#### **Selective Laser Melting of magnesium alloys**

L Jauer<sup>1</sup>, B Jülich<sup>1</sup>, M Voshage<sup>2</sup>, W Meiners<sup>1</sup>

<sup>1</sup> Fraunhofer Institute for Laser Technology ILT, Aachen, Germany <sup>2</sup> Chair for Laser Technology LLT, RWTH-Aachen University, Aachen, Germany

**INTRODUCTION:** Additive Manufacturing (AM) technologies enable the realisation of most complex parts. The AM technology Selective Laser Melting (SLM) uses laser radiation to subsequently melt and fuse thin layers of powder according to a sliced CAD-model. SLM allows for manufacturing e.g. individualised implants with designed, interconnected porosity.

METHODS: During this study, a laboratory SLM setup is used. The optical setup consists of a single mode ytterbium fiber laser (IPG YLR-200) with 230W maximum output power, a galvanometric scanner (SCANLAB hurrySCAN 20) and a f-theta focussing lens (SILL S4LFT 3254/126). The process chamber enables processing in an argon inert gas atmosphere with oxygen content below 10ppm. The materials used are gas atomized powders out of WE43 and AZ91 with almost spherical particle shape (MSE Clausthal). The powders are sieved to particle sizes 25-63µm before SLM processing. To build various SLM test specimen, the main SLM process parameters such as laser power, scan speed, hatch distance and exposure strategy are varied. SLM test specimen are analysed by means of SEM, EDS and light microscopy.

**RESULTS:** According to EDS analysis of crosssections of SLM-specimens out of AZ91 the magnesium content of the SLM-specimens compared to the aluminium content is linearly dependent on the energy input per unit volume. The higher the energy input the more magnesium is evaporated (Fig. 1 left). On the other hand, the part density is usually higher for higher energy input (Fig. 1 right).

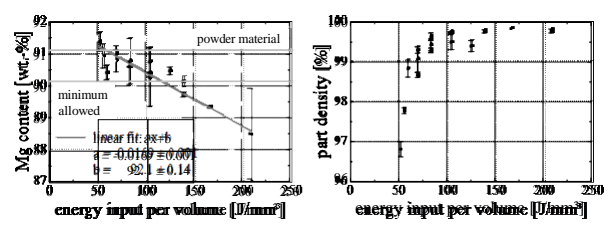


Fig. 1: Effect of energy input per unit volume on magnesium content (left) and part density (right)

Besides processing AZ91, first experiments for manufacturing scaffold-like structures with interconnected porosities out of WE43 were conducted.

The resulting parts show strong sintering of particles (Fig. 2 left). However, these adhering particles can be removed by e.g. sandblasting (Fig. 2 right). Sandblasted parts exhibit almost dense struts with thicknesses down to 300µm.

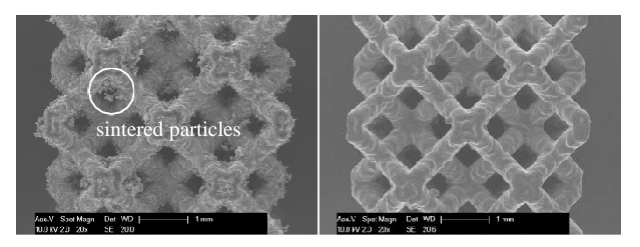


Fig. 2: SEM image of WE43 structure asprocessed (left) and after sandblasting (right)

**DISCUSSION & CONCLUSIONS:** When processing AZ91 by means of SLM, the energy input influences the part quality in two competing ways. For higher energy input the amount of magnesium content in test specimens is reduced but the part density is increased. Nevertheless, a process window which allows for producing almost dense (>99.5%) specimens complying with the alloy specifications exists.

In addition, it is possible to fabricate scaffold-like structures with designed interconnected porosity out of WE43 by means of SLM (Fig. 3). This is a first step towards manufacturing individualised implants with designed, interconnected porosity.

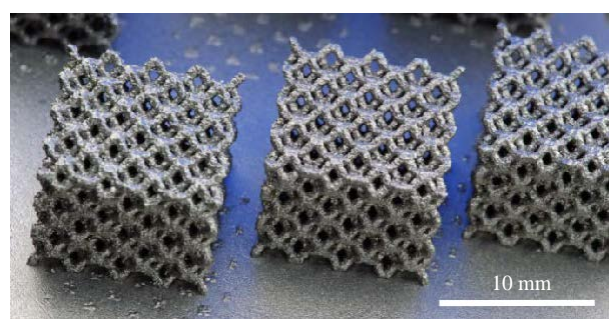


Fig. 3: scaffold-like structures with designed interconnected porosity out of WE43 made by SLM

**ACKNOWLEDGEMENTS:** This work was supported by Fraunhofer Internal Programs under Grant No. MAVO 824682 (DegraLast).

#### Selective laser melting of pure Fe and pure Zn for biodegradable implants

M Montani<sup>1</sup>, AG Demir<sup>1</sup>, E Mostaed<sup>1</sup>, M Vedani<sup>1</sup>, B Previtali<sup>1</sup>

<sup>1</sup> Department of Mechanical Engineering, Politecnico di Milano, Milan, Italy

**INTRODUCTION:** Laser based additive manufacturing processes have become an enabling technology for the production of customized biomedical implants in the past years. Selective laser melting (SLM) enables obtaining personalised products with complex shapes and controlled density and porosity, which are all advantageous for biomedical implants manufacturing [1]. Concerning metallic implants, titanium alloys and stainless steel have been by far the most widely studied with SLM. Although, the novel biodegradable metals are highly interesting for application requiring customized implants such as the orthopaedic ones, only few works on Mg and alloys are present in literature [2], whereas Fe and Zn have not been studied. In this work, SLM of Fe and Zn is presented. Manufacturability and mechanical properties of these materials were compared to a common bio-implant material AISI 316L.

**METHODS:** The used prototype SLM system consisted of a multimode 1 kW fibre laser equipped with a scan head generating 213 μm beam diameter at focal point. The powder grain sizes were  $31\pm8\mu m$ ,  $41\pm19\mu m$  and  $42\pm18\mu m$  for AISI 316L, Fe and Zn respectively. The powder bed was placed in a gas chamber with Ar flowing at 20Nl/min. Focal position was placed on powder surface. Laser power (P) was varied at two levels: 200 and 300 W, while scan speed (v) was varied between 150-1900 mm/s. The samples with minimum porosity (p) were characterized in terms of density (ρ), Vickers hardness (HV) and compression yield stress (CYS).

**RESULTS:** Figure 1 reports the microscopy images of the deposited materials with the lowest porosity achievable. summarizes the processing conditions used with the resulting porosity and density levels. It can be seen that both AISI 316L and pure Fe allow complete melting of the powder and generate low levels of porosity. The porosity generated on Zn remains above 10%, due to its low vaporization point (907 K). As a matter of fact, with 300W laser power the process was unstable, as deposited Zn layers showed porosity levels higher than 20%. On the other hand, the deposited Zn was characterized by foam-like structure with high surface area. The Vickers hardness of AISI 316L and pure Fe was

245±8 and 157±5 respectively (pure Zn was not characterized due to high porosity). The CYS values of the laser melted materials are shown in Figure 2. High CYS was achieved with AISI 316L, whereas the CYS of laser melted Fe and Zn are very similar to the human bone.

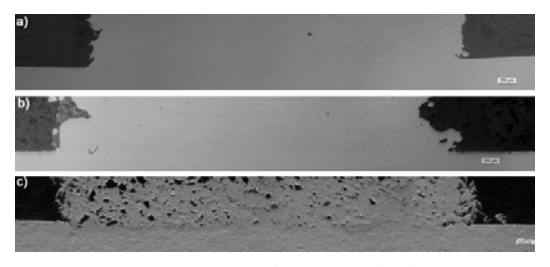


Fig. 1: Cross-sections of laser melted a) AISI 316L, b) pure Fe, and c) pure Zn.

*Table 1. SLM conditions for the tested powders.* 

Material	P [W]	v [mm/s]	p [%]	ρ [g/cm <sup>3</sup> ]
316L	300	150	1.5	7.87
Fe	300	150	1.1	7.82
Zn	200	600	14	6.1

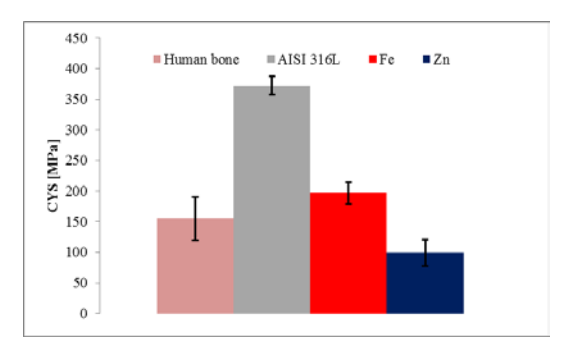


Fig. 2: CYS of the laser melted AISI 316L, pure Fe and Zn with comparison to human bone [3].

DISCUSSION & CONCLUSIONS: Both laser melted Fe and Zn appear to be highly appealing for biomedical applications such as orthopaedic implants, stents and scaffolds. The processability of pure Fe with the SLM is quite close to the widely used AISI 316L. Moreover the intrinsic foam-like porosity obtained in Zn can be also beneficial for cell integration and controlled biodegradation. On the other hand improving the controlled gas atmosphere can be solutions to obtain fully dense Zn.

#### Fabrication of porous pure magnesium sheet by selective laser melting

N Sato<sup>1</sup>, K Hanada<sup>1</sup>, T Shimizu<sup>1</sup>, S Nakano<sup>1</sup>

<sup>1</sup> National Institute of Advanced Industrial Science and Technology (AIST), Tsukuba, Japan

**INTRODUCTION:** Selective laser melting (SLM) is one of 3D printing technologies that can fabricate products designed by CAD from metal powder [1]. This process enables fabricating products with porous structure by controlling laser conditions such as power, scan speed, and scan interval. In medical field, porous implants are expected as one of the promising applications. For example, porous titanium alloy sheets have been fabricated by the SLM process for dental implant [2].

Magnesium and its alloy have attracted much attention as biodegradable materials for less-invasive medical devices. A porous magnesium sheet is expected to be applied as biodegradable bone scaffold for healing the large bone defects. In this study, to develop the porous magnesium sheets, we conduct SLM processing of pure magnesium powder at various conditions.

**METHODS:** Porous sheet samples were fabricated using SLM machine shown in *Figure 1*. This machine is equipped with a quasi-continuous wave fiber laser of 1064 nm wavelength. The spot size of the laser is about 175 min diameter.

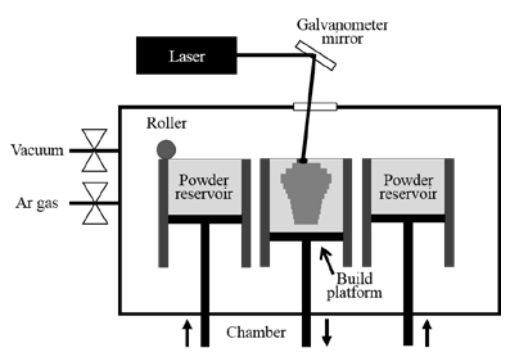


Fig. 1: Schematic illustration of SLM machine used in this study.

The pure magnesium powder for SLM experiment was prepared by cutting and mechanical milling. The pure magnesium ingot of commercial purity (>99.9 mass%) was cut into fine chips in air. Subsequently the cutting chips were mechanically milled at 200 rpm for 30 min in Ar atmosphere, and were passed through #140 sieve. The obtained pure magnesium powder had angular particle morphology and the average particle size was approximately 120  $\square$ m. The powder put on the build platform was irradiated within 10 mm square area in Ar atmosphere by laser. The laser power

and scan speed and scan interval were changed to examine the effect of the process conditions, as shown in *Table 1*.

Table 1. SLM process conditions.

Laser power	Scan speed	Scan interval
40 - 360 W	100 - 1000 mm/s	0.1, 0.2 mm

**RESULTS:** Under all processing conditions in Table 1, the sheet samples could be fabricated. As the laser power increased, the pore morphology and degree of oxidation were changed. *Figure 2* shows the porous pure magnesium sheet obtained at laser power 50 W, scan speed 1000 mm/s and scan interval 0.1 mm. This porous sheet had light gray colored surface and indicated ductility. The microstructure of the sheet had open cell structure formed by melting angular shaped pure magnesium particles.

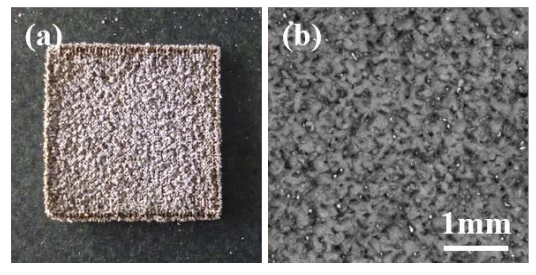


Fig. 2: Porous pure magnesium sheet: (a) appearance, (b) close-up view.

**DISCUSSION & CONCLUSIONS:** Porous pure magnesium sheets could be successfully fabricated by SLM process, and it indicates the possibility of controlling the porous structure and size for biodegradable implant applications, and of its tailor-making. However, it is necessary to optimize of the SLM conditions, and to examine the mechanical and corrosion properties as well as the biocompatibility of the porous sheet.

#### Safety recipient for controlled selective laser melting of magnesium

S Böhringer<sup>1</sup>, A Kessler<sup>1</sup>, J Rüegg<sup>1</sup>, R Schumacher<sup>1</sup>, E Schkommodau<sup>1</sup>, <u>M de Wild</u><sup>1</sup>

<sup>1</sup> University of Applied Sciences Northwestern Switzerland, School of Life Sciences, Institute for Medical and Analytical Technologies, Muttenz, CH

**INTRODUCTION:** Additive manufacturing opens new perspectives towards novel implant shape and function. Technological progress has led to reproducible manufacturing of implants by selective laser melting (SLM) out of metallic materials like titanium<sup>1</sup> or NiTi<sup>2</sup>. However, only few attempts with magnesium (Mg) have been reported<sup>3,4</sup> aiming to resorbable implants. Due to the materials reactivity, the process of selective laser melting on Mg requires special precautions. In this study, we developed and validated a prototype for a safety recipient for the controlled operation inside a commercial SLM machine.

**METHODS:** In order to limit the reaction volume, a hermetic container was constructed in which the SLM process can be studied under a protective gas atmosphere inside an SLM Realizer 100 machine, see Fig. 1. The 100 W continuous wave Ytterbiumfibre laser with a wavelength between 1068 and 1095 nm passes a borosilicate glass on top of the container with negligible absorption. A Ti or Mg substrate serves as the building platform and is covered by a powder layer of controlled thickness.



Fig. 1: Safety recipient and building platform (\$\phi65\$ mm) with selectively melted powder areas.

Experiments were first done with thin layers of Ti powder of approx.  $30~\mu m$  thickness (Ti grade II, SLM solutions, Germany), later with atomized Mg powder (AZ91, SFM, Switzerland). The particle size distribution was determined (Helos, Sympatec GmbH, Germany). The particle shape and chemical composition were analysed by SEM/EDX (TM-3030Plus, Hitachi, Japan).

**RESULTS:** The used Mg powder has a  $d_{50}$ -value of 57 µm and the particle express a spherical morphology (Fig. 2) which is important for a good flowability. After passing the quartz lid, the laser beam accurately irradiates the powder bed on the

building platform according to the predefined scan trajectories, see Fig. 3. Ti powder as well as AZ91 powder can be successfully fused to the substrate (Fig. 1 right and Fig. 3).

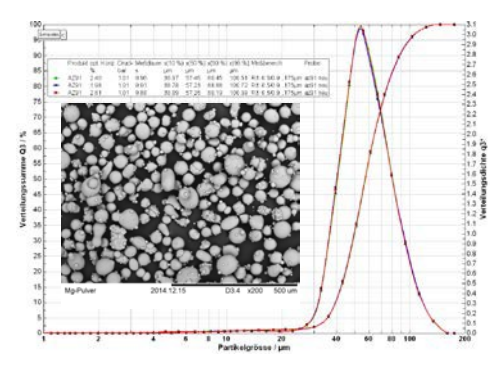


Fig. 2: Particle size distribution of the AZ91 powder, logarithmic scale from 1  $\mu$ m – 200  $\mu$ m. The inset shows a SEM image of the spherical particles. Scale bar 500  $\mu$ m.

DISCUSSION & CONCLUSIONS: The developed safety recipient allows controlled experiments to study the SLM process of Mg powder with various substrates, types of powder, process parameters and environments (protective gas composition and pressure). Single SLM layers of Mg have been created.

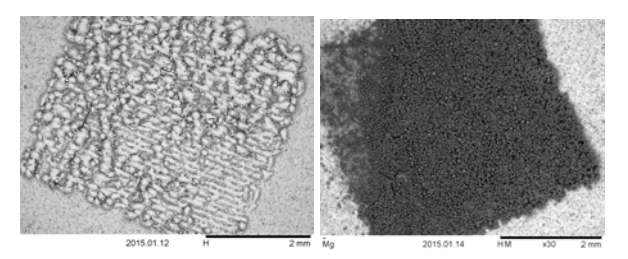


Fig. 3: Powder selectively fused to Ti substrate. Left: Ti powder, right: Mg powder. Bar = 2 mm.

**ACKNOWLEDGEMENTS:** This work was supported by the *stiftung***fhnw**.

### Comparison of additive manufactured porous magnesium and titanium implants using primary osteoblasts and primary stem cells

J Matena<sup>1</sup>, M Gieseke<sup>2</sup>, M Teske<sup>3</sup>, S Petersen<sup>3</sup>, A Kampmann<sup>4</sup>, I Linke<sup>4</sup>, L Roland<sup>1</sup>, M Grau<sup>1</sup>, H Murua Escobar<sup>5</sup>, NC Gellrich<sup>4</sup>, H Haferkamp<sup>6</sup>, I Nolte<sup>1</sup>

<sup>1</sup>University of Veterinary Medicine Hannover Foundation, Small Animal Clinic, Hannover <sup>2</sup>Laser Zentrum Hannover e.V., Hannover

<sup>3</sup>Rostock University Medical Center, Institute for Biomedical Engineering, Rostock <sup>4</sup>Hannover Medical School, Department of Oral and Maxillofacial Surgery, Hannover <sup>5</sup>University of Rostock, Division of Medicine Clinic III, Hematology, Oncology and Palliative Medicine, Rostock

<sup>6</sup>Leibniz Universitaet Hannover, Institut fuer Werkstoffkunde, Hannover

**INTRODUCTION:** Craniofacial implants for the reconstruction of critical size defects which are biodegradable and provide initial stability have currently not been realized. An initial stable and biodegradable porous scaffold should enable vascularization and bone remodelling. provides magnesium favorable mechanical properties such as biodegradability and stability [1], this material was examined in terms of its suitability as implant material in comparison with a titanium implant.

A defined porous structure can be achieved by different additive manufacturing methods. In this study Selective Laser Melting (SLM) was utilized for processing magnesium and compared with titanium, that was examined in an earlier study [2]. As magnesium corrosion often is increased PCL and P(3HB) were used as a polymer coating.

**METHODS:** Magnesium and titanium implants with interconnected cavities were manufactured using the SLM process and coated with polymers (PCL and P(3HB)). The different implant materials were compared in a cell culture setting and magnesium corrosion was evaluated measurement of the pH value changes and mass loss. In this study a cell visualization method was used based on Live Cell Imaging (LCI) allowing a real time cell tracking. For this purpose the implants were vitalized with primary stem cells or osteoblasts and imaged with LCI using a specially manufactured teflon holding device. The new method was compared with commercially available proliferation and vitality Additional histological investigations completed the evaluation

**RESULTS:** Open porous magnesium and titanium implants were successfully manufactured using SLM and could be examined in in vitro studies (Fig. 1). The results obtained in this study proved LCI to be a powerful method for examination of implant material. The cytocompatibility of PCL

was slightly reduced in comparison to P(3HB). Nevertheless, a complete polymer coating and protection against corrosion was successfully achieved solely for PCL. The porous implant structure allowed cell proliferation even in the inner parts of the porous implant.

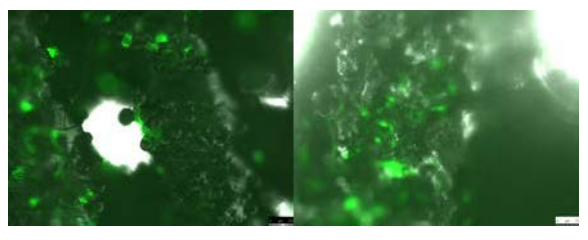


Fig. 1: Titanium (left) and magnesium (right) PCL implant seeded with GFP-Osteoblasts

**DISCUSSION & CONCLUSIONS:** Open porous magnesium implants generated with SLM and coated with a polymer might be a beneficial approach to overcome the lack of biodegradable and stable implants adapted to the requirements of craniofacial surgery.

#### Fabrication of zinc alloy minitubes for biodegradable stent applications

E Mostaed<sup>1</sup>, M Sikora-Jasinska<sup>1, 2</sup>, S Lofferdo<sup>1</sup>, D Mantovani<sup>2</sup>, M Vedani<sup>1</sup>

<sup>1</sup>Department of Mechanical Engineering, Politecnico di Milano, Milan, Italy. <sup>2</sup>Lab. for Biomaterials & Bioengineering (CRC-I), Dept. Min-Met-Materials Engineering, Laval University, Québec City, Canada

INTRODUCTION: Two classes of biodegradable metallic materials have been widely investigated: Mg- and Fe- based alloys. Mg degrades too fast, releasing large amounts of hydrogen gas, while degradation rate of Fe is too slow. Newly, zinc has been proposed as an alternative candidate for biodegradable applications. According to the standard electrode potential Zn has a corrosion rate faster than Fe but slower than Mg. Moreover Zn is any of section of the standard electrode potential values as ports of callular metabolisms.

Thus, Zn is believed to be a promising candidate for degradable stent.

**METHODS:** Zn-Mg alloys were prepared by melting pure Zn (99.995%) and Mg (99.95%) at  $500^{\circ}$ C. Microstructure was characterized by optical microscopy. Mechanical properties were assessed by tensile test. Corrosion behavior of the alloys was compared to those of pure Zn and Mg by performing potentiodynamic polarization and static immersion tests in Hanks' modified solution. The solution temperature and pH were adjusted to  $37 \pm 1^{\circ}$ C and 7.4, respectively.

**RESULTS:** Microstructure of the extruded tubes shows a remarkable evolution of large Zn dendrites into small equiaxed grains. Moreover, eutectic mixture disappeared and instead precipitates segregated along grain boundaries.

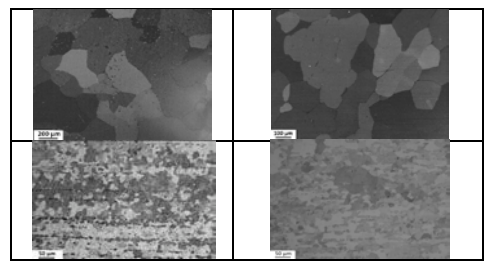


Fig. 1: Microstructure of the extruded samples: (a)Zn,(b) Zn-0.15Mg,(c)Zn-0.5Mg and (d)Zn-1 Mg.

Mechanical properties of the extruded alloys consistently increases with Mg concentration (Fig.2). Among all the investigated alloys, Zn-0.15Mg shows a proper mechanical strength, while keeping a fairly high tensile ductility. Fig. 3 shows the corrosion behavior of the investigated samples. As seen, regardless of the Mg content, corrosion

rates of Zn alloys are lower than that of pure Mg. The effect of Mg on corrosion parameters of Zn alloys is small owing to the low concentration of alloying elements used in this study (0.15 - 3%).

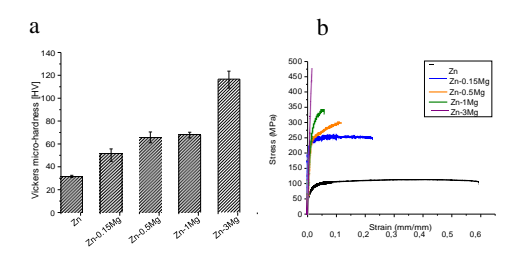


Fig. 2: Mechanical properties of the extruded samples: (a) Vickers micro-hardness and (b) Tensile properties.

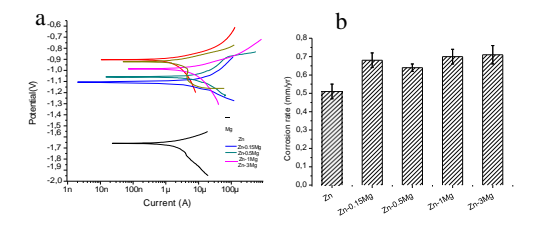


Fig. 3: a) Potentiodynamic polarization curves b)Degradation rate of Zn alloys.

**DISCUSSION & CONCLUSIONS:** Zn-Mg alloy minitubes with different concentrations have been proposed for biodegradable stent applications. Hot tube extrusion led to a considerable grain refinement in all samples. All produced minitubes featured equiaxed grain structure along with segregation of the precipitates along grain boundaries. With increasing Mg content mechanical properties of the alloys improved due to the increasing volume fraction of the hard Mg<sub>2</sub>Zn<sub>11</sub> intermetallic phase. Among all the investigated alloys, Zn-0.15Mg showed a proper strength and ductility, making it stand out for stent application. Influence of Mg on corrosion properties of Zn is not significant. Extruded alloys revealed slightly higher corrosion resistance than their cast counterparts.

#### Absorbable filament design with three-fold device function

JE Schaffer<sup>1</sup>, A J Griebel<sup>1</sup>

<sup>1</sup> Fort Wayne Metals Research Products Corp., Fort Wayne, IN, USA

**INTRODUCTION:** An absorbable platform provides not only mass but also form as a time-dependent variable by use of shape memory alloy (SMA). The localized corrosion behaviour in metallic implants is at least a function of materials selection, processing and the final *in situ* materials stress state [1-2]. Relatively noble nitinol SMA filaments were used to prevent form loss in the reinforced-composite-wire textile shown in Figure 1 (right) [3]. Herein, SMA filaments are used to achieve motion in an absorbable device via a preprogrammed terminal scaffold shape.



Fig. 1: Images showing wire-based scaffolds after 4 weeks in 37°C bovine serum: (left) high strength Ø 200 µm Fe-Mn wire scaffolds are susceptible to break up by corrosion-assisted fracture in contrast to (right) SMA-embedded design.

**METHODS:** Drawn-filled tube (DFT) composite wires were produced with an antiferromagnetic iron – 35 wt.% manganese (FeMn) sheath. Binary Ni-49.2 at.% Ti (NiTi) SMA was used in the wires composite and manufactured conventional medical material processes [4]. Closing-mode (CM) devices were made by forming cold-worked 0.20 mm wires around a 0.81 mm diameter stainless steel mandrel as shown in Figure 3d, followed by heat treatment in air at 773 K for 300 s. A portion of the 1.2 mm diameter coil was plastically straightened by stretching as shown in Figure 3a. Opening-mode (OM) devices were made by a simple juxtaposition of processing steps: wires were first heat set at 773 K while constrained straight before coil forming over the same 0.81 mm mandrel as shown in Figure 3d. For concept demonstration, both CM and OM devices were placed in 60°C, 25 v/v % nitric acid in order to force FeMn dissolution and resultant shape evolution over a period of minutes.

**RESULTS:** Figure 3 shows a time image sequence of shape change during scaffold dissolution. Panels a-c show contraction of a straightened coil as the absorbable species dissolves into the acidic milieu. Panels d-f show length and diametral expansion over a similar dissolution course. Total elapsed time in both cases was under 300 s.

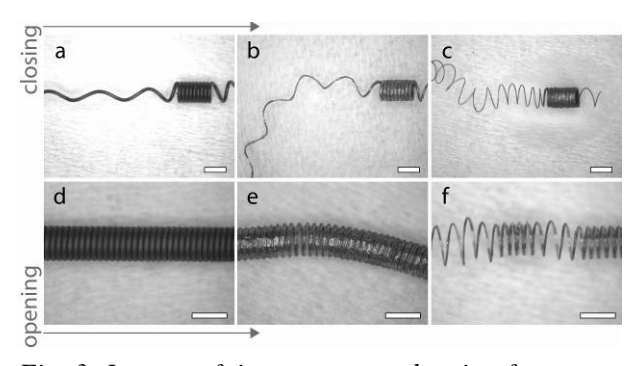


Fig. 3: Images of time sequence showing form closing (a to c) and form opening (d to f) during exterior corrosion dissolution. Note: end form matched programmed memory in underlying shape memory filament; white scale bars are 1.2 mm.

DISCUSSION & CONCLUSIONS: It is shown that plastic forming of an absorbable and composited metal component can provide initial device form where an embedded shape memory alloy can drive motion and provide programmed end-point geometry. Combined with wire format capabilities (Fig. 2), this technology may provide unique three-fold function driven by (i) therapy associated with initial form, degradation-associated motion, and the final modified form.

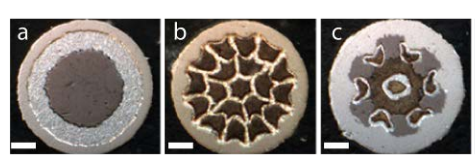


Fig. 2: Images of multiscale and multi-element wire composites that provide a toolbox for smart absorbable filament design, scalebar is 25 µm.

**ACKNOWLEDGEMENTS:** J Christ (textile fabrication), D Braaten & DL Snider (wire).

# Magnetron sputtered, structured iron based foils as biodegradable implant material for minimal invasive vascular surgery applications

T Jurgeleit<sup>1</sup>, E Quandt<sup>1</sup>, C Zamponi<sup>1</sup>

<sup>1</sup>Chair for Inorganic Functional Materials, Institute for Materials Science, Faculty of Engineering, University of Kiel, Germany

**INTRODUCTION:** The use of biodegradable metals like magnesium and iron is a promising approach to fabricate non-permanent implants e.g. for minimal invasive vascular surgery.

While for magnesium it is attempted to slow down the degradation rate and reducing the hydrogen evolution [1], the task for iron is to accelerate the degradation or improve the mechanical properties in order to reduce the amount of material necessary to resist the mechanical load on an implant [2].

Goal of the present work is the improvement of the degradation behavior and of the mechanical properties of iron based alloys and composites fabricated by magnetron sputtering. In combination with lithographic techniques a direct structuring during the deposition is possible.

The technique allows the fabrication of homogeneous metal films and furthermore the combination of various non-compounding materials.

**METHODS:** Different approaches were pursued to achieve the given aims. The grain structure of pure iron samples was influenced by annealing. Multilayer systems of iron and various non compounding elements where fabricated and homogenized afterwards, to achieve small, finely distributed precipitates.

The microstructure, topography and composition was investigated by electron microscopy and X-ray diffraction methods. Tensile tests were performed the mechanical characterization. degradation behavior was studied by in vitro corrosion tests via linear polarization measurements and immersion testing in hanks buffered salt solution at 37 °C where the pH-value of the solution was held at 7.4 by carbon dioxide inlet was performed.

**RESULTS:** Annealing of the pure iron film leads to a grain coarsening that involves an increase of the corrosion rate from 0.06 mm/year to 0.10 mm/year. The tensile strength decreased from 634 MPa to 343 MPa, while the strain at fracture increased up to 20 %. Annealed iron-gold samples

showed depending on the gold content tensile strengths between 416 MPa and 609 MPa.

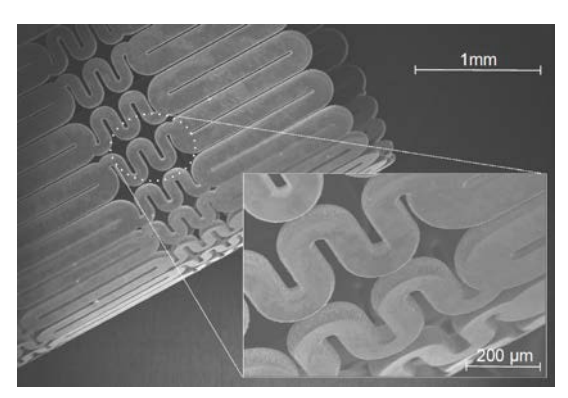


Fig. 1: SEM Images of stent graft shaped freestanding, pure iron structures. The structures where produced by lithographic structuring and magnetron sputtering.

**DISCUSSION & CONCLUSIONS:** Free-standing, structured pure iron and iron based foils where produced by magnetron sputtering. The foils show a high strength and strain at fracture, which in some extent can be tailored.

Magnetron sputtering offers a good process controllability, due to a number of possibilities influencing the microstructure and therefore the relevant material properties.

The method offers a promising new approach to produce iron based, biodegradable implants.

**ACKNOWLEDGEMENTS:** The Authors would particularly like to thank the DFG for financing this project.

#### Biodegradable magnesium alloy wires preparation and application study

LL Tan<sup>1</sup>, JL Li<sup>1</sup>, FF Liu<sup>2</sup>, K Yang<sup>1</sup>

<sup>1</sup> <u>Institute of Metal Research</u>, Chinese Academy of Sciences, Shenyang, China.

<sup>2</sup> <u>Dong Guan Eontec Co.</u>, Dong Guan, China

**INTRODUCTION:** Suture materials for surgical dressings have already been available to humans for a few centuries[1]. Initial tests using magnesium wire in the field failed duo to the poor plasticity of the magnesium alloy wires[2]. For this reason, the aim of this work was to develop new kind of magnesium alloy wires with excellent mechanical properties to satisfy the requirement as degradable suture material.

**METHODS:** The magnesium alloy wires with diameter of 0.3 mm were prepared by the combination of rotary swag and drawing technologies. Tensile samples with a length of 30 mm were cut from as-drawn magnesium alloy wires. The tensile property data were based on the average of 10 tests. The magnesium wire was used to suture the muscle cut of the mouse and the degradation of the wire was observed.

**RESULTS:** Fig. 1 shows the macro morphology of as-drawn magnesium alloy wires.

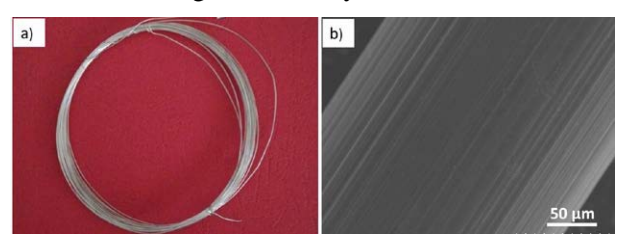


Fig. 1: a) Photo of  $\Phi 0.3$ mm Mg alloy wire in drawn condition, b) Micrograph of Mg alloy wire surface

The tensile properties of the wires at room temperatures are summarized in Table 1. The strength of the NZ20 wire suffers minimal losses after knotted. Therefore, the NZ20 wire seems to be the most suitable alternative as suture material.

Table 1 Tension strength of the Mg-Zn-Nd alloy wires under straight pull and knot pull

Alloys	Straight pull/N	Knot pull/N	Knot pull /Straight pull
ZN20	23.5±0.5	$15.8 \pm 0.9$	0.67
ZN40	$24.4\pm0.3$	$11.1 \pm 0.8$	0.46
NZ20	$19.7 \pm 0.2$	$17.6 \pm 0.2$	0.89

Fig. 2 shows the surgical procedure that NZ20 wire was used to suture the cut of the mouse. During the

surgery, the NZ20 wire kontted easily and the cut of the muscle was sutured successfully.



Fig. 2: Images of surgical procedure using NZ20 alloy wire, a) suturing the cut, b) knoting wire

Fig. 3 shows the macro morphology of the NZ20 wire after implatation for one and two weeks. It can be seen that the NZ20 alloy wire showed less obvious degradation after implatation for one week. And the wire became thin at the location where the wire suffered larger deformation during the knotting process.



Fig. 3: Photos of NZ20 alloy wires after implantation for 1week (a) and 2 weeks (b)

**DISCUSSION & CONCLUSIONS:** The tension strength of the wires decreased when they were in the knotted state. The NZ20 alloy wire was successfully used to suturing the muscle cut. And slight degradation was observed after the NZ20 wire was implanted for 2 weeks.

**ACKNOWLEDGEMENTS:** This work was supported by the National Basic Research Program of China (973 Program, NO. 2012CB619101).

# Microstructures and corrosion behaviour of an Mg-3Zn-0.5Zr/5HA composite prepared by casting and plastic deformation

J Li<sup>1,2</sup>, L Zhou<sup>1</sup>, Y Huang<sup>1</sup>

<sup>1</sup> BCAST, Inst. of Materials &Manufacturing, Brunel University London, Uxbridge, UB8 3PH UK. <sup>2</sup>National Engineering Research Centre for Special Metal Materials of Tantalum and Niobium, Yejin Road, Shizuishan, Ningxia 753000, China.

INTRODUCTION: Magnesium alloy matrix and hydroxyapatite(HA) particle reinforced composites have shown great potential for orthopaedic applications with controllable mechanical strength and degradability. However, their synthesis is difficult due to HA particle segregation and their corrosion behaviour is not fully understood. The present work was carried out to study the evolution of HA particle distribution and microstructures during processing and their effect on the corrosion resistance of the material.

**METHODS:** Spherical HA particles of 20-50nm in diameter were mixed into a commercially pure Mg-3wt.%-0.5wt.%Zr alloy melt by using a high shear rotor-stator device at 670°C. The molten Mg/HA composite was then either cast into an ingot in a book-shaped steel mould or cast by a twin roll caster into 2.5mm thick strip at a speed of 4m/min. 15×15×100mm bars were machined from the as-cast ingot for equal channel angular pressing, which was conducted at 350°C in a 120° die to a total of 6 passes for each sample (total true strain~4). The twin roll casting strip was further hot rolled at 400°C to 1mm, giving a reduction of 60%. Optical and electron microscopy was carried out to characterize the HA particle distribution and microstructures for the as-cast samples and deformed samples. The point analysis, line scan and area mapping of chemical compositions were performed by EDS. Immersion tests were conducted in the HBSS at 37°C for 72h according to ASTM-G31-T2, using a WE-3 immersion oscillator. During the tests, the solution was constantly replaced with the fresh one to maintain its pH value at a level of 7.4±0.2. The mass loss per unit area was measured as a function of time and the corrosion rate was determined accordingly.

**RESULTS & DISCUSSION:** High shear mixing produced a globally uniform distribution of HA particles in the Mg matrix during normal casting (Fig. 1a). TRC provided higher cooling rate and plastic deformation, giving a finer grain structure and improved particle distribution (Fig. 1b).). 6 pass ECAP resulted in a fine and elongated microstructure (Fig. 2a), leading to the breakdown

of HA particle aggregates and the formation of HA particle dispersion in the matrix (Fig. 2b).

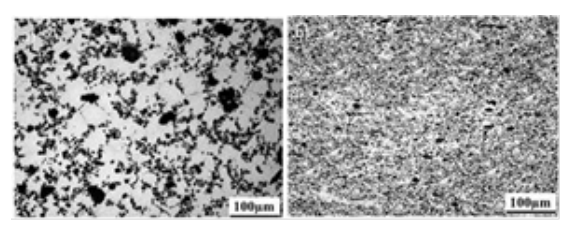


Fig. 1: Optical micrographs of the as-cast composite: a) Ingot; b) TRC strip (TD plane).

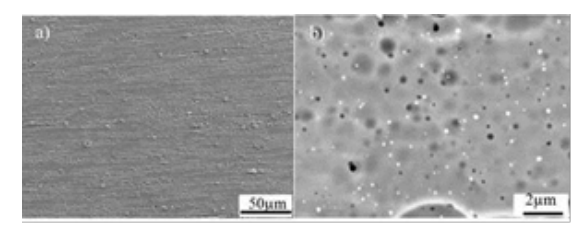


Fig. 2: SEM micrographs for an ECAP processed sample (6 passes), showing a) the improved particle distribution and refined microstructure; and b) the formation of HA particle dispersion.

The average corrosion rates over the first 36h in the immersion tests were measured to be 0.147, 0.223 and 0.094 mg/cm²/h for the as-cast ingot, ascast TRC strip and 6 pass ECAP samples. The refined microstructure, improved HA particle distribution and chemical homogeneity were attributed to the reduced corrosion rate for the ECAP samples. The poor corrosion resistance for the as-cast TRC strip was most likely due to the contamination during processing as EDS results showed that its Fe content was ~30% higher than that in the as-cast ingot, although it exhibited finer microstructure and better HA particle distribution. Hot rolling did not show improvement.

**CONCLUSIONS:** High shear mixing and ECAE was effective in the control of microstructure and HA particle distribution in the Mg/HA composite with improved corrosion resistance. Increased Fe level was critically detrimental to the corrosion resistance of the material.

**ACKNOWLEDGEMENTS:** This research was supported by the EPSRC, UK and CSC, China.

# Microstructure and mechanical properties of thin nanostructured hydroxyapatite coating deposited on the surface of AZ31 magnesium alloy via RF-magnetron sputtering at a substrate bias

R Surmenev<sup>1,2</sup>, M Surmeneva<sup>1</sup>, T Mukhametkaliyev<sup>1</sup>, A Tyurin<sup>3</sup>, T Pirozhkova<sup>3</sup>, R Stolyarov<sup>3</sup>

<sup>1</sup> <u>Department of Theoretical and Experimental Physics</u>, National Research Tomsk Polytechnic University, Tomsk. <sup>2</sup> Fraunhofer Institute for Interfacial Engineering and Biotechnology (IGB), Stuttgart. <sup>3</sup> G.R. Derzhavin Tambov State University, Tambov

**INTRODUCTION:** There is an increasing interest in investigations of different ways of surface modification to enhance physico-chemical and mechanical properties of magnesium (Hornberger, 2012) [1]. The objective of this study was to modify the surface of bioresorbable magnesium alloy AZ31 by the use of a thin nanostructured coating of HA fabricated by RF-magnetron sputtering deposition and investigation of physico-chemical and mechanical properties of the prepared biocomposites.

**METHODS:** AZ31 magnesium alloy (GoodFellow) was used as substrate. A commercially available apparatus with an RF (13.56 MHz, COMDEL) magnetron source was

used to deposit thin HA coatings. The phase composition and structure of the CaP coatings were identified by X-ray diffraction (XRD-7000, Shimadzu, Japan). Local physico-mechanical properties of the biocomposites were studied using TI-950 Triboindenter (Hysitron, USA) with a Berkovich indenter according to Oliver-Pharr method [2].

**RESULTS:** Structure and mechanical properties of the nanostructured HA coatings prepared at the biased substrate (50 V, duty cycle 10 %) were obtained. Nanocrystalline HA coating provides enhancement of the mechanical properties of AZ31 alloy (fig. 1). Nanohardness H and Young's modulus E of the coatings prepared on the surface of the alloy at the penetration depth of  $h_c = 50 \text{ nm}$ are  $3.65 \pm 1.2$  and  $54.58 \pm 19.67$  GPa (Table 1), respectively. The values of H/E and  $H^3/E^2$  for HA coating (0.067 and 0.0163 GPa, respectively) are significantly higher than that of the uncoated substrate (0.024 and 0.0005 GPa). Thus, HA coatings deposited on magnesium alloy AZ31 via RF-magnetron sputtering resulted in enhancement of its mechanical properties (high values of abrasive and erosion wear).

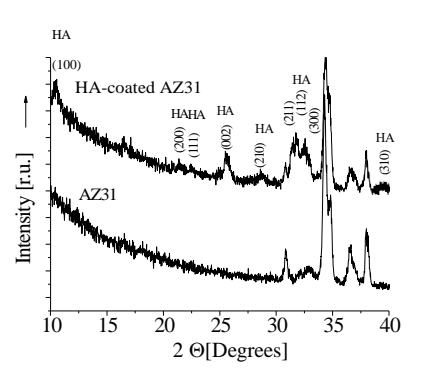


Fig. 1. Typical XRD-patterns of HA-coated and initial AZ31 substrate

Table 1. Local physico-mechanical characteristics of the investigated samples at the penetration depth of  $h_c = 50$  nm.

Sample type	H [GPa]	E [GPa]
AZ31 alloy	$0.90 \pm 0.80$	$37.01 \pm 22.30$
HA-coated AZ31 alloy	$3.65 \pm 1.2$	$54.58 \pm 19.67$

**DISCUSSION** & **CONCLUSIONS:** The deposited HA coating is nanocrystalline with the crystallite size in the range 14-17 nm. After nanostructured HA coating deposition such physico-mechanical characteristics as nanohardness H, Young's modulus E, H/E ratio and  $H^3/E^2$  were significantly improved.

**ACKNOWLEDGEMENTS:** We thank Mr. M. Syrtanov for the help with the XRD measurements. The authors acknowledge the support of the Russian Science Foundation (project number 14-13-00274).

#### Design and manufacture of commercially viable absorbable magnesium alloys

R Thornton<sup>1</sup>, I Syed<sup>1</sup>, P Lyon<sup>1</sup>

Magnesium Elektron, Manchester, UK

INTRODUCTION: Research in absorbable magnesium for short term implants has been hugely popular over the past 10 years, with research groups around the world looking at bespoke biomedical alloy compositions and processing routes. However designing alloy chemistry and thermo-mechanical processing is only half the development process to producing a successful commercial alloy. A manufacturing route which answers the demands of alloy design (chemistry and process), risk and economic models must be created to ensure commercial viability and patient safety. This presentation gives an overview of the steps taken at Magnesium Elektron to bring research ideas to a full industrial process.

**DISCUSSION:** Magnesium Elektron is a manufacturer of high performance magnesium alloys having supplied into a range of markets from aerospace to nuclear, however over the last 10 years has been heavily involved in the research and development of alloys for absorbable implants. During this time over 100 alloy designs were investigated for their suitability as implants. Designing an alloy system does not end at the discovery of successful chemical, biocompatible and mechanical properties; but it fact is a complex interaction driven by the application, economics and physical form (see figure 1). For a truly successful commercial alloy, the end goal is a manufacturing route, chemistry and thermomechanical process which work together.

During scale up investigations, it was found that certain alloys which show outstanding mechanical properties were actually highly unstable for the casting process due to cracking issues not seen on small diameter billets. This occurred on a number of alloying systems and shows how important it is to consider the final casting route before designing alloy chemistry. Alloys which relied on very small grain size for mechanical and stress corrosion properties had to be produced on a bespoke extrusion press to ensure the natural variability in the process did not vary properties along the length of extrusion or extensively batch to batch. Another alloy series which had yield strengths in excess of 300MPa and corrosion rates below Elektron WE43 seemed incredibly promising for load bearing

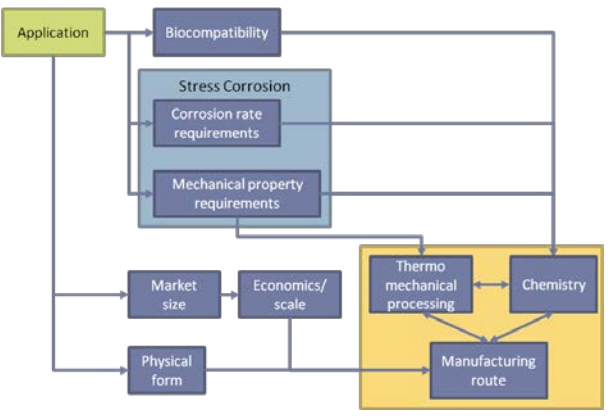


Fig. 1: The various factors and complex interaction between them in order to produce commercially successful magnesium alloy

applications; however the alloy content and strengthening mechanisms lead to extrusion conditions requiring very narrow processing parameters. This in turn makes the economics and ability to hit target specifications, and relevant dimensions incredibly difficult.

It was realised over the 10 years of development, manufacturing these alloys in an aerospace environment and to aerospace quality management systems was not suitable. A new facility specifically, for biomedical alloys, was built and gains in alloy performance and process consistency were achieved. It was also found that running ISO 13485 for design and manufacturing activities although arduous compared to AS9100 or ISO9001, gave greater control of risk management which is so important for bio-absorbable materials compared to permanent metals.

Magnesium Elektron now has a pipeline of alloys currently in *in vitro*, *in vivo* and clinical stages ready to fulfil the specific requirements of a variety of applications. The alloy properties, balance between manufacturing route, chemistry and thermo-mechanical process as well as the lessons learned during up-scaling activities will be discussed.

#### Cold-drawn Mg alloy composite wires minimize risk through galvanic coupling

AJ Griebel<sup>1</sup>. JE Schaffer<sup>1</sup>

<sup>1</sup> Research & Development, Fort Wayne Metals Research Products Corp., Fort Wayne, IN, USA

INTRODUCTION: One of the most significant risks in the pursuit of absorbable medical devices is that of premature device failure due to localized corrosion or stress corrosion cracking [1]. Premature failure can lead to an ineffective treatment at best and an unsafe one at worst, with dangers like embolus formation or arterial perforation a real possibility. In an effort to minimize such risk, drawn-filled tube (DFT®) wire composites with absorbable ferrous shells and nonabsorbable core filaments were produced [2]. These wires demonstrated excellent cohesiveness throughout the corrosion process, leaving behind only an extremely thin, flexible filament. An ideal wire for absorbable medical devices would incorporate this fracture-preventing filament, wherein the filament also degrades. To achieve such a material, core and shell materials with proper galvanic relationships must be selected. The three main metal groups of interest for absorbable devices, in order of most anodic to least, are magnesium (Mg), zinc (Zn), and Iron (Fe). An ideal construction would place the more anodic material over the cathodic (e.g. Mg over Zn or Mg over Fe), so that the central filament may be galvanically protected from corrosion until the majority of device degradation is complete. The purpose of this work is to demonstrate the feasibility of cold-drawn Mg alloy composite wires with core materials allowing advantageous galvanic coupling, building on recent efforts to develop cold-drawn Mg alloy wire [3, 4].

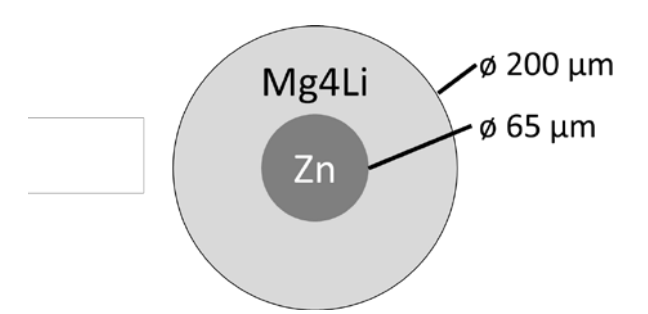


Figure 1. Mg4Li-DFT-10%Zn wires were drawn to 200  $\mu$ m diameter.

**METHODS:** 200  $\mu$ m diameter DFT composite wire was produced with a 68  $\mu$ m thick Mg-4wt%Li shell and 65  $\mu$ m diameter 99.99% pure Zn, so that Zn comprised 10% of the cross-

sectional area (Fig.1). This wire was cold drawn to 80% cold area reduction.

To assess the cohesiveness of the Zn core after drawing and corrosion of the Mg4Li shell, 2.5 mm coils were made to serve as a crude representation of a stent. One end of these coils was etched in a 3% sulphuric acid solution to remove the Mg4Li and expose the underlying Zn.

**RESULTS:** The 200  $\mu$ m wires had an ultimate tensile strength of 310 MPa, yield strength of 250 MPa, and elongation at failure of 4.3%. After etching the coils, the Zn core remained intact and elastically recovered to a slightly larger coil diameter (Fig. 2).

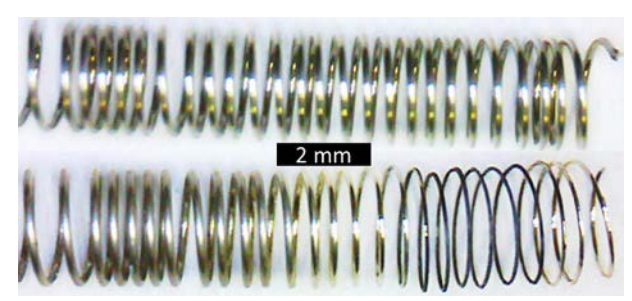


Figure 2: 200 µm Mg4Li-DFT-10%Zn were formed into 2.5 mm coils (top) and then partially etched (bottom, right) to expose the Zn core.

**DISCUSSION & CONCLUSIONS:** The wire concept presented herein could effectively reduce the risk of premature device failure in wire-based absorbable implants. The potential for galvanically accelerated corrosion of the shell must be investigated. Other configurations, combining Mg and Fe, dissimilar Mg alloys, and Mg and radiopaque materials are currently being pursued and will be discussed at the upcoming meeting.

**ACKNOWLEDGEMENTS:** The continued support of FWM leadership is gratefully acknowledged.

# New kind of bio-functional Mg-Cu alloy with enhanced osteogenesis, angiogenesis and long-acting antibacterial performance

C Liu<sup>1</sup>, XK Fu<sup>2</sup>, Y Zhao <sup>2</sup>, LL Tan<sup>1</sup>, Q Zhang<sup>3</sup>, HB Pan<sup>2</sup>, K Yang<sup>1</sup>

<sup>1</sup> <u>Institute of Metal Research</u>, Chinese Academy of Sciences, Shenyang, China.
<sup>2</sup> <u>Shenzhen Institutes of Advanced Technology</u>, Chinese Academy of Sciences, Shenzhen, China.
<sup>3</sup> <u>Chinese PLA General Hospital</u>, Beijing, China

INTRODUCTION: With progress in research and development on biodegradable magnesium based implants, some biomedical functions of them during degradation were also explored, which might subsequently promote the possible clinical applications [1]. The biodegradable magnesium based implants with both regenerative and antimicrobial properties will achieve a great progress in orthopedic applications [2]. A series of binary magnesium-copper (Mg-Cu) alloys were designed as a novel biofunctional material to induce osteogenesis, stimulate angiogenesis and provide a long-acting antibacterial performance while with appropriate degradation.

**METHODS:** The Mg alloys doped with X-wt.% of Cu element (X = 0.05, 0.2, 0.5) were as casted-fabricated. The antibacterial test was employed to examine the effect of Mg-Cu alloys against Staphylococcus aureus that may induce infections in the biological systems. The effects of the ionic extracts from Mg-Cu alloys on osteogenic differentiation of Murine calvarial preosteoblasts (MC3T3-E1), proliferation of human umbilical vein endothelial cells (HUVECs) and the related mechanisms were investigated.

**RESULTS:** The high alkalinity and continuous Cu ions releasing along with Mg matrix degradation had demonstrated a long-acting antibacterial performance of Mg-Cu alloys. Mg-Cu extracts could enhance cell viability, alkaline phosphatase (ALP) activity, matrix minerilazation of MC3T3-E1 cells, and stimulate cell proliferation, migration and endothelial tubule-forming of HUVECs due to the release of Mg ions and Cu ions in the biological environment.

**DISCUSSION & CONCLUSIONS:** Mg-Cu alloy is much potential to be a new biodegradable metal combined with osteogenesis, angiogenesis and anti-infection ability for orthopedic application.

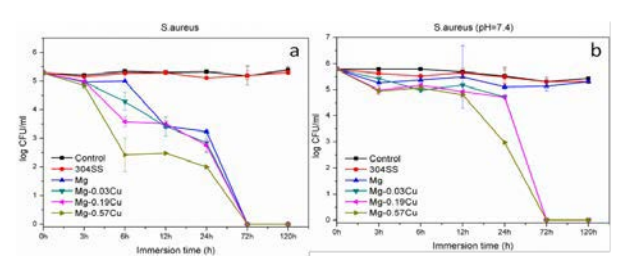


Fig. 1: Colony-forming unit/mL of S. aureus for various intervals under normal pH values (a) and neutral pH value (pH = 7.4) (b).

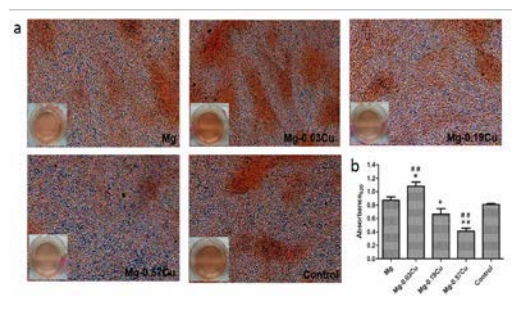


Fig. 2: The extracellular matrix mineralization of MC3T3-E1 cells after 15 days of incubation in the different extracts (a) and colorimetrically quantitative analysis (b).

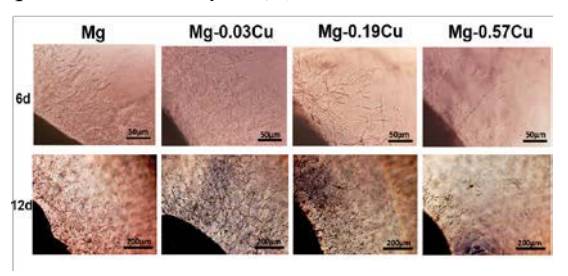


Fig. 3: Microvessel outgrowths arising from the edges of SD rat thoracic aortic rings embedded in rat tail collagen gels and cultured in the different extracts after 6 and 12 days of incubation.

**ACKNOWLEDGEMENTS:** This work was supported by National Basic Research Program of China (No. 2012CB619101)

#### Study on the preparation and properties of Mg/PLA composite for bone screw

J Ni<sup>1</sup>, C Zhao<sup>1</sup>, H Wu<sup>1</sup>, Y Chen<sup>1</sup>, W Chen<sup>1</sup>, F Zhang<sup>1</sup>, Q Xia<sup>1</sup>, S Zhang<sup>2</sup>, X Zhang<sup>1</sup>

School of Materials Science and Engineering, Shanghai Jiao Tong University, Shanghai, China.

Suzhou Origin Medical Technology Co. Ltd., Jiangsu 215513, China.

INTRODUCTION: Degradable poly lactide acid (PLA) has good biocompatibility [1]. Magnesium (Mg) with good biocompatibility and bioactivity is beneficial to the growth of bone cells [2]. As a composite phase, Mg can improve greatly the mechanical strength and biocompatibility of PLA and especially neutralize the local acid environment caused by degradation of PLA, reducing irritation to biological tissue [3]. This work aims to prepare Mg/PLA bone screws by blending dispersion-heat fusion method and to investigate their physicochemical and biological properties.

**METHODS:** Chloroform war poured separately into four dry beakers with 10 g PLA raw material. After full dissolution of PLA, 0 g, 0.2 g, 0.5 g, 1.0 g Mg powder were added into PLA-contained chloroform solution and were stirred for 30 min to dissolve fully. These four mixed solutions were exposed in air for 24 h for complete volatilization of chloroform. The Mg/PLA mixture with different Mg concentration were poured into the molds, and then heated to 170 °C and kept 20 min before cooling. Mg/PLA composite could be processed into the samples for next property tests.

The influence of Mg particles on the crystalline, molecular weight, mechanical performance of biodegradable PLA was investigated by XRD, EDX, DSC, bending test, respectively. The Mg/ALP composite was soaked into simulate body fluid (SBF) to study the in vitro degradation properties.

**RESULTS:** Homodisperse Mg/PLA composite with no obvious cracks and holes was successfully prepared by blending dispersion-heat fusion method (see Fig. 1a). XRD results confirmed there was no reaction between Mg powders and PLA, which kept their respective phases. DSC testing demonstrated that the crystallization degree of PLA was enhanced by Mg particles (see Fig. 1b). The bending properties of Mg/PLA composite were weakened by the addition of Mg particles compared with that of PLA, but the bending properties of Mg/PLA would rise with the increase of Mg content. Alkalinity derived from Mg degradation could neutralize the local acid

environment caused by ALP degradation. The increase of the Mg content was beneficial to the deposition of calcium and phosphorus. Furthermore, Mg particles could accelerate the degradation of PLA molecular weight and the fall range of molecular weight of PLA grew with the increase of Mg content.

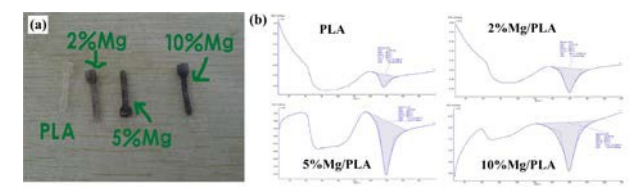


Fig. 1: (a) Bone screws of Mg/PLA composite prepared by blending dispersion-heat fusion method; (b) The DSC curves of PLA, 2% Mg/PLA, 5% Mg/PLA, 10% Mg/PLA.

DISCUSSION & CONCLUSIONS: In this work, the physicochemical and biological properties of Mg/PLA were studied. It was speculated that physical combination between Mg particles and ALP and stress concentration were the primary causes of the decline of Mg/ALP bending properties compared with that of ALP itself. The addition of Mg could improve the local acid environment and enhance the deposition of Ca and P, leading to better cell adhesion on Mg/ALP. We believe that degradable Mg/PLA composite has a good application prospect as orthopedics repair materials.

**ACKNOWLEDGEMENTS:** This work was supported by the National Natural Science Foundation of China (No. 51271117, No. 51401126) and Shanghai Committee of Science and Technology, China (No. 14441901800).

# Tailoring the bioactivity of AZ31 alloy by nanofibrous PCL/HA composite coatings for degradable metallic implant applications

T Hanas<sup>1,2</sup>, TS Sampath Kumar<sup>1</sup>

<sup>1</sup>Medical Materials Laboratory, IIT Madras, Chennai – 600036, India. <sup>2</sup> School of Nano Science and Technology, NIT Calicut, Calicut, Kerala- 673601, India.

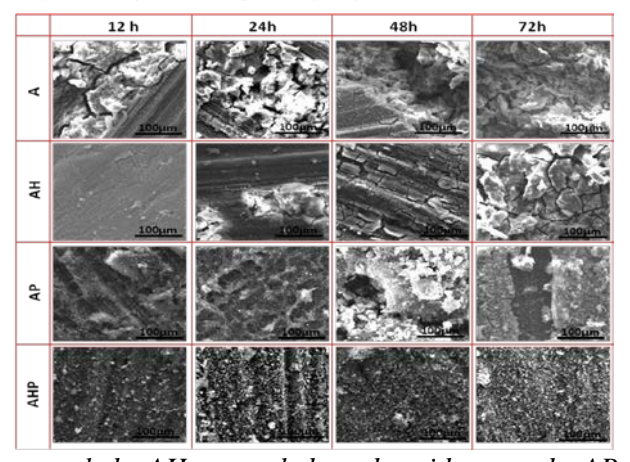
**INTRODUCTION:** Magnesium and its alloys are excellent choice for degradable metallic implant development as their mechanical properties are similar to that of human bone [1]. However, the high reactivity of magnesium in physiological environment result in faster degradation rate that needs to be controlled [2]. Surface modification treatments, protective coatings and metallurgical modifications [3] are some of the methods used to reduce the degradation rate. We have shown earlier that electrospun PCL coating can be adopted to control the degradation of magnesium<sup>4</sup>. In this work, the role of enhanced bioactivity to tailor the degradation was investigated bv polycaprolactone/hydroxyapatite (PCL/HA) composite fibers using electrospinning on the surface treated AZ31 alloy.

**METHODS:** Locally procured AZ31 alloy sheets were cut into 10 x10 x 2mm size samples, polished to 2000 grade and annealed at 340° C. Samples were then exposed to 1M HNO<sub>3</sub> treatment for controlled period [4] and subsequently coated with PCL/HA composite nanofibres with known wt.% of HA (prepared by wet chemical synthesis [5]) containing PCL solution (chloroform and methanol electrospinning technique. mixture) using Bioactivity and degradation studies of the coated samples were conducted by immersing the samples in supersaturated stimulated body fluids upto 3 days. Samples before and after immersions were well characterised using scanning electron microscopy (SEM), X-ray diffraction technique (XRD) and water contact angle measurements.

RESULTS: Microstructural and morphological analysis confirmed that the samples were uniformly coated with a PCL/HA composite mat of fibrous morphology with fibers of ~ 200 nm diameter. Contact angle measurements showed that PCL/HA coating is more hydrophilic compared to PCL coating. Surface morphology of the samples after the immersion tests is shown in Fig.1. Annealed samples indicates severe pitting corrosion during the immersion test compared to acid treated sample which was able to resist the initial degradation with a protective Mg(OH)<sub>2</sub> layer. However, with increase in immersion time, later sample showed cracks in the layer and

subsequent removal of the layers. All the composite coated samples were stable during the initial hours of immersion, but with increase in immersion time, the coating on the annealed samples developed cracks and peeled off from the surface. However, coating on the acid treated samples remained stable till 72 h of immersion test and also showed apatite layer formation with a Ca/P ratio varying from 1.6 to 1.7.

Fig. 1: Surface morphology after immersion test. A



annealed, AH annealed and acid treated, AP annealed and composite coated and AHP annealed, acid treated and composite coated.

**DISCUSSION & CONCLUSIONS:** The stability of the sample surface is an important factor for better tissue-implant interaction. The protective layer that has formed by acid treatment seems to protect of the surface during the initial hours of immersion. This stability assists in developing the apatite layer on the composite coated samples which further reduces the degradation rate<sup>3</sup>. Hence, HNO<sub>3</sub> surface treatment combined with the PCL/HA composite coating may be used to tailor the degradation of the Mg alloys.

#### Silane coatings for surface modification of magnesium alloy

S Agarwal<sup>1, 2</sup>, J Curtin<sup>2</sup>, B Duffy<sup>1</sup>, S Jaiswal<sup>1</sup>

<sup>1</sup>Centre for Research in Engineering and Surface Technology, FOCAS Institute, DIT, Ireland <sup>2</sup>School of Food Science and Environmental Health, Cathal Brugha Street, DIT, Ireland

INTRODUCTION: Biodegradable magnesium implants have been explored as potential alternative of permanent implants for orthopaedic applications due to high biocompatibility, mechanical property close to bone, no repeated surgeries and cost effective [1]. However, clinical use of Mg is deterred due to its rapid corrosion in physiological conditions, resulting in rapid pH change and evolution of subcutaneous cytotoxic H<sub>2</sub> gas. Silane coatings have been used as a protective coating for metals. Herein, multilayer MTES-TEOS and APTES sol-gel surface modification of Mg alloy have been employed as a potential corrosion resistant coating.

METHODS: WE43 Mg alloy disks (5mM thick and 12mm diameter) were polished 320 to 1200 grit SiC paper. The samples were ultrasonically cleaned, and immersed in 3N NaOH for 2h to generate surface OH groups. The different molar ratios of TEOS: MTES (MT 2:1) or APTES (2 molar fraction) silanes were prepared. The NaOH-activated Mg alloy substrates were dip coated sequentially in MTES-TEOS and APTES sols, and cured at 120°C for 1h at each step. The coatings were characterised by FTIR, FTA contact angle and SEM. All data are expressed as mean ±S.D.

**RESULTS:** In order to develop the corrosion resistant coatings, Mg-OH layer was treated with hydrolysed MTES-TEOS and APTES. The two layer coatings were prepared through siloxane bond which was confirmed by FTIR studies (Fig. 1). FTIR spectra show the peak around 1045 (Si-O) and 1127 cm<sup>-1</sup> (Si-O-Si). Subsequent coating with APTES shows new peak at 3296 cm<sup>-1</sup> (-NH<sub>2</sub> stretching) which are consisted with the reported literature [2-3].Contact angle measurements showed the influence of silane coatings on surface wettability. The bare Mg alloy exhibits contact angle of 41.65°±1.18. Treatment with NaOH  $22.78^{\circ} \pm 1.15$ . reduces contact angle to Incorporation of MTES-TEOS increases the hydrophobicity to 79.89°±2.63, whereas coating with APTES exhibits lower contact angle 64.62°±1.89. The surface morphology of coatings was examined by SEM (Fig.2). The image of

multi-layered MTES-TEOS-APTES (molar ratio; MTA 2:1:2) shows crack free coatings as compared to corresponding controls.

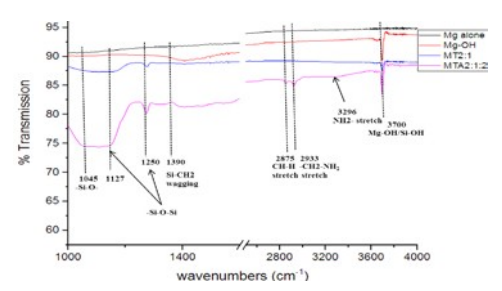


Fig.1: FTIR of Mg alloy surface modifications.

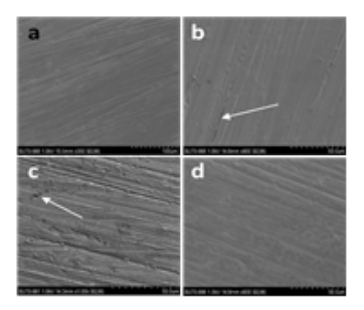


Fig.2: SEM images (a) Mg alloy (b) Mg-TEOS, (c) Mg-MTEOS and (d) (MTA 2:1:2) (Arrows showing cracks, scale bar-50 µm)

DISCUSSION & CONCLUSIONS: The FTIR and contact angle measurement studies indicate the functionalisation of silane coating on Mg alloy. The Mg-OH and Si-O-Si/Si-O- hydrophobic network could enhance the corrosion resistance to Mg alloy, whereas surface amine group could facilitate the functionalization with other polymers to increase the biocompatibility [3]. Hence, these newer surface modifications have potential to enhance the corrosion resistance of Mg alloy for orthopaedic applications.

**ACKNOWLEDGEMENTS:** DIT, Dublin, Ireland Fiosraigh scholarship program.

#### **Phase Diagrams:**

#### Which informations you can get from them for alloy and process design?

N Hort<sup>1</sup>, CL Mendis<sup>1</sup>, P Maier<sup>2</sup>

<sup>1</sup> Magnesium Innovation Centre, Helmholtz-Zentrum Geesthacht, Geesthacht, Germany <sup>2</sup> University of Applied Sciences Stralsund, Stralsund, Germany

**INTRODUCTION:** Melting and casting are the first steps in making a new alloy. Additionally, in numerous cases heat treatments and further processing (e.g. extrusion, rolling, forging etc.) are applied. In all cases, phase diagrams can be used.

A phase has its own chemical composition with its own set of physical, chemical and mechanical properties and is separated from other phases by a boundary region. Due to their own physical properties phases determine the property profile of materials with respect to their size and volume fraction. Phase diagrams describe the existence of phases with respect to temperature and composition at a constant pressure in equilibrium. However, phase diagrams are also useful under non-equilibrium conditions. They can be used to estimate phase transformations during solidification and also with respect to heat treatments. Which information can be obtained from a binary phase diagram will be exemplarily shown for the Mg-Gd system (fig. 1).

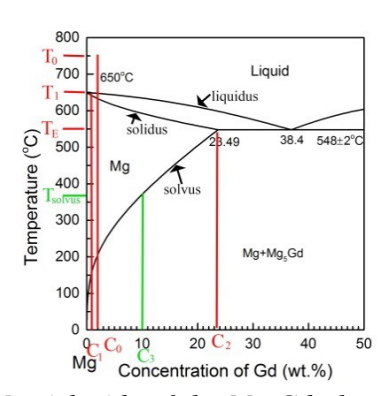


Fig. 1: Mg rich side of the Mg-Gd phase diagram (calculated with Pandat software)

**SOLIDIFICATION:** For a composition,  $C_0$  we can illustrate what happens during solidification. When cooling from a temperature  $T_0$  the liquidus line will be reached at temperature  $T_1$ . This is the temperature where a nucleus may form with the composition  $C_1$ . The composition of the newly formed grain follows the solidus line until full solidification at the eutectic temperature,  $T_E$ , with the composition  $C_2$ . At  $C_2$  the remaining liquid forms an eutectic structure via  $L\rightarrow\alpha$  (Mg)+ $\beta$  (Mg<sub>5</sub>Gd). Thus, all Mg-Gd alloys with a hypo-eutectic composition should contain  $\alpha$  (Mg) grains and eutectic

structures at the grain boundaries (fig. 2). And this is different from equilibrium conditions where the solubility of Gd in Mg is high enough and an eutectic structure would not appear. Additionally grains form with a composition in the centre ( $C_1$ ) that is different from the composition at the grain boundary ( $C_2$ ). This segregation can have a tremendous effect on properties and especially on corrosion behaviour; most  $\beta$  phases are nobler than the  $\alpha$  matrix, which causes anodic-cathodic coupling.

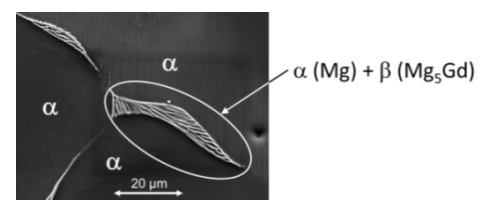


Fig. 2: Mg2Gd as cast:  $\alpha$  (Mg) grains and eutectic structure at grain boundary  $\alpha$  (Mg) +  $\beta$  ( $Mg_5Gd$ )

**HEAT TREATMENT:** As seen before, after casting an eutectic structure exists as well as concentration gradients. To get rid of both heat treatments should be applied. However, during heating the material would start melting at TE regardless composition. This limits the upper heat treatment temperature to temperatures lower than T<sub>E</sub>. Additionally the lower heat treating temperature must be above the solvus line at a temperature, T<sub>solvus</sub>, to dissolve the existing β phase. Therefore the range between  $T_{solvus}$  and  $T_E$  determines the temperatures for an initial solution heat treatment directly after casting (exemplarily shown for composition C<sub>3</sub>). If a solution heat treatment as already been undertaken, temperatures higher than T<sub>E</sub> can be applied to a material, which consists completely of the α matrix. However, it also has to take into regard that grain growth will occur at a time where all intermetallic phases have disappeared (Ostwald ripening).

**SUMMARY:** Phase diagrams contain information about the presence of phases with respect to composition and temperature. This information can be used to estimate properties and to design heat treatments.

#### Microstructure of as-cast and T4 heat-treated Mg2Gd-x(Ag,Ca) ternary alloys

Y. Lu<sup>1</sup>, Y. Huang<sup>1</sup>, F. Feyerabend<sup>1</sup>, R. Willumeit-Römer<sup>1</sup>, K. U. Kainer<sup>1</sup>, N. Hort<sup>1</sup>

<sup>1</sup>Institute of Materials Research, Helmholtz-Zentrum Geesthacht, Max-Planck-Strasse 1, 21502 Geesthacht, DE

INTRODUCTION: The previous work about Mg-xGd (x=0, 0.5, 1 and 2 wt%) alloys has shown that Mg2Gd alloy combines promising mechanical and corrosion properties for biomedical application. The addition of Ag was reported to improve the ductility and its ion Ag+ can prevent bacterial infections<sup>1</sup>. Ca can refine the microstructure of ascast Mg alloys, and improve their strength and plasticity. In this work, Mg2Gd alloy was modified with Ag or Ca elements. The microstructures of the as-cast and heat-treated ternary Mg2Gd-x(Ag,Ca) alloys were investigated to study the effects of T4 (solution treatment) on it.

**METHODS:** Four ternary alloys of Mg2Gd-xAg (x=1, 2 wt%), Mg2Gd-xCa (x=0.4, 0.8 wt%) were prepared by permanent mould casting<sup>1</sup>. For all the alloys, solution treatment was carried out at 510 °C for 48 h (T4) under Ar protective atmosphere and quenched in water at room temperature. The microstructure was investigated using optical microscope (OM), scanning electron microscope (SEM) and energy-dispersive X-ray spectroscopy (EDS). The specimens for OM were prepared by grinding with SiC waterproof abrasive paper, polishing with a lubricant containing 1 diamond particles and 0.05 µm colloidal silica (OPS), and etching in an etchant containing 30 ml deionized water, 140 ml ethanol, 7 ml glacial acetic acid and 8 g picric acid.

**RESULTS:** The optical and scanning electron micrographs of Mg2Gd-x(Ag,Ca) alloys in as-cast (F) and T4 heat-treated conditions are shown in Fig. 1, and Fig. 2, respectively.

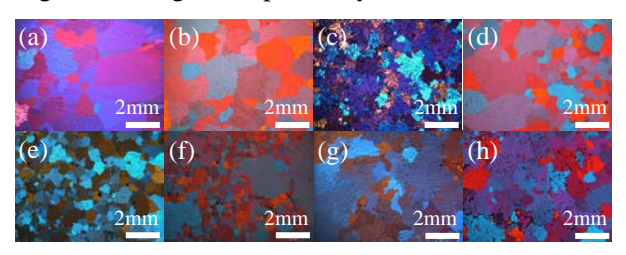


Fig. 1: Optical micrographs of as-cast Mg2Gd1Ag alloy (a) and after T4 (b), as-cast Mg2Gd2Ag alloy (c) and after T4 (d), as-cast Mg2Gd0.4Ca alloy (e) and after T4 (f), as-cast Mg2Gd0.8Ca alloy (g) and after T4 (h).

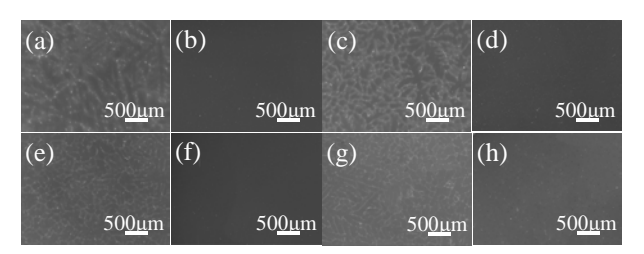


Fig. 2: Scanning electron micrographs of as-cast Mg2Gd1Ag alloy (a) and after T4 (b), as-cast Mg2Gd2Ag alloy (c) and after T4 (d), as-cast Mg2Gd0.4Ca alloy (e) and after T4 (f), as-cast Mg2Gd0.8Ca alloy (g) and after T4 (h).

As seen, all the alloys have a quite coarse grain. With more addition of Ca, the grain size becomes even larger. However, after alloying with 2 wt% Ag, the grain size is reduced. With more additions of Ag or Ca alloying elements, the volume fraction of the intermetallic phase (IMP) is increased. Due to the segregation, the alloys have a dendritic microstructure in as-cast condition. In contrast, after T4 heat treatment, the dendrites were eliminated and grain growth occurs.

**DISCUSSION** & **CONCLUSIONS:** The additions of Ag and Ca and T4 heat treatment alter the microstructures of the alloys. The amount of intermetallic phase is significantly decreased after T4 heat treatment, which means the IMPs were totally dissolved in the matrix.

**ACKNOWLEDGEMENTS:** This project is funded by the Helmholtz Virtual Institute VH-VI-523 (In vivo studies of biodegradable magnesium based implant materials).

#### Mg-Zn-Ca alloys processed by equal channel angular pressing

M Krystian<sup>1</sup>, M Bammer<sup>1</sup>, A Ostertag<sup>2</sup>, J Hofstetter<sup>3</sup>, S Beck<sup>4</sup>, B Mingler<sup>1</sup>

<sup>1</sup> Biomedical Systems, Health & Environment Department, AIT Austrian Institute of Technology GmbH, Wr. Neustadt, Austria <sup>2</sup> Kühr GmbH, Wr. Neudorf, Austria <sup>3</sup> Laboratory of Metal Physics and Technology, Department of Materials, ETH Zurich, Switzerland <sup>4</sup> Synthes GmbH, Oberdorf, Switzerland

INTRODUCTION: Our approach in developing new Mg alloys with highest biocompatibility for medical applications is to use only low amounts (< 1wt.%) of highly biocompatible alloying elements (i.e. Zn, Ca). These dilute alloys combine good mechanical properties with low degradation rates [1]. However, equal channel angular pressing (ECAP) offers the possibility to modify the microstructure of Mg alloys towards ultrafine grains with a more homogeneous grain size distribution as well as to further improve mainly the mechanical properties [2].

**METHODS:** Several Mg–Zn–Ca alloys in the form of cylindrical bolts (diameter: 12 or 20 mm, length: 90-100 mm) were processed with different ECAP dies having a channel intersection angle of  $90^{\circ}$  or  $120^{\circ}$ . Multiple passes with route B<sub>c</sub> ( $90^{\circ}$  rotation of the samples in the same direction after every pass) were applied. Starting usually at  $300^{\circ}$ C the temperature of the ECAP process was decreased stepwise after every pass.

Recently, a completely new ECAP die, specially designed for Mg alloys, was developed and manufactured. This new ECAP die consists of three channels with two different intersection angles (90° and 120°). Thus, it enables extremely high deformation per every single pass resulting in a significant reduction of the total number of passes. Currently first experiments with this new ECAP die are being carried out with promising results.

Alloys in two conditions (as extruded and after additional ECAP processing) were compared in terms of microstructure, mechanical (hardness, strength...) and degradation properties. The latter were measured electrochemically as well as with immersion tests using different buffers (TRIS,  $CO_2$ ).

**RESULTS:** Figure 1 shows the typical microstructure of ECAPed low-alloyed Mg. In contrast to the as extruded condition the grain size after ECAP is significantly smaller (down to < 1  $\mu$ m) and the grain size distribution is much more

homogeneous. This results in a huge increase in mechanical properties. For example, the hardness of low-alloyed Mg could be raised by ECAP from  $46 \text{ to } 75 \text{ HV}_{30}(+60\%)$ .

Measurements with different test setups showed that ECAP hardly influences the degradation rate of these alloys - both a minor decrease as well as a slight increase of the degradation rate were observed depending on the alloy composition as well as the ECAP parameters.

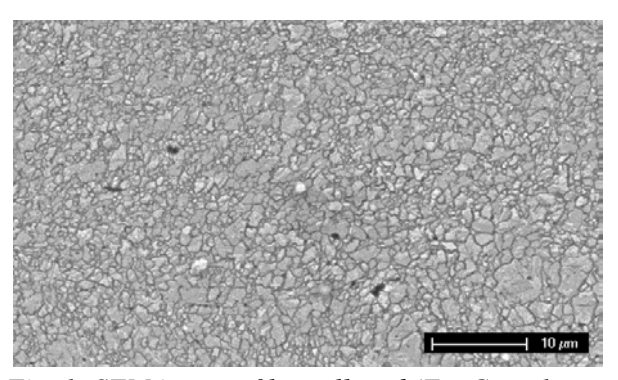


Fig. 1: SEM image of low-alloyed (Zn, Ca < 1 wt%) Mg - the microstructure consists of ultrafine grains with homogeneous grain size distribution.

DISCUSSION & CONCLUSIONS: ECAP is a powerful method to generate an ultrafine grained and homogenous structure in Mg alloys. This unique microstructure is the reason for improved mechanical properties like hardness and strength. ECAP has its biggest potential when applied to low-strength materials which makes it the ideal method to optimize low-alloyed Mg. With the new developed ECAP die it is expected to even surpass the results achieved to date. However, more work is needed to bring light upon the contradictory results regarding the impact of ECAP on the degradation rate.

**ACKNOWLEDGEMENTS:** The authors appreciate support via the K-project OptiBioMat, FFG – COMET program, Austria.

### Variations in degradation of ultrahigh-purity MgZnCa alloys by thermal treatment

JD Cao<sup>1</sup>, J Hofstetter<sup>1</sup>, M Cihova<sup>1</sup>, WW Trinh<sup>1</sup>, B Mingler<sup>2</sup>, PJ Uggowitzer<sup>1</sup>, JF Löffler<sup>1</sup>

<sup>1</sup> <u>Laboratory for Metal Physics and Technology</u>, Department of Materials, ETH Zurich, 8093

Zurich, Switzerland; <sup>2</sup> <u>Biomedical Systems</u>, Health & Environment Department, AIT Austrian Institute of Technology GmbH, 2700 Wr. Neustadt, Austria

**INTRODUCTION:** Mg-based alloys have the potential to be deployed as biodegradable implant material in a broad biomedical context. Slow and homogeneous degradation is required to allow for sufficient stability of the temporary implant, whereas the ability to tune the degradation rate is desired to accommodate for varying implant geometries. We thus investigate in this study the potential of further improving the properties of ultrahigh-purity (XHP) Mg-1.0Zn-0.3Ca (ZX10) [1] for biodegradable implant applications.

In the Mg-Zn-Ca system, intermetallic particles (IMPs) are formed whose electrochemical properties differ from the Mg matrix [2]. By modifying the type of the IMPs the degradation rate of ZX10 can be modified. Since the presence and type of IMPs is dependent on the applied heat treatments, here we studied their formation as a function of annealing temperature based on simulations using MatCalc with the new database mc\_mg\_v1.09. It was the aim of this study to confirm solvus temperatures above which IMPs dissolve and to verify their effect on alloy degradation.

**METHODS:** Extruded cylindrical rods of XHP ZX10 were cut and heat-treated at 325, 350, 375, 400 and 425°C in environmental atmosphere. The required time of heat treatment for achieving nearequilibrium was determined to be 1 h for 375°C and calculated for all other temperatures under consideration of equal thermal load. The types of IMPs formed were analysed using transmission electron microscope (TEM). The resultant grain sizes as a function of heat-treatment temperature were determined using metallography. The biodegradation of the annealed samples was tested by immersion in TRIS-buffered simulated body fluid (SBF) at 37°C. Evaluation of degradation was based on the hydrogen (H<sub>2</sub>) evolution method [3].

**RESULTS:** Energy dispersive x-ray spectroscopy (EDX) elemental mapping using TEM illustrated the presence and types of IMPs at different annealing temperatures. As predicted from thermodynamic calculations, a change of IMPs was detected and critical temperatures fit the

predictions with good accuracy. Furthermore, the solvus temperature for complete dissolution of IMPs predicted by MatCalc was validated via microstructural analysis (Fig. 1): a sudden increase of grain size at an annealing temperature of 400°C supports the expected absence of IMPs, which are assumed to act as barrier to grain growth [4].

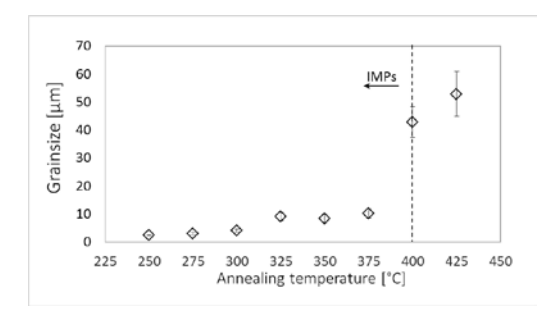


Fig. 1: Dependence of grain size on the annealing temperature; dashed line: temperature for complete IMPs' dissolution according to MatCalc.

Finally, biodegradation studies in SBF revealed the slowest degradation for XHP ZX10 alloys which contain no IMPs and fastest degradation for ZX10 with the more noble Zn-rich ternary IMPs. Thus, it is shown here that XHP ZX10 degradation can be modified by appropriate heat treatment.

**DISCUSSION & CONCLUSIONS:** In this study we experimentally confirmed the predicted critical temperatures influencing the presence and types of IMPs within XHP ZX10. Preliminary degradation studies showed the great promise of heat treatment to modify the degradation rate in XHP ZX10.

**ACKNOWLEDGEMENTS:** The authors appreciate support by the SNF Grant No. 200021-157058 and by the K-project OptiBioMat, FFG – COMET program, Austria.

# In situ synchrotron radiation diffraction during solidification of Mg4Y2Nd and Mg4Y2Ag1Nd alloys

G Szakács, CL Mendis, B Wiese, D Tolnai, A Stark, KU Kainer, N Hort Institute of Materials Research, Helmholtz-Zentrum Geesthacht, Germany

**INTRODUCTION:** Mg-RE alloys are potential candidates to be used as degradable implants [1]. The addition of Ag provides antibacterial properties to the implant material [2]. Casting plays an important role in the production of these alloys, since the microstructure, and consequently, the macroscopic properties are determined during solidification. *In situ* synchrotron radiation diffraction is a unique tool to follow the evolution of various phases. This contribution reports the findings from the solidification of Mg4Y2Nd and Mg4Y2Ag1Nd.

MATERIAL & METHODS: Samples for the solidification experiments were cut from as-cast ingots and placed in stainless steel crucibles. The solidification experiments were conducted with a cooling rate of 10 K/min at the BW2 beamline of HASYLAB at DESY. The beam energy was set to 100 keV, the acquisition time was 25 s. The measurement was performed in the chamber of a DIL 805A/D dilatometer in Ar flow [3]. The microstructures of the alloys were examined with a Carl Zeiss Gemini Ultra 55 Scanning Electron Microscope attached with an EDAX energy dispersive X-ray spectrometer (EDXS).

**RESULTS & DISCUSSION:** The line profiles from the azimuthal integration of the 2D diffraction patterns acquired during the solidification experiments are shown in Figure 1. The solidification of both alloys starts with the nucleation of the  $\alpha$ -Mg phase followed by the formation of  $Mg_{24}Y_5$ . This correlated with the thermodynamic calculations using Scheil model. In the case of Mg4Y2Nd the solidification is complete at 550 °C with the formation of Mg<sub>41</sub>Nd<sub>5</sub> or Mg<sub>12</sub>Nd. The thermodynamic calculation predicts the formation of Mg<sub>41</sub>Nd<sub>5</sub> at 523 °C. In the Mg4Y2Ag1Nd alloy in addition to Mg<sub>24</sub>Y<sub>5</sub> phase Mg<sub>2</sub>NdAg phase was observed. However, the Mg41Nd5 and phases predicted with thermodynamic software were not observed. The SEM analysis of the investigated alloy shows the presence of two different intermetallic particles. The EDXS analysis of the phases suggests that one phase contains Mg, Nd and Ag the other Mg and Y corresponding to Mg<sub>2</sub>NdAg and Mg<sub>24</sub>Y<sub>5</sub> phases.

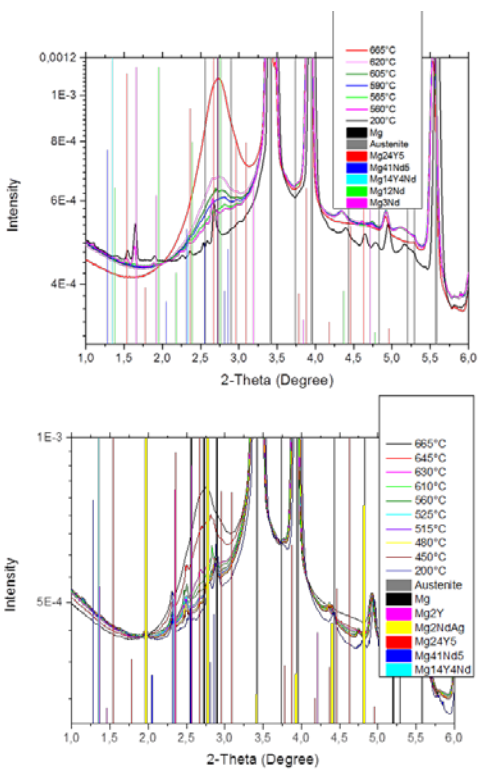


Fig. 1: XRD line diagrams acquired during solidification of Mg4Y2Nd (a) and Mg4Y2Ag1Nd (b)

**CONCLUSIONS:** *In situ* synchrotron radiation diffraction during solidification was performed on two Mg alloys and the experimental results were correlated with thermodynamic calculations. The formation of the ternary Mg<sub>2</sub>NdAg phase cannot be predicted by thermodynamic calculations. Thus, the applied technique can provide a new approach to revise or explore the phase evolution during solidification.

**ACKNOWLEDGEMENTS:** The authors acknowledge the DESY for the provision of synchrotron radiation facilities in the framework of the proposal II-20100225, and the European Union FP7-PEOPLE-ITN-2011 program under REA Grant Agreement No 289163: MagnIM project for the financial support.

#### Can defects improve properties of metallic biomaterial?

B Wiese, CL Mendis, KU Kainer, N Hort

<u>Magnesium Innovation Centre</u>, Helmholtz-Zentrum Geesthacht, Geesthacht, Germany

**INTRODUCTION:** Every metal contain a significant amount of defects within the microstructure. These defects have an effect on the mechanical and corrosion properties of a metal. Tailoring the profile of properties of metallic biomaterial is important for different applications, e.g., for cortical implants or vascular stents. The field of materials development offers a wide range of techniques to adjust the required properties for a given application.

The defects in metallic materials can be used to tailor the mechanical and corrosion properties. Three different groups of defects will be illustrated in connection with their impact on the properties of materials. The groups of defects are ordered according to the geometries of defects which are 0D, 1D and 2D (dimensional) [1]. These groups have different reasons and impacts on the overall properties of metallic materials (Table 1).

Table 1. Dimension (D) of the defects with type of defects of the group and the process or reason, which generated this type of defects [1].

D	<u>Defects</u>	Process/Reason	
	vacancy, an	alloying, impurities,	
0	interstitial defect	solidification, heat	
U	or substitution	treatment and	
	atom	radiation	
1	dislocations	deformation	
1	distocations	rapid solidification	
2	grain boundaries, phases boundaries, stacking fault and twinning	solidification, heat treatment, deformation and recrystallization	

Every defect has an impact on the properties of material. In alloy more than one defect type is used to increase the strengths of the material. However, every property is affected by these defects, such as corrosion, ductility etc. This talk will introduce the types of defect and how the production processes influence the prevalence of such defects, will be demonstrated using the examples from Mg alloys.

**DEFECTS; THERE REASONS AND IMPACTS:** 0D defects are point defects, which occur only at or around a single crystal structure

point. A typical 0D defect in the crystal structure is a vacancy (missing atoms), an interstitial defect (in the general crystal structure) or substitution atom (with larger or smaller atoms). 0D defects increased the thermodynamic free energy of the metal. A 0D defect arises from an alloying element, under radiation and during rapid cooling from the melt.

1D defects are line defects, which occur after a deformation in a crystal structure. 1D defects are dislocations from deformation, e.g., from extrusion, rolling or bending. These can be defined as edge dislocation, screw dislocation and mixed dislocations combining aspects of both types. A 1D defect arises from an external force together with a movement of the atomic plains or by a defect.

2D defects are planar defects, which are not defects with the crystal. These defects occur due to mismatch between two crystals and occur at the interfaces, as grain boundaries, phase boundaries, stacking fault and at twins. These defects occur in with grain growth during solidification or recrystallization. Twins form during deformation of a crystal with a low number of slip systems, e.g. Mg. Twins can also occur during recrystallization.

All defects block the dislocations movement and increase the force to move new dislocation through the crystal. This increase the yield strength and hardness but reduce the deformability; heat and electrical resistances. Only the grain boundaries and in some particular cases twin boundaries increased the yield strength and deformability concurrently. The corrosion rate is correlated with the defects, as defects change a perfect crystal. However, a larger density of defects increases the corrosion rate in general.

**CONCLUSIONS:** The defects can not only improve properties of metallic biomaterial, they are an effective way to tailor them. However, the influence of defects on mechanical properties and corrosion has to be balanced for any application.

#### Planar defects in magnesium alloys

B Smola, I Stulíková, T Kekule, M Vlach

Faculty of Mathematics and Physics, Charles University, Prague, Czech Republic

**INTRODUCTION:** Metastable phases in form of planar defects are responsible for the top strength in many Mg alloys, especially with rare earth elements (RE) (Y included) [1] and affect their corrosion. Orientation of these defects in the α-Mg matrix determines strictly their hardening effect. Peak hardening in Mg-RE alloys is reached by dense triangular arrangement of prismatic plates, whereas basal plates have only a moderate effect on basal dislocations slip. The Zn addition in the alloys leads to a decrease of stacking fault (SF) energy and consequently to formation of variety of thin basal planar defects [1]. Moreover, Zn addition was proved to favourably influence corrosion and biocompatibility of some of these alloys (e.g. Mg2Y1Zn in wt. % [2]).

METHODS: Mg4Y (WZM411), Mg3Y2Nd (WEZM3211) alloys with 1Zn and 1Mn and Mg2Y (WZ21), Mg2Y1Nd (WEZ211) alloys with 1Zn addition respectively were squeeze cast in Ar + 1% SF<sub>6</sub> atmosphere. The last two alloys were also gas atomized in Ar+1%O<sub>2</sub>. Powder was sieved and consolidated by hot extrusion (PM). Microstructures and their development by heat treatment are compared to alloys properties (see [3] for all methods details).

**RESULTS:** : Grain size of as cast alloys is in the range of 50 - 90 µm. Grain boundaries are decorated by grain boundary eutectic phase rich in Nd and/or Y with exception of WZ21 alloy. Addition of Nd depresses formation of the LPSO 18R particles. Individual very thin basal plates with SFs image attributes ( $\gamma$ ' or  $\gamma$  phase of the Mg-Y-Zn sequence) are present in grain interiors of all alloys. Step by step annealing up to  $\sim 620 \text{ K} - 660$ K corresponds to the highest α-Mg purification in all cast alloys. Moderate hardening due to this annealing is observed only in the WEZM3211 alloy where  $\gamma$ " plates of the Mg-Nd-Zn sequence develop together with prismatic plates of the stable β phase (Fig. 1). Almost no strengthening was detected in other heat treated alloys, because the only microstructure change is an increased number density of the  $\gamma$ ' planar features. The bulk LPSO 18R phase transforms into 14H type (stable y phase) in both annealed alloys without Nd.

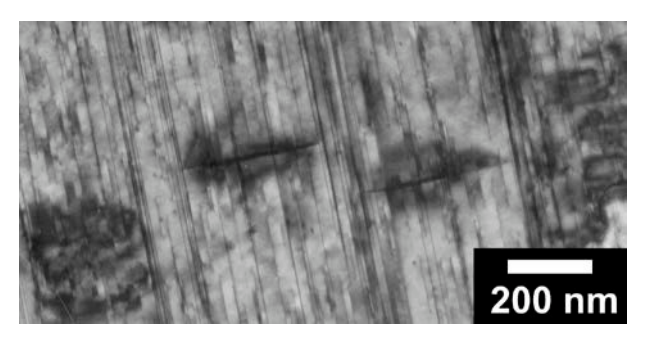


Fig. 1: TEM image of  $\gamma$ ' basal plates and  $\beta$  phase prismatic plates in WEZM3211 alloy at 633 K.

Neither LPSO nor planar defects of metastable phases were detected in both PM produced alloys. Dynamically recovered grains of  $\sim 2~\mu m$  and well developed dislocation substructure forming subgrains of  $\sim 300~nm$  size are typical features of as prepared PM alloys. Boundary regions are decorated by particles rich in RE and Zn. Hardness of PM alloys ( $\sim 80~HV0.5$ ) is about 50% higher than in cast alloys due to Hall-Petch effect and is extremely stable up to  $\sim 650~K$ .

Corrosion measured by polarisation resistance in aerated physiological solution at 37°C proceeded preferentially along basal planar defects and is therefore lower in both PM alloys. The Nd addition deteriorates corrosion resistance in all alloys. Lower corrosion was observed in alloys with lower RE content.

**CONCLUSIONS:** Basal planar defects have only moderate effect on hardness but enhance corrosion. Both basal and prismatic plates can be developed simultaneously by annealing of the WEZM3211 alloy. Higher RE content decreases corrosion resistance. Corrosion resistance is improved in PM alloys.

**ACKNOWLEDGEMENT:** Research leading to these results has received funding from the People Programme (Marie Curie Actions) of the European Union's Seventh Framework Programme FP7/2007-2013/ under REA grant agreement No. 289163.

#### Investment casting of biodegradable Mg-Ca-Zn alloys

NA Zumdick<sup>1</sup>, SF Fischer<sup>2</sup>, P Weiß<sup>2</sup>, A Bührig-Polaczek<sup>2</sup>, D Zander<sup>1</sup>

<sup>1</sup> <u>Chair of Corrosion and Corrosion Protection,</u> RWTH Aachen, Germany <sup>2</sup> <u>Foundry Institute,</u> RWTH Aachen, Germany

**INTRODUCTION:** Biodegradable magnesium is currently applied as screws for bone fixation or as tubular, grid-type coronary stents <sup>1</sup>. Both devices are produced using ingot casting and subsequent machining. An alternative and cost-effective manufacturing method utilized in order to create filigree structures with high geometric freedom is investment casting, with possible products including meshes or foams that serve as a bone scaffolds or as textured plates for bone fixation.

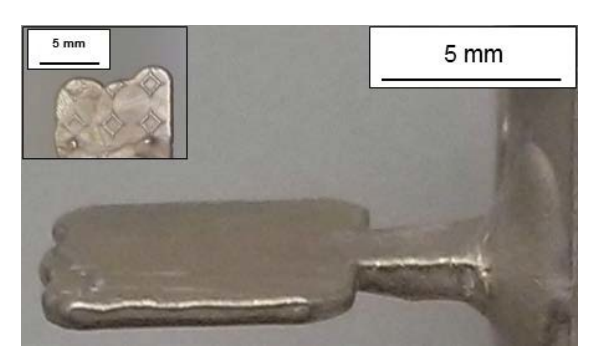
During investment casting, the melt is poured into a ceramic shell or a gypsum-based mould. Up to today, the investment casting process has been established for a broad range of materials and is used to produce components with extremely fine structures, such as open-cell aluminium foams with a strut thickness in the range of hundreds micrometres<sup>2</sup>. Nonetheless, the investment casting of magnesium remains a major challenge due to the critical combination of a high reactivity of magnesium together with a large surface area. The aim of this work is to investigate the feasibility of adapting the established investment casting procedures of aluminium to magnesium in order to produce mesh-shaped or foam structures. In a further step, the influence of surface quality (e.g. casting skin) on the in-vitro corrosion performance is evaluated.

**METHODS:** A wax-model, consisting of an ingate with two different sample geometries, was assembled. In order to produce the mould, the wax model was placed in a cuvette and recast by the gypsum based moulding material that consisted of SiO<sub>2</sub>, CaO and SO<sub>3</sub> (Goldstarpowders, UK). By firing, the wax was extracted from the mould; the mould dried and increased in strength. Prior to casting, the mould was heated to 350°C and flooded with argon. The melt was cast at 720°C. Subsequently, the microstructure and the boundary layer were investigated via optical light microscopy and SEM with EDX.

**RESULTS:** Plates with and without a surface texture with the dimensions 12x12x1.5 mm were produced by investment casting, as presented in Fig. 1. The microstructural analysis showed a homogeneous microstructure with minimal porosity. Fig. 2 shows a nm thick surface layer that was observed via SEM. This layer contained traces

of Si, Ca and S that resulted from the contact of the liquid melt with the mould material.

Fig. 1: Macroscopic image of the plates with and



without texture

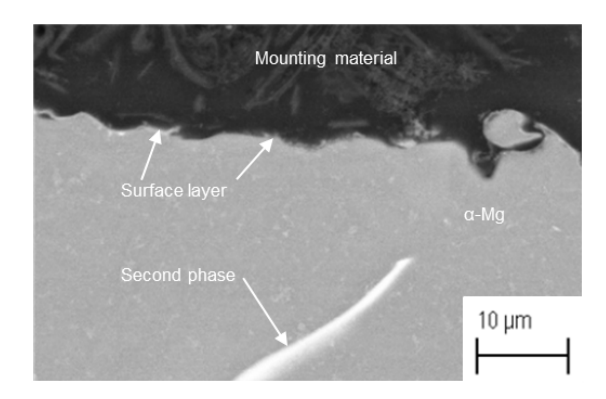


Fig. 2: SEM image of the cross-section showing a thin surface layer

DISCUSSION & CONCLUSIONS: Investment casting was evaluated and confirmed as a valid alternative for producing fine structured magnesium components. The utilized mould material and process parameters are valid for producing smooth and textured plates by investment casting. Further modification of experimental parameters and of the moulding material composition is required in order to achieve finer structures.

**ACKNOWLEDGEMENTS:** The authors would like to thank Ingo Braun, Martina Thönnißen and Tatiana Kutz for assistance.

# Effect of composition on the microstructure and properties of candidate Mg-Si-Sr alloys for resorbable material applications

A Gil-Santos<sup>1</sup>, G Szakacs<sup>2</sup>, I Marco<sup>1</sup>, N Moelans<sup>1</sup>, N Hort<sup>2</sup>, O Van der Biest<sup>1</sup>

Department of Materials Engineering, KU Leuven, Leuven, Belgium. Magnesium Innovation Centre (MagIC), Geesthacht, Germany

**INTRODUCTION:** Mg base alloys with Si and Sr as alloy elements have been investigated for their use in bioresorbable applications. Several compositions in the Mg rich corner of the ternary system (Table 1) were produced and analyzed. From the characterization of their as cast microstructure the presence of ternary phases and other intermetallics has been determined and quantified based on SEM-EDX, EPMA, image analysis and XRD measurements.

Table 1. Phase percentage estimated by image analysis (ImageJ software) for the different compositions

	Quantification of intermetallic phases				
Alloy wt %	wt%	wt%	wt%	wt%	
	$Mg_2Si$	$Mg_{17}Sr_2$	MgSrSi <sub>2</sub>	MgSrSi	
Mg 0.38Si 0.51Sr		3.12	1.09	2.38	
Mg 0.47Si 0.26Sr	2.16		6.63		
Mg 0.13Si 0.27Sr		6.02		1.32	
Mg 0.29Si 0.24Sr		4.35		0.96	
Mg 0.14Si 0.07Sr			4.16		

**METHODS:** All the alloys were prepared by permanent mold gravity casting using a steel crucible and commercial high purity raw materials. Compression tests and Vickers hardness measurements were done in order to correlate the microstructures with the mechanical behavior. Also the degradation performance has been evaluated by both polarization experiments in PBS with rotating disc electrode (RDE) and immersion test in DMEM (with 10 vol.% fetal bovine serum in 5 vol.% CO<sub>2</sub>) by mass loss.

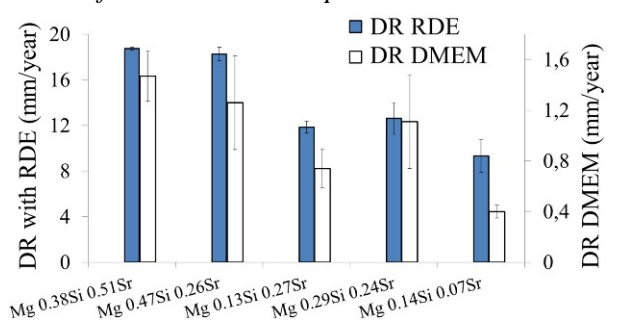
**RESULTS:** The presence of the binary phases Mg<sub>17</sub>Sr<sub>2</sub> and Mg<sub>2</sub>Si appear to be related with higher hardness and compressive strength values (Table 2). While higher amounts of Mg<sub>17</sub>Sr<sub>2</sub> cause an increase in the ultimate deformation values, the presence of Mg<sub>2</sub>Si can be related with low ductility. This intermetallic has been described before as a brittle phase at low temperature[1]. The presence of the ternary compounds MgSrSi and MgSrSi<sub>2</sub> appears to generate higher values for hardness and compressive strength as well as a reduction in ductility. This can be stated for a big particles size (>2□m) but the opposite effect is happening for finer microstructures.

Table 2. Hardness and compression strengths for the studied compositions in the Mg-Si-Sr system

Alloy wt %	HV0.25	Compressive strenght MPa (0.2% strain)	% Compression at ultimate Comp. strenght
Mg 0.38Si 0.51Sr	$46.3 \pm 3.4$	$89.5 \pm 3.6$	$18.6 \pm 1.3$
Mg 0.47Si 0.26Sr	$45.0 \pm 2.3$	$72.5 \pm 1.9$	$16.0 \pm 0.5$
Mg 0.13Si 0.27Sr	$41.6 \pm 6.5$	$60.4 \pm 1.3$	$25.0 \pm 4.9$
Mg 0.29Si 0.24Sr	$36.8 \pm 3.3$	$57.1 \pm 2.3$	$24.4 \pm 2.8$
Mg 0.14Si 0.07Sr	$32.2 \pm 3.3$	$42.0 \pm 1.3$	$19.8 \pm 2.3$

In general, as shown in Table 3, this system shows a degradation rate (DR) under physiological conditions between 0.4 and 1.5 mm/year. By RDE proportional but higher DR values are obtained from 9.3 to 18.7 mm/year.

Table 3. DR for both RDE and immersion tests in DMEM for the studied compositions.



**DISCUSSION & CONCLUSIONS:** The presence of different ternary phases and binary intermetallics has been related with mechanical behavior of the alloys in the Mg-Si-Sr system. Different degradation test methods have been used to study the DR and they show a similar trend in the mentioned alloy compositions.

**ACKNOWLEDGEMENTS:** The research was supported by the PEOPLE programme (Marie Sklodowska-Curie Action) of the EU FP7 Programme FP7/ 2007-2013/ under REA grant agreement n289163.

### Effect of grain size, extrusion ratio and extrusion temperature on the texture development in Mg-xZr alloys (x=0~1 wt. %)

S Yarmolenko<sup>1</sup>, Z Xu<sup>1</sup>, R Kotoka<sup>1</sup>, S Neralla<sup>2</sup>, J Sankar<sup>1</sup>

<sup>1</sup>NSF-ERC Center for Revolutionizing Metallic Biomaterials, North Carolina A&T State University, Greensboro, NC USA. <sup>2</sup>Jet-Hot, Inc., Burlington, NC USA

INTRODUCTION: Extrusion of magnesium alloys typically leads to reduction of grain size and development of preferred orientation of grains (texture). However, extrusion of as-cast alloys having large grain sizes frequently does not allow receiving uniform grain size distribution. To evaluate the effect of grain size we studied extrusion of pure Mg with different grain size controlled by small amounts of Zr as grain nucleation agent.

**METHODS:** Mg-xZr alloys (x=0, 0.25, 0.5, 0.75 and 1.0 wt. %) were prepared from 99.95% Mg and Mg-30Zr master alloy. They were extruded at different extrusion ratios (ER) and extrusion temperatures (ET).

**RESULTS:** Texture sharpness values (MAX) for extruded Mg-Zr alloys were obtained using pole figures (PF) for 5 crystallographic planes (typical set is shown in Fig.1 for cross-section surface). Pure Mg with extremely big grains cannot develop strong texture after extrusion while pure Mg with grain size below 100 µm exhibit strong texture (MAX values increase, Fig. 1B). Fig. 2 shows effect of ER and ET on sharpness of texture. These observations indicate that properties of extruded alloys vary significantly depending on compressive stresses (related to ER) and temperature. Elevated processing temperatures also activate partial recrystallization of extruded material which can reduce texture strength of final alloy. Fig. 3 shows mechanical properties of Mg-Zr alloys at produced at different ER and ET.

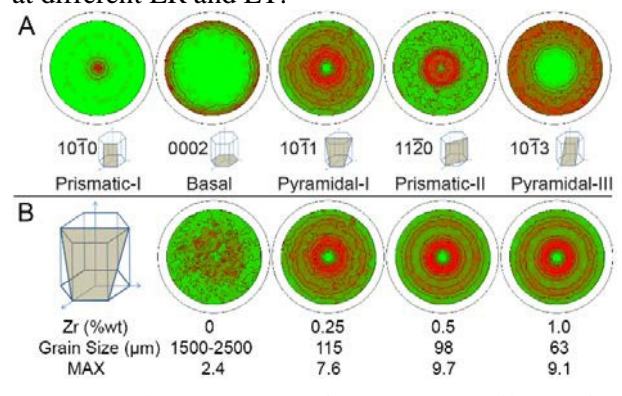


Fig. 1: Pole figures for different crystallographic planes of Mg-0.25Zr extruded at 300°C with ER 30 (A). Effect of Zr content on Mg grain size and texture sharpness after extrusion (B).

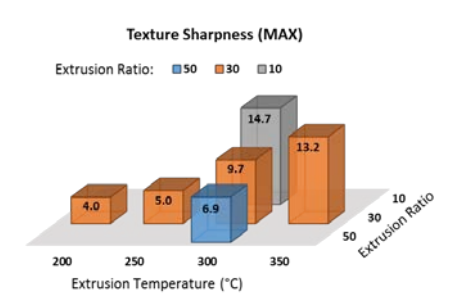


Fig. 2: Effect of ER and ET on MAX values.

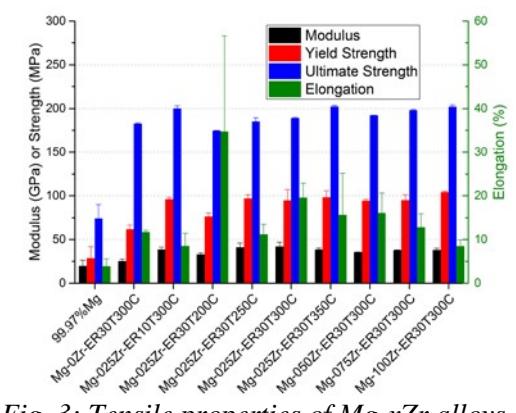


Fig. 3: Tensile properties of Mg-xZr alloys.

**DISCUSSION & CONCLUSIONS:** (a) Grain size reduction significantly improves strength of alloys (from 75 to 175 MPa). Fig. 4 shows additional improvements in mechanical properties due to texture. At similar grain size, ~20% of strength can be gained due to texture (from weak 2.5 to strong 14 MAX values). The maximum yield strength can be achieved only at MAX >5. (b) Best results from extrusion of Mg alloys can be achieved at initial grain size below 100 μm.

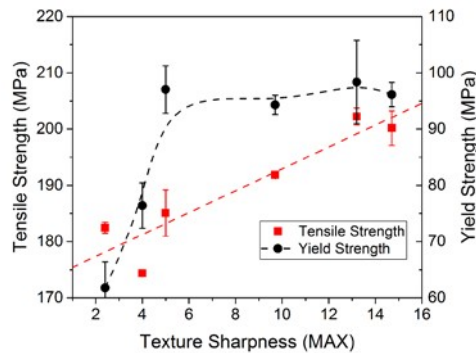


Fig. 4: Texture effect on strength of Mg-xZr alloys.

**ACKNOWLEDGEMENTS:** This work has been supported by NSF-ERC Center for Revolutionizing Metallic Biomaterials (EEC 0812348).

### Investigation of impurity levels of biodegradable Mg-materials and their influence on biocorrosion

M Wolff<sup>1</sup>, JG Schaper<sup>2</sup>, M Dahms<sup>2</sup>, N Rüder<sup>3</sup>, C Vogt<sup>4</sup>, T Ebel<sup>1</sup>, F Feyerabend<sup>1</sup>, R Willumeit-Römer<sup>1</sup>, T Klassen<sup>5</sup>

<sup>1</sup><u>Helmholtz-Zentrum Geesthacht</u> <sup>2</sup>University of Applied Sciences, FH Flensburg <sup>3</sup>Technical University Hamburg Harburg TUHH <sup>4</sup>Leibnitz Univ. Hannover <sup>5</sup>Helmut Schmidt Univ., Hamburg

**INTRODUCTION:** Recent Mg-based biometals research focusses on different magnesium alloys like Mg-Gd/Dy/Zn, Mg-Ag, Mg-Ca, or pure Mg. However, next to the influence of the chosen alloying elements on biodegradation, the impact of theirs impurity level on biocorrosion shall also be mentioned [1-2]. This impact can overlap the influence of the alloying elements. This may result in misinterpretations of chosen Mg alloys and can lead to wrong decisions in the future of Mgbiometals. To avoid this, full knowledge about the impurity level of used base materials and their impact on biocorrosion is essential for the total understanding of the biodegradation processes. This study gives an introduction how impurity levels of homogeneous PM-Mg-base materials (powder metallurgy) can be determined and how they influence biodegradation.

METHODS: Different pure Mg powders (SFM-Switzerland; ESM-SMT, USA; Geesthacht, Germany) and CA containing (Master Alloy Powder) (ZfW-Clausthal, Germany) were used. For the degradation testing DMEM + 10% FBS, the powders were pressed to cylinders of 4 mm diameter by applying 1200 MPa of surface pressure. In a second processing route, powders were also pressed at 100 MPa and subsequent sintered at 635-645 °C for 8-64h under Argon atmosphere in a hot wall furnace (Xerion, Germany)[3-4]. XRF, ICP-MS and (spark emission spectroscopy) were applied on untreated raw materials under compliance of clarity during sampling. For the determination of O and N levels, a LECO TC 436 was used. The microstructure was studied using light microscopy (Olympus PGM 3) and SEM, EDX (Zeiss DSM 962). Photoshop- and analySYS pro software as well as Archimedes method were used to investigate porosity and Young's moduli were density, respectively. determined by using resonant ultrasonic spectroscopy, (RFDA, IMCE, Belgium).

**RESULTS:** Pitting corrosion, as shown in fig.1, 2 (upper image), is the undesirable form of

biodegradation, leading to fast loss of load bearing capacity of the implant. Fe-particles, identified by EDX, are found on the bottom of pitting holes. ICP-MS and XRF analysis confirm 38ppm Fe and 8ppm Ni in the base material. Sintered specimens obtain a near dense condition (1.71 g/cm<sup>3</sup>) down to 2 % residual porosity.

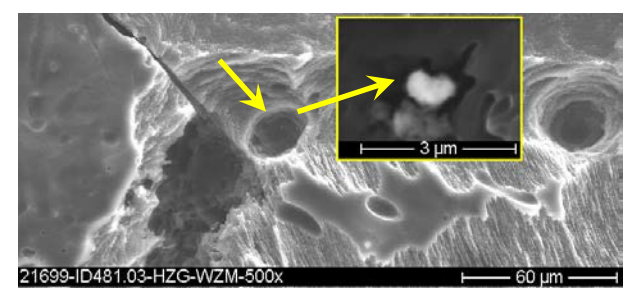


Fig. 1: SEM images of sintered and corroded surface of Mg-0.9Ca part showing pitting holes and Fe-particles (arrow).

**DISCUSSION & CONCLUSIONS**: Biodegradation of Mg is not influenced by choosing suitable alloying elements and amounts, only, it is also highly affected by tiny amounts of e.g. Fe, Ni and Cu, too. These elements lead to pitting corrosion as shown in fig. 2.





Fig. 2: Mg-0.9Ca: left: sintered and spark-eroded part; right: pitting corrosion after 7 days under cell culture conditions.

#### **Properties of deformed Mg-Gd alloys**

I Stulíková, B Smola, J Čížek, M Vlček, F Lukáč

Faculty of Mathematics and Physics, Charles University. Prague, Czech Republic

**INTRODUCTION:** Mg alloys generally suffer from their hexagonal structure resulting in low ductility at ambient temperature. Simultaneously a sufficient low deformation temperature is needed in production of final product shapes to prevent undesirable phase transformations deteriorating mechanical properties.

**MATERIALS:** Binary Mg-Gd alloys (up to 15 wt.%) were squeeze cast under a protective gas (Ar+1% SF<sub>6</sub>) and solution treated in an air furnace followed by quenching. A part of material was cold rolled to various reduction of thickness (up to 29%) and a part was severely deformed by high pressure torsion (HPT) at room temperature up to true strain  $\varepsilon = 7$  under high pressure of 6 GPa.

RESULTS: Solution treatment (ST) of Mg-9wt.%Gd resulted in a coarse grained and well annealed structure with ~ 150 µm grain size and microhardness value HV0.1 = 67. A uniform ultra fine grained structure (mean grain size ~ 100 nm) and a high density of dislocations uniformly distributed was observed in the HPT alloy – Fig.1 accompanied with extremely high HV0.1 value equal to 168. This value decreases to 120 during annealing at 80°C/20 min where internal stresses release. Tiny particles of  $\beta$ " and  $\beta$  phases [1] precipitate successively in both ST and HPT alloys during isochronal annealing leading to a slight precipitation hardening. Dislocation density of the HPT alloy decreases in the range 100°C-240°C, but grains do not grow until isochronal annealing to ~ 300°C - Fig.2. Whereas ductility of the ST alloy deformed in tensile test at strain rate of 10<sup>-3</sup> s<sup>-1</sup> <sup>1</sup> and 400°C is 45% and the test shows dynamic recrystallization features, superplastic character with elongation to fracture 580% was observed in the HPT alloy [2].

Decomposition in course of isochronal annealing in the supersaturated Mg-15wt.%Gd alloy proceeds gradually according to the sequence

SSSS 
$$\rightarrow \beta$$
" (D0<sub>19</sub>)  $\rightarrow \beta$ " (cbco)  $\rightarrow \beta$  (fcc) [1].

Prismatic plates of the c-based centred orthorhombic structure developed at 280°C step of annealing are the most effective barriers for dislocation motion and cause peak hardening effect (35%) [1].

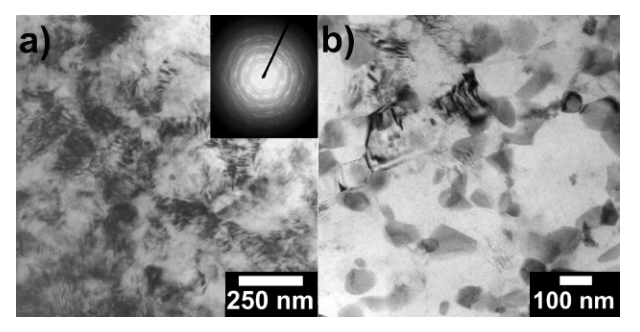


Fig. 1: Bright-field TEM image of HPT Mg9Gd alloy – a) as prepared, b) annealed up to 300°C

Deformation strengthening increasing with cold rolling deformation was measured in ST Mg-15wt.%Gd (HV0.1 increases about 25% after 29% thickness reduction) [3]. Precipitation of the  $\beta$ ' phase is responsible for the peak hardening again. The peak hardening temperature is about 40°C lower in the alloy cold rolled to 29%. It is due to an increase of nucleation sites concentration by introduction of dislocations and enhancement of diffusion of Gd atoms by pipe diffusion.

If both ST Mg-Gd alloys are hold at ambient temperature, natural aging appears leading to microhardness increase after 500 hours (Mg-9wt.%Gd) and 5 hours (Mg-15wt.%Gd) [4]. The increase is almost saturated after 200 hours in the latter alloy.

**CONCLUSIONS:** HPT increases significantly microhardness of ST Mg-9wt.%Gd. It deforms superplastically at 400°C. Cold rolling shifts peak hardening temperature to lower temperatures in ST Mg-15wt.%Gd. Natural aging occurs in both ST alloys.

ACKNOWLEDGEMENTS: The research leading to these results has received funding from the People Programme (Marie Curie Actions) of the European Union's Seventh Framework Programme FP7/2007-2013/ under REA grant agreement N° 289163.

#### Tensile and microstructural properties of annealed Mg10Gd-alloy wires

M Bartosch<sup>1</sup>, H Peters<sup>1</sup>, B Schmitt<sup>1</sup>, F Berger<sup>1</sup>, N Hort<sup>2</sup>, F Witte<sup>3</sup>

<sup>1</sup> Deutsches Herzzentrum Berlin, Germany. <sup>2</sup> Helmholtz-Zentrum Geesthacht. <sup>3</sup> Julius Wolff Institut, Charité. Berlin, Germany

**INTRODUCTION:** During the development of degradable magnesium-based implants, multiple alloying systems, manufacturing routes and post-treatments can be considered, making a preselection mandatory before the final implant can be tested in vivo. Bowen et al. suggested tensile testing of wires for initial selection [1]. Recently, our group presented a novel approach for in vivo degradation testing using a carrier stent with wires sewn on [2]. Combining both methods yields a reliable procedure for evaluating new degradable materials. Tensile tests narrow the initial selection and allow analysis of the remaining mechanical integrity after explantation. For stent applications, this represents the relevant parameter of corrosion.

An advanced setup for tensile testing of short wires was developed. Two drawing routes and different heat treatments were evaluated by analyzing the tensile and microstructural properties of wires (Mg10Gd, 0.4mm diameter).

**METHODS:** Mg10Gd wires were hand- (hd) or machine-drawn (md) to 0.4 mm diameter, followed by annealing (400°C or 450°C; 30, 60 or 90 minutes). Wires were cut to a length of 30 mm, cleaned and etched. A mould was designed for embedding both wire ends in cylinders fitting into custom-made fixtures for mounting on universal testing machines. Toothpicks stabilizing the wire during mould removal were embedded and cut after mounting in the fixtures (see figure 1).

**RESULTS:** The microstructure of the wires asdrawn showed elongated grains aligned in drawing direction. md-wires showed uniform grain size and distribution after heat treatment, whereas hd-wires had coarser grains along with more heterogeneous size distribution.

Elongation at break was between 11 % and 13.4 % for most annealed wires. The ultimate tensile strength (UTS) ranged from 150 MPa (hd) to 225 MPa (md).

**DISCUSSION & CONCLUSIONS:** Compared to the plastic deformation of the as-drawn wires (0.35 % hd, 0.7 % md), annealing lead to significantly improved plasticity. Mean values were similar for

all materials and annealing parameters with higher dispersion of the hd-wires (6.8 – 15.7 %). UTS was reduced from 217 MPa to 158 MPa (hd) and from 378 MPa to 228 MPa (md).

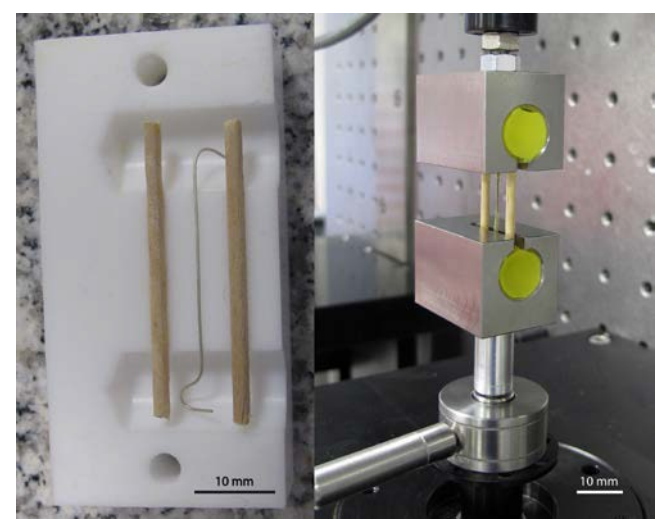


Fig. 1: Mould with wire and toothpicks. Test sample mounted in universal testing machine.

The large variations and slightly lower values of elongation for hd-wires along with the low tensile strength can be attributed to non-uniform drawing speed, variable lateral alignment and the relatively high number of intermediate annealing procedure after every two drawing steps.

Metallography showed a disturbed microstructure of 10-20 microns from the surface. Thus, the next step is the optimization of the pickling protocol followed by implantation using the carrier stent approach.

**ACKNOWLEDGEMENTS:** The authors thank Gert Wiese (Helmholtz-Zentrum Geesthacht) and Dag Wulsten (Julius Wolff Institut, Charité).

### Shape optimization for a biodegradable magnesium alloy stent using computer simulation

CX Chen<sup>1,2</sup>, W Wu<sup>2</sup>, F Migliavacca<sup>2</sup>, GY Yuan<sup>1</sup>, WJ Ding<sup>1</sup>

<sup>1</sup> National Engineering Research Center of Light Alloy Net Forming and State Key Laboratory of Metal Matrix Composite, Shanghai Jiao Tong University, Shanghai 200240. <sup>2</sup> Dept. of Chemistry, Materials and Chemical Engineering 'Giulio Natta', Politecnico di Milano, Milan, Italy.

**INTRODUCTION:** Compared to permanent stents, biodegradable magnesium alloy stents have inferior mechanical performance and show corrosion damage during their life when implanted. Optimization techniques based on finite element analysis (FEA) are efficient tools to improve the stent designs. In this study, some new stent optimization methods were developed via morphing the stent strut unit while conceding both creeping and dilation deformation.

METHODS: The stent material is as-annealed Mg-Nd-Zn-Zr tubes, fabricated in our previous work [1]. It has a modulus of 45GPa; yield strength of 123MPa and elongation of 26%. The middle surface of stent strut unit was modelled with 736 shell elements for 2D shape optimization. Boundary conditions and displacement loadings were applied to the 2D model in plane to simulate the crimping and expansion procedures. The shape morphing was controlled by algorithm based on global response surface method (GRSM).

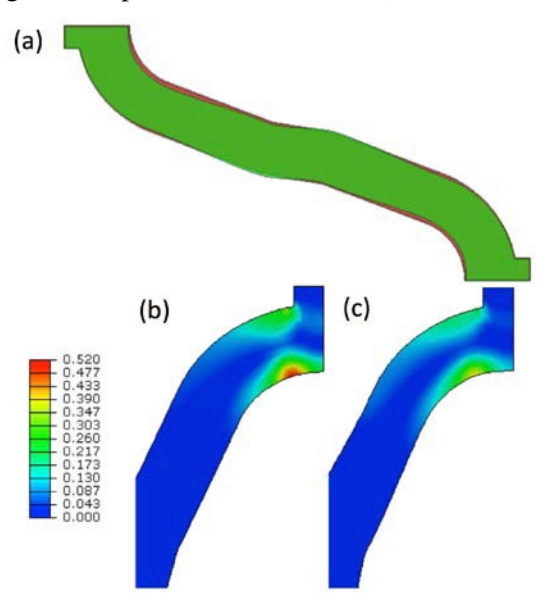


Fig. 1: (a) The overlap of stent shapes, red is the original, green is the optimized result of Type C; The PEEQ distribution of the 2D unit: (b) original design and (c) optimized result of Type C

Different responses were chosen as objectives for the optimization. Type A's objective was minimizing the Equivalent plastic strain at the end of crimping. Similarly Type B's was at the end of expansion and Type C's was considering both crimping and expansion. After optimization, 3D models were built and expanded into an arterial vessel to confirm the design's performances.

**RESULTS:** The shape and PEEQ distribution of the original strut unit and optimized results for Type C is shown in Fig.1. The mechanical performances of 3 cases of optimization are shown in Table 1. Type B performed best in Max Principle strain at the end of expansion. However Type A and Type C worked better for the stress and recoiling performances.

Table 1. Result summary of 3D model testing

	Type A	Type B	Type C
Max. Principle strain	0.184	0.174	0.182
Max. Mises stress after recoil (MPa)	218.8	231.7	201.6
Recoil with vessel (%)	5.71	6.15	6.17

**DISCUSSION & CONCLUSIONS:** In a previous shape optimization investigation for biodegradable magnesium stent [2], the expansion process and corrosion behaviour were always the main focus. Neglecting the crimping deformation some optimized solutions are not considered. Indeed, lower residual stresses might lead to lower corrosion speed and longer corrosion life. The crimping procedure is also a key factor in shape optimization for magnesium stent.

**ACKNOWLEDGEMENTS:** This work is supported by the National Key Technology R&D Program of China (2012BAI18B01). Wei Wu is supported by the PIF (Politecnico International Fellowship) grant.

#### Tailored Mg-Zn-Ca alloy for biomedical application

HJ Roh<sup>1,2</sup>, HS Han <sup>2</sup>, JW Lee<sup>4</sup>, HK Seok <sup>2,3</sup>, DH Kim <sup>1</sup>, YC Kim <sup>2,3</sup>

<sup>1</sup>Nano structural Material laboratory, Yonsei University, Korea. <sup>2</sup>Center for bio-materials, Korea Institute of Science and Technology, Korea. <sup>3</sup>Department of Bio-medical Engineering, University of Science & Technology, Korea. <sup>4</sup>Kookmin University, Korea

**INTRODUCTION:** Research on Mg-Zn-Ca alloy to develop new biomedical application has been increasing due to their excellent biocompatibility and outstanding mechanical properties. However, one of the main problems with current alloy system is low corrosion resistance accompanied by the precipitation hardening. According to recent studies, Mg<sub>6</sub>Ca<sub>2</sub>Zn<sub>3</sub> can act as a local corrosion barrier depending on its distribution and content. Moreover, Mg<sub>6</sub>Ca<sub>2</sub>Zn<sub>3</sub> can also significantly improve the mechanical properties of alloy system. Thus, the selective use of Mg<sub>6</sub>Ca<sub>2</sub>Zn<sub>3</sub> in alloy system may offer advantages in both mechanical and corrosion properties. Purpose of this study was to optimize the alloy composition of Mg-Zn-Ca alloy so that it only contains Mg<sub>6</sub>Ca<sub>2</sub>Zn<sub>3</sub> phase. To avoid formation of the other phases and reduce absolute volume of Mg<sub>6</sub>Ca<sub>2</sub>Zn<sub>3</sub>, 2 wt% Zinc and small varying addition of Calcium were used as alloying elements.

**METHODS:** The billets of 2Zn-xCa(x: 0, 0.1, 0.3 wt%) were prepared with high purity (99.9%) Mg, Ca and Zn. Prepared billets were then heat treated and extruded. For analysis of microstructure and evaluation of corrosion property, extruded alloys were cut into coin samples with a diameter of 8 mm and a thickness of 1 mm. SEM was used to observe microstructure and immersion test was conducted to measure the corrosion rate. Tensile test was conducted according to ASTM B557-10.

RESULTS: After solution heat-treatment, most of the Mg<sub>6</sub>Ca<sub>2</sub>Zn<sub>3</sub> of the as-casts samples were dissolve<sub>d</sub>i<sub>nto</sub> the matrix. However, Mg<sub>2</sub>Ca phase, which transformed from Mg<sub>6</sub>Ca<sub>2</sub>Zn<sub>3</sub> was observed in 0.3Ca samples. Extruded samples without Ca had no secondary phase and 0.1Ca (Fig1.a) had fine (~200nm) and well-dispersed Mg<sub>6</sub>Ca<sub>2</sub>Zn<sub>3</sub>. 0.3Ca (Fig1.b) had both coarse (~4um) Mg<sub>2</sub>Ca and Mg<sub>6</sub>Ca<sub>2</sub>Zn<sub>3</sub>. After immersed in hanks solution, 2Zn and 0.1Ca (Fig1.c) had uniform and thin corrosion layer. However, severe pitting corrosion was observed in 0.3Ca (Fig1.d). Fig.1e shows that mechanical property is in inverse ratio to the corrosion rate. It was interesting to observe the

drastic increase in toughness of 0.1Ca samples when its corrosion rate was similar to 2Zn.

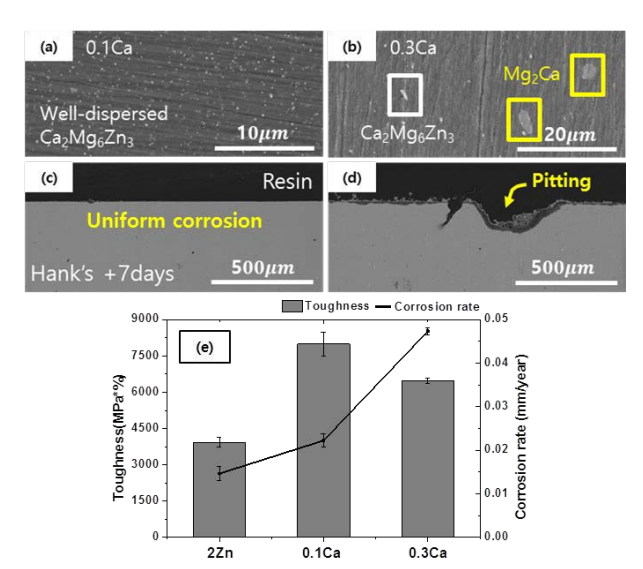


Fig. 1: Microstructure of Mg-Zn-Ca alloy with varying Ca quantity and cross sectional view after immersion in hanks solution.

**DISCUSSION & CONCLUSIONS:** Mg-2Zn alloy shows excellent corrosion resistance due to completely dissolved alloying elements in Mg matrix. However its low mechanical properties are not sufficient for application in load bearing implant materials. Formation of the coarse Mg<sub>2</sub>Ca in 0.3Ca significantly improved mechanical strength, which caused severe decrease in elongation and corrosion resistance. However, addition of 0.1 wt% Ca, resulted in fine and welldispersed Mg<sub>6</sub>Zn<sub>3</sub>Ca<sub>2</sub> phase and showed excellent corrosion properties without pitting corrosion. Also, it showed good mechanical when compared to the other two alloy system. The results from this study indicated that the Mg-2Zn-0.1Ca system showed most optimum mechanical and corrosion properties for Mg-Zn-Ca alloy system.

**ACKNOWLEDGEMENTS:** This research was supported by KIST Project (2E25260).

#### Heat treatment of Mg-Y-based alloys with addition of Ca or Ag

M Vlček<sup>1</sup>, F Lukáč<sup>1</sup>, I Stulíková<sup>1</sup>, B Smola<sup>1</sup>, H Kudrnová<sup>1</sup>, M Vlach<sup>1</sup>, V Kodetová<sup>1</sup>, G Szakács<sup>2</sup>, N Hort<sup>2</sup>

<sup>1</sup> <u>Faculty of Mathematics and Physics</u>, Charles University in Prague, Czech Republic. <sup>2</sup> <u>Institute</u> for Material Research, Helmholtz-Zentrum Geesthacht, Geesthacht, Germany

**INTRODUCTION:** Possibility to improve the quality of healthcare and to remove the necessity of second surgery brings attention to biodegradable magnesium implants. In this work we study novel Mg-Y-based alloys with addition of Ca or Ag envisaged for production of biodegradable implants.

**METHODS:** Samples of Mg-Y-based alloys with compositions Mg-4.1wt.%Y-1.1wt.%Ag (WQ41) and Mg-4.0wt.%Y-0.6wt.%Ca (WX40) were prepared by direct-chill casting under protective atmosphere. Solution treated samples were subjected to isochronal annealing with step 20°C/ 20 min. Isothermal annealing was used to determine annealing time for solution treatment and artificial aging. Each annealing step was finished by quenching into room-temperature water. Measurements of electrical resistivity were performed by DC four-point method at -196°C with relative accuracy of 10<sup>-4</sup>. Current reversal was used to suppress parasitic thermoelectromotive forces. Mechanical properties of samples were characterized by Vickers hardness HV0.5 which was measured on polished samples at room temperature. Microstructure of the samples was examined by optical metallography and scanning electron microscopy on Tescan MIRA I equipped with Bruker EDX analyzer.

**RESULTS:** As cast samples of WX40 alloy exhibit equiaxial grain with Ca rich eutectic along grain boundaries. On the other hand, as cast WO41 has dendritic structure with inhomogeneous distribution of solutes in the matrix. Solution treatment (T4) temperatures of 500°C and 525°C were selected for WX40 and WQ41 alloys, respectively. Electrical resistivity sharply increases at the beginning of solution treatment and then slowly converges to the final value. Hardness of the samples decreases during solution treatment as phases secondary dissolve. SEM performed after solution treatment testified that practically all particles of secondary phases have been dissolved and distribution of solute atoms becomes homogeneous. Measurements of hardness and electrical resistivity during isochronal

annealing were used to monitor precipitation processes in solution treated samples.

The WX40 alloy shows quite complex sequence of precipitation processes while the WQ41 exhibits only single precipitation process associated with minimum of electrical resistivity and increase of hardness at 160°C. Hardness measurement during isothermal annealing at temperatures 150°C, 200°C, 250°C for WX40 alloy and 125°C, 150°C, 200°C, 250°C for WQ41 alloy was used to determine heat treatment parameters for artificial aging (T6) shown in table 1. Effect of heat treatment on hardness of WX40 and WQ41 alloys is shown in table 2.

Table 1. Heat treatment parameters for studied alloys

	T4	T6
WX40	500°C/8 h	200°C/16 h
WO41	525°C/3 h	150°C/16 h

Table 2. Hardness of studied alloys

	As cast	<u>T4</u>	<u>T6</u>
WX40	$57.8 \pm 1.6$	$56.0 \pm 1.2$	$63.0 \pm 0.6$
WQ41	$57.5 \pm 1.2$	$49.2 \pm 1.2$	$58.7 \pm 0.9$

**DISCUSSION & CONCLUSIONS:** Although studied alloys exhibit lower hardness than commercial high-strength Mg alloys [1], low content of alloying elements is advantageous for medical applications. Concentration of solutes in matrix can be also adjusted by heat treatment which suggests possibility to adjust the corrosion rate.

ACKNOWLEDGEMENTS: The research leading to these results has received funding from the People Programme (Marie Curie Actions) of the European Union's Seventh Framework programme FP7/2007-2013/ under REA grant agreement N° 289163.

### Influence of solid-solution treatment on microstructure, mechanical property and corrosion behaviour of biodegradable Mg-Zn-Ca alloy

XN Ly, S Yang

School of Materials Science and Engineering, Nanjing University of Science and Technology, Nanjing 210094, China

INTRODUCTION: Magnesium with a low density, the elastic modulus closest to that of the human bone than other traditional metallic alloys. In addition, magnesium is biodegradable, making it an ideal biological metallic material. However, magnesium in physiological environment have high degradation rate and insufficient mechanical properties that limit its applications [1-2]. In the research, Mg-Zn-Ca alloys with different Ca content were prepared, and then studies the influence of solid-solution treatment on mechanical property and corrosion behaviour of magnesium alloy.

**METHODS:** The magnesium alloy were prepared from pure magnesium (99.95%), pure zinc (99.99%) and Mg-30%Ca intermediate alloy (mass fraction) through smelting in a graphite crucible in a resistance furnace protected by flux. The melt was held at 720°C for 10 min and casted at 690°C into a steel mold. The final composition of alloys is given in Table 1. The sample were cut from the ascast ingot to solid-solution treatment, which were carried out at 445°C for 12h in the air with protected by carbon powders, and then cooled in water at room temperature.

Table 1. Chemical composition of the magnesium alloys in wt.%

Alloy	Mg	Zn	<u>Ca</u>
Ι	Re	6.52	0.46
II	Re	5.62	0.98
III	Re	5.46	1.90

Mechanical properties was tested on electronic universal testing machine, corrosion behaviour were conducted by polarization and immersion testing in Hank's solution at 37°C.

**RESULTS:** After solid solution treatment, the microstructure of magnesium alloys had significantly changed, a large number of the second phase ( $Ca_2Mg_6Zn_3$ ,  $Mg_2Ca$ ) dissolved into the  $\alpha$ -Mg matrix reached a supersaturated state and grains size is bigger than before; the mechanical properties are obviously improved, especially the tensile strength of 0.5wt.% Ca content of Mg alloy

reached 220MPa and the ductility reached 16.6%. Compared with as-cast sample, the corrosion potential after solid solution treatment slightly shifted positive, but the corrosion current density is significantly decreased with the increase of Ca. With the increase of immersion time, the corrosion rate of Mg alloys after solid-solution treatment is increased. The surface morphologies of alloy I after cleaning the corrosion product are shown in Fig.1.

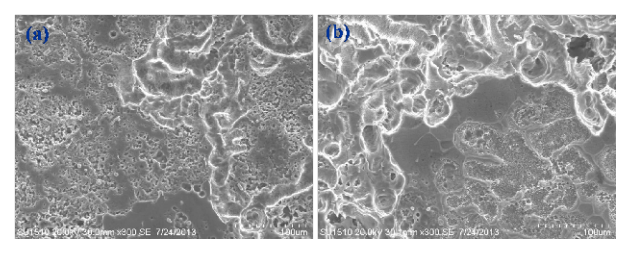


Fig. 1: Micro-corrosion morphologies of alloy I after immersion for 3days (a) as-cast (b)solid-solution treatment

**DISCUSSION & CONCLUSIONS:** After solid solution treatment, the microstructure of Mg alloys is more uniform than before, which resulted in the mechanical properties were improved. The corrosion mode of Mg alloys was started from pitting corrosion which along surface direction and depth direction grew up at the same time, the solid-solution treatment decreased the barrier to prevent the corrosion, lead to corrosion rate increased rapidly.

**ACKNOWLEDGEMENTS:** The author wish to acknowledge the financial supports from NSFC (Grant No. 50871055, 51474132), PAPD and Jiangsu Key Lab of Micro-nano Materials and Technology.

### Corrosion behaviour of sintered biodegradable iron materials with hydroxyapatite film

R Oriňaková<sup>1</sup>, A Oriňak<sup>1</sup>, M Kupková<sup>2</sup>, M Hrubovčáková<sup>2</sup>

<sup>1</sup> <u>Department of Physical Chemistry</u>, PJ Šafárik University, Slovak Republic, <sup>2</sup> <u>Institute of Materials</u> <u>Research</u>, Slovak Academy of Science, Slovak Republic

INTRODUCTION: Biodegradable metallic materials have attracted considerable interest due to their use for temporary medical implants [1]. Coating of metallic implants by bioactive materials like hydroxyapatite (HAp) ceramics is widely used to improve the osteointegration and to ensure the lasting clinical success [2]. The biodegradable iron material was produced by sintering of carbonyl iron powder and electrochemically coated with hydroxyapatite and manganese-doped HAp (MnHAp) ceramics layer. The electrochemical and static immersion corrosion behaviour of developed materials in Hank's solution was studied.

**METHODS:** The carbonyl iron powder was cold pressed at 600 MPa into pellets (Ø 10 mm, h 2mm) and sintered in a tube furnace for 1 hour at 1120°C in reductive atmosphere. Cathodic electrochemical deposition of bioceramic coating layer was carried out using an potentiostat with conventional threeelectrode system. Deposition of HAp layer was realised in an electrolyte composed of 4.2 x 10<sup>-2</sup> M Ca(NO<sub>3</sub>)<sub>2</sub>, 2.5 x 10<sup>-2</sup> M NH<sub>4</sub>H<sub>2</sub>PO<sub>4</sub>. Deposition of MnHAp layer was conducted from the same electrolyte with addition of 3.0 x 10<sup>-3</sup> M Mn(NO<sub>3</sub>)<sub>2</sub> under the following parameters: pH  $4.3 \pm 0.5$ , current density  $0.85 \text{ mA/cm}^2$ , 40 min,  $65 \pm 0.5 \text{ °C}$ . After deposition, the samples were immersed in 1M NaOH solution at 65 °C for approximately 2 h, washed in distilled water, dried at 80 °C for 2 h and then sintered at 400 °C for 2 h in N<sub>2</sub>.

**RESULTS:** The corrosion potential  $(E_{corr})$  and corrosion current density  $(j_{corr})$  were calculated from the intersection of the anodic and cathodic Tafel lines extrapolation. The average corrosion were extracted from potentiodynamic polarisation curves using polarisation resistance method. The values of  $E_{corr}$  shifted to the less negative potential side for both bioceramic coated samples indicating the increased corrosion resistance of coated samples as compared to bare Fe sample. The highest corrosion susceptibility was observed for MnHAp coated sample. Corrosion potential of Fe was about -500 mV, while  $E_{corr}$  of the HAp coated and MnHAp coated iron substrate was about -452 mV and -478 mV. The increased corrosion resistance of coated materials was proved also by decreasing values of

*j<sub>corr</sub>* and corrosion rate. The corrosion rate as high as 0.4853 mm/y, 0.1578 mm/y and0.2762 mm/y were obtained for Fe, Fe+HAp and Fe+MnHAp, respectively. The value of in vitro degradation rate in Hank's solution for the sample with MnHAp coating layer was nearly two times higher than that of the HAp coated Fe sample, which could be associated with presence of Mn in coating layer. This result shows that the incoherent bioceramic coatings layer served as a slight barrier layer against corrosion.

The mass losses of the samples during static immersion test in Hank's solution for 13 weeks were determined. The highest corrosion rate after two weeks of immersion was proved for bioceramic coating layer with pre presence of Mn. However, also the corrosion rate for HAp coated sample was higher than that of uncoated material. The HAp presence in both coating layers enhanced the surface hydrophilicity and was thus considered to decrease the corrosion resistance of bioceramic coated samples. The corrosion rates as high as 3.458 mg/m<sup>2</sup> d, 1.992 mg/m<sup>2</sup> d, and 2.674 mg/m<sup>2</sup> d were obtained after 13 weeks for uncoated, HAp coated and MnHAp coated sample, respectively.

**DISCUSSION & CONCLUSIONS:** From the results of degradation studies it can be concluded that the presence of Mn in the bioceramic coating increased corrosion rate and decreased corrosion resistance of MnHAp coated iron material, particularly in the first stages of degradation.

**ACKNOWLEDGEMENTS:** The authors are thankful for the financial support provided by the Slovak Research and Development Agency, the APVV-0677-11 and APVV-0280-11 projects, and the Grant Agency of the Ministry of Education of the Slovak Republic, Grant No. 1/0211/12.

### In vitro cytotoxicity studies of powder metallurgy biodegradable materials from phosphated carbonyl iron powder

A Oriňak<sup>1</sup>, R Oriňaková<sup>1</sup>, M Kupková<sup>2</sup>, M Hrubovčáková<sup>2</sup>, M Giretová<sup>2</sup>, Ľ Medvecký<sup>2</sup>

<sup>1</sup> <u>Department of Physical Chemistry</u>, PJ Šafárik University, Slovak Republic, <sup>2</sup> <u>Institute of Materials Research</u>, Slovak Academy of Science, Slovak Republic

**INTRODUCTION:** Biodegradable metallic implants are of significant importance in the replacement of bones or the repair of bone defects. A degradable, iron-based alloys potentially usable as matrix material for cellular structures with biomechanically tailored properties were produced by the powder metallurgical approach by Wegener [1]. This study evaluates the effects of iron phosphate coating of carbonyl iron powder and of the addition of manganese on the microstructure and in vitro cytotoxicity of sintered materials. The iron phosphate-coated carbonyl iron powder (Fe/P) was produced by the phosphating method. The Fe/P-Mn alloy was prepared by sintering of the Fe/P powder mixed with the manganese powder.

**METHODS:** The carbonyl iron powder was coated in a phosphating solution using the modified precipitating method [2]. The phosphated iron powders were dried at 60°C for 2 hours and calcined at 400°C in air for 3 hours. The samples with the addition of Mn were prepared from a mixture of 30 wt.% of Mn and the phosphated carbonyl iron powder. For the cytotoxicity test, the powder mixtures were pressed into cylinders (Ø 10 mm, h 2 mm) at 600 MPa and sintered at 1120°C in reductive H<sub>2</sub> for 1 hour. The Fe/P samples were sintered at 1050°C to avoid liquid-phase sintering. The density, distribution and morphology of the L929 cells were evaluated on the tested samples using fluorescence optical microscopy live/dead staining based on fluorescein diacetate (FDA)/propidium iodide (PI). After 24 hours of culturing, the in vitro cytotoxicity extracts were evaluated by the MTS proliferation test assay. The absorbance of formazan was determined at 490 nm by a UV VIS spectrophotometer.

**RESULTS:** The fibroblast viability in the extracts from the Fe and Fe/P substrates exhibited reduction in viability in relation to negative control (polystyrene (PS) microplate), at about 40%. No cell viability was observed in the extracts from the Fe/P-Mn samples, which verified their severe cytotoxicity. The extracts from the Fe and Fe/P substrates were potentially cytotoxic, as their viabilities decreased below the critical level of 70%.

An analysis of the extracts revealed a considerable amount of Fe in all solutions obtained from the iron-based experimental samples. The highest released ion concentration, resulting from a high degradation rate, was observed in the Fe/P-Mn sample. The released ion concentration detected in the Fe/P sample was slightly lower. The concentration of released phosphorus was generally low, but it was higher in the Fe/P sample than in the Fe/P-Mn sample.

During the 4 hours after the seeding of cells, a large amount of cells in the Fe/P-Mn sample was damaged. The density of live fibroblasts found on the surface of this sample was very low. In the case of the Fe and Fe/P substrates, the amounts of initially adhered and live cells were practically the same, but they were lower than on the surface of the stainless steel sample. No live cells were observed on the surface of the Fe/P-M sample after 72 hours of fibroblast cultivation. The distribution and morphology of cells were, again, approximately the same for the Fe and Fe/P substrates, and around

30 % of the cells were damaged (dark red cells).

phosphate coating has a moderately negative effect on the cytotoxicity. Addition of Mn resulted in higher surface inhomogeneity, porosity and roughness as well as in increased cytotoxicity.

**ACKNOWLEDGEMENTS:** The authors are thankful for the financial support provided by the Slovak Research and Development Agency, the APVV-0677-11 and APVV-0280-11 projects, and the Grant Agency of the Ministry of Education of the Slovak Republic, Grant No. 1/0211/12.

#### Biodegradable open-celled magnesium scaffolds for bone tissue engineering

GZ Jia, JL Niu, H Huang, GY Yuan\*

<u>School of Materials Science and Engineering</u>, Shanghai Jiao Tong University, Shanghai 200240, China

INTRODUCTION: Magnesium has been widely studied as a potential material for biomedical implants due to its unique biodegradability and comparable Young's modulus to the hard tissue<sup>1</sup>. In particular, porous magnesium with excellent biocompatibility has shown its promising advantages for bone tissue engineering scaffold. The open-celled structure can not only accelerate the vascularization but also promote the reconstruction and regeneration of the defected bone, which will realize reliable osseointegration<sup>2</sup>. The present study is to develop an open-celled magnesium scaffold for biodegradable implants, and to investigate the microstructure and the mechanical properties.

METHODS: Pure liquid Mg was infiltrated into a pre-prepared sodium chloride template possessing controllable interconnectivity of particles fabricated by spherical NaCl particles. The magnesium ingot was placed on the template, after its molten at 720°C infiltration was carried out with the pressure of 0.2MPa. NaOH solution was used to dissolve the salt in order to decrease the corrosion of the magnesium during the remove process of the NaCl particles. The pore structure and the NaCl residues were directly evaluated by microcomputer tomography and the scanning electron microscope (SEM) equipped with an energy dispersive X-ray spectrometer (EDS). The mechanical properties of the open-celled magnesium were characterized by the uniaxial compressive tests. The tests were conducted on the specimens with dimensions of  $\phi 10 \text{mm} \times 15 \text{mm}$ under displacement control with the crosshead speed of 1mm/min.

**RESULTS:** The μ-CT image indicated that there were neither NaCl particles nor closed pore residual inside the scaffold as shown in Fig 1a. In Fig 1b, it can be seen that the main pores (700μm) and the interconnected pores (300μm) are almost rounded with a uniform size and homogeneous distribution, which virtually inherited the shape and size of the NaCl particles. The EDS analysis indicated that there was few Mg(OH)<sub>2</sub> remaining on the pore wall. The nominal stress-strain cure of the open-celled sample was shown in Fig. 2. The mechanical properties were about 1.25 MPa of yielding strength and 0.12 GPa of Young's

modulus for the open-celled magnesium scaffold with a 76.6% porosity.

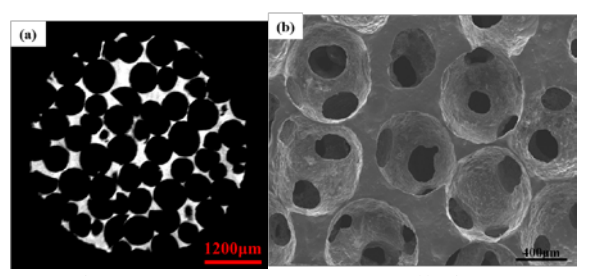


Fig.1 The pore structure of open-celled magnesium scaffold, (a) is  $\mu$ -CT image and (b) is SEM image.

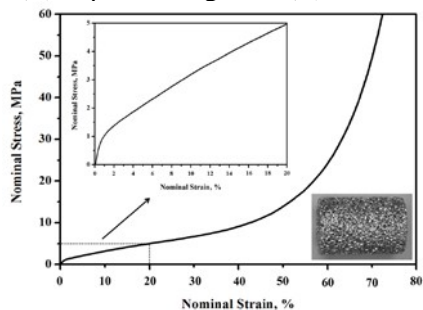


Fig.2 Nominal stress-strain cure of the open-celled magnesium scaffold.

DISCUSSION & CONCLUSIONS: It is worth noting that each main pore has at least six interconnected pores on its cell wall, which will certainly be beneficial to the vascularization and transportation of the nutrients or metabolic products. Moreover, the mechanical properties of the open-celled magnesium scaffold exhibits comparable strength and Young's modulus to the cancellous bone. Therefore, such open-celled magnesium scaffold possessing excellent pore morphology and comparable mechanical properties to the nature bone is a prospective material for bone tissue engineering.

ACKNOWLEDGEMENTS: This work was supported by the National High Technology R&D Program("863"Program) of China(No. 2015AA033603).

### Poly-lactic acid based composites reinforced with biodegradable magnesium alloys

X Li <sup>1,2</sup>, L Zhou<sup>1,2</sup>, J Zhang<sup>1,2</sup>, C Wang<sup>1,2</sup>, CL Chu <sup>1,2,\*</sup>, J Bai <sup>1,2</sup>, C Guo <sup>1,2</sup>, F Xue <sup>1,2</sup>, P Lin <sup>1,2</sup>

<sup>1</sup> School of Materials Science and Engineering, Southeast University, Nanjing, 211189, China.

<sup>2</sup> Jiangsu Key Laboratory for Advanced Metallic Materials, Southeast University, Nanjing, 211189, China.

**INTRODUCTION:** Biodegradable poly-lactic acid (PLA) and magnesium alloys attract huge interest for bone fixation implants. Composites composed with these two components have favorable mechanical and degradation properties [1,2]. This paper presents several PLA based composites reinforced with magnesium alloy products for various bone fixations.

**METHODS:** Mg alloy wires (MAW), Mg alloy sheets (MAS), and Mg alloy rods (MAR) were employed to reinforce PLA. The methods for the fabrication of the composites involved heat-compression, heat-drawing and injection. Mechanical properties were assessed by tensile and bending tests. *In vitro* tests were applied to determine the *in vitro* properties.

**RESULTS:** Mechanical properties of the composites exhibit versatility, varying from 45 MPa to 300 MPa for tensile strength and 80 MPa to 300 MPa for bending strength (Fig 1). With the corporation of proper interface modification, the composites exhibit favorable degradation and interface strengthening behaviors.

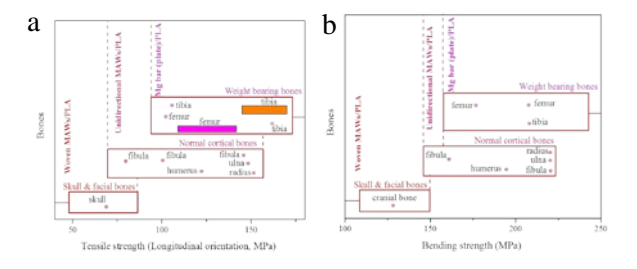


Fig. 1: Illustration of tensile (a) and bending (b) strength of the composites reinforced with different magnesium alloy products.

**DISCUSSION & CONCLUSIONS:** This kind composite could meet the fixation requirements of different bones, involving the anisotropic-tough humerus and the isotropic-frail skull through proper interface modification or internal distribution of Mg products. The versatility and designability of this kind composite suggests it

would be promising candidate for bone fixation implants.

ACKNOWLEDGEMENTS: This work was jointly supported by the Scientific Research Foundation of Graduate School of Southeast University, Science and Technology Support Program of Jiangsu Province (BE2011778), Natural Science Foundation of Jiangsu Province (BK2012869).

# Possibilities and limitations of electrochemical measurement techniques to assess the degradation behaviour of Mg and Mg - alloys for biomedical application – an overview

WD Mueller<sup>1</sup>,

 $^{\it I}$  Dental and Biomaterial Research Gr., CC3 Charité Universitaetsmeizin Berlin D

Various reviews have been published focusing on several aspects concerning the application of Mg and Mg-alloys for biomedical applications [1-3]

The assessment of degradation of these new developed alloys is possible via immersion tests, hydrogen evolution measurements and electrochemical measurements.

Electrochemical measurements are commonly used but there is a lack of comparability of data which was a theme during the Biometal symposium in 2010 and the question appears, how reliable they are?

Based on literature data an overview about techniques, set up's and strategies for data assessment will be given.

Following points are presented more in detail: measured date, calculated results, measurement conditions, measurement set up's, necessity to use independent measurements.

The open circuit potential  $E_{OCP}$ , corrosion density  $i_{corr}$ , polarization resistance  $R_p$  are the key data for assessment of corrosion rate (CR) using the Faraday law. In case of Mg degradation reaction (1) is well accepted.

(1) 
$$Mg + 2H_2O \Leftrightarrow Mg^{2+} + 2H_2 + 2OH^-$$

But in aqueous solutions the hydrogen evolution is one of the key problems because of its influence on the electrochemical measurements. That is linked with the galvanic process and the creation of MgH<sub>2</sub> at the surface [4].

These caused problems by calculation of CR which is normally based on reaction (1).

Before this can be discussed in detail the point of measurement conditions and set up's has to be summarized.

The set up's go from macro to ultra-micro techniques. This is related to the applied measurement area and resolution. Usually 1 cm<sup>2</sup> measurement area will be used with the disadvantage of embedding the specimens and

don't have any real control about the corrosion reaction which takes place in the interfaces [6].

Even the classical protocols from standards, made for steel, are not very helpful.

Reduction of measurement area, avoiding the embedding procedure can improve the quality of measured data. But also here some disadvantages have to be considered as the reduction of time frame for measurements, which can be minimized by using of an adapted measurement protocol.

The application of ultra-micro electrodes in scanning electrochemical microscopy produce new data which describe the interface conditions more in detail as the ph gradient or the favoured local places at the surface for hydrogen evolution [7,8].

At least the question, what kind of measurements should be done, voltammetry or impedance spectroscopy, has to be illuminated.

These concerning the measurement conditions as artificial electrolytes as ringer solution, or SBF, or cell culture medium, or at least blood, as a special focus in relation to a common accepted protocol for electrochemical measurements.

All these will be presented and summarized and demonstrate the power of electrochemical measurements as tool for assessment of degradation of Mg and Mg alloys for biomedical applications.

### The use of rotating disk electrode to improve Mg degradation characterization by polarization experiments

I Marco, O van der Biest Department of Materials Engineering (MTM), KU Leuven, Belgium.

INTRODUCTION: For the characterization of Mg alloy degradation different approaches are electrochemistry, applying immersion testing and in vivo implantation. However, results found in literature discordance [1-3]. Potentiodynamic polarization (PDP) experiments give a comparison of different Mg alloys behaviour by assessing the rate at which the anodic and the cathodic reactions take place [4]. The rotating disc electrode (RDE), where the working electrode is a disc in rotation, is a better approach for characterization with PDP [5, 6]. This RDE makes a fluid flow which removes the dissolved Mg<sup>2+</sup> ions from the surrounding of the Mg surface avoiding the formation of a corrosion layer influencing the measurement [7]. The goal of this work is to clarify the effect of the rotation  $(\omega)$ on the polarization results with RDE.

**METHODS:** Open circuit potential (OCP) during 120s and PDP experiments are carried out in PBS at 37°C with the RDE. The working electrode is a pure Mg disc, with a surface of 50 mm², placed in a sealed clamp and connected electrically to the potentiostat. The disc surface is ground with SiC sandpaper (4000 grits) and polished with diamond suspension (3 $\mu$ m). Pt mesh as counter electrode and Ag/AgCl saturated with KCl as reference electrode complete the cell. The scanned potential range is  $\pm 250$  mV against the OCP, and the scan rate is 5 mV/s.

**RESULTS:** The influence of the rotation speed on the open circuit potential and the first PDP of pure Mg in PBS at 37 °C is shown in figure 1.

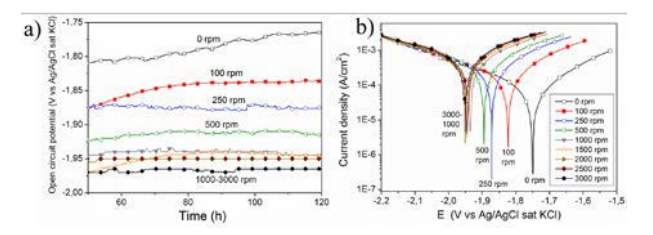


Fig. 1 OCP (a) and first PDP (b) at different ω, show the decreasing influence of the corrosion layer formation at higher rotation speeds.

The OCP gets stable around -1.95V at  $\omega$  higher than 1000rpm. At lower  $\omega$  values down to zero (no rotation) there is a considerable potential increase showing the effect of the forming corrosion layer

(figure 2), which increases constantly the OCP during the first 120 seconds of immersion. In addition, the first PDP at different  $\omega$  depicts the corrosion potential ( $E_{corr}$ ) increase and current density ( $i_{corr}$ ) decrease due to the protective precipitated corrosion layer.

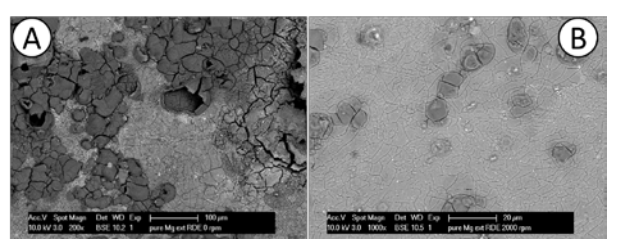


Fig.2 Corrosion layer SEM imaging at 0rpm (a) and 2000rpm (b), after the same testing.

CONCLUSIONS AND DISCUSSION: The presence of dissolved magnesium (Mg<sup>2+</sup>) during polarization experiments induces a corrosion layer, of mainly Mg(OH)<sub>2</sub>, which covers the sample. This layer and the increase in the stationary boundary layer thickness at lower  $\omega$  in the fluid, which controls Mg ions diffusion, shift the corrosion potential towards more anodic values and slows down the current flow. The RDE use reduces this influence and experimentally the appropriate ω range is defined between 1500rpm and 2000 rpm. With this RDE technique it is possible to measure the intrinsic response of a particular Mg alloyelectrolyte system avoiding the corrosion layer dependence in which the defects become degradation rate controlling.

**ACKNOWLEDGEMENTS:** Research supported by the PEOPLE Programme (Marie Skłodowska-Curie Actions) of the European Union's Seventh Framework Programme FP7/2007-2013/ under REA grant agreement n° 289163 (MagnIM).

### Challenges for accurate determination of rare earth elements in degradable Mg allovs

C Vogt<sup>1</sup>, F Zimmermann<sup>1</sup>, N Hort<sup>2</sup>

<sup>1</sup> Leibniz University Hannover, Institute of Inorganic Chemistry, Hannover, Germany <sup>2</sup> Helmholtz Zentrum Geesthacht, Magnesium Processing, Geesthacht, Germany

INTRODUCTION: Rare earth elements (REE), especially gadolinium, europium, neodymium and dysprosium, are nowadays added to Mg alloys (among other alloying components) to tune the mechanical and chemical properties and the degradation behaviour in vitro and in vivo. Due to availability and cost reasons mixtures of several REE are often applied in the alloys within a typical concentration range from 1 to 10 wt%. Although these REE show comparable degradation chemistry, the interaction with the biosystems could differ significantly. Thus an accurate determination of concentrations of all alloyed REE is necessary to interpret toxicity and biocompatibility studies properly.

**METHODS:** A determination of REE could be performed on the solid material by XRF methods or after digestion with concentrated acids by Optical Emission spectroscopy (ICP-OES) or Mass spectrometry (ICP-MS). Due to the chemical and physicochemical similarity of the REE, interferences are observed for all methods which hamper an accurate quantification. To investigate and solve these problems several preparation and measurement strategies have been tested for different Mg alloys.

**RESULTS:** Quantification by external calibration with matrix matched standards is commonly used to overcome matrix effects. Nevertheless detailed knowledge of the samples and, depending on the analyte concentrations, absolutely pure matrix materials are essential.

If one or both conditions are unknown, quantification by standard addition is used. It is one of the most reliable quantification methods since samples and standards undergo the same matrix effects. However, signal overlaps remain crucial and this method fits only perfect for few samples. Due to the large preparation effort, it is not practicable for large sample numbers or routine analytics without proper automation.

In ICP-OES measurements, solutions with relatively high Mg concentrations (matrix) cause intensity enhancement or reduction of the signals of the other alloy components compared to

solutions without matrix. An adjustment of the spectral observation height in the plasma (radial view) by shifting the torch box can solve this problem. At a certain tuning position the matrix effect is compensated (Fig. 1).

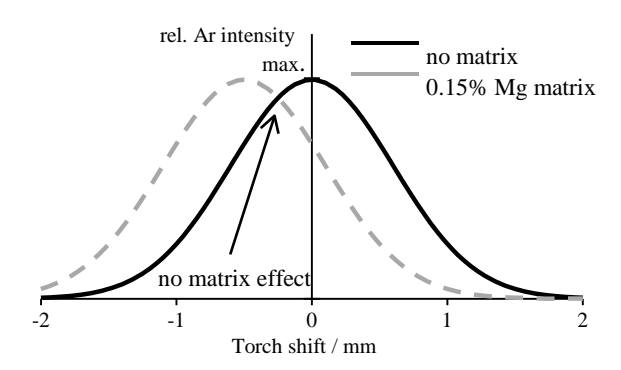


Fig. 1: Schematic illustration of matrix effects on ICP-OES measurements.

Based on the chemical similarity of REE, emission lines may also overlap in OES and XRF. Diluting the samples (if possible) at an expense of the LODs is often the only possibility besides higher spectral resolutions.

All REE have at least one isotope which could be determined in mass spectrometry without isobaric interference. In several cases the usage of collision cell technology, which allows to minimise polyatomic interferences, leads to significantly improved results. Otherwise high resolution mass filters have to be used for an accurate quantification of several REE in the same sample.

DISCUSSION & CONCLUSIONS: In principle an accurate determination of REE in Mg alloys or degradation products is possible, although the proper method to choose strongly depends on the given task and the composition of the alloy. Pros and Cons for the most commonly applied methods have been discussed. Furthermore the adaptation of additional strategies like flow injection analysis or isotope dilution could be interesting.

### Three dimensional in silico study of coating debonding for biodegradable magnesium alloy stents

W Wu<sup>1</sup>, M Mercuri<sup>1</sup>, C Petroni<sup>1</sup>, L Petrini<sup>2</sup>, F Migliavacca<sup>1</sup>

<sup>1</sup> Chemistry, Materials and Chemical Engineering Department, Politecnico di Milano, Italy. <sup>2</sup> Civil and Environmental Engineering Department, Politecnico di Milano, Italy

**INTRODUCTION:** The debonding phenomenon of the coated magnesium alloy stents (MAS) is a drawback for this promising cardiovascular method. Although a few 2D finite element models have been built to study this phenomenon [1], further work of 3D model should be done to better understand the mechanism of the debonding of MAS coating.

METHODS: The 3D stent model was built based on the geometry of the Magic stent (Biotronik, Bulach, Switzerland). Only one unit was chosen because of its structural symmetry (Fig.1). A polycaprolactone coating of 0.01 mm was modeled around the stent (the green layer in Fig. 1). The bonding of the stent and coating was realized through CZM using special cohesive elements, which are zero thickness and connected top and bottom to the adjoining bodies to represent the bond. As Fig. 1 shows, the cohesive elements bond the stent and coating meaning that the coating can be ruptured during stent expansion, which cannot be simulated in 2D models. The CZM relates the tractional stresses (T) to the displacements  $(\delta)$ , between the bonded interfaces through a tractionseparation law. Only one parameter is obtained from peeling tests: the fracture energy per unit area of crack growth,  $G_c$ . With the penalty parameter  $\delta$ set through pre-test of simulations, the CZM can simulate the debonding behaviour of coated MAS. In this study the balloon expansion is not included and the deformation of the model is controlled by vertical displacement at one stent end.



Fig. 1: One ring of the investigated stent (left), one strut unit showing coating layer (middle) and cohesive elements bonding stent and coating (right).

**RESULTS:** When the stent had the maximum expansion, not only the coating deboning from stent occurred, but also the coating rupture along

the stent edges can be observed; both are located at tensile side of the curved part of the stent unit,

where the metallic substrate was subjected to high plastic deformations (Fig 2a). At the same locations, the cohesive elements were mainly stressed by traction forces orthogonally towards the separation interface (separation mode I), until failed to maintain interfaces bonded (Fig 2b). The coating rupture led to an opening gap between stent and vessel, where human body fluids can eventually accumulate and enhancing localized stent corrosion.

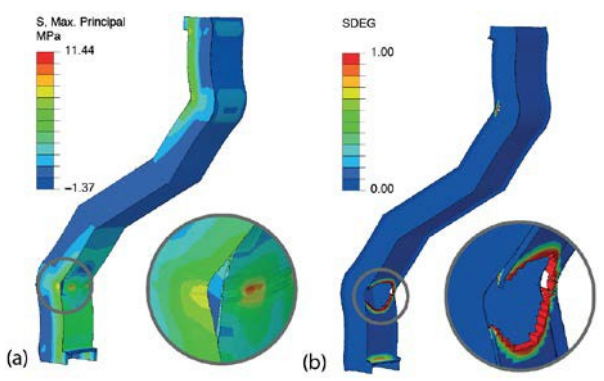


Fig. 2: (a) Maximum stress distribution of the coating at the end of stent expansion. Inset shows how the debonding and rupture of coating happened. (b) Damage of the cohesive elements at the same time. The cohesive elements reaching damage factor of 1 were failed and eliminated.

modelling of coating delamination on magnesium alloy stent can reflect the coating rupture phenomenon which cannot be observed in the 2D simulation studies<sup>1</sup>. Furthermore, the 3D model can include contact behaviour to study the influence of the balloon expansion. Thus this novel model could provide a more accurate and useful tool for the in silico study to prevent the debonding of coated magnesium alloy stent.

**ACKNOWLEDGEMENTS:** WeiWu is supported by the International Fellowship Program (PIF).

#### Investigation on adjustment for biodegradation behaviour of iron-based metal

XM Yu, X Lu, LL Tan, K Yang

Institute of Metal Research, Chinese Academy of Sciences, Shenyang, China

**INTRODUCTION:** As one of potential material candidates for biodegradable stents, the degradation behaviour of iron-based alloy has been investigated[1,2]. Without changing the alloy composition, the crevice corrosion was adopted to enhance the degradation rate. Changes of the degradation rate were studied through *in vitro* immersion test and the related mechanism was analysed based on the experimental data and phenomenon.

**METHODS:** An Fe-30Mn-1C alloy was cut into size of 10mm×10mm×0.2mm. Sample surfaces were grounded up to 2000 gritsand paper, and then mirror polished with 1μm diamond grinding paste. Pore matrix (16×16 holes) was fabricated by a CO<sub>2</sub> laser device. The pitch of holes was 0.5mm, and the pore size was set as 0.07mm, 0.10mm and 0.15mm, respectively. The immersion test was conducted in Hank's and 0.9% NaCl solutions at pH of 7.4. The ratio of sample area to the solution volume was 1cm<sup>2</sup>: 10mL. The container was kept at 37 °C in a 5% CO<sub>2</sub> incubator. The immersion solution was changed each two days. The degradation product was cleaned, and the degradation rate was calculated by:

$$CR = 8.76 \times 10^4 W/At\rho$$
 (1)

CR: degradation rate(mm/year), W: weight loss (g), A: superficial area (cm $^2$ ), t: immersion time (h),  $\rho$ : density (g/cm $^3$ ). The morphology of surface layer on samples was examined under a scanning electron microscope (SEM).

**RESULTS:** Because of a pore structure, degradation rate of the Fe-based alloy was dramatically increased up to about 200% in Hank's solution, as shown in Fig.1.

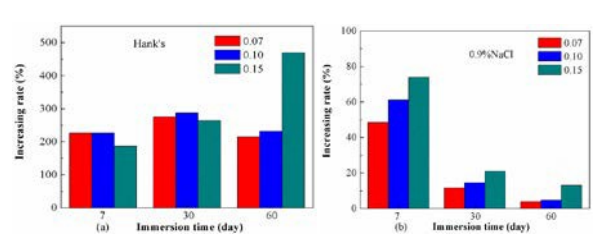


Fig. 1: Increasing rates of degradation of Fe-30Mn-1C alloy with different-size pores immersed in Hank's (a) and 0.9% NaCl (b) solutions.

The crevice corrosion took place for all samples with different pore sizes. In Hank's solution, the degradation first took place around pores, and then the degradation product increased and contacted with each other. In 0.9% NaCl solution, the degradation was similar with the control group.

**DISCUSSION & CONCLUSIONS:** As shown in Fig.2, in Hank's solution, a heavy degradation was observed inside pores, while not obvious outside pores. As the crevice corrosion was the first factor. the degradation rate was dramatically enhanced due to the pore structure. But 0.9% NaCl solution was relatively more corrosive, the degradation was similar on the whole sample and the crevice corrosion became the secondary factor. In the initial stage, the crevice corrosion took place for different pore sizes. However, the degradation rate of sample with pore size of 0.15mm was maintained at higher level. The reason was that the accumulation of degradation product, which could prevent the corrosion, was relatively less for the larger pore size. Therefore, variation of pore size affected the crevice corrosion. Moreover, increase of the surface area could also improve degradation, but the increasewas no more than 10% and the effect was limited.

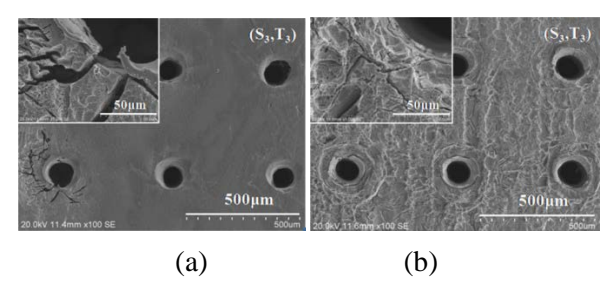


Fig. 2: SEM morphologies of Fe-30Mn-1C alloy with pore size of 0.15mm in Hank's (a) and 0.9% NaCl (b) solutions for 60 days

**ACKNOWLEDGEMENTS:** The authors would like to thank the financial support of the National Basic Research Program of China (973 Program, No.2012CB619101)

#### Uniformed and accelerated degradation of pure iron patterned by Pt electrode

T Huang<sup>1</sup>, Y Zheng<sup>1</sup>, LQ Ruan<sup>2</sup>

<sup>1</sup> State Key Laboratory for Turbulence and Complex System and Department of Materials Science and Engineering, College of Engineering, Peking University, Beijing 100871, China 
<sup>2</sup> Magnesium Research Center, Kumamoto University, Kumamoto-shi 860-8555, Japan

**INTRODUCTION:** The safety of stents made of pure iron has been verified by a plenty of animal experiments[1]. However, the degradation rate *in vivo* of pure iron is too slow to meet clinic requirements. Therefore, Strategies to accelerate corrosion rate of pure iron are sorely needed.

METHODS: Two different designs of platinum disc arrays, including sizes of  $\Phi$ 20  $\mu$ m  $\times$  S5  $\mu$ m (Φ20 μm means the diameter of the platinum disc is 20 µm, S5 µm means the space between two nearest platinum discs is 5  $\mu$ m) and  $\Phi$ 4  $\mu$ m  $\times$  S4 um, have been coated on the surface of pure iron through photo-etching technique and electron beam evaporation. The micro-topography of specimens were observed by ESEM (AMRAY-1910FE). In the immersion test, specimens were mounted in silicone, and only remained exploded surface of 10×10 mm<sup>2</sup> in area. Then, mounted specimens were immersed into Hank's solution at the temperature of 37 °C for one week. The surface morphologies after immersion test were observed by ESEM (AMRAY-1910FE). And the corrosion rates were calculated by mass loss method.

**RESULTS:** Fig.1 shows the microstructure of the pure iron coated with platinum disc arrays. As can be seen from Fig. 2, galvanic corrosion can be observed obviously. To some extent, Platinum patterned pure iron transferred the localized corrosion mode of pure iron to a more uniform one. Platinum arrays has higher standard potential (+1.2 V) than that of iron (-0.44 V). Then, the platinum discs (as cathodes) and the surrounded iron matrix (as anode) formed a large number of galvanic cells when immersion into the Hank's solution. Table 1 gives the information of mean corrosion rates of platinum electrodes coated pure iron after immersion in Hank's solution for a week, uncoated pure iron as control. According to these values, the coated of platinum electrode can significantly speed up the degradation rate of pure iron matrix. Furthermore, platinum patterns with the size of  $\Phi$ 4 µm × S4 µm exhibited the fastest corrosion rate.

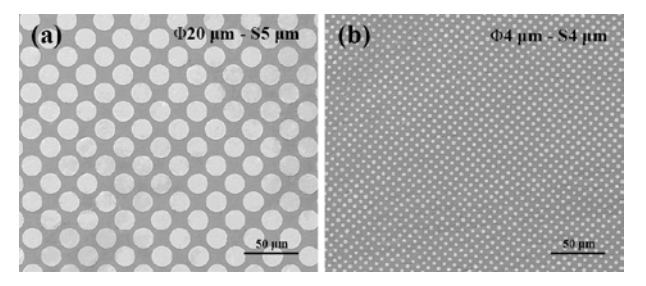


Fig. 1: Platinum disc arrays coated pure iron.

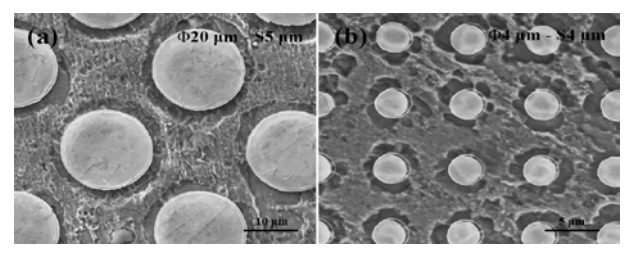


Fig. 2: Platinum disc arrays coated pure iron after immersion in Hank's solution for a week.

Table 1. Mean corrosion rates after immersion in Hank's solution for a week.

Materials	Corrosion rate (mg·cm <sup>-2</sup> ·d <sup>-1</sup> )
Uncoated pure Fe	$0.12025 \pm 0.038537$
$\Phi$ 4 μm × S4 μm	$0.173913 \pm 0.027551$
$\Phi$ 20 μm × S5 μm	$0.152331 \pm 0.027271$

**DISCUSSION & CONCLUSIONS:** Coating platinum electrodes on the surface of pure iron can form a plenty of galvanic cells to accelerate the degradation rate. Meanwhile, due to the designable of platinum electrode's shape, size as well as distribution, pure iron coated with platinum electrodes may realize the controllable degradation rate as well as uniformity of pure iron matrix.

ACKNOWLEDGEMENTS: This work was supported by the National Basic Research Program of China (973 Program) (Grant No. 2012CB619102), National Science Fund for Distinguished Young Scholars (Grant No. 51225101), National Natural Science Foundation of China (Grant No. 51431002 and 31170909).

#### The effect of nonlinear dynamic characteristics of AMS on its corrosion speed

ZW Zhu<sup>1</sup>, YX Kong<sup>1</sup>, WD Zhang<sup>1</sup>, J Xu<sup>1</sup>

<sup>1</sup> Department of Mechanics, Tianjin University, Tianjin 300072, China.

INTRODUCTION: The corrosion problem of absorbable magnesium stent (AMS) has gained considerable attention. The traditional ways to improve the AMS's corrosion resistance is surface modification technology. However, single coating can not meet the all requirements from human body's environment. In this paper, the effect of the AMS's nonlinear dynamic characteristics on corrosion speed is studied, and a new physical way to control the AMS's corrosion speed through adjusting its parameters and design is proposed.

**METHODS:** The dynamic model of an AMS subjected to the viscous force from blood is developed as follows:

$$\rho h r^{2} \frac{\partial^{2} w}{\partial t^{2}} = q r - \frac{\partial^{2} M}{r \partial \theta^{2}} N_{\theta} (1 - \frac{\partial^{2} w}{r \partial \theta^{2}} + F_{v})$$
 (1)

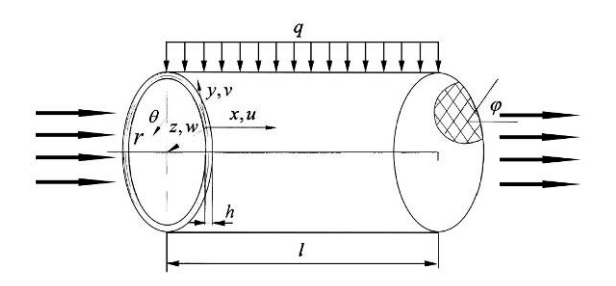


Fig. 1: Mechanical model of AMS subjected to radial pressure from vascular wall and axial viscous force from blood.

The dynamic equation of the AMS's radial vibration amplitude can be solved from Eq. (1) as follows:

$$\dot{x} + 2\eta \dot{x} + \omega^2 x + ax^3 = ex(\sin\Omega t + \sigma B(t)) \quad (2)$$

**RESULTS:** The stationary probability density (SPD) of the system's response is shown as follows:

$$f(H) = \overline{A}H^{-\frac{4\eta\omega}{De^2}} \exp\left[-\frac{\omega_2}{De^2}H - \frac{a_2}{2De^2\omega}H^2\right]$$
 (3)

The results of numerical simulation are shown in Fig.1. We can see that: In area 1, the steady-state probability density of H=0 is the maximum, and there is a crest in the SPD of the system response; in area 2, there is a crest and a loop in the SPD of the system response; in area 3, there is a loop in the SPD of the system response, the loop has the maximum SPD. It means that the system's motion

is the stochastic vibration near a periodic orbit, which can increase the AMS's corrosion speed. The experimental results are shown in Table 1.

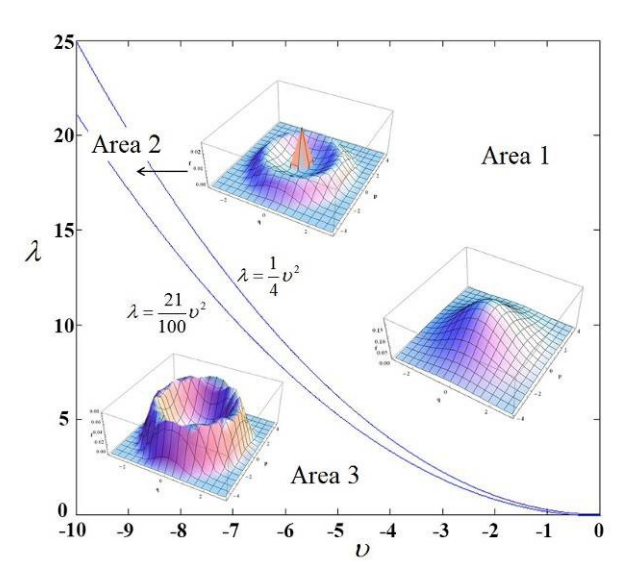


Fig. 1: Stationary probability density (SPD) of the system's response in different parameter areas.

Table 1. Vibration amplitude and corrosion speed of AMS in different parameter areas.

	Vibration	Corrosion Speed
	Amplitude (µm)	(mm/a)
Area 1	0.07	0.29
Area 3	0.23	0.76

**DISCUSSION & CONCLUSIONS:** Numerical simulation and experimental results show that there are jumping phenomena of the system's vibration amplitude when the parameters varies, and stochastic Hopf bifurcation occurs in the process, which effects the AMS's corrosion speed.

4

### Bioreactor-based *in vitro* degradation testing for biodegradable magnesium alloys

Y Yun<sup>1</sup>, Y Koo<sup>1</sup>, J Wang<sup>1,2</sup>, B Collins<sup>1</sup>, V Shanov<sup>3</sup>, J Sankar<sup>1</sup>

<sup>1</sup> Engineering Research Center for Revolution Metallic Biomaterials, North Carolina A&T State University, NC, USA. 2 Key Lab. of Advanced Materials Technology, Ministry of Education, School of Materials Science and Engineering, Southwest Jiaotong University, China.3 Department of Biomedical, Chemical & Environmental Engineering, University of Cincinnati, OH, USA

**INTRODUCTION:** Developing proper *in vitro* degradation testing method is critical, allowing fast alloys screening and lowering burden of animal test. However, simplifying complex nature of biology and finding the influential factors to affect degradation *in vivo* are first critical step. Here, we report the impact of cyclic loading, diffusion, and fluidics on magnesium degradation as well as we suggest pseudo-physiological testing methods for orthopaedic and cardiovascular simulation.

**METHODS:** *Cardiovascular model*. Two asdrawn magnesium (Mg) wires (99.9 %, 250 ± 25 μm dia.) were located into the lumen and intima of the porcine abdominal aorta. We flew medium at flow rate 100 ml/min, pulsed pressure range 80 - 120 mmHg. *Orthopaedic model*-Degradation test of the as-drawn Mg rods (99.9 %, 1.6 mm dia., 5 mm length) was performed under the three different environments based on flow rate 1.5 ml/min, cyclic loading period 3 hours/day, 10 N/sample. Both tests were kept in the incubator at 37 °C and 5 % CO<sub>2</sub> and Dulbeco's modified Eagle's medium (DMEM) with 10 % Fetal Bovin Serum (FBS) and 1 % Penicillin-Streptomycin was used as a pseudo-physiological medium.

**RESULTS:** Mg (red) degradations under the dynamic flow conditions are significantly faster than other conditions (Fig. 1). More corrosion products (yellow) accumulated on the Mg surface at static conditions.

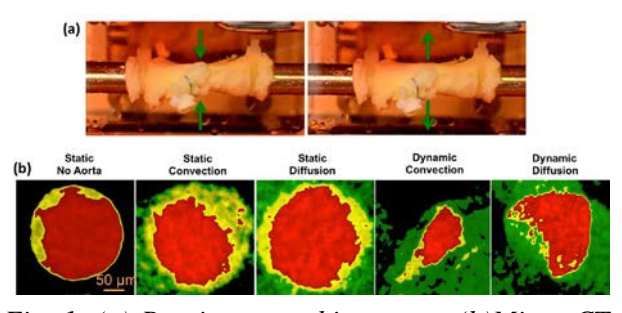


Fig. 1: (a) Porcine aorta bioreactor. (b)Micro-CT 2D slices under static condition with the aorta (No Aorta), in the lumen (Static Convection) and under the intima static condition, in the lumen (Dynamic

Convection) and under the intima (Dynamic Diffusion) at bioreactor for 3 days.

Mg rod was tested under three different environments using mechanical stimulating bioreactor (Fig. 2). The corrosion rate was increased under cyclic loading with diffusion environment.

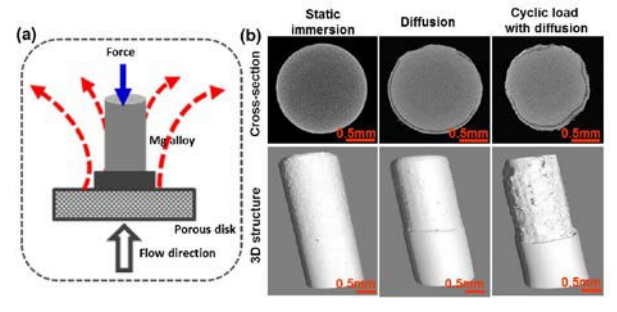


Fig. 2: (a) Schematic of the reactor inside,(b) reconstructions of X-ray micro-CT 2D with corrosion products, and 3D morphologies without corrosion products at standard static immersion and at bioreactor for 14 days.

**DISCUSSION & CONCLUSIONS:** The hydrodynamic and stress with diffusional flow microenvironments significantly affect on the different degradation behavior of magnesium. It can be considered in developing *in vitro* test that hold potential for being predictive of *in vivo* behavior.

**ACKNOWLEDGEMENTS:** This work was supported by NIH grant (1SC3GM113728-01) and NSF-ERC for revolutionizing metallic biomaterials (NSF-0812348).

#### Remaining strength of cold drawn and aged WE43 wires after corrosion

P Maier<sup>1</sup>, AJ Griebel<sup>2</sup>, O Scheffler<sup>1</sup>, JE Schaffer<sup>2</sup>

<sup>1</sup>University of Applied Sciences Stralsund, Stralsund, Germany. <sup>2</sup>Fort Wayne Metals Research Products Corp., Fort Wayne, IN, USA.

INTRODUCTION: Magnesium (Mg) alloy wire may have utility in a host of medical applications. Cold-drawn Mg wire offers mechanical advantages compared to warm worked metal [1], however; the influence of this cold work on corrosion is poorly understood. Mechanical testing of Mg wires after corrosion provides an estimate of performance in vivo [2]. WE43 is a high-performance alloy that exhibits an acceptable biological response [3]. The purpose of this research was to determine the remaining strength of cold-drawn WE43 wires with varying thermal treatments after corrosion in Ringer solution at body-temperature.

**METHODS:** Wires drawn to 1.6 mm through repeated cold-drawing and annealing steps were annealed at 723 K and cold-drawn to 1.0 mm. From here, 4 material conditions were produced. As Drawn wires had no thermal treatment after drawing, Aged were treated at 523 K, Anneal 1 at 673 K, and Anneal 2 at 773 K. A TIRA28100 machine was used for mechanical testing. Samples for tensile tests after corrosion had a length of 50 mm (speed 2 mm/min), for 3-point bending of 30 mm (span of 25 mm, speed 1 mm/min, radius of curvature at the load tip 5 mm). Ringer-Acetate was used in the corrosion tests due to its similarity to human blood. Wires were corroded in 500 ml electrolyte at  $310 \pm 2$  K.

**RESULTS:** High tensile strength was observed for precipitation hardened material (Aged) and moderate strength with high ductility for the fine grained recrystallized microstructure (Anneal 1), see Fig. 1. However, ductility of the wires can be better shown under 3-point-bending, where no material condition fractured or cracked.

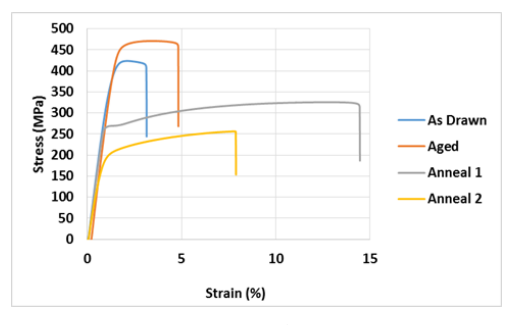


Fig. 1: Representative tensile stress-strain curves (here: 127mm gauge length, speed 25.4 mm/min)

The charts in Fig. 2 show the remaining ultimate strength of corroded wires, Fig. 2a for tensile and Fig. 2b for bending strength. Only the aged state corroded over 20 days failed during bending (at maximum strength; remaining ductility of 50%).

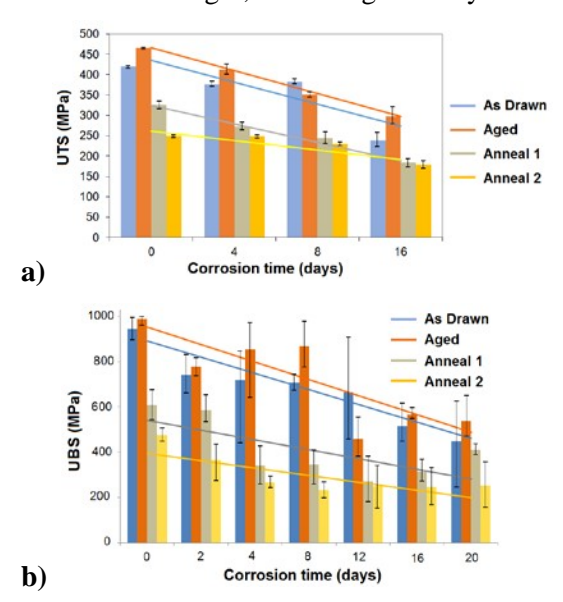


Fig. 2: Strength loss over corrosion time, ultimate tensile (a) and bending (b) strength

**DISCUSSION & CONCLUSIONS:** All wires form an oxide layer during corrosion, and retain approximately 50% initial strength after 16-20 days. Aged wires show the highest strength before and after corrosion. Combined with the higher ductility compared to as drawn wires (Fig. 1), the aged state may be suitable in high-strength applications. Annealing reduces initial strength, but has negligible impact on corrosion rates. Especially the fine grained micro-structure (Anneal 1) has a positive effect on longer corrosion and may be suitable for applications requiring high ductility. Micrographs, presenting corrosion form and oxide layer thickness and surface hardness measurements are used to explain corrosion mechanisms.

The consistency of relative strength values over time for all conditions seems to indicate that cold drawing does not increase the corrosion rate.

#### The need of bioactive coatings for biodegradable implants

A Eliezer<sup>1,4\*</sup>, C Gasqueres<sup>4</sup>, KS Lips<sup>3</sup>, L Heimann<sup>2</sup>, E Dingeldein<sup>2</sup>,

<sup>1</sup> Corrosion Research Center, Nano-Bio & Advanced Materials, Shamoon College of Engineering, Bialik/Basel Sts. P.O.B. 950, Beer-Sheva, 84100, Israel

<sup>2</sup> aap Biomaterials GmbH, Lagerstraße 11-15, 64807 Dieburg, Germany

<sup>3</sup> Justus-Liebig-Universität Gießen, Klinik für Poliklinik und Unfallchirurgie, Labor für Experimentelle Unfallchirurgie, Kerkraderstraße 9, 35394 Gießen, Germany

<sup>4</sup> aap Implantate AG, Lorenzweg 5, 12099 Berlin, Germany

INTRODUCTION: Today there is a demand for short term biodegradable implants. The general question is why after so many years very few biodegradable implants have succeeded to reach the product level. This study will focus on coated and uncoated biodegradable magnesium alloys as well as on the importance of corrosion research and development of in-situ experimental units. The main problem is that these materials are very reactive and may undergo environmentally induced degradation during service Coatings can address the ability of a controlled degradation biomaterial behavior under different environments.

**METHODS:** Cannulated Interference W4 (96% magnesium, 4% yttrium) screws and their runners which were produced by die casting were investigated under in-vitro (electrochemical and gas formation experiments) and in-vivo (sheep) and (rats) conditions. The study will also discuss other alloys such as pure magnesium alloys. The coating was obtained by plasma electrolytic oxidation (PEO). The PEO technology is an electrochemical surface conversion treatment. Metal components are exposed to a liquid electrolyte, and an electrical potential is applied to form an oxide-based ceramic. The electrochemical measurements were under 0.9% NaCl solution and corrosion was quantified electrochemically by electrochemical impedance spectroscopy (EIS) .The experimental setup for EIS consisted of a unique bio-reactor system In order to mimic the tissue conditions as closely as possible the solution was adjusted to 36.5–40°C and pH 7.35–7.45. The flow rate of the solution between the reactor (3000 ml) and the electrochemical cell (500 ml) was chosen to be 100 ml/min. The coating topography was investigated by scanning electron microscopy (SEM) and two in-vivo studies were performed on sheep's femur 6 and 12 weeks and on rat's femur ( W4 Pins) 6 and 12 weeks.

**RESULTS:** The study has demonstrated the development of importance the understanding it's mechanism and adhesion to the bulk material. The in-vitro measurements showed a significant decrease in corrosion for magnesium PEO coated samples compared to the uncoated samples by up to 90% both in EIS and gas formation. It was also shown that PEO coating screws resulted in a significant improvement of gas formation in-vivo for the rat's femur after 12 weeks implantation as well as for the sheep model. Figure 1 shows a HA regimen 2 coating after 12 in rat's femur once gas formation is not observed.



Figure 1: Coating Regimen 2 after 12 weeks

**DISCUSSION & CONCLUSIONS:** 1.Effective tailoring of corrosion by CaP- PEO nano coating for W4 magnesium alloy lead to a reduction of corrosion by up to 90%. 2. The results lead to the conclusion that in order to effectively tailor and control the biodegradation of advanced bio-active magnesium implants, there is a for such coated surfaces.

#### Corrosion behavior of Mg-Ca-Zn alloys in artificial saliva

N Zumdick<sup>1</sup>, S Ubber<sup>1</sup>, A Modabber<sup>2</sup>, E Goloborodko<sup>2</sup>, S Neuß-Stein<sup>2</sup>, <u>D Zander</u> <sup>1</sup>

<u>Chair of Corrosion and Corrosion Protection</u>, RWTH Aachen, Germany

<u>Uniklinik RWTH Aachen, Germany</u>

**INTRODUCTION:** A new prospective application field for biodegradable magnesium alloys could include oral and maxillofacial surgeries, e.g. facial reconstruction or jawbone traumata. During these treatments, the implant is inserted orally in order to generate as little aesthetical damage as possible. This implies that the implant stays in contact with the patients' saliva until wound closure. Therefore, such an implant initially undergoes different environmental conditions compared to those found in blood vessels or bone tissue. Corrosion tests, in order to predict biodegradation behavior, should conducted in electrolytes that simulate these specific conditions. In this work, the corrosion behavior of two low alloyed Mg-Ca-Zn alloys with varied Zn-content will be investigated in Artificial Saliva according to Klimek et al.<sup>1</sup>.

**METHODS:** Two Mg-0.6Ca-x·Zn alloys, x=0.8, 1.8 wt.%, were produced as described in Ref. 2. Polarization testing and hydrogen collection experiments<sup>3</sup> were conducted in Artificial Saliva<sup>1</sup>, prepared with high-purity chemicals and bidistilled water (see Table 1), at  $37 \pm 1$  °C. The pH of 6.8 to 7.5 was maintained by the manual addition of H<sub>3</sub>PO<sub>4</sub>. Both experiments were conducted with the same parameters and surface conditions as in Ref. <sup>2</sup> and at least three repetitions per material were undergone. Cross sections of post-immersion samples were observed in a Zeiss SEM with EDX.

Table 1. Chemical composition for 1000 ml Artificial Saliva according to Klimek et al<sup>1</sup>.

<b>KH<sub>2</sub>PO<sub>4</sub></b> 0,330 g	Na <sub>2</sub> HPO <sub>4</sub> 0,340 g	KCl 1,270 g	NaSCN 0,160 g	NaCl 0,580 g	CaCl <sub>2</sub> 0,128 g
NH <sub>4</sub> Cl	Urea	Glucose	Ascorbic	acid	Mucin
0,160 g	0,200 g	0,030 g	0,002 g		2,700 g

**RESULTS:** Potentiodynamic polarization and immersion curves of both Mg-Ca-Zn alloys are presented in Fig. 1. The  $i_{corr}$  of both materials lie in a small range of 1.0 to  $2.25 \,\mu\text{A/cm}^2$  and thus result in similarly low corrosion rates; however, Mg-0.6Ca-0.8Zn reveals to lower corrosion rates. This is confirmed by long-term immersion experiments with increasing time. Cross-sections (Fig. 2) show the corrosion attack (green) with a Mg/O of

 $0.4 \pm 0.1$  and multiple layers (blue), one with a Ca/P of  $1.0 \pm 0.1$  (dark blue) and one mainly consisting of C and O.

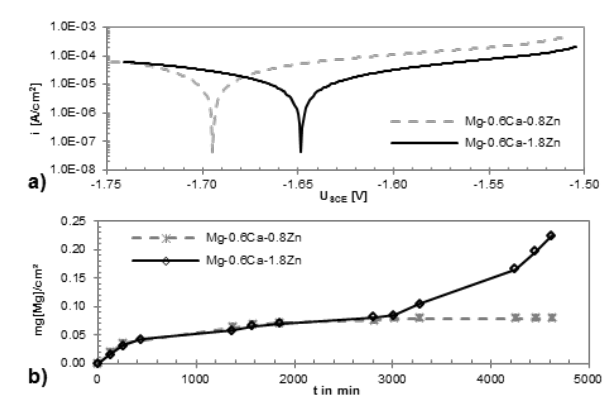


Fig. 1: a) Potentiodynamic polarization curves and b) mass-loss curves of Mg-0.6Ca-x·Zn in Artificial Saliva at 37°C.

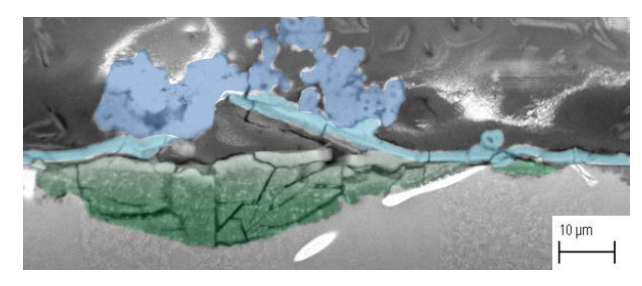


Fig. 2: Cross-section of corroded Mg-0.6Ca-1.8Zn after 5-day immersion showing multiple layers.

DISCUSSION & CONCLUSIONS: Mg-0.6Ca-0.8Zn shows lower corrosion rates in Artificial Saliva, possibly due to fewer micro-galvanic elements. In addition, the corrosion attack and layers appears more homogeneous for Mg-0.6Ca-0.8Zn. Low chloride contents and possible mucin lead to low corrosion rates in Artificial Saliva. Additionally, multiple, partially very thin layers were formed on the surface; similar in appearance when compared to those formed when exposed to other electrolytes.<sup>2</sup>

### Surface modification of magnesium alloys using electrophoretic deposition of chitosan and bioactive glass

H Hornberger, S Heise, M Hoehlinger, L Cordero-Arias, AR Boccaccini, S Virtanen Friedrich-Alexander-University Erlangen – Nuremberg, Germany

INTRODUCTION: The use of magnesium and its alloys as temporary implants fails mainly due to the missing control of the corrosion rate. Surface modifications are an appropriate method to reduce the degradation of Mg alloy components [1]. The aim of this study is to develop chitosan-bioactive glass layer systems onto Mg alloy substrates via electrophoretic deposition (EPD) [2] and to understand the degradation of such systems, which takes place in several steps. Every degradation step is influencing the following step but also inversely, for example in case of pitting corrosion. The adhesion of the applied organic coating to the substrate plays thereby an important role.

METHODS: Suspensions of chitosan and bioactive glass are produced using acetic acid and ethanol. WE43 substrates are pre-treated in order to enhance the adhesion of the following chitosan coating as well as to protect the substrate against corrosion during the coating procedure. The coating layer of chitosan and bioactive glass is deposited onto WE43 substrates via EPD, see Fig. 1. The EPD parameters are carefully adapted to low voltages. Various counter electrodes are applied to optimize the coating. The resulting adhesion is studied by pull off tests. The corrosion behavior is studied using mini cell system [3].



Fig. 1: Experimental set up for electrophoretic deposition. The parameters for Mg alloy substrates have to be carefully adapted.

**RESULTS:** The resulting EPD coating is made of a composite of chitosan and bioactive glass, see Fig. 2. Using EPD the adhesion of the coating can be improved in comparison with simply dip coated layers. The EPD parameters for Mg alloy

substrates, including the effect of counter electrode appear different than for other substrates as magnesium is very active. Using an appropriate pre-treatment of the alloy samples the adhesion of chitosan is further increased. The reason for this is mainly the increased surface roughness of the pre-treated substrates. The best results so far are achieved using substrate surfaces, which are pre-treated by etching in phosphoric acid as well as by anodization. Polarisation measurements can show that the current corrosion density is decreased due to the coating. Special interest is shown in the occurrence of pitting corrosion as also observed in other organic coating systems [4].

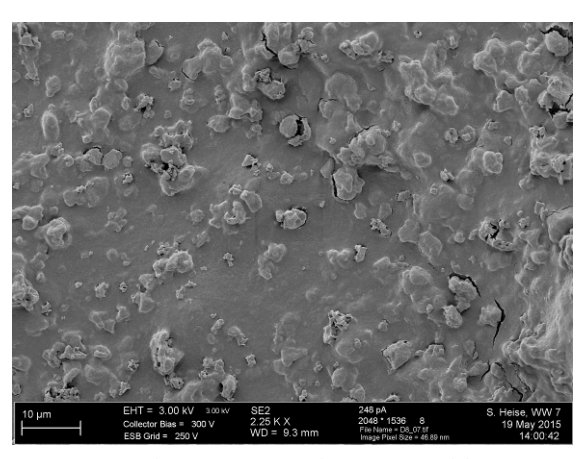


Fig. 2: EPD deposition of chitosan and bioactive glass onto WE43 substrate.

**DISCUSSION & CONCLUSIONS:** The present study focuses on the development of a new family of bio-adaptive coatings. EPD of chitosan-bioactive glass coatings on magnesium alloy shows promising results with the aim to improve adhesion to the substrate. Pitting corrosion occurs in dependence on the degree of adhesion.

**ACKNOWLEDGEMENTS:** This study is supported by German Science Foundation (DFG).

#### Self-assembling alkyl-silane anticorrosion coatings for resorbable Mg devices.

E Beniash<sup>1,2,3</sup>, A Patil<sup>2,3</sup>, O Jackson<sup>2</sup>, L Fulton<sup>2</sup>

<sup>1</sup>Department of Oral Biology, School of Dental Medicine; <sup>2</sup>Department of Bioengineering; <sup>3</sup>Center for Craniofacial Regeneration, University of Pittsburgh, Pittsburgh, PA 15261, USA

INTRODUCTION: Magnesium (Mg) and its alloys represent promising candidates for transient orthopedic devices<sup>1</sup>. Mg is highly biocompatible, since Mg<sup>2+</sup> is one of the essential ions and is present naturally in the body. It is also low weight and has mechanical properties compatible to bone. One of the obstacles for use of Mg in clinical application is its initial massive corrosion reaction leading to the formation of gas pockets around the implantable devices. To regulate the rate of corrosion we propose to use self-assembled alkylsilane (AS) coatings. Such coatings decrease the rate of corrosion by isolating a metallic devise from the liquid environment. Importantly, the surface chemistry and biological activity of AS coatings can be modified via covalent attachment of molecules of interest to the coating.

**METHODS:** Mg disks (99.9% purity) were polished and etched with HNO3 and some of them were passivated with NaOH prior to the coating procedure. Amphyphilic AS decyltriethoxysilane (DTES) and tetramethoxysilane (TMOS) were copolymerized for 90 min and the Mg disks were dipcoated in the solution and dried at 37°C. Some of the coatings were aminated with 3- Aminopropyltriethoxysilane (APS). Corrosion dynamics was assessed using H<sub>2</sub> evolution method potentiodynamic polarization as described elsewhere<sup>2</sup>. Scanning electron microscopy (SEM) energy dispersive spectroscopy (EDS) characterization of the coatings was conducted to assess their structural integrity. MC3T3 cells were cultured on the AS coated Mg disks for 15 days under routine tissue culture conditions.

**RESULTS:** The SEM revealed a homogeneous smooth 1 µm thick AS film covering entire area of the disk (Fig. 1A). Analysis of the scratch made with a razor blade has revealed a laminar structure of the layer. H<sub>2</sub> evolution analysis showed that AS coating has dramatically decreased the rate of corrosion (Fig. 1B). Similarly the potentiodynamic polarization experiments demonstrate almost 2 orders of magnitude reduction in Icorr from 995 μA/cm<sup>2</sup> for bare Mg to 12.5 μA/cm<sup>2</sup> for AS coated aminated samples. Contact measurements show that AS coating hydrophobic (120° for the coated sample vs. 60° for bare Mg). However, when AS coatings were functionalized with APS the contact angle

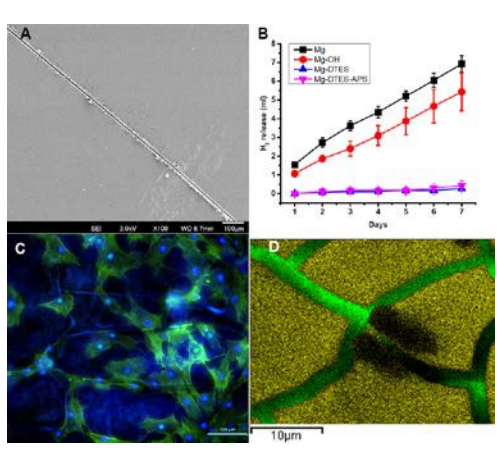


Figure 1. Figure 1.A SEM micrograph of an AS coated Mg disk, scratched with a razor blade. B H<sub>2</sub> evolution profiles of bare (black); NaOH passivated (orange), DTES coated (blue) and DTES/APS coated (magenta) Mg disks. C. Epifluorescence micrograph of MC3T3 cells cultured for 14 days on the DTES/APS coated Mg disks. Blue lines in the background correspond DAPI stain absorbed in the cracks. Green- F-actin IF; Blue DAPI staining. D. EDS map of an AS caoated Mg disk after 2 weeks in the tissue culture. Green- Mg K edge, Gold- Si K edge.

decreased to 70°. The results of the tissue culture studies demonstrate that cells survive for 2 weeks on the surface of AS coated Mg disks (Fig. 1C). The analysis of the coating surface after 2 weeks in the cell culture conditions revealed that the surface of the coating has cracked leading to a cobblestone appearance, however by and large the coating remained on the surface of the metal (Fig 1.C,D).

**DISCUSSION & CONCLUSIONS:** The resuts of our study demonstrate that self-assembled AS coatings can provide a viable solution for the regulation of the corrosion rates of the implantable Mg devices. Furthermore, these coatings can support cell attachment and proliferation.

#### **REFERENCES:**

<sup>1</sup>Witte, F. *Acta Biomater* **2010**, *6*, 1680. <sup>2</sup>Cui, W.; Beniash, E.; Gawalt, E.; Xu, Z.; Sfeir, C. *Acta Biomater* **2013**, *9*, 8650.

## Comparative study on degradation behaviour of magnesium alloys Mg-Y-RE and Mg-Ca-Zn in a dynamic bioreactor testing setup

D Porchetta<sup>1</sup>, J Gonzales<sup>2</sup>, F Feyerabend<sup>2</sup>, R Willumeit-Römer<sup>2</sup>, M Behbahani<sup>1</sup>, C Ptock<sup>3</sup>, A Kopp<sup>3</sup>

**INTRODUCTION:** Since magnesium is currently attracting attention as a potential candidate for resorbable orthopedic implants, decelerating, controlling and in particular predicting the resorption rate of magnesium materials would allow standardized forecasting of the in vivo implant performance prior to medical use, thus saving time, costs and animal lives. The non-trivial difficulty in performing degradation tests lies with the use of adequate boundary conditions and the cross-correlation between in vitro and in vivo resorption rates. Currently established electrochemical and static immersion tests in simulated body fluids take into account the chemistry of human body, but not the influence of fluid exchange and interactions at the site of implantation. Hence, it seems obvious, that previously mentioned models are not entirely capable of accurately estimating in vivo degradation rates of implants in animal or even human use. In this study, we carried out degradation testing under dynamic flow conditions, additionally performed by two independent research groups, in order to validate dynamic testing, compare different approaches on flow chambers and correlate different measuring methods for the determination of magnesium degradation rates.

METHODS: Specimen of magnesium alloys WE43 (4% yttrium, 3% rare earths) and ZX21 (2% calcium) were evaluated electrochemical measurements and dynamic in vitro testing utilizing two different flow chambers. electrochemical For measurements. potentiodynamic polarization (PDP) impedance spectroscopy (EIS) were used to compare both alloys qualitatively and semiquantitatively in terms of corrosion resistance as well as to calculate corrosion rates. To compare these theoretical values with real in vitro measurements, corrosion rates of geometrically identical specimen were quantified over a time span of 14 days in two different chamber designs under equal flow conditions. By combining gravimetric loss analysis and hydrogen gas evolution measurements the material loss was

examined and compared in fixed intervals. In addition, *in vitro* cytocompatibility was assessed using indirect XTT-, BrdU- and LDH- and direct live-dead staining.

**RESULTS:** Stained L929-fibroblasts, seeded directly on the surface, showed unsteady colonization with living and dead, rounded cells, with limited viability. Indirect testing by XTT-, BrdU-, as well as LDH-assays gave no evidence for cytotoxicity by the material-extracts, but showed diminished metabolic cell activity in dependence of the extract concentration, indicating an early interference with initial corrosion. This was confirmed by electrochemical measurements generally showing comparable corrosion with a slightly increased resistance for WE43. By employing dynamic degradation testing we were able to validate this tendency and show that quantitative measurements not only depend on conditions, but also on geometry. Notwithstanding, there is a strict constant of proportionality between different testing setups as well as measuring methods allowing the calibration of hydrogen gas method to real gravimetric loss and comparison of results derived from different setups.



Fig. 1: One of the two dynamic bioreactor setups used within the scope of presented comparative study on degradation of different magnesium alloys

**DISCUSSION & CONCLUSIONS:** First time systematic investigation of degradation testing in different flow chambers showed that dynamic testing better approaches real degradation than static immersion testing. Furthermore, it seems feasible to derive constants of proportionality between different setups and measuring methods.

<sup>&</sup>lt;sup>1</sup>Aachen University for Applied Sciences, Medical Engineering and Technomathematics, Aachen.

<sup>&</sup>lt;sup>2</sup> Helmholtz-Zentrum Geesthacht, Centre for Materials Research, Division Metallic Biomaterials, Geesthacht. <sup>3</sup> Meotec GmbH & Co. KG, Aachen.

### Potentiodynamic evaluation of Fe-Mn-C TWIP alloy in three pseudophysiological solutions

E Mouzou<sup>1</sup>, R Toulei<sup>1</sup>, P Chevalier<sup>1</sup>, C Paternoster<sup>1</sup>, H Hermawan<sup>1</sup>, D Mantovani<sup>1</sup>

Lab. for Biomaterials & Bioengineering (CRC-I), Dept. Min-Met-Materials Engineering & CHU de

Quebec Research Center, Laval University, Québec City, Canada

**INTRODUCTION:** High manganese austenitic steels such as Fe-20Mn-1.2C, with twinning induced plasticity (TWIP) effect, were developed primarily for automotive industry due to their exceptional high strength and deformation<sup>1</sup>. The low corrosion resistance in Cl<sup>-</sup> rich environment <sup>2</sup> and the presence of Mn whose excess<sup>3</sup> was reported as non-toxic in cardiovascular system make this material an interesting candidate for use in cardiovascular devices, although only few studies were reported on its degradation properties in biological environment<sup>4</sup>. Therefore the aim of this work was to investigate the potentiodynamic evaluation of Fe-20Mn-1.2C in three different pseudo-physiological solutions.

**METHODS:** Three different pseudo-physiological solutions, Sol1(Hank's commercial: HC), Sol2 (Dulbecco's phosphate buffered saline with protein: DPBS) and Sol3 (Hanks' modified solution: HM), were used for potentiodynamic tests, on the basis of ASTM G59-97. Princeton Applied Research model K47 corrosion cell system at a scan rate of 0.166 mV/s and at an applied potential of  $\pm 0.5$  V. The corrosion solution was used in an aerated environment at  $37^{\circ}$ C and mechanically stirred. The surface area exposed to the solution was 0.16 mm<sup>2</sup>. The calculation of the corrosion rate (CR) was obtained by using:

 $CR = 0.003272 * i_{corr} * EW/d$  (1) where  $i_{corr}$  is the corrosion current density  $(\mu A/cm^2)$ , EW the equivalent weight (grams) and  $\rho$  the density (grams/cm<sup>3</sup>).

Scanning electron microscopy (SEM-EDS), atomic absorption spectroscopy (AAS), and stylus profilometer (Dektak) were used to characterize degraded surface and corrosion products.

**RESULTS:** The potentiodynamic degradation rate of Fe-20Mn-1.2C were influenced by solution chemical composition. The degradation rate in HC was 3 times higher than DPBS and 3.5 times higher than HM. Dekatat, SEM and EDS analysis revealed the formation of craters (Fig.1) along with iron hydr(oxide) and manganese oxide

precipitation inside these craters. In the three solutions, Fe ion release was higher than Mn ion ones, however the difference between concentration of these two ions was more relevant in solution 2.

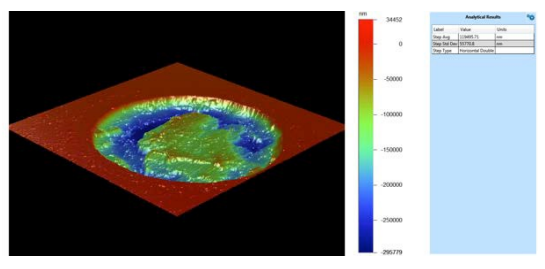


Fig. 1: Dektak image of Fe-Mn-C sample surface after potentiodynamic polarisation test in DPBS

DISCUSSION & CONCLUSIONS: Degradation rate, craters depth, concentration of ions release depends on chemical composition of test solution. For the three solutions the higher degradation rate was obtained for HC, but the high quantities of Fe and Mn ions released was obtained for DPBS solutions. HM samples has the lowest degradation rate and and also in terms of quantity of Fe and Mn ions released. These results were correlated with high quantity precipitate and low depth of crater observed for the samples of this solution.

ACKNOWLEDGEMENTS: The Authors would like to thank S. Turgeon at CHSFA de Québec, M. Choquette Ph.D, A. Ferland, V. Dodier, D. Marcotte and M. Larouche, of Min-Met-Materials Eng at Laval University They would also acknowledge ACDI and AUCC for scholarship to Essowè MOUZOU. Research was partially funded by natural Sciences and Engineering Research Council of Canada and CHU de Quebec Research Center

#### Corrosion and biocompatibility of gadolinium-containing magnesium alloys

D Bian<sup>1</sup>, N Li<sup>1</sup>, YF Zheng<sup>1,\*</sup>, YH Kou<sup>2</sup> BG Jiang<sup>2,\*\*</sup>

<sup>1</sup> Department of Materials Science and Engineering, College of Engineering, Peking University, China. <sup>2</sup> Department of trauma and orthopedics, People's Hospital Peking University, China.

INTRODUCTION: Magnesium and its alloys have been recognised as one kind of potentially revolutionary biomaterial in recent years [1]. The remained disadvantages of bio-absorbable magnesium are mainly about its corrosion regulation and biocompatibility. Moreover, insufficient mechanical property is problem to be faced in some loading bearing orthopaedic applications [2]. Based on literature investigations, it can be conclude that Mg-Zn-Gd alloy system exhibits a good combination of strength and ductility. Whether this kind of magnesium alloy can be used in the orthopaedic field attracts our great interest. Therefore, three Mg-Zn-Gd alloys are designed and fabricated in the present study and their potential in orthopaedic applications is studied.

**METHODS:** Three Mg-Zn-Gd alloys were cast and hot rolled into 1.5 mm thick sheets. The microstructure and mechanical property have been studied. Electrochemical measurements in Hank's solution have also been investigated. The indirect cell assays were taken to evaluate the cytotoxicity to two kinds of bone related cells, namely human osteoblast-like MG63 cell line and rat primary osteoblasts.

**RESULTS:** Mg-1.7Zn-0.2Gd was composed of single α-Mg phase, while Mg-1.0Zn-2.4Gd and Mg-1.9Zn-0.8Gd consisted of α, Mg<sub>5</sub>Gd and Mg<sub>3</sub>Gd<sub>2</sub>Zn<sub>3</sub> phases. The addition of Zn and Gd elements improved the strength and elongation of magnesium. Mg-1.7Zn-0.2Gd and Mg-1.9Zn-0.8Gd exhibited the favourable combination of strength and ductility. Electrochemical results implied that Mg-1.7Zn-0.2Gd alloy has the lowest corrosion rate of 0.117 mm/y, even lower than high magnesium. Besides, the morphology of Mg-1.7Zn-0.2Gd was uniform. In cell assay, enhanced cell viability of MG63 cells and rat primary osteoblasts was found in the Mg-1.7Zn-0.2Gd extract.

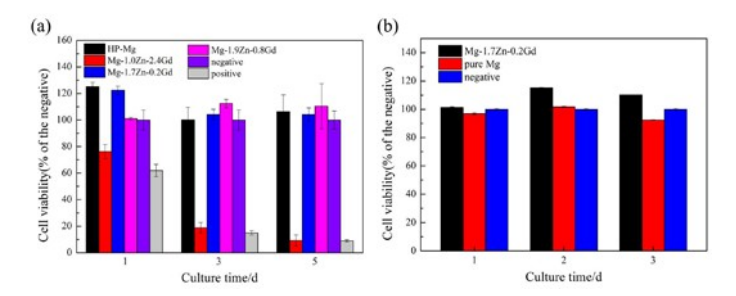


Fig. 1: Cell viability expressed as a percentage of the viability of cells cultured in negative control in the Mg-Zn-Gd alloy extracts: (a) MG63 and rat primary osteoblasts.

Table 1. Electrochemical corrosion data of three Mg-Zn-Gd alloys in Hank's solution.

Material	$i_{corr}(\mu A/cm^2)$	$V_{corr}$ (mm/y)
HP-Mg	$8.38 \pm 0.74$	0.1914±0.0170
Mg-1.0Zn-2.4Gd	$16.87 \pm 3.34$	$0.3853 \pm 0.0763$
Mg-1.7Zn-0.2Gd	$5.13 \pm 0.51$	$0.1172 \pm 0.0117$
Mg-1.9Zn-0.8Gd	13.93±3.09	0.3183±0.0707

**DISCUSSION & CONCLUSIONS:** From all the comprehensive and systematic investigations, we can conclude, Mg-1.7Zn-0.2Gd alloy has a favorable combination of strength and ductility, a low corrosion rate without obvious cytotoxicity. It's one kind of promising biodegradable magnesium alloy in orthopedics.

**ACKNOWLEDGEMENTS:** This work supported by the National Basic Research Program of China (973 Program) (Grant No. 2012CB619102), National Science Fund for (Grant Distinguished Young Scholars 51225101), National Natural Science Foundation of China (Grant No. 51431002 and 31170909), the NSFC/RGC Joint Research Scheme (Grant No. 51361165101), State Key Laboratory Mechanical Behavior of Materials (Grant No. 20141615).

### Improvement of coating adhesion ability on magnesium by femtosecond laser surface modification

J Park<sup>1,2</sup>, HS Han<sup>1</sup>, S Lee<sup>1</sup>, J Park<sup>1</sup>, YC Kim<sup>1</sup>, M OK<sup>1</sup>, HK Seok<sup>1</sup>, S Chung<sup>2</sup>, J Lee<sup>3</sup>, H Jeon<sup>1</sup>

<sup>1</sup> <u>Center for Biomaterials</u>, Biomedical Research Institute, Korea Institute of Science and Technology, Seoul, Korea

<sup>2</sup> <u>Small+integrative device laboratory</u>, Department of Micro/Nano system, Korea University, Seoul, Korea

<sup>3</sup> School of Advanced material Engineering, Kookmin university, Seoul, Korea

INTRODUCTION: Laser surface engineering is emerging as a new tool for micro/nano structure modification of materials due to its simple and effective process. Recently, technology utilizing the femtosecond (fs) laser has been highlighted in the field due to various advantages, which includes laser texturing technique one-step process to easily form macro/nano structure on materials [1]. Changes of surface structure results in alteration of several properties such as roughness, surface energy, and wettability. In this study, surface wettability of Mg was modified into superhydrophilic state to achieve improvement in adhesion using fs coating laser modification method. Modified surfaces were coated with biodegradable polymers and compared with that of pure Mg.

**METHODS:** Pure Mg strips (Kojindo Japan.) with 99.9% purity were prepared (8 mm x 8 mm x 1 mm) for surface modification. The irradiating laser source was constituted by a regenerative amplified ytterbium ( $\lambda$ =343 nm) delivering 400 fs pulse at a repetition rate of 1 kHz. Average pulsed power was 160  $\mu$ J and scan speed was 0.5 mm/s. Poly (L-lactic acid) (PLLA, L 214 S), Poly(lactide-coglycolide)(PLGA, LG 857 S) were spin-coated on the surface of laser treated Mg.

**RESULTS**: Top inset images from Figure 1 (a) and (b) shows the difference in microstructures formed by laser modification, which results in significantly different contact angle. Compared non-laser treated control samples, laser treated group shows significantly lower contact angle (Control: 55±10.5°, Laser treated: <10°). This result indicated that the surface property of pure Mg changed into hydrophilic wettability by laser irradiation, which could lead to improvement in adhesion strength of the coating layer at the modified surface. We observed superior adhesion strength and greater contact surface area for both polymer coating on super-hydrophilic Mg. In the immersion test and cell viability test also showed noticeably improved corrosion properties when compared to the control group.

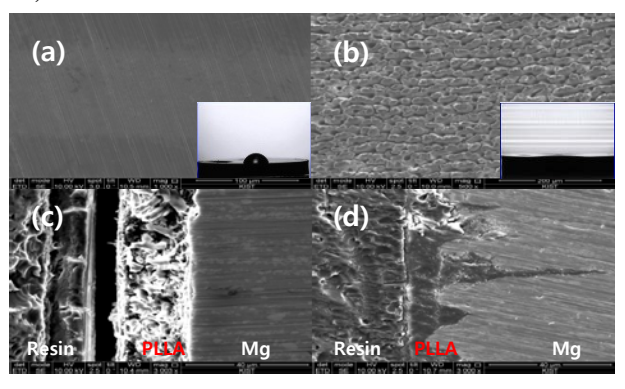


Fig. 1: Surface profile, and contact angle (inset) of (a) control and (b) laser modified surface and cross-section images of PLLA coating layer on (c) control and (d) laser modified surface.

DISCUSSION & CONCLUSIONS: In this study, through a surface modification using the fs laser texturing, the surface morphology of the Mg was changed into micro/nano structure resulting in improvement of adhesion strength due to imbedded coating layer between pits and grooves. Change in surface structure turned Mg surface property into hydrophilic state, which allowed formation of more adhesive, quicker and denser coating layer using biodegradable polymers. Such technology can be applied in wide range of biomedical application.

**ACKNOWLEDGEMENTS:** This research was supported by Basic Science Research Program through the National Research Foundation of Korea (NRF) funded by the Ministry of Education (2009-0093814) and KIST Project (2E25260)

#### Precipitation hardening on hardness, grain size and corrosion of WE32

R Peters<sup>1</sup>, P Maier<sup>1</sup>, C.L. Mendis<sup>2</sup>, N Hort<sup>2</sup>

<sup>1</sup>University of Applied Sciences Stralsund, Stralsund, Germany. <sup>2</sup>Helmholtz-Zentrum Geesthacht, Geesthacht, Germany

**INTRODUCTION:** Precipitation hardening is one of four strengthening mechanisms available for Mg alloys. Strength and hardness increase due to the formation of extremely small uniformly dispersed particles within the matrix can be very high. This is accomplished by phase transformation through appropriate heat treatments. The solution heat treatment (T4), results in a single phase (solid solution supersaturated with B atoms) and precipitation heat treatment (T6), where βprecipitates form as finely dispersed particles, causing peak hardness, followed by overaging (hardness decrease). The change in properties during heat treatment depends on the alloy itself (solubility of B in α-phase, diffusion and formation of β-phase). Improvement in mechanical properties will affect corrosion properties (by microgalvanic corrosion of nobel β-phase and less nobel  $\alpha$ -matrix).

MATERIAL & METHODS: The Mg-alloy used in this study is Mg3Y1.5Nd0.4Gd0.4Dy (WE32). The WE43 (alloy with a similar composition) has shown acceptable biological response [1]. Alloy was T4 heat treated for 8h quenched in cold water. T6 was at 250°C for times up to 10h. Hardness was evaluated with a Zwick Hardness Tester ZHU/Z2.5. Corrosion properties were investigated with potentiodynamic polarization (3-electrode cell, Ringer solution, 37°C, scan rate 50mV/min, circulating electrolyte, Ø 10mm²).

**RESULTS:** The extruded alloy has a hardness of 67HV1. Fig. 1 shows influence of heat treatment on hardness. The supersaturated  $\alpha$ -phase (T4) shows a hardness decrease. Ageing up to 8h causes an increase in hardness, followed by a decrease (overaging).

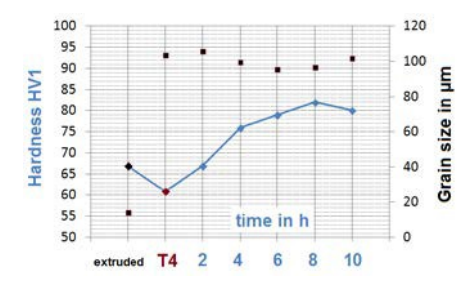


Fig. 1: Influence of T4 and T6 heat treatment on hardness and grain size of extruded WE32

Fig. 2 shows the influence of heat treatment on corrosion (by potentiodynamic polarization): fine grained extruded material and peak aged alloy (T6) indicate lower current density (no breakdown up to 4000mV for extruded material, breakdown at 3600mV for T6). T4 shows highest corrosion rate.

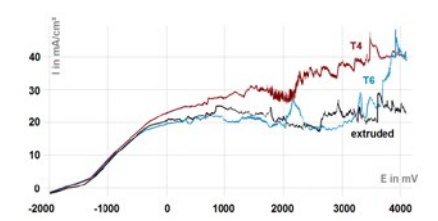


Fig. 2: Influence of heat treatment on current density -voltage curves.

Micrographs (Fig. 3 for the extruded condition) reveal the form of corrosion after exposure to 4000mV. The corroded area and depth as well as change in weight have been used for comparison.

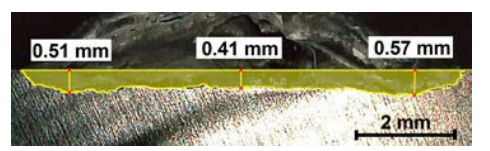


Fig. 3: Corroded WE32-T6, evaluated at 4000mV

**DISCUSSION & CONCLUSIONS:** Hardness decrease of the supersaturated  $\alpha$ -phase (T4) is mostly due to the increase in grain size during heat treatment. At the peak hardness finely dispersed β' precipitates were observed. The oxide layer formed during T6 treatment is resistant up to breakdown voltage of 3600mV due to microgalvanic corrosion of precipitates and  $\alpha$ -matrix. The as-extruded condition does not show breakdown; finer grains seem to decrease corrosion (~5mm<sup>2</sup>). T4 reveals the largest corroded area of ~11mm<sup>2</sup>, illustrating the highest current density. All conditions tend to pitting corrosion, causing stress peaks by notch effects when additionally loaded. Dangerously narrow and deep pits were observed in extruded condition (coarse β-phases). Less harmful pits (wide, shallow) are found in T6, due to uniformly distributed fine β'-phase, which has the lowest current density within passivation and smallest corroded area, Fig. 3.

[1] F. Witte et al. (2005) Biomaterials 26:3557

#### Effect of mechanical stress on degradation of Mg-based biodegradable metals

Y Koo<sup>1</sup>, Y Jang<sup>1</sup>, GL Song<sup>2</sup>, J Sankar<sup>1</sup>, Y Yun<sup>1</sup>

<sup>1</sup> Engineering Research Center for Revolution Metallic Biomaterials, North Carolina A&T State University, NC, USA. <sup>2</sup> Oak Ridge National Laboratory, TN, USA. Email:yyun@ncat.edu(Y.Yun)

**INTRODUCTION:** Biodegradable metallic implants in human body undergo complicated stress conditions such as tensile, compressive, shear stress [1]. The relationship between the healing process and mechanical resistance integrity is critical during gradually degraded in the body. Here, we report the effect of mechanical stress on corrosion and overall integrity of biodegradable metals.

METHODS: Stress corrosion cracking (SCC) test was conducted with two magnesium alloys (AZ31B and ZE41A) in Hank's Balanced Salt solution followed by ASTM G39 standard (Four points loaded). Stress was applied with 120 MPa, mimicking physiological condition for 30 days and 90 days. Standard immersion test as a control was also performed without stress. SEM with EDX and CT were used to perform to characterize morphology and four point bending test was done using Instron machine.

**RESULTS:** We observed the difference of the SCC mechanism between AZ31B and ZE41A shown in Fig. 1. Transgranular stress corrosion cracking (TGSCC) of AZ31B was progressed with the localized corrosion area, whereas intergranular stress corrosion cracking (IGSCC) was progressed in ZE41A [2].

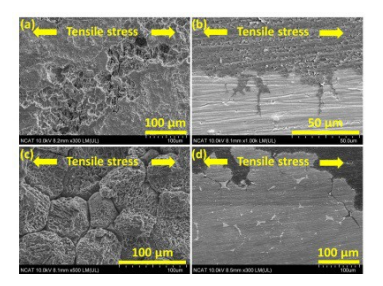


Fig.1: The SEM images of surface and cross-section. (a), (b) for AZ31B, and (c), (d) for ZE41A after stress corrosion test for 30 days.

After long-term four-point bending test, flexural stress-strain curves of AZ31B and ZE41A were acquired (Fig. 2a). Mechanical properties (elastic modulus and yield strength 0.05 % offset) were reduced and weight of the tested AZ31B and ZE41A alloys under stress were decreased slightly (Fig. 2b).

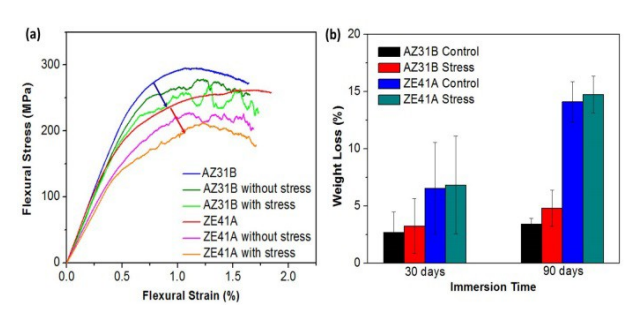


Fig.2: (a) Representative flexural stress-strain curves of AZ31B and ZE41A for 90 days, and (b) Weight loss after 30 and 90 days.

Fig. 3 shows the surface area and depth of localized corrosion. We observed that stressed AZ31B and ZE41A samples show more localized corrosion.

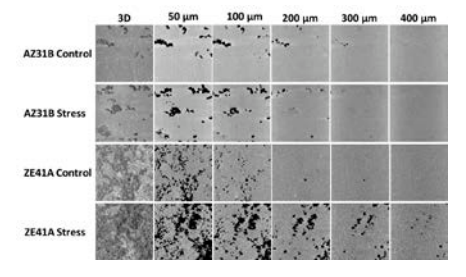


Fig.3: (a) Representative flexural stress-strain curves of AZ31B and ZE41A for 90 days, and (b) Weight loss after 30 and 90 days.

**DISCUSSION & CONCLUSIONS:** Stress corrosion cracks were observed in both AZ31B and ZE41A alloys. Effect of stress for corrosion rate and susceptibility of SCC were observed in AZ31B than ZE41A.

**ACKNOWLEDGEMENTS:** This work was supported by NIH grant (1SC3GM113728-01) and NSF-ERC for Revolutionizing Metallic Biomaterials (NSF-0812348).

### Assessment of electrochemical data for calculation of degradation of Mg and Mg-alloys

WD Mueller<sup>1</sup>, F Goetze<sup>1</sup>, F Feyerabend<sup>2</sup> and Biomaterial Research Gr., CC3 Charité Universitaetsmediz.

<sup>1</sup> Dental and Biomaterial Research Gr., CC3 Charité Universitaetsmedizin Berlin D

<sup>2</sup> Helmholtz Centre Geetshacht D

**INTRODUCTION:** Electrochemical measurements are commonly used to assess the degradation behaviour of Mg and Mg-alloys for biomedical applications. Easy handling and a lot of data which contain information about the conditions in the interface are the reason therefore.

At least the interpretation of the data is less as easy and so systematic failures can be seen in the literature. The aim of this paper is to show the possibilities of interpretation of electrochemical measurement data from voltammetry and impedance spectroscopy.

**METHODS:** Pure Mg and Mg-Ag-alloys (HZG) (Mg6Ag and Mg8Ag) were used for the electrochemical measurements which performed solution. in cell culture measurements were made by using the Mini-Cell-System with a measurement area of 0.5 mm<sup>2</sup> at room temperature and at 37 °C. All specimens were treated with 2500 SiC paper and cleaned in ethanol 96 % prior to measurements. Various measurement protocols have been realised. 1. Open circuit measurements (OCP) for 15 min and 2. cyclic voltammetry (CV) measurements starting at a distance of 0.5 V and 1.0 V vs. OCP in cathodic direction and 0.5 V vs. OCP in anodic direction with a scan rate of 10 mV/s, for 5 cycles. 3. Electrochemical Impedance spectroscopy (EIS) was performed, with 3 different amplitudes, 5mV, 10mV and 15 mV.

**RESULTS:** Depend on the quality of the specimens, in case of pure Mg some variations in the electrochemical behaviour can be observed. After the second cycle the interface activity seems to be equilibrated. The Mg-Ag alloys show some variations with time. Fig.1 shows an example of measurement on pure Mg in cell culture solution and an extraction of back ward scans for analysing the corrosion rate. The results are shown in Fig. 2. Depend on the number for exchanged electrons z=2 or z=4 in case of considering MgH<sub>2</sub> as a part of the back ward reaction.

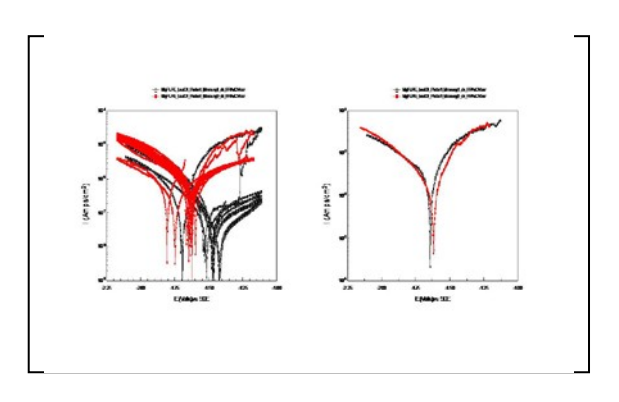


Fig. 1: I vs E curves of Mg (pure) in cell culture medium, 10mV/s: left: whole cycles at two different time points; right only one back ward scan

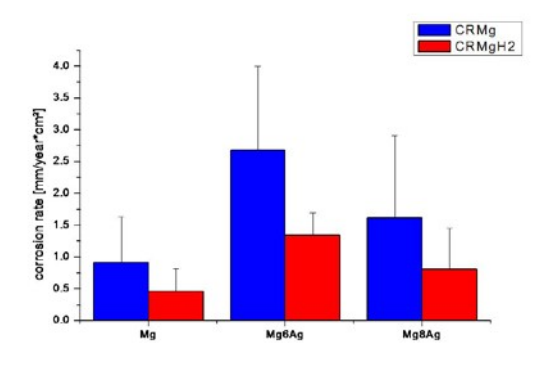


Fig. 2: Calculated corrosion rate for Mg, Mg6Ag and Mg8Ag in cell culture medium, using two different approaches.

**DISCUSSION & CONCLUSIONS** It is clear to see that depend on the way of assessment of corrosion rate different values can be obtained. The question is, which are the reliable one's? Based on the assumption of the reaction pathway for the forward scan as:  $Mg + 2H_2O \Leftrightarrow Mg^{2+} + H_2 + 2OH^{-} \text{ (1)} \text{ and the backward scan as:} MgH_2 \Rightarrow Mg^{2+} + 2H^{+} + 4e^{-} \text{ (2)}$ A more or less reliable set of data about the degradation rate of Mg can be obtained. Of course a more detailed description of the parameter of measurement is demand.

### Laser surface structuring: a method to change topography, promote coating deposition and reduce corrosion rate

AG Demir<sup>1</sup>, TB Taketa<sup>2</sup>, R Tolouei<sup>3</sup>, V Furlan<sup>1</sup>, C Paternoster<sup>3</sup>, MM Beppu<sup>2</sup>, D Mantovani<sup>3</sup>, B Previtali<sup>1</sup>

**INTRODUCTION:** High degradation rate of Mg alloys is an important limitation for their use in biomedical implants [1]. The deposition of a biodegradable coating is a well-established strategy allowing the control of the degradation rate [2]. Morphology, structure and adhesion of the deposited layer are strongly affected by the substrate topography, so that a surface pretreatment, for example by laser, plays a fundamental role in the definition of the final properties of the coating [3]. In this work, a Mg alloy (AZ31) surface was laser treated to produce a series of finishing with different features; the treated surfaces were then coated with a layer by layer (LbL) technique, to produce a multi-layered polysaccharide coating. The relation between surface topography and corrosion mechanism is analysed.

METHODS: AZ31 Mg-alloy samples were laser cut from sheet with 0.4 mm of thickness (R<sub>a</sub>= 255±10 nm). Pulsed fibre laser source was used to obtain surfaces at higher roughness (R<sub>a</sub>=1069±50 nm) and lower roughness ( $R_a=216\pm10$  nm) [4]. The treated surfaces were evaluated by the sessile drop method for contact angle assessment: the nonstructured surface showed a contact angle of 61°, while the high and low roughness surface showed respectively a contact angle of 22° and 69° Both as-received and laser treated surfaces were coated by a cellulose acetate (CA) primer, followed by LbL alternate layers of carboxymethyl cellulose (CMC) and chitosan (CHI). In order to compare the degradation behaviour of all the treated samples, a static immersion test was carried out in phosphate buffer saline solution for 14 days according to ASTM NACE/ASTMG31-12a.

**RESULTS:** Figure 1 shows SEM images of coated samples with different surface topographies. The surface topography exhibits high influence on the generated coating morphology. Non-structured and surfaces with reduced roughness show porous and non-homogeneous coating. On the contrary surface with increased roughness presents a denser coating morphology. This result is related to the evidences of degradation test. As it is showed by results in

table 1, surface with increased roughness exhibits the lowest average corrosion rate value.

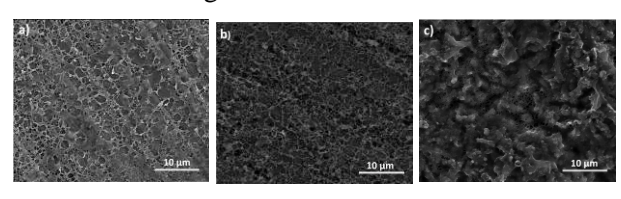


Fig. 1: Coating morphologies on a) nonstructured, b) reduced roughness, c) increased roughness.

Table 1. Average corrosion rates (CR) different sample types

	Non-coated	Coated
Surface	CR [mm.yr <sup>-1</sup> ]	CR [mm.yr <sup>-1</sup> ]
Non-structured	$1.37 \pm 0.02$	$1.17 \pm 0.05$
Increased roughness	$1.52\pm0.05$	$1.27 \pm 0.01$
Reduced roughness	$1.32 \pm 0.01$	$1.15\pm0.01$

**CONCLUSIONS:** The bio-degradation rate of Mg alloys can be significantly decreased with the proposed coating strategy. Moreover, the coating morphology is highly influenced by the underlying surface morphology and wettability. This gives way to tailoring surface morphologies to enhance and control the bio-degradation rate of Mg alloys.

**ACKNOWLEDGEMENTS:** The authors acknowledge the support from São Paulo Research Foundation and Quebec Government for partially funding the research under Project Number 08.205.

<sup>&</sup>lt;sup>1</sup><u>Department of Mechanical Engineering</u>, Politecnico di Milano, Milan, Italy, <sup>2</sup> <u>School of Chemical Engineering, University of Campinas</u>, Campinas, São Paulo, Brazil, <sup>3</sup> <u>Lab. for Biomaterials and Bioengineering, Laval University</u>, Quebec City, Canada.

### In-vitro corrosion behaviour of Mg-2Nd-1Y-0.5Mn-0.5Zn-0.4Zr alloy with double-layered thin film

K Hanada<sup>1</sup>, H Ueda<sup>2</sup>, M Inoue<sup>2</sup>, K. Matsuzaki<sup>1</sup>

<sup>1</sup> <u>Advanced Manufacturing Research Institute</u>, National Institute of Advanced Industrial Science and Technology (AIST), JAPAN. <sup>2</sup> <u>Product and Research Development Division</u>, Fuji Light Metal Co., Ltd., JAPAN

**INTRODUCTION:** Mg and its alloy show promise as base materials for biodegradable medical implants in cardiovascular and orthopedic and oral surgeries. However, tailoring their biodegradation periods to various implants' needs is not easy, and many studies on the surface coating and surface modification have been conducted to achieve the biodegradation control [1,2]. Here, we report the surface modification of Mg-2Nd-1Y-0.5Mn-0.5Zn-0.4Zr alloy and its invitro corrosion.

**METHODS:** Mg-2Nd-1Y-0.5Mn-0.5Zn-0.4Zr designed for biodegradable allov medical applications was prepared in Ar atmosphere by RF induction melting at 720°C and by casting into a low carbon steel crucible. The alloy billet was extruded at 400°C with an extrusion ratio of 24 and was rolled repeatedly at 350°C until 90% reduction in thickness. Then the rolled sheet was cut into the plate shape (W9×D15×t1.4 mm) for immersion test, and the plate samples were mechanically polished up to #1000 grit and were treated in acid solution (pH 0.3) to modify their surfaces. The modified surface of the sample was analyzed using the pulsed RF GD-OES (GD-profiler2, HORIBA) and FE-SEM (Gemini, ZEISS). The plate samples were immersed in bovine serum at 37°C. The corrosion behaviour was observed and then the corrosion rate was determined by mass loss.

**RESULTS:** Figure 1 shows the cross-sectional image of the surface modified sample. The sample obviously has a double-layered thin film, and the top and bottom layers are approximately 50 nm and 70 nm in thickness, respectively. Figure 2 shows the depth profiling result. This result indicates that the top layer mainly consists of hydroxides derived from Mg, Mn, Zn, and Nd, whereas the bottom layer mainly consists of oxides derived from Mg, Zn, Nd, and Y. The corrosion rate of this sample is 1.1 mm/y, and this is 63% lower than that of the as-polished sample, 3.0 mm/y. Moreover, the surface modified sample shows uniform corrosion, against the local corrosion of the as-polished sample.

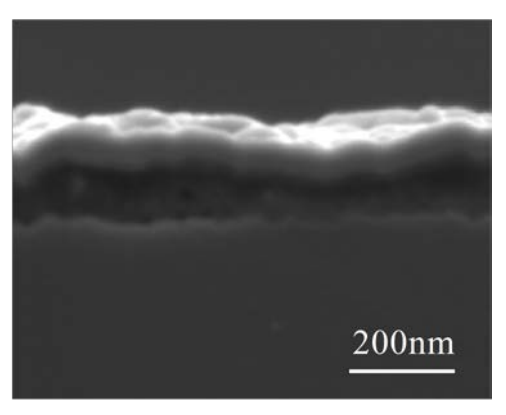


Fig. 1: Cross-sectional SEM image of the plate sample for immersion test.

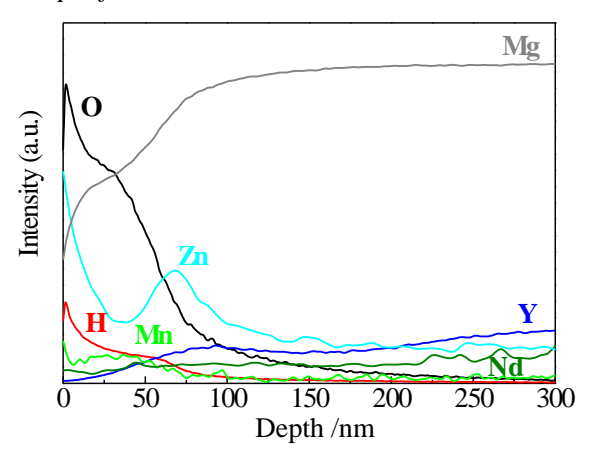


Fig. 2: Depth profile of the plate sample by pulsed RF GD-OES.

**DISCUSSION & CONCLUSIONS:** The Mg-2Nd-1Y-0.5Mn-0.5Zn-0.4Zr alloy had double-layered thin film derived from its alloy compositions by surface modification with acid solution, and the consequent corrosion resistant was much improved. These results obtained in this study shows great potential of material design considering surface modification for controlling the biodegradation of Mg-based implants.

#### In vitro degradation of HA-silica coated AZ91 magnesium alloy in SBF

Y. Moharrer<sup>1</sup>, S. Saber-Samandari<sup>2</sup>, Gh. Rouhi<sup>1</sup>

**INTRODUCTION:** The high corrosion rate of biodegradable magnesium alloys the physiological environment results degradation before the complete healing of the tissue [1]. Depositing Hydroxyapatite (HA) on the surface of the Mg alloys using Electrophoretic Deposition (EPD) technique can improve the bioactivity and corrosion behavior of Mg alloys. However, controlling the adhesion of HA to the surface using EPD is difficult. Silica is a bioactive substance with therapeutic properties that increases the adhesion of deposited HA to the surface of the substrate [2, 3]. This work intends to investigate the in-vitro corrosion behavior of HA-silica coated by EPD on AZ91 Mg alloy.

**METHODS:** Three rods of AZ91 (D: 3mm, L: 40mm) were coated by HA particles (6gr/l) dispersed in the ethanol solution under constant voltage and time (30 V, 1min). Three other rods with the similar dimensions were, first, coated by silica nano particles (6gr/l) dispersed in ethanol solution under constant voltage and time (30V, 10 min). Subsequently, HA powders were deposited on the silica-coated substrates to produce HA-silica coated samples. Three rods of each group including uncoated, HA coated, and HA-silica coated were immersed in SBF solution (suggested by [4]) for one, two and three weeks. The concentration of magnesium ions in the SBF solution was measured by ICP-AES. The corrosion rate of the samples was measured by weight loss method. The coating morphology and the surface characteristics of the samples after one week of immersion were analyzed by SEM.

RESULTS: SEM analysis of HA-silica coated samples shows interlocking between two layers (HA and silica) at their interface (Fig 1.a). SEM analysis also showed the formation of apatite layer (rich in calcium and phosphorous) on the surface of the HA-silica coated sample after one week of immersion (Fig. 1.b). Bioactive samples can bond to a living bone via this apatite layer. According to the results extracted from ion release and weight loss, although HA coated samples have the lowest corrosion rate compared to the others, the implant completely corroded after three weeks of

immersion (high amount of sedimentation) (Fig. 2, a, b). In contrast, corrosion rate for HA–silica coated samples decreases with a more uniform speed compared to other samples, moreover HA-silica coated samples produce less sediment compared to the other samples (the sample was not corroded completely after three weeks of immersion) (Fig. 2, a, b).

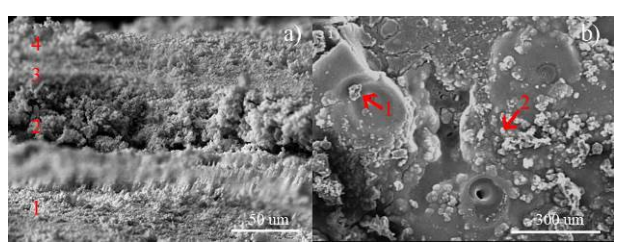


Fig. 1: a) Microstructure of HA-silica coated sample: substrate (1), silica layer (2), interface (3), HA Layer(4), b) formation of calcium phosphate particles on the HA-silica coated sample after 1 week immersion in SBF: granular apatite particles (1), Calcium and Phosphorus (2).

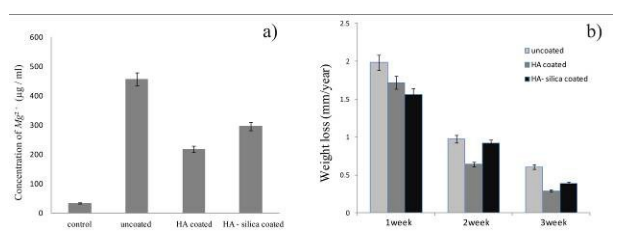


Fig. 2: a) The magnesium concentration of the SBF after three weeks immersion, b) weight loss of the samples in three consecutive weeks.

**DISCUSSION & CONCLUSIONS:** Results indicate improved in-vitro corrosion behaviour for the HA-Silica coated sample, which relates to the better adhesion of HA layer to the substrate's surface using silica intermediate layer. However to verify the efficiency further in-vivo degradation studies are required.

<sup>&</sup>lt;sup>1</sup> <u>Faculty of Biomedical Engineering</u>, Amirkabir University of Technology, Iran

<sup>&</sup>lt;sup>2</sup> <u>New Technologies Research Center</u>, Amirkabir University of Technology, Iran

#### In vitro corrosion behaviour of MAO and silica coated AZ91 magnesium alloy

Y Moharrer<sup>1</sup>, S Saber-Samandari<sup>2</sup>, Gh Rouhi<sup>1</sup>

<sup>1</sup> <u>Faculty of Biomedical Engineering</u>, Amirkabir University of Technology, Iran, <sup>2</sup> <u>New Technologies Research Center</u>, Amirkabir University of Technology, Iran

**INTRODUCTION:** Although biodegradable magnesium and its alloys are promising new materials as bone implants [1], but their high corrosion rate limits their applications in the physiological environment [2]. It is known that applying protective biocompatible coatings can greatly reduce their corrosion rate [1]. This research investigates the corrosion behaviour (evaluated by in vitro degradation experiment) and the average hardness (measured by nano indentation test) of AZ91 magnesium alloy coated Micro Arc Oxidation (MAO), Electrophoretic Deposition (EPD) method.

METHODS: six rods (D: 3mm, L: 40mm) and two plates (L: 9mm, W: 9mm, H: 3mm) of AZ91 were coated by MAO method (in a solution which contained KOH (40 gr/l), NaOH (200 gr/l), and NN<sub>2</sub>SSS<sub>3</sub> (960 gr/l), under constant voltage and time (45 V, 5 min)) and EPD method, (in a suspension which contained silica nanoparticles (6 gr/l, and ethanol, under constant voltage and time (30 V, 10 min)). Three rods of each group including uncoated, MAO coated, and silica coated were immersed in SBF solution (suggested by [3]) for one, two and three weeks to measure their corrosion rate by the weight-loss method. Microstructure of the coating layers and corroded surface of the samples were evaluated by SEM. The average hardness for coated layers deposited on the plates was also measured by nano indentation test.

**RESULTS:** The SEM micro-structural analysis of the MAO layer shows the existence of the higher level of the porosities on its surface in contrast with silica layer (Figure 1.a, b). Table 1 shows the in vitro degradation rate and hardness of the samples. According to Table 1, silica coated samples have the lowest corrosion rate which decreases with a more uniform speed in comparison to the other samples as times goes on . The SEM micro-structural analysis of the corroded surface of the coated samples revealed that the pitting corrosion is higher on the surface of the MAO layer compared to silica layer (Figure 2.a, b).

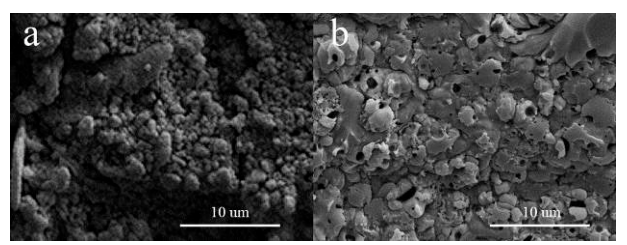


Fig. 1: SEM micrographs of a) MAO layer b) silica layer.

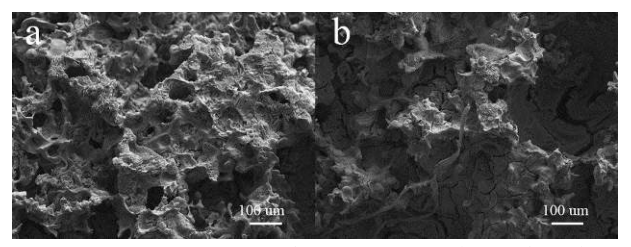


Fig. 2: SEM micrographs of a) MAO layer b) silica layer after 1 week immersion in SBF.

Table 1. Corrosion rates in three consecutive weeks and hardness of the samples.

	Corrosion rate (mm.yr <sup>-1</sup> )			Hardness (GPA)
	1 st	2 <sup>st</sup>	3	
Uncoated	1.98	0.97	0.60	<u>-</u>
MAO coated	2.17	0.96	0.53	$6.7 \pm 0.1$
Silica coated	1.7	0.87	0.39	$0.13 \pm 0.15$

DISCUSSION & CONCLUSIONS: According to Table 1, both MAO and EPD coating techniques reduce the corrosion rate of AZ91 to the noticeable extent. The pitting corrosion in MAO layer is higher than that of silica layer, due to the more penetration of the corrosive medium as a result of the higher level of the porosity of MAO surface. Additionally, the surface corrosion of the MAO coated sample is less uniform than the surface corrosion of the silica coated sample due to the higher hardness of the MAO layer. Further research is needed to find an optimal corrosion rate and corrosion mechanism for AZ91 Mg alloy.

#### Bioactive iron foam modified with CaP coating for bone scaffold applications

Y Su<sup>1, 2</sup>, S Champagne<sup>1</sup>, H Hermawan<sup>1</sup>, D Mantovani<sup>1</sup>

<sup>1</sup> <u>Lab. for Biomaterials & Bioengineering</u>, Dept. Min-Met-Materials Engineering & University Hospital Research Centre, Université Laval, Québec City, Canada.

**INTRODUCTION:** Porous iron was proposed for biodegradable metal-based bone scaffolds due to its strength, degradability and essential roles in human body metabolism [1, 2]. The foam structure greatly enhanced its degradation rate, but its excessive degradation could be harmful to the wound healing, especially at the early stage of operation [3]. Coating can therefore be developed to modulate the degradation rate of the iron foam structure. In this work, the degradation of pure iron foam was controlled by calcium phosphate (CaP) coating, which also has the potential to increase surface bioactivity toward bone cell proliferation.

**METHODS:** Open-porous pure iron foam (purity 99.9%, pore size = 800 um, porosity = 88%) was used as the substrate material. Before the coating process, the substrate was pre-treated in the 2% HNO<sub>3</sub> solution to remove the oxide on the surface. CaP coating was deposited by chemical conversion method. The electrolyte was prepared by dissolving 0.1 mol/L Ca(NO<sub>3</sub>)<sub>2</sub> in 10 ml/L H<sub>3</sub>PO<sub>4</sub> at pH 2.8 and 60 °C. After deposition, the specimens were rinsed in distilled water and then were dried. Corrosion resistance of the pure iron and CaP coated iron foam were evaluated by potentiodynamic polarization in Hanks' solution.

**RESULTS:** The typical surface morphology of the CaP coated iron foam is shown in Fig. 1. It can be observed that the foam is fully covered with the CaP coating with random distributed flakes. The EDS result showed that both of the Ca and P contents are around 13at%, while the Fe content is 1.3at%. The Ca/P atom ratio is 1.1, slightly higher than that of dibasic calcium phosphate dihydrate (DCPD). The potentiodynamic polarization curves are shown in Fig.2. Corrosion rate for the coated foam is estimated to be more than one order of magnitude lower than that of the uncoated foam.

**DISCUSSION & CONCLUSIONS:** The CaP coating surface has a high roughness, which could be helpful for the cells to infiltrate into the foam implants then to accelerate the healing of damaged bone. The lower corrosion rate for the coated foam is helpful to decrease the harmful degradation

products of pure iron implants at the early stage of operation.

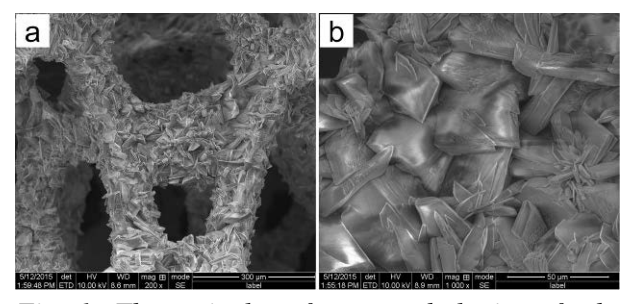


Fig. 1: The typical surface morphologies of the CaP coated iron foam (a: lower magnification, b: higher magnification).

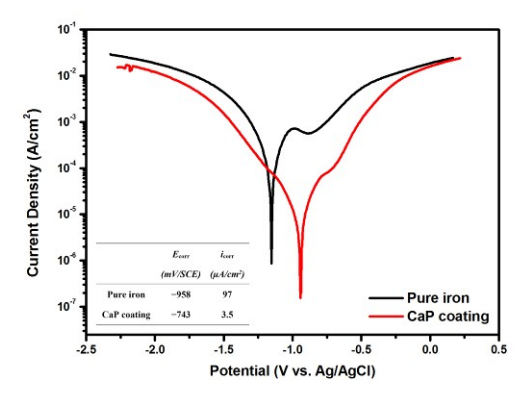


Fig. 2: The potentiodynamic polarization curves of the pure iron and CaP coating in Hanks' solution. Inset: Estimated corrosion rates from derived from the polarization curves.

**ACKNOWLEDGEMENTS:** This work was supported by the Natural Science and Engineering Research Council of Canada and the China Scholarship Council (CSC).

<sup>&</sup>lt;sup>2</sup> <u>The Key Lab of Automobile Materials</u>, Ministry of Education, College of Materials Science and Engineering, Jilin University, Nanling Campus, Changchun, China.

#### Effect of grain size on mechanical and corrosion properties of pure zinc

M Sikora-Jasinska<sup>1,2</sup>, E Mostaed<sup>1</sup>, D Mantovani<sup>2</sup>, M Vedani<sup>1</sup>

<sup>1</sup>Department of Mechanical Engineering, Politecnico di Milano, Milan, Italy
<sup>2</sup>Lab. for Biomaterials & Bioengineering (CRC-I), Dept. Min-Met-Materials Engineering & CHU de Quebec Research Center, Laval University, Québec City, Canada

**INTRODUCTION:** Zinc is considered as a promising candidate for a series of biomedical applications associated with blood vessels. Zn has been widely explored as an alloying element in Mg-based biodegradable alloys.

This work focused on the degradation behavior of pure Zn having different grain size in modified Hanks' solution. We hope to achieve some guidelines for a future design of biodegradable Znbased alloys. Comprehensive evaluations on *in vitro* corrosion behaviors of zinc were conducted in this work.

MATERIALS & METHODS: Warm rolling was carried out on samples cut from a Zn ingot with different reduction ratio of 10, 20 and 50%. Potentiodynamic and static immersion tests were carried out to identify the corrosion rate of the samples. Experiments were performed in Hanks' modified solution. Samples were immersed for 2 weeks in a controlled environment. Microstructure was characterized by optical and scanning electron microscopy. Mechanical properties were evaluated by tensile test. Ions released from the samples were assessed by atomic absorption spectroscopy (AAS).

**RESULTS:** Fig. 1 shows that after 10% of reduction grain size was remarkably decreased. However, no significant further grain refinement was observed after 20 and 50% reduction.

Table 1 summarizes the mechanical properties obtained from tensile test. As seen, the initial sample showed very poor mechanical properties which was attributed to its coarse grain structure. Nevertheless, remarkable grain refinement led to a meaningful improvement of tensile strength as well as elongation. Interestingly, regardless of the level of deformation mechanical properties are nearly similar for all rolled conditions.

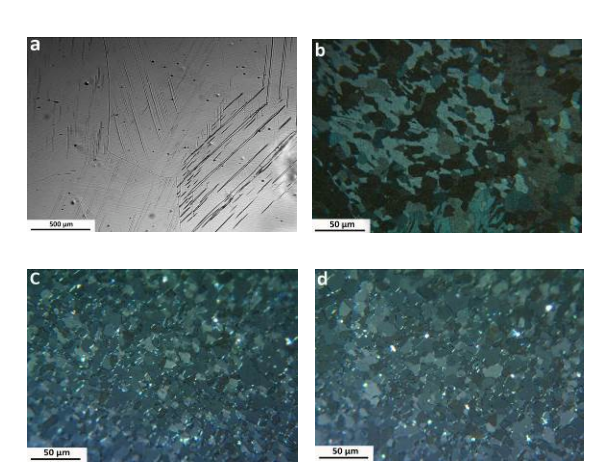


Fig. 1: Optical micrographs of pure Zn a) ingot, b) Zn 10% reduction, c) Zn 20% reduction d) Zn 50% reduction.

*Table 1. Tensile properties of all the samples.* 

Sample condition	TYS	UTS	E%
Ingot	22	26	0.5
10%	59	115	52
20%	53	110	46
50%	56	112	42

Fig. 2 shows that the corrosion rate reduced slightly with decrease of grain size in both static immersion test and potentiodynamic polarization.

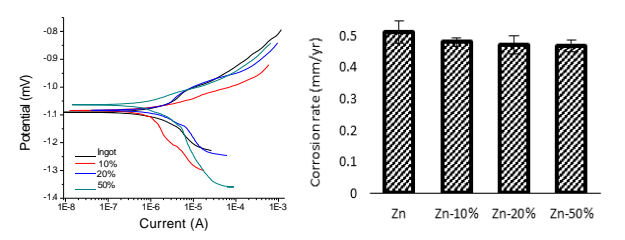


Fig. 2: a) Potentiodynamic polarization curves of Zn with different grain size b) degradation rate of Zn

**CONCLUSIONS:** The results confirmed that tensile strength and ductility of pure Zn were strongly influenced by grain size, improving with grain refinement. The corrosion rate obtained by potentiodynamic and immersion tests slightly decreased with decreasing grain size.

#### Cytotoxicity and antibacterial property of Mg-Ag alloys

Z Liu<sup>1</sup>, R Willumeit-Römer<sup>1</sup>, N Hort<sup>2</sup>, R Schade<sup>3</sup>, F Feyerabend<sup>1</sup>

<sup>1</sup> <u>Metallic Biomaterials</u>, Helmholtz-Zentrum Geesthacht, Germany. <sup>2</sup> <u>MagIC – Magnesium</u> <u>Innovation Center</u>, Helmholtz-Zentrum Geesthacht, Germany. <sup>3</sup> <u>Institute for Bioprocessing and</u> <u>Analytical Measurement Techniques</u>, Heilbad Heiligenstadt, Germany.

**INTRODUCTION:** Magnesium has a certain degree of antibacterial properties due to alkaline pH during corrosion [1]. However, there is room for improvement facing the challenge of clinical infection and arising of antibiotic-resistant bacteria [2]. To achieve better antibacterial behaviour of Mg alloys, effect of Mg-Ag alloys with different processing and silver content were studied.

**METHODS:** Extruded and T4 treated discs were used in this study. Cytocoxity and antibacterial property were characterized and compared with pure magnesium. Two different methods, live/dead staining and MTT were used to evaluate cytotoxicity. Human primary osteoblasts were seeded on the discs directly. Extracts of pure Mg and Mg-Ag alloys were prepared according to ISO 10993-12-2004. There is more silver existing in Mg8Ag extract (table 1). Extracts were diluted 1:5 and 1:10 by cell culture medium (CCM). Osteoblasts were pipetted into 96-wells plate. Cocultured *S. aureus* and *S. epidermidis* were used for antibacterial test in a bioreactor system (Fig. 1 a). Applied parameters are shown in table 2.

Table 1. Silver concentration in primary extracts.

Extracts	Pure Mg	Mg6Ag	Mg8Ag
Conc. (mg/L)	< 0.1	0.31	0.64

Table 2. Parameters of bioreactor system.

Ratio	Quantity	Flow (mL/min)	Temp. (°C)	Time (h)
1:1	$10^{6}$	0.3	37	15

**RESULTS:** Osteoblasts can attach and grow on pure Mg, Mg6Ag and Mg8Ag discs (Fig. 2 a). The amount of dead cells slightly increased with raising silver content. Nearly 50% of control cells can survive in pure extracts of pure Mg and Mg6Ag. Viability of osteoblasts in 1:5 extracts was at 75% of the control which is determined as no cytotoxic potential (Fig. 2 b). Viability of bacteria on Mg8Ag is significantly lower than viability on pure Mg (Fig. 1 b). There is no biofilm forming on Mg-Ag alloys (Fig. 3).

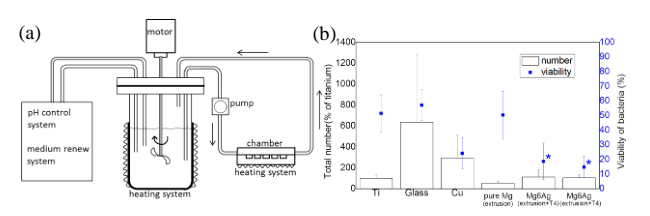


Fig. 1: (a) bioreactor system, (b) total number and viability of bacteria on discs.

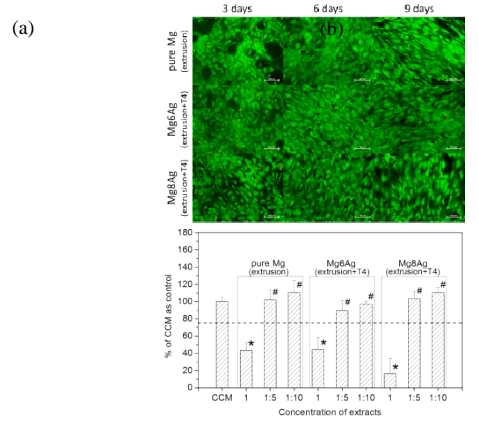


Fig. 2: (a) Live/dead staining of human primary osteoblasts, (b) viability of human primary osteoblasts in extracts.

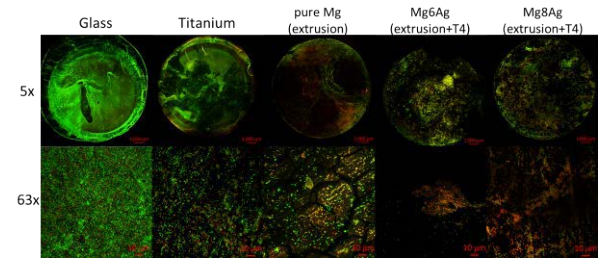


Fig. 3: Overview of biofilm and its details. Glass and titanium are internal control group.

**DISCUSSION & CONCLUSIONS:** Osteoblasts can attach and survive on both pure Mg and Mg-Ag discs, although pure extracts showed cytotoxic effects. Diluted extracts showed comparable cell viability to CCM. The Mg-Ag alloys have favourable antibacterial property, especially Mg8Ag, due to the higher silver release.

**ACKNOWLEDGEMENTS:** Juliane Zirm is thanked for her help in bioreactor run and bacteria count.

#### Molecular pathways involved in the immune response on magnesium alloys

MD Costantino<sup>1</sup>, BJC Luthringer<sup>2</sup>, R Willumeit-Römer<sup>1</sup>

<sup>1</sup> Helmholtz-Zentrum Geesthacht, Zentrum für Material- und Küstenforschung, Germany. maria.costantino@hzg.de

INTRODUCTION: Magnesium alloys are attractive materials in orthopaedics due their biodegradability and mechanical properties. The biological impact of the elements released during biodegradation on cells activities is still unclear. After implantation, cells of immune system are activated and molecules named "cytokines" are released. Macrophages are one of the most important sources of cytokines. Aim of this study was to analyse the influence of magnesium alloys elements on cytokines release.

**METHODS:** In order to investigate the influence of the degradation process of magnesium alloys on cytokines release, U937 cells line differentiated into macrophages with 5nM of phorbol 12 myristate 13 acetate (PMA) for 24h. Cells were exposed to extracts of commercial pure magnesium (CPMg, Mg10Gd and Mg2Ag) for 1 day. Extracts were obtained incubating discs (1mm x 10mm) of magnesium samples in cell culture media (0.2g/ml) under cells culture conditions for 72h. Defined concentration of magnesium, silver and gadolinium were obtained using mass spectrometry (ICP-MS). Subsequently, 1 to 10 diluted extracts (to decrease osmolality) were used to stimulate the cells<sup>1</sup>. The influence of mg alloys on targeted molecules released (Figure 1) using ELISA test was performed. In addition real time Polymerase Chain Reaction (RT-PCR was used to elucidated the contribution of Mg alloys on gene involved on macrophages activation (such as NFKB (nuclear factor-*kappa B*), IL 1β (interleukin 1β), CD36 (cluster of differentiation 36), OPN (osteopontin).

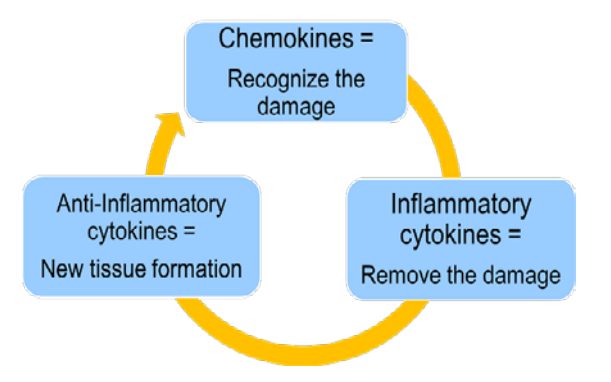


Fig. 1: Biological effect of 3 groups of cytokines analysed

**RESULTS & DISCUSSION:** Results obtained show a clear influence of magnesium alloys on macrophages activity. Anti-inflammatory cytokines such as IL-10 (interleukin-10) and IL1ra (interleukin-1 receptor antagonist) are upregulated, whereas inflammatory cytokines such as IL 1 $\beta$  and tumour necrosis factor alpha (TNF $\alpha$ ) are down regulated after stimulation with Mg2Ag and Mg10Gd extracts. Significant up regulation of TNF $\alpha$  was detected after stimulation with CPMg extracts.

PCR analysis show an increased expression of the inflammatory gene nuclear factor-*kappa B* (NFkB) in presence of CPMg. Genes involved in the (1) activation of macrophages (such as toll like receptor 2, TLR2 and, CD36) and (2) recruitment of macrophages on the site of damage (e.g., intercellular adhesion molecule 1, ICAM-1) are down regulated.

**CONCLUSION:** Our results suggest that the biological impact of Mg alloys on macrophages strongly influenced cytokines release. A common anti-inflammatory effect on the 3 different materials analysed was detected.

ACKNOWLEDGEMENTS: The research leading to these results has received funding from the People Programme (Marie Curie Actions) of the European Union's Seventh Framework Programme FP7/2007-2013/ under REA grant agreement n° 289163.

#### Alter increased magnesium levels the cell functionality in vitro?

A Bruinink<sup>1</sup>, Y Elbs-Glatz<sup>1</sup>

<sup>1</sup>Lab for Biointerfaces, Empa, St. Gallen, CH.

INTRODUCTION: The interest in degradable metal implants is steadily growing especially because of their mechanical properties. In case of magnesium-based degradable implants increased levels of Mg<sup>2+</sup>-ion at and nearby the implant-tissue interface will be present during degradation. Magnesium is thought to have anti-inflammation effects<sup>1</sup>. Various reports have been published regarding cellular reactions increased on magnesium levels, however, mostly without adequate controls. The aim of the present study was to fill this gap by comparing effects of Mg<sup>2+</sup> on differentiation of fibroblasts and macrophages by adding MgCl<sub>2</sub> and MgSO<sub>4</sub> to the cultures and using NaCl and Na<sub>2</sub>SO<sub>4</sub> at corresponding concentrations as controls. Fibroblasts macrophages are two cell types which play an important role in reactions on implants but also in wound healing processes.

METHODS: Primary human dermal fibroblasts (HDF) were cultured in RPMI-1640 medium containing 1% FCS, 2ng/ml TGF\u03b31 (to induce differentiation towards myofibroblasts) and Mg<sup>2+</sup> at a final concentration of 0.4, 1, 5 or 20mM. After 5 days the functional state of cells were assessed using the MTS assay and, in order to assess the degree of differentiation towards myofibroblasts, the percentage of  $\alpha$ -smooth muscle actin ( $\alpha$ -SMA) positive cells using flow cytometry. To explore the effects of increased magnesium levels on monocytes the human THP-1 monocytic leukemia cell line was taken. They were cultivated on thermoresponsive poly(N-isopropylacryl-amide) coated cell culture dishes and activated to resting state macrophages using 100nM phorbol-12myristate-13-acetate (PMA) (Bruinink et al, in preparation. They were subsequently polarized towards inflammatory M1 macrophages using medium containing LPS an interferon-y. In the next step M1 cells were harvested by cooling down the cultures. The harvesting step was included to exclude interfering effects of remaining bound LPS. Isolated cells were reseeded onto tissue culture treated polystyrene plates in culture medium with different concentrations of Mg<sup>2+</sup>. mRNA was extracted 24h thereafter. Quantitative real-time PCR was performed to assess the degree of M1 polarization by determining the relative expression of CD197, TNFα and CXCL10.

**RESULTS:** Independent from the salt added magnesium was able to significantly stimulate MTS conversion in HDF cultures with a maximum at 5 mM (Fig. 1). Such effect was not seen using the equivalent concentration of sodium salts. Preliminary results suggest that myofibroblast differentiation was not largely affected by magnesium ions. Currently, the effects on M1 macrophages are measured.

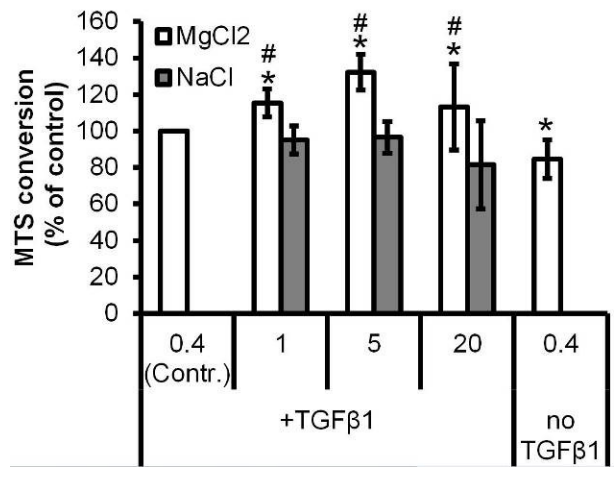


Fig. 1: Effects of Mg ions (mM) on MTS conversion in HDF cultures as measured after 5 days exposure. \*: significant different from control. #: significant different from cultures treated with equivalent concentration of NaCl in terms of chloride concentrations.

**DISCUSSION & CONCLUSIONS:** Based on the effects seen on HDF with equivalent Cl<sup>-</sup> and SO<sub>4</sub><sup>2-</sup> concentrations it may be concluded that slightly elevated levels (1-20mM) may modify specifically in this case total culture metabolic activity without affecting the state of differentiation.

**ACKNOWLEDGEMENTS:** We thank V Malheiro for her help in performing qRT-PCR. This project was part of the Empa internal project TECIT.

#### Influence of magnesium alloys degradation on human undifferentiated cells

F Cecchinato1, N Ahmad2, F Feyerabend2, R Jimbo1, R Willumeit-Römer2, A Wennerberg<sup>1</sup>

Department of Prosthodontics, Faculty of Odontology, Malmö, Sweden. 2 Helmholtz-Zentrum

Geesthacht, Geesthacht, Germany

INTRODUCTION: There is an increasing attention on magnesium as resorbable biomaterial for bone regeneration in orthopaedic and maxillofacial conditions. Initial cell adhesion and spreading after implant insertion into the host tissue are essential biological processes for establishing a stable crosslink for the upcoming cellular events around the implant surface [1]. Magnesium degradation has a direct influence on these processes, as its degradation is accompanied with hydrogen evolution and hence alkalinisation of the environment [2]. A further question is, whether the topographical features and chemical composition of the degraded surface can influence cell adhesion and development on the implant surface. In this study, the degradation properties of Mg2Ag, Mg10Gd and Mg4Y3RE alloys were analysed under cell culture conditions. The shortterm cell response of human umbilical cord perivascular cells (HUCPV) was investigated in terms of cell viability and adhesion.

METHODS: Discs of Mg2Ag (1.89% Ag, Mg Bal.), Mg10Gd (8.4% Gd, Mg Bal.) and Mg4YRE (3.45%, Y, 2.03% Nd, 0.84% Ce, Mg Bal.) were used in this study. High-purity magnesium (99.97% Mg) was used as control. Degradation parameters were analysed after 24 h, 48 h and 72 h incubation in culture medium of  $(\alpha$ -MEM+15%FBS+1%p/s) and cell culture conditions by means of mass loss determination, osmolality and pH-measurement, and energy dispersive x-ray spectroscopy (EDX). Surface topographical degradation was investigated with atomic force microscopy (AFM). Changes in cell viability and adhesion were evaluated culturing HUCPV on 24, 48 and 72 h pre-incubated materials with two staining assays: LIVE/DEAD staining and actin cytoskeleton/focal adhesion staining.

**RESULTS:** The pH and osmolality of the medium increased with increasing degradation rate, and this was most pronounced for Mg4YRE. The biological observations showed that HUCPV exhibited a more homogeneous cell growth on Mg alloys compared to high-purity Mg, where they showed a clustered morphology. Cells exhibited a slightly higher density on Mg2Ag and Mg10Gd in comparison to Mg4Y3RE, due to the lower

alkalinisation and osmolality of the microenvironment. However, cells grown on Mg10Gd and Mg4Y3RE generated more developed and healthy cellular structures, leading to better adhesion on the surface. This can be attributable to a more stable degradation layer that prevents further localized degradation on the surface.

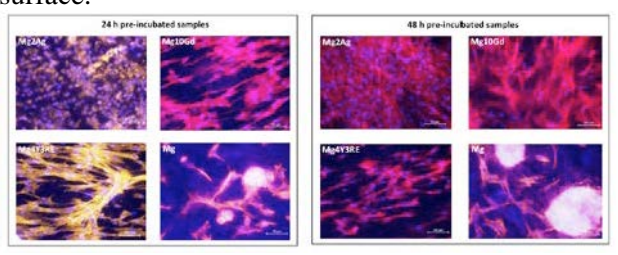


Fig. 1: Confocal fluorescence microscopy of focal adhesion and actin cytoskeleton in HUCPV cells cultured for 24h on 24 and 48h pre-incubated samples.

**DISCUSSION & CONCLUSIONS:** This work shows how the degradation parameters, the surface topography and chemistry of the magnesium-based materials influence the initial cell adhesion and spreading. It can be suggested that Mg10Gd alloy may represent a suitable alternative to the commercially available Mg4Y3RE alloys, since it possessed a reduced and more constant initial degradation that allows undifferentiated cells to properly adhere and spread on it.

ACKNOWLEDGEMENTS: The research leading to these results has received funding from the People Programme (Marie Curie Actions) of the European Union 's Seventh Framework Programme FP7/2007-2013/ under REA grant agreement n°n289163.

#### Effects of magnesium alloys on chondrogenic differentiation of HUCPV

AH Martínez-Sánchez<sup>1</sup>, F Feyerabend<sup>1</sup>, B Luthringer<sup>1</sup>, R Willumeit-Römer<sup>1</sup>

<sup>1</sup> <u>Helmholtz-Zentrum Geesthacht:</u> Zentrum für Material- und Küstenforschung GmbH, Geesthacht, Germany

INTRODUCTION: Magnesium and Mg alloys have been shown in previous studies to be suitable for the treatment of cartilage disorders, where combination with cell therapy is necessary. In children, the risk of bone fracture is strongly high, due to the underlying skeletal fragility. Damages in growth plate (mainly constituted cartilaginous tissue) can give rise to malformations during further bone growth. Therefore, it is important to consider the influence of the degradation of the implants on the growth plate. Human umbilical cord perivascular cells (HUCPV) are a relatively new source of mesenchymal cells that exhibit a high potential to be employed *in vitro* for evaluating the chondrogenic differentiation, due to their strong capability to differentiate into osteoblasts and chondrocytes [1].

METHODS: Both direct and indirect tests were performed with HUCPV and two different materials: PMg, and Mg10Gd. In extracts the Mg content was kept constant to evaluate possible effects due to the alloying elements. Life/dead staining was performed after 7d of cell culture directly on the samples and in extracts. Cytocompatibility was checked using MTT normalized DNA. The chondrogenic differentiation of HUCPV was induced in a 3D model. After 21d, analysis of the gene expression of several chondrogenic markers (COL2A1, ACAN, SOX9), as well as osteogenic markers (OPN) was carried out by rtPCR. Furthermore, Glycosaminoglycans (GAG) released progressively by the HUCPV pellets was 2-9-dimethyl-methylene quantified by blue (DMMB) colorimetric assay.

RESULTS: The surface of Mg10Gd, as well as extracts showed higher number of cells and a more homogenous distribution all over the samples (Fig. 1). The cells exhibited a bigger size and rounded-shape in Mg10Gd, while the morphology was mainly polygonal in PMg. No significant differences were detected in the gene expression of chondrogenic markers regarding the control in differentiaiton medium. Up-regulation of OPN was detected in both PMg and MG10Gd. Release of GAG into supernatants was increased when cells were cultured under the influence of PMg and

Mg10Gd. Finally, cells showed a higher metabolic activity when exposed to Mg10Gd extracts.

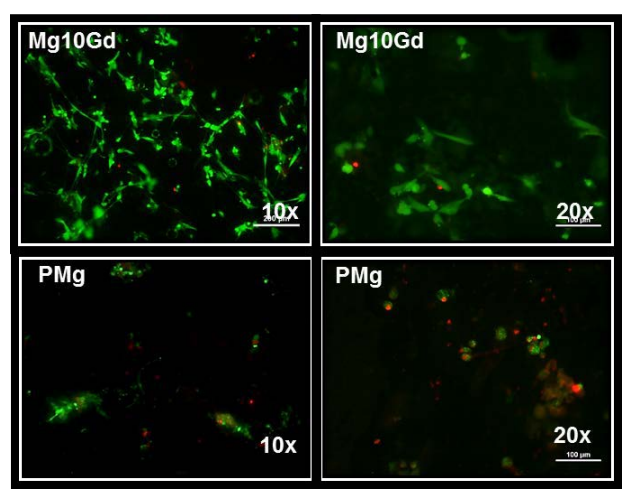


Fig. 1: Images of HUCPV on the surface of Mg10Gd and PMg discs after 7 days of culture. Life/dead staining.

DISCUSSION & CONCLUSIONS: The results indicate that Mg10Gd samples are suitable for HUCPV growth and survival. Both Mg10Gd and PMg seemed to induce terminal chondrogenic differentiation and transition to the ossification stage, as indicated by the up-regulation of OPN. Mg10Gd and PMg extracts also induced a progressive increase in the synthesis of GAG along the 21 days of study, showing chondrogenic effects. Furthermore, Mg10Gd extracts increased cell metabolism, which could be associated with a faster terminal differentiation.

ACKNOWLEDGEMENTS: This project is funded by the Helmholtz Virtual Institute VH-VI-523 (In vivo studies of biodegradable magnesium based implant materials). The Asklepios Klinik Altona is acknowledged for providing the human umbilical cord samples.

### Resorption of magnesium materials and its effect on human mesenchymal stem cells *in vitro*.

O Charyeva1, 2, F Feyerabend3, R Willumeit3, G Szakacs3, F Cecchinato4, N A Agha3, N Hort3, A Wennerberg4, O Dakischew2, C Heiss2, RSchnettler2, KS Lips2

<sup>1</sup> aap Biomaterials GmbH, Lagerstrasse 11-15, 64807 Dieburg, Germany. <sup>2</sup> Justus-Liebig University Giessen, Laboratory for Experimental Trauma Surgery, Schubertstrasse 81, 35392 Giessen, Germany. <sup>3</sup> Institute for Material Research, Department of Macromolecular Structure Research, Helmholtz-Zentrum Geesthacht, Max-Planck-Str. 1, 21502 Geesthacht, Germany. <sup>4</sup>Malmö University, Faculty of Odontology, Department of Prosthodontics, Malmö, Sweden

**INTRODUCTION:** Magnesium has attracted much attention for its potential use in trauma and orthopedics fields due to its excellent mechanical properties, biocompatibility, biodegradability and ability to stimulate bone formation. It is desirable for magnesium-based alloys to have slow degradation rate so that the fractured bone heals before the implant resorbs. It is thus crucial to design alloys with slow corrosion rate and high biocompatibility.

METHODS: Corrosion properties of Mg2Ag, Mg10Gd, WE43 and 99.99 % pure Mg were studied under near physiological conditions with and without the presence of human bone mesenchymal stem cells. The samples were placed in DMEM containing 10 % FBS and corrosion studied by immersion and gas evolution tests. The corrosion rate, osmolality, pH and calcium ion concentrations were determined with even intervals for up to 28 days. Cellular reaction was observed.

**RESULTS:** WE43 had the fastest degradation of all materials tested – 1.057 mm/year – which is almost twice higher than in the other samples. The presence of cells slowed down corrosion of all materials tested. Mg2Ag and Mg10Gd caused similar cellular reaction – vitality decreased up to the 7<sup>th</sup> day but at the 14<sup>th</sup> day and forward the amount of viable cells increased. Differentiation of mesenchymal stem cells (MSC) to osteoblasts was not affected by magnesium alloys. All magnesium alloys stimulated calcification and formation of crystals on materials' surface.

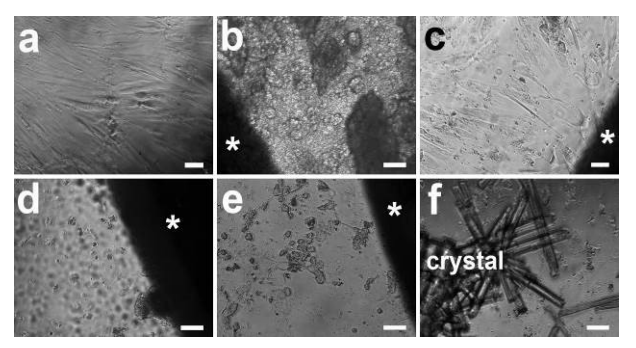


Fig. 1: Morphology of MSC at 21 days. a. Control group, the well in densely covered with the cells. b. Pure Mg, almost no cells compared to control. c. Mg2Ag, the well in densely covered with the cells. d. Mg10Gd, much fewer cells compared to control but more than at day 7. e. WE43 similar appearance to Mg10Gd with somewhat more cells than at day 7. f. Crystal formation was observed for all materials. The image shows pure Mg's well. Legend: asterix = magnesium disc. Scale bar represents 100 μm.

**DISCUSSION** & **CONCLUSIONS:** The corrosion slowed down at day 7 due to formation of protective layer. All alloys stimulated calcification which is beneficial for orthopedic applications. Mg2Ag was the most promising out of all studied materials in respect to cellular reactions and degradation.

**ACKNOWLEDGEMENT:** This project receives funding from the People Programme (Marie Curie Actions) of the European Union's Seventh Framework Programme FP7 (2007-2013) under REA Grant Agreement No 289163.

#### In vitro cytotoxicity evaluation of vascular cells after exposure to zinc

ER Shearier<sup>1</sup>, PK Bowen<sup>2</sup>, J Drelich<sup>2</sup>, J Goldman<sup>1</sup>, F Zhao<sup>1</sup>

<sup>1</sup> <u>Department of Biomedical Engineering</u> <sup>2</sup> <u>Department of Materials Science and Engineering</u>, Michigan Technological University, Houghton, Michigan, USA

**INTRODUCTION:** Endovascular stent research in the last decade has focused on the development of bioabsorbable materials of both polymeric and metallic composition. When considering metallic base materials, zinc (Zn) and its allows have been proposed as a promising material in comparison to more traditional bioabsorbable materials such as iron or magnesium [1]. The low corrosion rate does not appear to damage adjacent tissue in vivo, which can serve as a benchmark for an in vitro evaluation of Zn. Human vascular cell types are used here for focused in vitro evaluation. These include endothelial cells, smooth muscle cells, and fibroblasts. Aqueous insult with Zn2+ using a method similar to that described by Feyerabend et al. [2] and direct metallic contact experiments were performed on these key cell types. In vitro experiments help to determine how these cells will react to Zn in a controlled environment, allowing the determination of detailed cellular mechanisms.

**METHODS:** The specific cell types used in these cytotoxicity tests included human dermal fibroblasts (hDF) to represent adventitial tissue, human aortic smooth muscle cells (AoSMC) to mimic the tunica media, and human aortic endothelial cells (HAEC) as a substitute for the tunica intima. Cells were cultured for 48 hours, and then insulted with a ZnCl<sub>2</sub> solution buffered with MES with concentrations ranging from 1 to 500 uM Zn<sup>2+</sup> for four hours, and allowed to recover for 24 hours. An XTT assay was performed to determine the relative number of viable cells. Live/dead stains were performed on samples ranging from 1 to 200 µM Zn<sup>2+</sup> in full media. Cells were also seeded directly on Zn foils, as well as a modified surface with an attached sheet of collagen. Scanning electron microscopy (SEM) and fluorescent microscopy were then performed.

**RESULTS:** Cell viability following  $Zn^{2+}$  insult, recovery, and analysis using the XTT assay was performed. The median lethal dose (LD<sub>50</sub>) values were 50  $\mu$ M for hDF, 70  $\mu$ M for AoSMC, and 265  $\mu$ M for HAEC. HAEC exhibited the greatest tolerance for  $Zn^{2+}$ . A similar result was seen in the live/dead imaging, as shown in Figure 1. A distinct

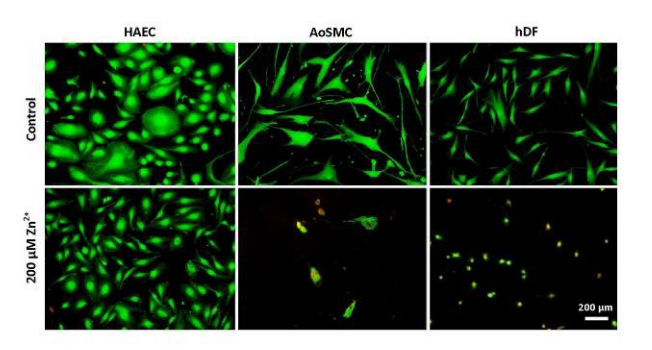


Fig. 1: Live/dead imaging of the three vascular cell types. Cells were exposed to media containing 1 to 200  $\mu$ M Zn<sup>2+</sup> in full media. Living cells show only green, whereas dead cells also fluoresce red.

change in morphology occurs in all cells, with HAEC exhibiting the highest viability in the presence of  $Zn^{2+}$ .

When cells were seeded directly on Zn discs for six hours and visualized with SEM and fluorescent imaging there were no living cells identifiable. To mimic the protein layer/proto-thrombus seen *in vivo*, Zn discs were then coated with a 200 µm layer of collagen gelatin. After 2 hours, living cells were still visible, albeit with a rounded morphology.

**DISCUSSION & CONCLUSIONS:** Zinc has already been demonstrated to be a possible biodegradable endovascular stent material. In this work, the response of key vascular cell types—HAEC, AoSMC, and hDF—to Zn *in vitro* was evaluated. HAEC appear to have the highest tolerance to both ionic Zn<sup>2+</sup> and metallic Zn. This is important *in vivo*, as they play vital role in the formation of a neoendothelium on an implanted stent. The evaluation of these vascular cell types helps to further our understanding of cellular reactions *in vivo*.

**ACKNOWLEDGEMENTS:** PKB was supported by an AHA fellowship. Project support from NIH NHLBI award no. 1R15HL129199-01.

#### Hemocompatibility of newly designed bioabsorbable Zn/ZnO composites

HT Yang<sup>1</sup>, ZH Wang<sup>2</sup>(co-first author), HF Li<sup>1</sup>, YF Zheng<sup>1,\*</sup>, YW Li<sup>2</sup> and R Li<sup>2</sup>

<sup>1</sup> Department of Materials Science and Engineering, College of Engineering, Peking University, Beijing 100871, China

2 Department of General Surgery, Zhengzhou University Affiliated Luoyang Central Hospital, Luoyang 471009, China

**INTRODUCTION:** Zn based biodegradable metal is a new research direction in the field of biodegradable metals(Bowen *et al.*, 2013). In this study, the Zn/ZnO composites were designed and the *in vitro* blood compatibility was investigated for potential usage as blood-contacting implants.

**METHODS:** The Zn/ZnO composites were fabricated by spark plasma sintering. Fresh human whole blood used in the experiments was obtained from health volunteers. Dilute blood was used for hemolysis rates test. Platelet-rich plasma, prepared by centrifuging the whole blood, was used for platelets adhesion test. The anticoagulant properties were evaluated by *in vitro* coagulation time tests, including Prothrombin Time(PT), Activated Partial Thromboplastin Time(APTT), and Thrombin Time(TT).

**RESULTS**: Hemolysis rates and number of adhered platelets, SEM morphologies of adhered platelets are shown in *Fig. 1*. The hemolysis rates of Zn/ZnO composites stand less than 2%, way below the safety-threatening threshold 5%, which demonstrates that the erythrocyte kept normal when interacting with Zn/ZnO composites. The density of adhered platelets on 0.25Zn/ZnO is less than the density of Zn while increasing the content of ZnO improves platelets' adhesion. The adhered platelets on Zn show fewer pseudopods than the

platelets on Zn/ZnO composites which demonstrates a more activated state of platelets on Zn/ZnO composites. *Table. 1* shows TT, PT, APTT times of Zn and Zn/ZnO composites. Zn and Zn/ZnO composites reduce the values of TT significantly when prolong the values of APTT greatly as compared to normal human blood plasma. As for the PT time, only slight prolongation is induced by samples. Higher content of ZnO has more significant effect on coagulation times.

**DISCUSSION** & **CONCLUSIONS:** The hemolysis rates of Zn/ZnO composites are far below the 5% standard. ZnO content higher than 0.5 wt.% enhances platelets' adhesion and

activation. Although Zn/ZnO composites induce the decrease of TT, the prolongation of PT and APTT demonstrates that Zn has anticoagulation effect on both intrinsic and extrinsic pathway of coagulation system. Together these results verify the promising hemocompatibility of Zn/ZnO composites.

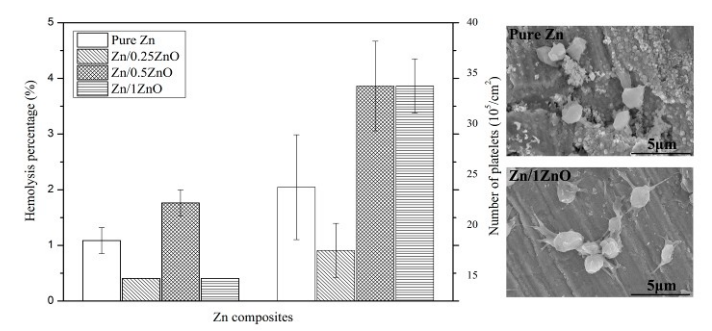


Fig. 1: Hemolysis rates, number and SEM image of adhered platelets on Zn/ZnO composites

Table. 1: TT, PT, APTT of Zn/ZnO composites

	TT(s)	PT(s)	APTT(s)
Pure Zn	11.00(0.28)	12.00(0.14)	42.90(0.57)
Zn/0.25ZnO	8.80(0.28)	12.25(0.07)	56.40(2.12)
Zn/0.5ZnO	7.20(0.42)	13.00(0.14)	59.55(2.19)
Zn/1ZnO	7.80(0.14)	12.75(0.07)	59.15(3.89)
Blood plasma	12.10(0.26)	11.40(0.17)	37.37(1.76)

ACKNOWLEDGEMENTS: This work was supported by National Science Fund for Distinguished Young Scholars (Grant No. 51225101) and Luoyang Municipal Science and Technology Development Fund (1301069A-3).

### In vitro degradation of PLA/Mg composites: relevance of matrix and filler nature

S.C. Cifuentes<sup>1,2</sup>, M. Lieblich<sup>1</sup>, R. Benavente<sup>2</sup>, J.L. González-Carrasco<sup>1,3</sup>

<sup>1</sup> Centro Nacional de Investigaciones Metalúrgicas <u>CENIM-CSIC</u>, Spain. <sup>2</sup>Instituto de Ciencia y Tecnología de Polímeros <u>ICTP-CSIC</u>, Spain <sup>5</sup>Centro de Investigación Biomédica en Red de Bioingeniería, Biomateriales y Nanomedicina <u>CIBER-BBN</u>, Spain.

INTRODUCTION: Resorbable medical devices must be developed in order to have an appropriate degradation rate in agreement with the healing rate of bone in the implantation site. This work deals with the in vitro degradation kinetics of novel PLA composites loaded with Mg particles of different shape and composition. The effects of the polymeric matrix nature, and crystallinity are also investigated. H<sub>2</sub> release, pH evolution, and weight variation are determined to monitor degradation rate during one month. Loss of mechanical properties is evaluated by means of compression tests. Degradation mechanism is explained by analysing the hydrolysis of the polymeric matrix and corrosion rate of Mg/MgZn.

**METHODS:** PLA/Mg cylinders of 9 mm high and 6 mm diameter were processed by extrusion and moulded by compression. Two polymers were used for the matrix: poly-L-lactic (PLLA) and poly-L,D-lactic acid (PLDA). As reinforcement, irregular flake-like Mg particles (IRR) and spherical Mg and Mg5Zn particles of less than 50 μm in size were used.

The study of the *in vitro* degradation behaviour and kinetics is addressed by hydrogen release assays, pH monitoring, water uptake, mass loss and changes in morphology. Compressive mechanical properties as a function of degradation time are also studied to analyse the *in vitro* strength retention of the composite.

**RESULTS:** The composite with the crystalline matrix presented the fastest degradation and the largest mass loss and water uptake, and also higher hydrogen release than its amorphous homologous. Within the amorphous matrices (PLLA and PLDA), PLLA allowed the highest hydrogen release rate.

Regarding the characteristics of the reinforcement, it was found that particle shape plays a very important role controlling the degradation behaviour of PLA/Mg composites. The lower surface of spherical particles reduced the reaction sites which decrease Mg particles corrosion rate, in comparison with irregular particles, and additionally retard the appearance of macroscopic

cracks in the composite. The composite reinforced with spherical Mg5Zn particles, exhibited better corrosion behaviour than the material reinforced with irregular Mg particles. This implies that particle shape played a more important role on controlling PLA/Mg degradation rate than particle nature (Fig. 1).

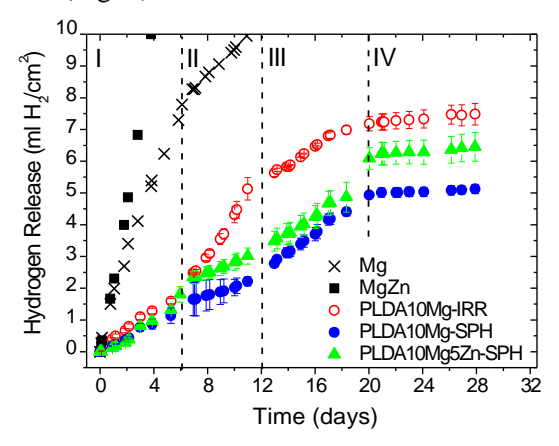


Fig. 1: Accumulated amount of hydrogen released as a function of immersion time in PBS

**DISCUSSION & CONCLUSIONS:** *In vitro* degradation behaviour of PLA/Mg composites can be tailored by changing the characteristic of the matrix and/or the metallic reinforcement.

The best *in vitro* degradation behaviour was obtained with the material composed by an amorphous PLDA matrix reinforced with spherical particles of Mg.

ACKNOWLEDGEMENTS: This work was supported by grants MAT2012-37736-C05-01-05 (MINECO, Spain). S.C. Cifuentes is supported by a European Social Fund for JAE-I3P Grant (CSIC). Special thanks are due to Amalia San Román and Jesús Chao (CENIM) for technical assistance.

### Biodegradable ferulic acid-loaded polymer coating for Mg stent application

E Zhang

Key Lab. for Anisotropy and Texture of Materials, Education Ministry of China, Northeastern University, Shenyang, 110819, China, Email: zhangel@atm.neu.edu.cn

**INTRODUCTION:** Magnesium stent has shown great advantage over stainless steel and Co-based stent due to its biodegradability. However, the fast degradation rate on the other hand resists it clinic application. As one of effective methods, biodegradable coating, especially drug-load coating can adjust the biodegradation rate, but also can promote the endothelialization due the released drug.

In this research, the coating includes biodegradable (hydroxybutyrate-co-hydroxyhexanoate) poly (PHBHHx) as drug-loaded material and ferulic acid as drug. First, blood compatibilities and degradation properties of PHBHHx with different molecular weights were studied by in vitro test methods. Second, the *in vitro* degradation property and the drug release property of the drug-loaded PHBHHx films were studied in this work. In addition, NaOH treatment was used to modify the surface of the coating film. The function of the ferulic acid and the NaOH treatment on the endothelialization and inhibition of the vessel smooth muscle cell (VMSCs) proliferation was also discussed.

**METHODS:** PHBHHx (containing 12mol% HHx) with different molecular weights were used as drug carries. Ferulic acid (FA) with a purity of ≥98% was used as drug. Briefly, 0.25 g of PHBHHx, 5% ferulic acid or 10% ferulic acid dissolved in 5 mL ethyl acetate to prepare 5% drug-loaded and 10% drug-loaded PHBHHx material, respectively. SEM was used to observe the surface morphology of the coating film. Degradation rate, drug release behaviour, cell proliferation were used to assess the biocompatibility of this coating film.

**RESULTS:** *In vitro* drug release result showed that the drug release from the drug-loaded PHBHHx films exhibited two stages: burst release and stabilization release. Primary mechanism of the drug release in the burst release stage was drug diffusion while the drug release in the stabilization release stage had a close relevancy and regularity to the degradation behaviors of the drug-loaded films.

In vitro biocompatibility test results showed that the ferulic acid release of the drug-loaded films had an obviously inhibition on the platelet aggregation and thrombosis and an effective improvement on the antihemolytic property and the anti-intrinsic and extrinsic coagulation properties of the drug-loaded films. Moreover, the human umbilical vein endothelial cells (HUVECs) adhesion and proliferation on the drug-loaded films could be significantly promoted and the VMSCs excessive proliferation could be effectively inhibited by the ferulic acid release.

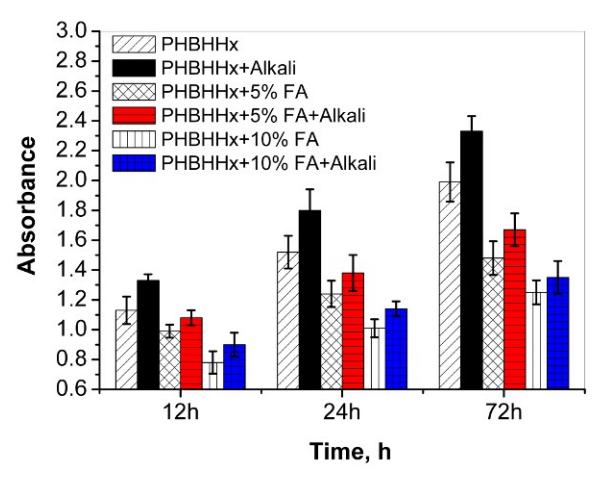


Figure 9 MTT assay of VSMCs proliferation on the drug-loaded PHBHHX before and after alkali treatment

It was found that the NaOH treatment could improve the hydrophilic property of the drug-loaded films, further improve the HUVECs adhesion and proliferation properties, and accelerate the endothelialization process. On the other hand, NaOH treatment could sharply reduce the content of ferulic acid on the sample surface due to the etching action of NaOH, and then weakened the inhibition on VMSCs excessive proliferation on the loaded films.

**CONCLUSIONS:** FA released from the coating film significantly promoted the adhesion and proliferation of HUVECs and inhibited the proliferation of on VMSCs. NaOH treatment was expected to control the cardiovascular restenosis by speeding up the endothelialization.

## Comparison of crystalline and amorphous versions of a magnesium-based alloy: corrosion and cell response

J Byrne<sup>1</sup>, ED O Cearbhaill<sup>1</sup>, DJ Browne<sup>1</sup>

<sup>1</sup>School of Mechanical and Materials Engineering, University College Dublin, Ireland

INTRODUCTION: Mg-Ca-Zn alloys have been identified as potential materials for bioresorbable orthopaedic implants – e.g. for bone fixation. It is important, however, to tailor the resorption rate of the alloy to the healing rate of the bone and the rate at which the metal ion release can be tolerated by the human body. Recent work has shown that bulk metallic glass (or amorphous) alloys corrode more than their conventional crystalline counterparts<sup>1</sup>, and the rate may be more suited to orthopaedic applications. It has also indicated a slower evolution of hydrogen gas during resorption<sup>2</sup>. This paper presents an experimental study on the casting of a Mg75-Zn22-Ca5 into bulk amorphous form, and testing of the resultant material in vitro for corrosion and cytotoxicity.

**METHODS:** The material was received as a prealloyed crystalline ingot. Samples were cast using a conventional muffle furnace flooded with argon gas to prevent magnesium oxidation and to keep the alloy pure. The molten alloy was poured into a  $\phi$  3mm copper mould. XRD was carried out on the samples to ensure they were amorphous.

Twelve 3mm x  $\phi$  3mm samples of both crystalline and amorphous forms of the alloy were prepared, as well as copper and stainless steel control samples. All were immersed in 6ml of DMEM for 24 h, at 37°C, and 5% CO<sub>2</sub> to form an elution media. The medium was aspirated and transferred to wells containing healthy human dermal fibroblasts. The cells were cultured for 24 and 48 h for indirect exposure. The samples were transferred to separate wells for 24 and 48 h direct cell exposure.

The corrosion samples were removed and soaked in alcohol to remove any biological contamination, then cleaned in soapy water and acetone to remove loose corrosion products before being examined. Cytotoxicity testing was carried out using CytoTox 96® assay, which measures the release of lactate dehydrogenase (LDH) signalling the loss of membrane integrity and thus levels of cell death.

**RESULTS:** The BMG samples corroded significantly slower than crystalline counterparts as can be seen in figure 1 for both the 48 and 72

hour tests. The BMG samples produced significantly less hydrogen gas.

The material was not as biocompatible as expected for similar materials<sup>1</sup>. The crystalline material showed results similar to that of the copper control samples, while the BMG sample showed LDH levels almost half that of the lysis control.

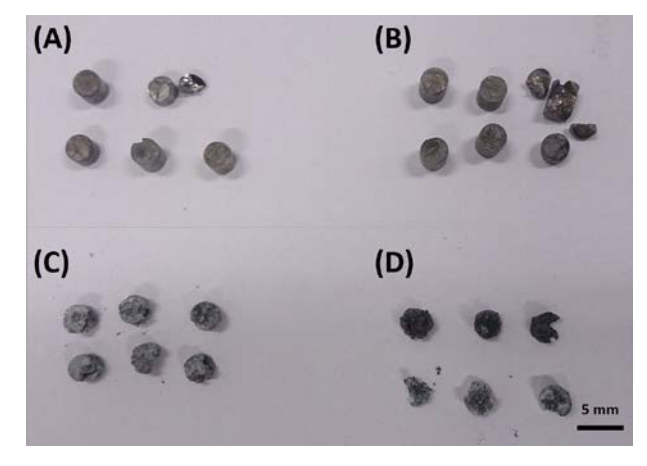


Fig. 1: Samples used for cytotoxicity testing (A) 21 hour BMG, (B) 45 hour BMG, (C) 21 hour crystalline alloy, (D) 45 hour crystalline alloy.

DISCUSSION & CONCLUSIONS: The amorphous material exhibited a more appropriate corrosion rate, as well as a reduced rate of hydrogen evolution. This points towards the usefulness of BMG in controlling the resorption rate of bioresorbable implants. Further analysis of the composition of the material showed traces of praseodymium, neodymium as well as aluminium, copper and lead. Trace amounts of these materials may be the cause of the adverse cell response. Future work is suggested.

**ACKNOWLEDGEMENTS:** The authors would like to thank Professor Eli Aghion, Ben-Gurion University of the Negev, Israel for supplying the alloy material, and Dr Tom Flanagan and the tissue engineering research group at UCD for assistance with cell work.

## The response of human endothelial and smooth muscle cells to high concentrations of magnesium

S Castiglioni, A Cazzaniga, JA Maier Università di Milano, Milano, I

**INTRODUCTION:** Biodegradable vascular stents in magnesium (Mg) alloys are a challenging alternative to conventional stainless steel metal stents [1]. As a results of corrosion of these Mg alloys, high concentrations of this element can be locally achieved. We therefore studied the effect of high concentrations of extracellular Mg on primary human endothelial and smooth muscle cells (EC and SMC, respectively), the principal constituents of the arterial wall.

**METHODS:** Human EC and SMC were cultured for 3-5 passages. Viability was tested by MTT assay and cell proliferation with a cell counter. Migration was studied by wound assay. Inflammatory cytokines were evaluated by protein array and ELISA. NO was evaluated by the Griess method and by mass spectrometry.

**RESULTS:** EC and SMC were exposed to various concentrations of extracellular Mg. Within 1 and 20 mM, the cells are viable, while concentrations of Mg higher than 20 mM reduce cell viability, partly through osmolality stress partly through an imbalance that might alter signal transduction. EC are growth stimulated and induced to migrate when cultured in high Mg. On the contrary, no effect on cell growth and an inhibition of migration was observed in SMC cultured in high Mg. It is noteworthy that in EC high Mg inhibits the inflammatory response and the generation of free radicals [2], both important events in driving endothelial dysfunction and atherogenesis. Moreover, high Mg stimulates endothelial synthesis and release of nitric oxide (NO) by upregulating endothelial nitric oxide synthase. NO stimulate smooth muscle cells guanylyl cyclase to produce 3',5'-cyclic monophosphate which causes relaxation of the blood vessels. Moreover, NO limits platelet activation, adhesion and aggregation, important events in preventing stent thrombosis [3].

**DISCUSSION & CONCLUSIONS:** High concentrations of Mg seem to be beneficial for vascular cells. Indeed, in SMC Mg prevents events involved in neointima formation. In EC Mg contrasts clot formation and reduces inflammatory and oxidative response. Recently, endothelial cells

were cultured on novel magnesium alloys containing rare earth element [1]. These alloys promoted endothelial attachment, spreading and growth.

These results indicate that Mg release from the stents might be helpful to accelerate vascular healing.

### Analysis of the response of bone cells towards magnesium alloys by proteomics

H Schlüter<sup>1</sup>, M Omidi<sup>1</sup>, M Kwiatkowski<sup>1</sup>, M Wurlitzer<sup>1</sup>, A Burmester<sup>2</sup>, Berengere Luthringer<sup>2</sup>, R Römer-Willumeit

<sup>1</sup><u>Mass Spectrometric Proteomics</u>, Department of Clinical Chemistry & Laboratory Medicine University Medical Center Hamburg-Eppendorf, Hamburg, G. <u>Centre for Materials and Coastal</u> Research, Helmholtz-Zentrum Geesthacht, Geesthacht, Germany <sup>2</sup>

**INTRODUCTION:** Implants made of magnesium alloys promise advantages over conventional implants. In the best case, the implant will have been disappeared after bone-healing will had been finished. However, the dissolving of the implant is associated with corrosion resulting in elevated Mg<sup>2+</sup>- concentrations as well as additional metal ions from the alloy, which might have toxic effects. Investigation of the proteomes [1,2] of bone cells in response to magnesium alloys and its corrosion products can give answers if these implants will have favourable or detrimental effects.

METHODS: Diverse cultured bone cells were incubated in the absence and in the presence of solid magnesium alloys as well as from their extracts. From the cells protein extracts were prepared and either applied to two-dimensional electrophoresis (2DE; top-down proteomics), selected spots (with differences in the spot intensities comparing 2 DE gels of control osteoblasts versus osteoblasts incubated with Mg<sup>2+</sup>) of separated proteins were picked and the proteins digested with the protease trypsin or the complete protein extracts were directly digested (bottom-up proteomics). The tryptic peptides were injected into a liquid chromatography (LC) system (nano-ultra pressure LC) coupled to tandem mass spectrometers. The resulting data were processed with OpenMS or Proteome-Discoverer and the proteins identified by a search engine (Mascot). Quantification was performed using MaxQuant.

**RESULTS:** Several thousand proteins were identified in each of the experiments. An example of a differential proteomics top-down approach applying 2DE is shown in Fig. 1. Each spot on both 2DE gels represent at least one protein. The intensity of the spots display the abundance levels of the individual proteins. For comparing the levels of the proteomes of two samples a comparison of the protein patterns is performed yielding dozens of proteins with same x-y coordinates but different spot intensities. These spots were selected for protein identification. As an alternative to the top-down approach the protein extracts of different incubation experiments were analysed by bottom-

up (shot-gun) proteomics. By label-free quantification up- or down-regulation of hundreds of proteins in the response of cultured bone cells towards magnesium compared to controls were observed.

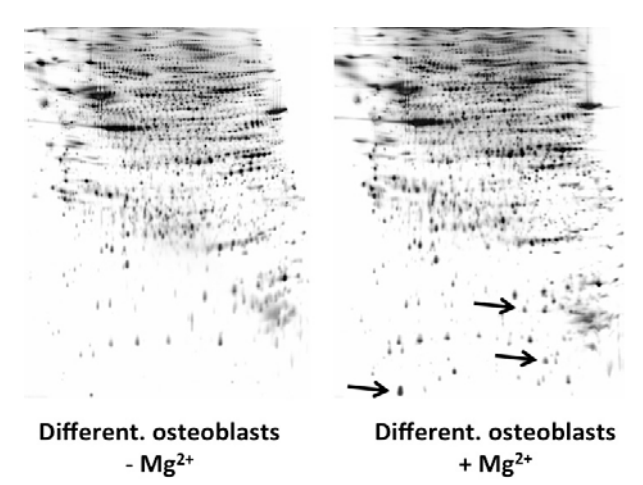


Fig. 1: Differential proteomics top-down analysis applying 2DE of cultured differentiating osteoblasts in the absence (left gel) and in the presence of Mg<sup>2+</sup>(right gel). The arrows show some of the many differences of protein intensities, which represent a differential regulation of protein levels.

**DISCUSSION & CONCLUSIONS:** In summary the diverse proteomics investigations showed that the presence of elevated magnesium ions support a physiological response of bone cells, which is beneficial for bone healing.

**ACKNOWLEDGEMENTS:** Financial support by the Helmholtz Society for the Helmholtz Virtual Institute MetBioMat is gratefully acknowledged.

### Understanding the response of skeletal tissue to magnesium alloy corrosion

D Maradze<sup>1</sup>, M Lewis<sup>2</sup>, Y Zheng<sup>3</sup>, Y Liu<sup>1</sup>,

<sup>1</sup> Wolfson School of Mechanical and Manufacturing Engineering, Loughborough University, UK <sup>2</sup> School of Sport, Exercise and Health Science, Loughborough University, UK. <sup>3</sup> College of Engineering, Peking University, Beijing, China

**INTRODUCTION:** Studies have shown that corrosion behaviour of Mg alloys observed in *in vitro* studies is not comparable to that observed *in vivo*. The aim of the current study is to generate a knowledge base for correlation of carefully-designed *in vitro* studies emulating *in vivo* environment to increase *in vitro* predictability. Furthermore we aim to understand the response of cells in skeletal tissue including; osteoblast, myoblasts and hMSCs to the corrosion of Mg biomaterial at local and systematic level.

**METHODS:** Mg and Mg-Ca1% were sterilised using ethanol and UV light and then immersed in DMEM for corrosion until saturation was reached. Conditioned medium containing products (100%) was diluted 1:10 (10%), 1:4 (25%) and 1:2 (50%) using fresh DMEM. For cell culture, conditioned medium was supplemented with 10% foetal bovine serum. Part of the conditioned medium was filtered to remove precipitates formed during corrosion (medium A) and the remainder remained with the precipitates (medium B). This was done in order to assess the effect of Mg ions and precipitates formed. ICP-OES was used to analyse the concentration of Mg ions in the conditioned medium. Cell viability was assessed using alamar blue assay. RT-PCR and immunohistochemistry was used to assess effect of the corrosion products at gene and protein level.

**RESULTS:** 1) <u>hMSCs</u>; the presence of corrosion products in high concentration reduced cell viability, however when the conditioned medium was diluted, cell viability was improved. Interestingly, we also observed the formation of bone-like nodules being formed in the presence of precipitates (Fig.1). Furthermore gene and protein analysis showed higher expression of osteogenic markers in cells cultured in conditioned medium B compared to conditioned medium A. 2) <u>Myoblasts</u>; the presence of precipitates in high concentration reduced the capability of myoblasts to fuse into myotubes (Fig.2), however as observed with the hMSCs the dilution of the conditioned medium improved myotube fusion. Interestingly

conditioned medium A and B did not have adverse effects on mature myotubes.

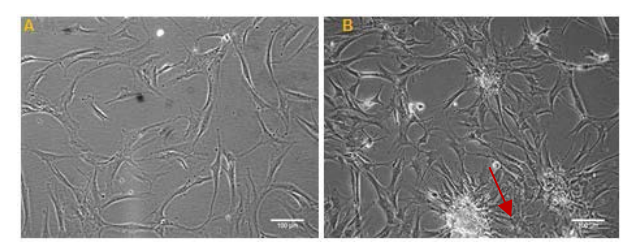


Fig. 1: hMSCs grown in A) control medium B) Mg-Ca 100% conditioned media. Arrow-formation of small bone-like nodules.

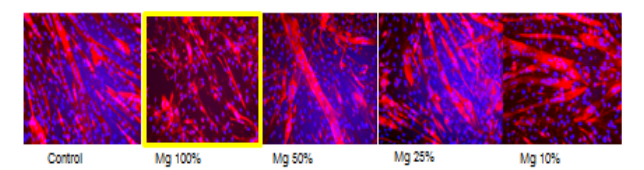


Fig. 2:  $C_2C_{12}$  myoblasts cultured in Mg conditioned medium. Series dilution was performed before culture.

DISCUSSION & CONCLUSIONS: With hMSCs, the presence of corrosion products in high concentration reduced cell proliferation but increased osteogenic marker expression. With myoblasts adverse effects are only seen during fusion, when cells were exposed to the highest concentration of Mg. Cells were able to tolerate up to 16mM Mg ion concentration, with the concentration between 9-10mM being favourable for cell growth and proliferation. This data can be used to build a knowledge base of magnesium corrosion behaviour that would allow the design of Mg-based implants that can function efficiently as orthopaedic implants.

**ACKNOWLEDGEMENTS:** We appreciate Yufeng Zheng and Wenting Li for providing Mg samples and EPSRC for funding.

## Evaluation of murine adipose derived mesenchymal stem cell behaviour on PCL and P(3HB)/P(4HB) coated magnesium scaffolds

M Grau<sup>1</sup>, J Matena<sup>1</sup>, L Roland<sup>1</sup>, M Gieseke<sup>2</sup>, M Teske<sup>3</sup>, S Petersen<sup>4</sup>, A Kampmann<sup>5</sup>, I Linke<sup>5</sup>, H Murua Escobar<sup>6</sup>, NC Gellrich<sup>5</sup>, H Haferkamp<sup>7</sup>, I Nolte<sup>1</sup>

<sup>1</sup> Small Animal Clinic, University of Veterinary Medicine Hannover Foundation, <sup>2</sup> Laser Zentrum Hannover e.V., <sup>3</sup> Institute for Biomedical Engineering, Rostock University Medical Center, <sup>4</sup> Fakultaet Ingenieurwissenschaften und Informatik, University of Applied Sciences, Osnabrueck, <sup>5</sup> Department of Oral and Maxillofacial Surgery, Hannover Medical School, <sup>6</sup> Division of Medicine Clinic III, Hematology, Oncology and Palliative Medicine, Rostock University Medical Center, <sup>7</sup> Institut fuer Werkstoffkunde, Leibniz Universitaet Hannover

INTRODUCTION: Magnesium as a biocompatible, degradable and osteoconductive implant material has recently come into of orthopaedic surgery<sup>1</sup>. To achieve adequate conditions for ingrowth of regenerated bone material and vascular supply porous three-dimensional scaffolds were manufactured by Selective Laser Melting (SLM)<sup>2</sup>. The main challenge connected with magnesium as implant material is the excessive generation of hydrogen gas caused by the corrosion process, which inhibits cell adhesion to the implant surface. In order to avoid this the scaffolds were coated with synthetic Poly-ε-caprolactone (PCL) and biological Poly(3-hydroxybutyrate)/Poly(4-hydroxybutyrate) (P(3HB)/P(4HB)) blend. To enable an early and proper osteointegration the coated implants were previtalized with murine Adipose Derived Mesenchymal Stem Cells (mADMSCs). Using Live Cell Imaging both biopolymer coatings were compared regarding their influence on the cell behaviour.

METHODS: Green fluorescent protein (GFP) labeled mADMSCs were seeded onto magnesium scaffolds coated with PCL or P(3HB)/(P4HB). These vitalized implants were incubated in DMEM with 10% FCS at standard cell culture conditions for seven days. Thereby the medium was substituted each day. In order to achieve an overview of the cell behaviour and growth upon the scaffold surface, each implant was photographed daily at four to five representative regions of interest.

**RESULTS:** The cells attached evenly onto the surface of both biopolymers and stayed vital for seven days. Fig. 1 shows the development of cell behaviour comparatively and representatively at one region of interest on the implant in hundredfold magnification right after vitalization (B, E) and on day three (C, F) and seven (D, G).

**DISCUSSION & CONCLUSIONS:** Both coating materials decrease the initial magnesium corrosion and thereby allow attachment and viability of mADMSCs on the implant surface. Thus both polymer matrices are proven to be suitable as implant coating materials.

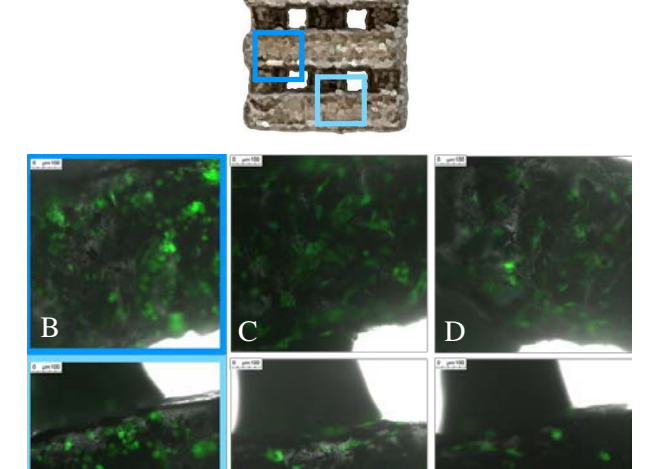


Fig. 1: mADMSCs on magnesium scaffolds (A) coated with PCL (B-D) or P(3HB)/P(4HB) (E-G).

## Investigation the impact of magnesium-implants compared to titanium-implant on protein composition in cultured osteoblast by label free quantification

M Omidi<sup>1</sup>, A Burmester<sup>2</sup>, P Kiani<sup>1</sup>, M Kwiatkowski<sup>1</sup>, B Luthringer<sup>2</sup>, R Willumeit<sup>2</sup>, H Schlüter<sup>1</sup>

<sup>1</sup> <u>Mass Spectrometric Proteomics</u>, Department of Clinical Chemistry & Laboratory Medicine,

University Medical Center Hamburg-Eppendorf, Hamburg, Germany, <sup>2</sup> <u>Centre for Materials and Coastal Research, Helmholtz-Zentrum Geesthacht</u>, Geesthacht, Germany

**INTRODUCTION:** Magnesium implants for bone healing offer the opportunity getting degraded by corrosion and thus avoiding a second surgery for removing them, because the implants in the best case will have been disappeared after bone healing will have been finished (1 and 2). By reason of removal surgery, bio-absorbable avoiding magnesium-based implants can be taken desirable than conventional permanent metal implants (3). The aim of this study was to investigate the response of osteoblasts to Mg-implant in comparison to conventional permanent titaniumimplant materials. Therefore, we studied the effect of elevated Mg<sup>2+</sup> compared to Ti<sup>3+</sup> levels on osteoblasts by proteomics.

METHODS: In this study, we investigated the proteomes of cultured osteoblast, in absence (control) and presence of Mg-Implants after 24 hours and 7 days incubation and Ti-Implants with the same incubation time. First, cell pellets were lysed; proteins of the cells were extracted, reduced, alkylated and finally incubated with trypsin. Tryptic digested peptides were subjected to a nano-UPLC-column coupled to a hybrid orbitrap system (Orbitrap-Fusion, Thermo Fisher scientific). Data analysis and data interpretation for comparison of relative protein abundance was performed with Proteome Discoverer by using spectral counting and MaxQuant based on precursor ion intensity.

**RESULTS:** 135,000 spectra were recorded in total yielding approximately 3,700 identified proteins including more than 89,000 peptides. The levels of hundreds of proteins increased respectively decreased in response to elevated concentrations of Mg<sup>2+</sup> and Ti<sup>3+</sup>. 19 proteins from up-regulated and 5 proteins from down-regulated proteins, in response to elevated concentration of Mg<sup>2+</sup>, have essential effect on bone remodeling (Fig. 1). For instance, A/C, Prelamin which is required osteoblastogenesis, was increased in osteoblasts through rising the incubation time with Mg-Implant, respectively decreased through rising the incubation time with Ti-Implant.

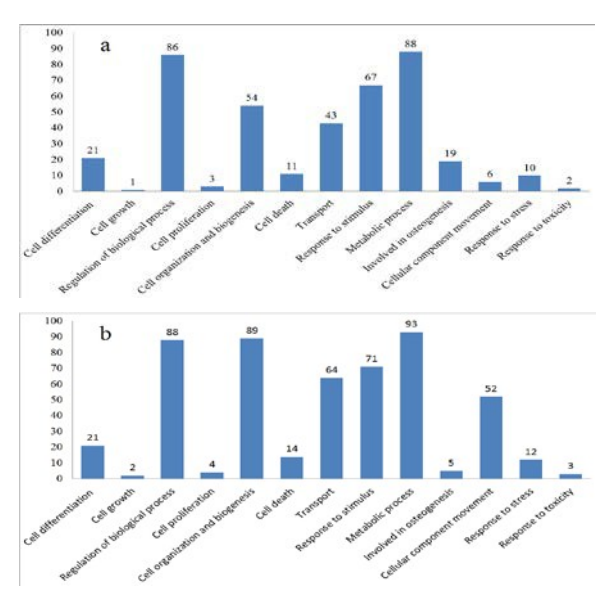


Fig. 1: Numbers of (a) up-regulated proteins and (b) down-regulated proteins in response to elevated concentrations of  $Mg^{2+}$  compared to  $Ti^{3+}$ , which are sorted according to their participation in cellular processes.

**DISCUSSION & CONCLUSIONS:** The investigation shows that the overall response of osteoblasts towards Mg-implants is more beneficial than the response towards Ti-implants. It can be assumed that Mg-implants will support bone healing.

**ACKNOWLEDGEMENTS:** Financial support by the Helmholtz Virtual Institute MetBioMat is gratefully acknowledged.

### In vitro degradation assessment of the bioabsorbable small scale Mg alloy specimens

S Agarwal, <sup>1</sup> E Galvin<sup>2</sup>, B Duffy<sup>1</sup>, S Jaiswal<sup>1</sup>

<sup>1</sup>Centre for Research in Engineering and Surface Technology, FOCAS Institute, DIT, Ireland <sup>2</sup>School of Mechanical and Manufacturing Engineering, Dublin City University, Dublin, Ireland

INTRODUCTION: Magnesium has become a potential candidate as a biodegradable bioactive substance [1]. Bioabsorbable stents have various advantages over permanent implants; non-surgical removal of implants, biocompatible and cost effective. However, Mg alloys are prone to rapid corrosion, thereby producing toxic subcutaneous H<sub>2</sub> gas [1]. Several studies have examined the mechanical properties of bulk WE43 specimens [1]. However, very few studies examined the microstructure and mechanical properties of very small Mg alloy specimens on the size scale of medical devices such as stents. This study elucidated the mechanical, corrosion and cytotoxic properties of small-scale WE43 specimens.

METHODS: The uniaxial tensile testing of WE43 Mg alloy wire specimen was carried out by using a materials testing machine (Z005, Zwick Roell) with a 5 kN load cell. Followed by mechanical studies, the corrosion studies of wire were examined in a container (with screw cap slightly open to allow gaseous exchange) with 25 ml Hank's balanced salt solution. These samples were subjected mass loss at different time points in physiological pH. Furthermore, cell cytoxicity assays were conducted using HUVECs cells.

**RESULTS**: The stress-strain mechanical property of Mg alloy is represented in Figure 1a. The mechanical integrity of the specimens was denoted by the UTS as shown Fig.1b. The mechanical properties and ductility of the specimens were reduced significantly with increasing immersion time (30 days).

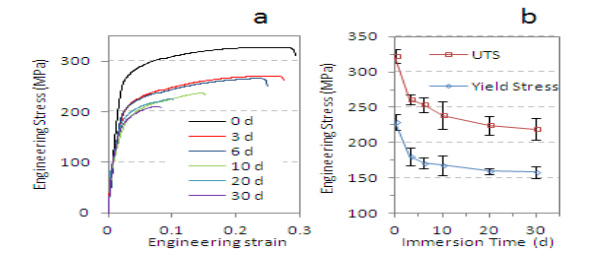


Fig. 1: (a) Representative engineering stress strain curves for corroded and non-corroded wire specimens (b) evolution of UTS and yield stress of wires over time.

Furthermore, the mass loss of wire is linear at fixed pH over a period of time. Moreover the surface morphology of specimens also changed significantly over 30 day's immersion period (Fig 2).

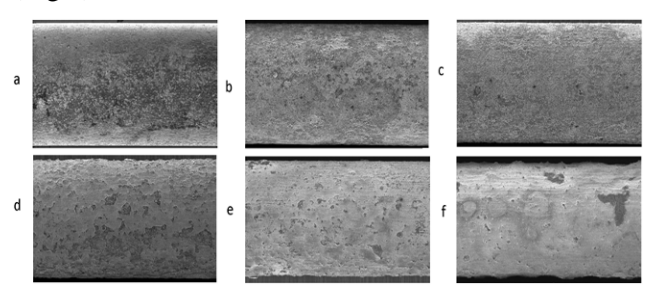


Fig. 2: SEM images of uncorroded and corroded wires after immersion times of (a) 0 d, (b) 3 d, (c) 6 d, (d) 10 d, (e) 20 d and (f) 30 d

This cytotoxicity assay result demonstrates that the Mg alloy extraction medium has a positive influence on the viability and proliferation of the HUVECs (Fig 3).

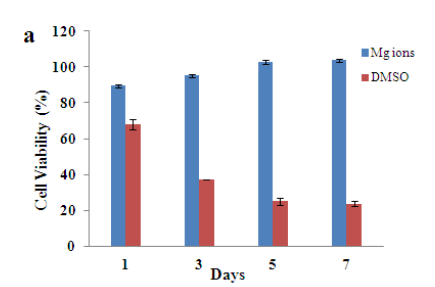


Fig. 3: The effect of Mg ions (103.3 ppm) on the HUVEC cells examined by MTT assay after 1, 3, 5 and 7 days of exposure

DISCUSSION & CONCLUSIONS: It has been concluded that WE43 Mg wire sustained showed sustained mechanical property over a period of time (30 days) at physiological pH. Furthermore, the Mg ions are less cytotoxic to HVECS cells. These results support the appreciable mechanical and biocompatibility of WE43 Mg wire for biomedical applications.

**ACKNOWLEDGEMENTS:** The authors would like to acknowledge the SFI funding for this work.

### Influence of sterilization on magnesium alloy Mg2Ag

F Feyerabend<sup>1</sup>, M Johannisson<sup>1</sup>, Z Liu<sup>1</sup>, R Willumeit-Römer<sup>1,2</sup>

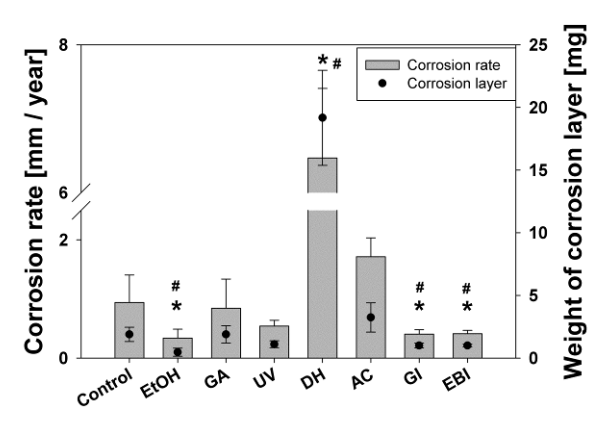
<sup>1</sup> <u>Helmholtz-Zentrum</u> Geesthacht, Institute of Materials Research, Geesthacht, DE. <sup>2</sup> <u>Christian-Albrechts University Kiel, Technical Faculty, Kiel, DE</u>

INTRODUCTION: Magnesium alloys specially designed for biomedical applications have been studied intensively and the first applications have been approved<sup>1</sup>. Especially for medical applications there are some further important requirements for the final before implantation like cleaning, sterilization and packaging, which have not yet been widely considered or studied. Due to the susceptibility of magnesium and its alloys to water all sterilization methods including liquids should be critically analyzed. Moreover, heat and radiation can also induce alterations in the material, which is an exclusion criterion for many polymers. The aim of this study was to determine the influence various sterilization methods on mechanical and corrosion properties.

METHODS: In this study the influence of 70 % ethanol (EtOH), glutaraldehyde (GA), autoclaving (AC), dry heat (DH), UV-, gamma (GI)- and electron beam-irradiation (EBI) on mechanical and corrosion parameters of the alloy Mg2Ag were analyzed. As mechanical parameters hardness and grain size were determined. The corrosion rate under physiological conditions, the weight of the corrosion layer and the corrosion morphology were determined. Osmolality and pH were analyzed for their correlation to the corrosion rate.

#### **RESULTS:**

Compared to the control (HV  $5 = 52.8 \pm 3.8$ ) most of the sterilization methods led to a slight decrease of the hardness values, associated by an increase of grain size. The determined corrosion rates were compared against an unsterilized control (Fig. 1). Dry heat dramatically increased the corrosion rate by a factor <6. Autoclaving also led to an increase of the corrosion rate; however the increase was not significant. In contrast, all other methods led to a decrease of the corrosion rate, which was significant for ethanol, gamma-irradiation and electron beam irradiation. Glutaraldehyde treatment showed values comparable to the control. The weight of the corrosion layers showed correlated behavior. Significant differences observed for the corrosion rate were also observed for the weight of the corrosion layer.



#### Sterilization method

Fig. 1: Influence of the sterilization methods on the corrosion rate (grey bars) and on the weight of the corrosion layer (dots). Significant differences (p<0.05) are indicated as stars (\*) for the corrosion rate and as hashtags (#) for the weight of the corrosion layer.

**DISCUSSION & CONCLUSIONS:** It could be demonstrated that irradiation treatments and 70 % ethanol are suitable methods, as they decrease the corrosion Heat-introducing methods rate. (autoclaving and dry heat) acted as incomplete ageing treatments on this alloy and therefore increased the corrosion rate. Furthermore. osmolality showed a better correlation to the actual corrosion rate than the pH. Therefore an optimum ratio between alloying system, implant and sterilization method has to be established, depending on the intended application.

ACKNOWLEDGEMENTS: The authors want to acknowledge Gert Wiese and Gabriele Salamon for expert technical assistance. Financial support of the Helmholtz-association (Helmholtz Virtual Institute VH-VI-523 -In vivo studies of biodegradable magnesium based implant materials) is gratefully acknowledged.

## Adhesion of two different cell lines (DH1+/+ and Mg63) on surface treated magnesium

V Wagener<sup>1</sup>, S Virtanen<sup>1</sup>

<sup>1</sup> <u>Chair for surface science and corrosion</u>, Department for Materials Science, University of Erlangen-Nuremberg, Germany

**INTRODUCTION:** Protein adsorption is crucial for cell adhesion and thus is an important factor influencing biocompatibility. Magnesium (cp) was coated with a linker molecule known to immobilize proteins and reduce corrosion in order to enhance biocompatibility.

METHODS: Magnesium samples were pretreated and afterwards coated with aminopropyltriethoxysilane + vitamin C (AV), according to Wagener et al. [1]. Cell tests up to 20 days were conducted with endothelial (DH1+/+)osteosarcoma (Mg63) cells. Among others, the cell spreading area was calculated in order to elucidate short- and long-term biocompatibility of the samples. The influence of cell growth on the corrosion behaviour of magnesium investigated by electrochemical impedance spectra (EIS).

#### **RESULTS:**

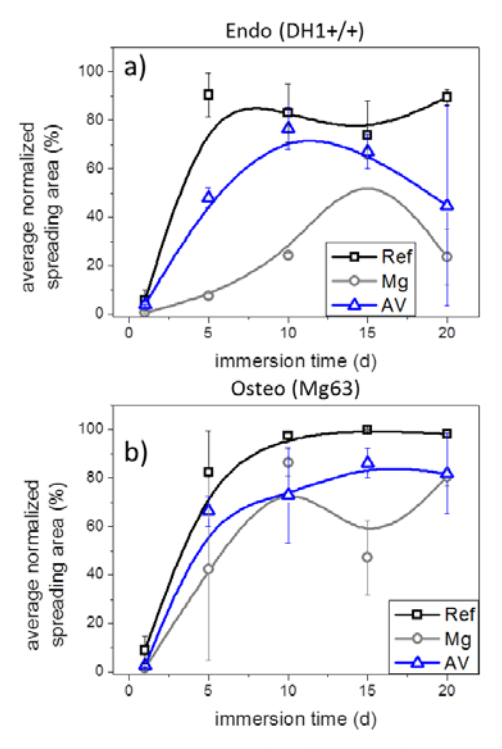


Figure 1: Average normalized spreading areas of the long-term cell test with DH1+/+ (a) and Mg63 (b) on cp Mg and after AV treatment. As reference tissue culture plastic was used.

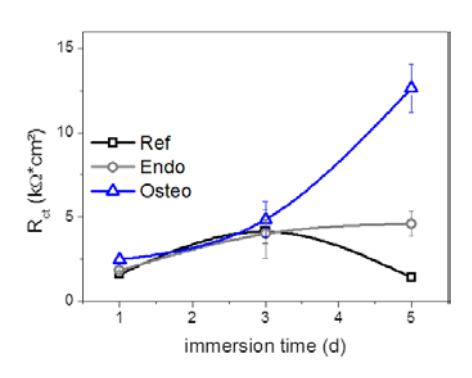


Figure 2: Calculated charge transfer resistances  $R_{ct}$  from EIS for cultivation of Dh1+/+ and Mg63 for 1, 3 and 5 days. As reference AV coated Mg immersed in cell culture medium was used.

**DISCUSSION & CONCLUSIONS:** Cell tests showed that growth of DH1+/+ and Mg63 is possible on cp Mg in general (Fig1), even if initial biocompatibility seems to be limited due to corrosion of Mg. The AV treatment leads to a faster increase of cell adhesion and spreading in the case of DH1+/+ (Fig1a) and shows better longterm stability of cell growth for Mg63 (Fig1b). These improvements are dedicated to the protein immobilizing effect of AV and the increased corrosion resistance by the coating leading to a decreased hydrogen evolution and surface alkalization. EIS measurements (Fig2) after 1 and 3 days show no effect of cell adhesion compared to the reference immersed in cell culture medium without cells. However, after 5 days an increase of R<sub>ct</sub> can be observed for both cell lines, with the one for osteosarcoma being very significant. The different influences of the two cell lines can be explained by different spreading and adhesion behaviour [2].

**ACKNOWLEDGEMENTS:** The Authors thank Prof. Fabry and the Chair for Biophysics, University Erlangen-Nuremberg for the cooperation.

### *In-vitro* cell culture study on Organosilane coated Mg discs

A Patil<sup>1,3</sup>, O Jackson<sup>1</sup>, L Fulton<sup>1</sup>, C Sfeir<sup>1,2,3</sup>, E Beniash<sup>1,2,3</sup>

<sup>1</sup>Department of Bioengineering; <sup>2</sup>Department of Oral Biology, School of Dental Medicine; <sup>3</sup>Center for Craniofacial Regeneration, University of Pittsburgh, Ph. 15261, US

**INTRODUCTION:** Degradable Magnesium (Mg) and its alloys have a great potential as a material for resorbable implantable devices<sup>1</sup>. Mg and its have several advantages such biocompatibility and their mechanical properties closely match to natural bone. However, rapid corrosion of Mg is hindering its use in clinical setting. One potential solution is to develop the coatings for highly corroding Mg surfaces. We used Organosilane (OS) coating to control the corrosion rate of Mg. The aim of this study was to test the hypothesis that OS multilayer selfassembled coating was cytocompatible and the surface modification of the coating will lead to higher rate of cells proliferation and decreased cells death.

**METHODS:** Self-assembled OS multilayer coating was formed on Mg discs using dip coating technique. The hybrid film formed via a simple sol-gel process based on the cohydrolysis and cocondensation of a mixture of alkyltriethoxysilanes and tetramethoxysilane. Furthermore, the OS coating was functionalized with 3-aminopropyltrimethoxysilane (APS) MC3T3-E1 preosteoblast cells were cultured on the OS coated and OS coated and aminated Mg disks for 15 days, to assess their cytocompatibility. Fluorescence dyes were used to visualize nuclei and cytoskeleton of the cells on the Mg discs. Cell viability was assessed using LIVE/DEAD assay.

#### **RESULTS:**

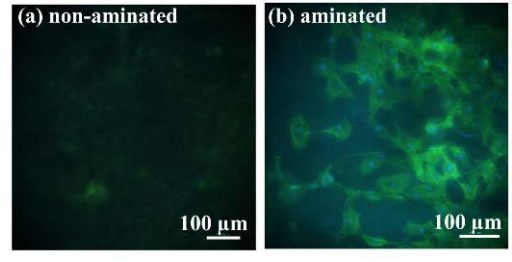


Fig. 1: Fluorescence imaging of the Mg discs exposed to MC3T3-E1 cells for 15 days: (a) non-aminated and (b) aminated OS coated Mg disc. The nuclei (blue) and actin filaments (green) indicate the presence of cells. Alexa Fluor® 488 dye for F-actin staining (green) and Hoechst 33342 dye for nuclei staining (blue) were used.

The fluorescence imaging results showed cell density on aminated OS discs was 28.40±0.73

cells/10,000  $\mu m^2$  significantly higher (p < 0.01) than 17.83±1.72 cells/10,000  $\mu m^2$  on OS coated discs after 15 days. These data indicate that amination of OS coating promoted cell attachment and/or cell proliferation due to the decrease in the surface hydrophobicity.

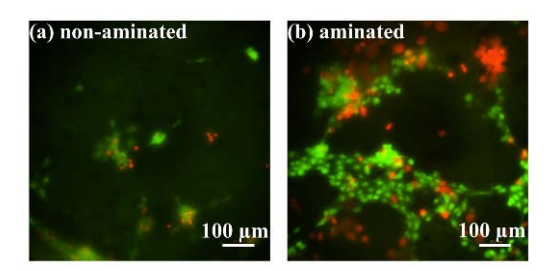


Fig. 2: Live/Dead cell assay after 11 days of culture on: (a) non-aminated and (b) aminated OS coated Mg disc.

The LIVE/DEAD cell viability assay confirmed that OS coated layer is cytocompatible. We observed 41% cell death on aminated OS coated discs compared to 87% cell death on non-aminated OS coated discs (p<0.029).

**DISCUSSION & CONCLUSIONS:** With twostep coating process we have developed an anticorrosive OS coating which is further functionalized with APS. We found that the cell viability and proliferation were highest when cultured on aminated OS compared to nonaminated OS. In summary, our study shows that organosilane self-assembled coating cytocompatible and has a potential for surface functionalization of the Mg implantable devices with bioactive molecules. Our results suggest that surface functionalization can improve biocompatibility and histointegration of orthopedic degradable devices.

**ACKNOWLEDGEMENTS:** The authors acknowledge the financial support from NSF ERC Center for Revolutionizing Metallic Biomaterials # 0812348.

### Initial degradation of magnesium in simulated and real body fluids

K Törne<sup>1,2</sup>, A Örnberg<sup>2</sup>, J Weissenrieder<sup>1</sup>

<sup>1</sup> KTH Royal Institute of Technology, Material Physics, 16440 Kista, Sweden. <sup>2</sup> St Jude Medical

INTRODUCTION: Before we can establish a predictive capability of any metal's in vivo degradation it is necessary to understand the processes underpinning its in vitro degradation. However, very few studies have investigated the corrosion of biodegradable metals in real body fluids, e.g. whole blood.1 Real body fluids as electrolyte provides insight into the influence of protein and cell adsorption on the degradation of Mg. In vitro immersion studies commonly use zwitterionic buffers such as 4-(2-hydroxyethyl)-1piperazineethanesulfonic acid (HEPES) to stabilize pH.<sup>2</sup> Recently HEPES was reported to increase the corrosion rate of Mg and its alloys. <sup>2,3</sup> The detailed mechanism behind the increased rate remains unclear. Electrochemical impedance spectroscopy (EIS) allows for *in situ* studies of the evolution of a corroding surface over time. In combination with carful ex situ investigation of the corrosion products formed and the surface morphology, a detailed understanding of the influence of proteins and buffer system may be formed.

**METHODS:** Pure Mg samples were immersed for 24 h in whole blood and for 24h and 30 days in modified simulated body fluid (m-SBF) with HEPES, denominated m-SBF(HEPES), and without HEPES, denominated m-SBF(CO<sub>2</sub>). The pH was regulated by CO<sub>2</sub> bubbling. EIS was measured regularly during the immersion. Post immersion examination included Fourier transform infrared spectroscopy (FTIR) and cross sectional scanning electron microscopy (SEM).

**RESULTS:** EIS spectra of magnesium immersed in the electrolytes presented in fig 1. The polarization resistance  $(R_p)$  was ~10 times higher in m-SBF(CO<sub>2</sub>) compared to the other solutions. The corresponding phase angle spectra showed a clear two time constant behavior. In the other solutions only one time constant was present. FTIR revealed the corrosion product formed in all solutions to be carbonated hydroxyl apatite (HA). The SEM cross section in m-SBF(CO<sub>2</sub>) (fig 1b) showed a thick inner layer of magnesium oxide/hydroxide, (MgO/OH), and a thin outer layer with HA. In m-SBF(HEPES) and whole blood only one layer was detected consisting of mainly HA (fig 1 d and f). These layers were

thicker and more porous compared to the HA layer formed in m-SBF(CO<sub>2</sub>).

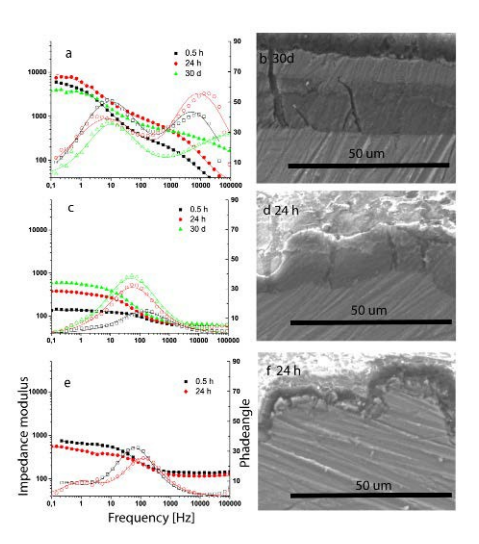


Fig. 1: EIS spectra and cross section SEM images a-b) m-SBF(CO<sub>2</sub>) c-d) m-SBF(HEPES) e-f) whole blood

DISCUSSION & CONCLUSIONS: The different morphologies of the HA layers formed in m-SBF(CO<sub>2</sub>) compared to m-SBF(HEPES) and whole blood may explain the observed decrease in corrosion rate. The dense HA layer in m-SBF(CO<sub>2</sub>) form an effective diffusion barrier and stabilize the protective layer of MgO/OH at the interface.<sup>4</sup> The porous HA layer formed in m-SBF(HEPES) and whole blood leads to rapid dissolution of formed MgO/OH and no protective layer can be formed. The interface formed in m-SBF(CO<sub>2</sub>) is similar to interfaces from *in vivo* trials.<sup>4</sup> m-SBF(CO<sub>2</sub>) is therefore the recommended environment for *in vitro* experiments.

**ACKNOWLEDGEMENTS:** St Jude Medical and the Swedish Research Council are acknowledged for their financial support.

#### Magnesium degradation influenced by cell interaction

N Ahmad Agha<sup>1</sup>, D Laipple<sup>1</sup>, R Willumeit-Römer<sup>1</sup>, F Feyerabend<sup>1</sup>

<sup>1</sup>Institute of Materials Research, Helmholtz-Zentrum Geesthacht, Geesthacht, DE

**INTRODUCTION:** If magnesium should be used as implant material, the cell-material interaction is of high interest. However, this interaction is only poorly understood. In this study we aim to elucidate the influence of primary osteoblasts on the degradation interface of three magnesium based alloys.

**METHODS:** Pure Mg (as control) and the magnesium alloys Mg2Ag and Mg10Gd were used in this study. Mg2Ag and Mg10Gd were cast by permanent mould gravity casting, whereas pure Mg was cast by permanent mould direct chill casting. The alloys were homogenized by T4 heat treatment, and extruded by indirect hot extrusion. Cylindrical samples ( $\emptyset$ = 10 mm, t = 1.5 mm) were machined from the extruded bars. Samples were sterilized by gamma irradiation at a dose of 29.2 KGy.

DMEM (Dulbecco's Modified Eagle's Medium) with 10 %FBS (Fetal Bovine Serum) and 1% P/S (Penicillin/Streptomycin) was used as cell culture and immersion medium. Immersion was done under cell culture conditions (37°C, 20% O<sub>2</sub>, 5% CO<sub>2</sub>, 95% rH). Samples were pre-incubated for 24 hours and then 100.000 primary human osteoblasts were seeded directly on the sample surface. The immersion time was 4 and 14 days in total (including pre-incubation). Each sample was immersed in 3 ml of immersion medium. The immersion medium was changed every 2 to 3 days to create a semi-static immersion and to exclude saturation effects. Samples without cells were subjected to the same immersion protocol and used as negative controls.

During immersion pH and osmolality were measured. After immersion, the mean degradation rate was calculated by mass loss. Cell viability was checked by Live/Dead fluorescent staining, and mineralization matrix formation was detected by Osteo-Image fluorescent staining. In addition, the chemical composition of the degradation interface after 14 days of immersion was investigated with FIB-SEM. Different areas were cut using focused ion beam (FIB), then followed by EDX line scans on the cross sections of these cuts. (1) osteoblasts with the degradation layer underneath, (2) degradation layer next to the osteoblast, and (3) cut on the control sample without cells

**RESULTS:** EDX results show that the presence of osteoblasts on the material surface altered the

degradation profile by mediating mineralization function and changing the chemical composition of the degradation profile. This qualitative measurement could be quantified by Osteo-Image measurements. The formation of hydroxyapatite by osteoblasts was mainly noticed after 14 days on Mg10Gd (where the measured stained area is 27%), and on pure Mg (10%), Mg2Ag deposition whereas on the hydroxyapatite seemed to be lower or slower by comparing the 14 days measurements of this alloy (1%) with the 4 days of Mg10Gd (4%) and pure Mg (2.4%).

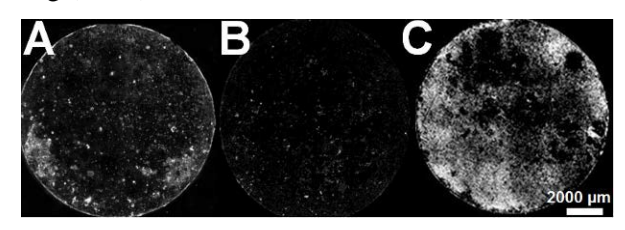


Fig. 1: Fluorescent images of Osteo-Image staining in monochromatic mode (Grey). Images taken after 14 days of immersion with primary osteoblasts cultured on. (A: pure Mg, B: Mg2Ag and C: Mg10Gd)

**DISCUSSION & CONCLUSIONS:** It could be shown that osteoblasts on the material induce the formation of mineralized matrix without osteogenic factors. The amount of matrix formed is dependent on the alloy. Further studies using coculture systems will be performed to analyse a more "Tissue-like" environment, including intercellular communication.

**ACKNOWLEDGEMENTS:** Research leading to these results has received funding from the People Program (Marie Curie Actions) of the European Union's Seventh Framework Program FP7/2007-2013/ under REA grant agreement n° 2891

## Ag-incorporated FHA coating on pure Mg: *in vitro* cell biocompatibility and antibacterial properties

C Zhao<sup>1</sup>, H Wu<sup>1</sup>, J Ni<sup>1</sup>, S Zhang<sup>2</sup>, X Zhang<sup>1,2</sup>

**INTRODUCTION:** Fluoride apatite (FHA) coating provided an improvement of corrosion resistance to biodegradable magnesium alloys [1]. Owing to its similarity with natural bone mineral, FHA coating has the ability to stimulate bone integration as Mg does. In order to protect against the bacterial invasion during Mg implantation as bone repair materials, silver-incorporated FHA coating was fabricated on high-purity Mg in this work. The *in vitro* cell response and antibacterial properties were studied.

**METHODS:** The Ag-containing FHA coating were conducted through electrodeposition on highpurity Mg disc samples. 0.042M Ca(NO<sub>3</sub>)<sub>4</sub>·4H<sub>2</sub>O, 0.1M NaNO<sub>3</sub>, 0.025M NH<sub>4</sub>H<sub>2</sub>PO<sub>4</sub>, 6 vol.% H<sub>2</sub>O<sub>2</sub> and 1×10<sup>-3</sup>M NaF were respectively dissolved into the deionized water at 60°C to be used as the electrolyte. After being processed at 0.5 mA/cm<sup>2</sup> current density for 2h, the sample were immersion in 1g/L AgNO<sub>3</sub> solution for 0.5h to load Ag. The sample were then washed and sterilized by ultraviolet irradiation. Mouse osteoblastic MC3T3-E1 cells were used to assess the biocompatibility of the Ag-incorporated FHA coating Mg samples. MTT assay were conducted according to ISO 10993-6 to evaluate the cytotoxicity. Cell morphology and fluorescence observation were performed as in ref [2]. S.aureus was used as a model to evaluate in vitro antimicrobial properties of FHA coating with Ag addition. In brief, 3 mL of the bacteria S. aureus suspension with a concentration of 1×10<sup>6</sup> (CFU mL<sup>-1</sup>) was added into the tubes containing samples and incubated for 24h. The number of bacteria were analysed by spread plate method as describe in ref [3].

**RESULTS:** The cell viability of the extraction for Ag-FHA/Mg was 104.9% after 24h incubation, which was comparable to the extraction of untreated Mg and FHA/Mg (114.0% and 108.5%, respectively). The cell viability in Ag-FHA/Mg group remained 90.2% after 72h, showing a good compatibility. Fig.1 showed MC3T3-E1 cells on both substrates of Mg and Ag-FHA/Mg samples were well attaching and spreading, and filopodia were stretching to connect with the packed

columnar crystals surface of the Ag-FHA/Mg sample. Fluorescence images demonstrated a slight lower density of cells, which was in accordance with the MTT assay results, indicating an inferior cell compatibility as compared to the untreated Mg and FHA/Mg. Nevertheless, the antibacterial effects against planktonic bacteria in the medium are relatively high in Ag-FHA/Mg group (89.7%) as compared to FHA/Mg group (26.6%), showing the good antimicrobial ability of the coating when incorporated with Ag.

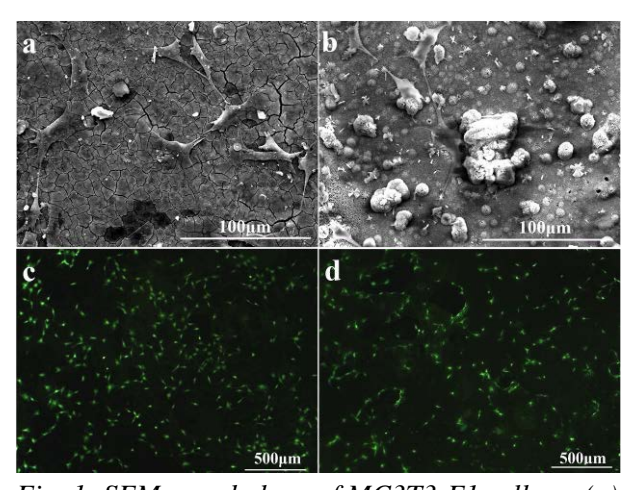


Fig. 1: SEM morphology of MC3T3-E1 cells on (a) Mg and (b) Ag-FHA/Mg after 72h incubation and their corresponding fluorescence images (c and d).

**DISCUSSION & CONCLUSIONS:** FHA coating incorporated with Ag has shown both cell biocompatibility and preferable antibacterial property, which is worth considering in surface modification of biodegradable Mg for bone repair materials.

**ACKNOWLEDGEMENTS:** The authors are grateful to the financial support of National Natural Science Foundation of China (51271117).

<sup>&</sup>lt;sup>1</sup> State Key Laboratory of Metal Matrix Composites, School of Materials Science and Engineering, Shanghai Jiao Tong University, China. <sup>2</sup> Suzhou Origin Medical Technology Co, Ltd., China,

### Magnesium ion promote proliferation of osteoblast cell

XZ Zhang<sup>1</sup>, F Cao<sup>1</sup>, DW Zhao<sup>1,\*</sup>

<sup>1</sup> Orthopedics Research Center, Affiliated Zhongshan Hospital of Dalian University, Dalian, China.

**INTRODUCTION:** Magnesium, a biodegradable metal, has been more and more applied as bone implant material in the clinical trials, and researchers have found the phenomenon of osteogenetic activity. But its molecular mechanism has not been clearly understood. In this study, molecular biological methods have been used to illustrate the mechanism which can provide theoretical foundation for magnesium application.

#### **METHODS:**

CCK-8 assay for cell viability: MG63 cells after irradiation were seeded in 96-well plates at a density of 3000 cells/well and cultured in an incubator for 1 to 7 day periods. The Cell Counting Kit-8 (CCK-8; Dojindo, Japan) was employed to quantitatively evaluate cell viability. The absorbance was determined at a wavelength of 450 nm.

Cell cycle analysis: Cells were cultured with MgSO<sub>4</sub> (200  $\mu$ M) for 24 or 48 h. The cell cycle were determined by cytofluorimetry. Cells treated in different ways were subjected to flow cytometric analysis for chromosomal DNA. DNA labeling was performed using the Cycle TEST<sup>TM</sup> PLUS DNA reagent kit (BD Biosciences Pharmingen, San Diego, CA, USA).

#### **RESULTS:**

Mg<sup>2+</sup> increase the viability of osteoblast cells. Cellular viability was assayed by treating MG63 cells with various concentrations of Mg<sup>2+</sup>, followed by analysis with the CCK-8 viability assay. At 24 h, 200 and 500 μM Mg<sup>2+</sup> increased viable MG63 cell number by 1.6 and 4.2 fold relative to Mg<sup>2+</sup> free medium. When the concentration of Mg<sup>2+</sup> exceed 500 μM, it did not lead to a further increase in cell viability. We observed that cellular viability was increased by Mg<sup>2+</sup> in a dose-dependent manner in the osteoblast cells (Fig.1).

Effects of  $Mg^{2+}$  on the cell cycle. Sustained incubation of the cells with  $Mg^{2+}$  for 24 h, the proportion of MG63 cells in the G2/M phase of the cell cycle was found to have significantly increased when exposed to  $Mg^{2+}$  (Fig. 2). This

finding indicated that Mg<sup>2+</sup> leading to accelerated G2/M phase transition contributes to enhanced cell

proliferation in MG63 cells. The concentration of  $Mg^{2+}$  used was 200  $\mu$ M.

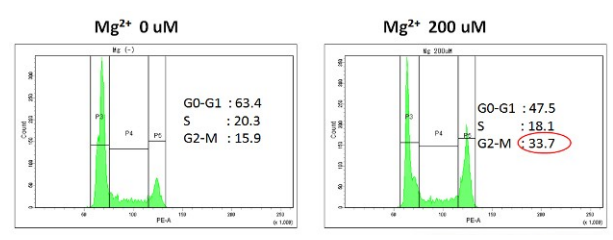


Fig. 1:  $Mg^{2+}$  increase viability in MG63 cells: Cell viability was determined by a CCK-8 viability assay. The cells were either vehicle-treated (PBS-control) or treated with increasing concentrations of  $Mg^{2+}$  (200–5000  $\mu$ M) for 24 h.

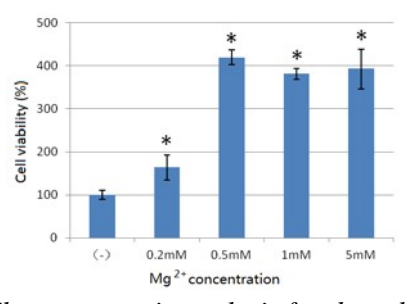


Fig 2. Flow cytometric analysis for the cell cycle: the proportion of G2/M phase significantly increased when MG63 cells were treated with Magnesium ions (200  $\mu$ M) for 24 h.

#### **DISCUSSION & CONCLUSIONS:**

This study indicated that magnesium ion could promote proliferation of osteoblast cell. Our finding could provide theoretical foundation and extensive application space in clinical othopedics. In the following experiment, next generation sequencing will be used to study the genetic regulation mechanism of osteogenetic activity.

### Mg-MOF biodegradable coatings for drug delivery on Mg temporal implants

I Marco, N Campagnol, J Fransaer, O van der Biest Department of Materials Engineering (MTM), KU Leuven, Belgium.

**INTRODUCTION:** Metal organic frameworks (MOF's) are novel materials designed for different applications with a growing interest in the last 10 years [1]. Horcajada et al. showed a drug delivery system based of MOF as drug nanocarriers, applying iron and 5 different organic linkers loading them with ibuprofen among other drugs [2]. Mg can also be used as the metal in the MOF structure (Mg-MOF), which has been successfully synthesised hydrothermally with DHTA (2,5dihydroxyterephthalic acid) as organic linker and MgNO<sub>3</sub> as a metal source, in two different structures CPO-26-Mg and CPO-27-Mg [3]. Moreover, DHTA has shown a low toxicity in animal experiments, which makes it a biomaterial candidate [4]. In this study, Mg-MOF structures are electrochemically synthesized and deposited on pure Mg only using Mg from the substrate. This could be the first step in biodegradable drug delivery system to control the post-implantation inflamation of bioabsorbable Mg implant.

**METHODS**: Pure Mg samples are cast, extruded and machined into discs (Ø10-1.5mm). These discs are embedded in epoxy resin and connected electrically to be used as working electrodes. Pt foil and Ag/AgCl saturated with KCl are used as counter and reference electrode respectively in the electrochemical cell. 60 mM DHTA, 10 vol.%  $H_2O$  and 90 vol.% absolute ethanol is the composition of the electrolyte used for the synthesis. 10 mL of this solution are used in the cell at 60 °C. Measured electrolyte conductivity and pH are 76  $\mu$ S/cm and 2.7, respectively. During potentiostatic dissolution 4 V vs OCP are applied for 1 h , and the same electrolyte was used with consecutive samples, keeping a similar distance between electrodes.

**RESULTS AND DISCUSSION:** As shown in figure 1a, the applied procedure consists in polarizing potentiostatically consecutive samples dissolving Mg, which increases Mg<sup>2+</sup> concentration, and pH due to the negative difference effect (NDE) [5]. Consequently, the charge passed in each synthesis increases, reaching a maximum after 2 samples and depositing a thicker but non-uniform layer. The next samples get a homogeneous thin Mg-MOF layer until terephthalic acid concentration decreases down to

a minimum value. This shows the importance of the electrolyte volume, which accelerates reaching a charge maximum and Mg<sup>2+</sup> ion saturation, and delays the linker concentration minimum.

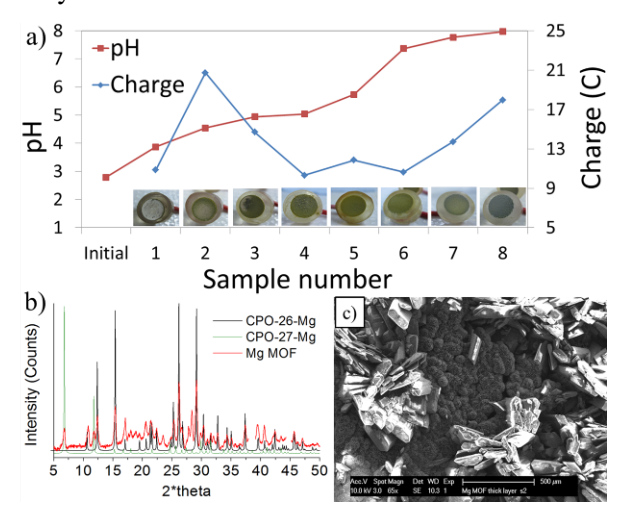


Fig. 1: a) pH and charge evolution over 8 consecutive Mg-MOF depositions in the same electrolyte and different Mg discs; b) its XRD spectrum compared with CPO-26-Mg and 27; c) SEM image showing both structures morphology.

The measured current densities are between  $150\mu\text{A/cm}^2$  and  $400~\mu\text{A/cm}^2$ , indicating the importance of low conductive electrolyte. Figure 1b shows XRD patterns comparing experimental Mg-MOF with its two theoretical structures, proving that these two structures are identified. Figure 1c depicts the deposited Mg-MOF morphology.

**CONCLUSIONS:** Mg-MOF is successfully deposited on pure magnesium as drug delivery system for biodegradable Mg implant. The key parameters of this process are the electrolyte composition, its low conductivity and volume; and the Mg dissolution applied potential and time.

**ACKNOWLEDGEMENTS:** Research supported by the PEOPLE Programme (Marie Skłodowska-Curie) of the European Union's Seventh Framework Programme FP7/2007-2013/ under REA grant agreement n° 289163.

### The influence of pH on the corrosion rate of high-purity Mg, AZ91 & ZE41 in bicarbonate buffered Hanks solution

S Johnston<sup>1</sup>, Z Shi<sup>1</sup>, A Atrens<sup>1</sup>

<sup>1</sup> The University of Queensland, Materials Engineering, School of Mechanical & Mining Engineering, Brisbane, Qld 4072, Australia

**INTRODUCTION:** The human body maintains pH at a relatively constant value between 7.35 & 7.45. However, some pH fluctuations in the body do occur. There have been evidence that the pH of a bone fracture site can drop to as low as 5.5 in the period immediately after implantation<sup>1</sup>. In order to ensure the integrity of any medical implants fashioned from Mg alloys, all aspects influencing their corrosion rate must be understood fully. This study aims to determine the influence pH has on the bio-corrosion of Mg alloys.

**METHODS:** Four solution pH levels were tested: 6.5, 7.0, 7.5 & 8.5. Samples of HP Mg, AZ91 & ZE41 were immersed in bicarbonate buffered hanks solution for 7 days. A schematic of the immersion testing apparatus is depicted in figure 1. The pH of the solution was maintained by either the addition of NaOH or CO<sub>2</sub>. The corrosion rate of all the samples was measured by mass loss  $(P_m)^2$ . The corrosion rate of half of the samples was also measured from hydrogen gas evolution (P<sub>H</sub>)<sup>2</sup>. The samples were split into two tanks: tank 1 samples were suspended freely in solution, tank 2 samples were suspended beneath a standard hydrogen capture apparatus<sup>2</sup>. This was done to determine if the stagnant flow conditions created by the hydrogen capture apparatus were influencing the corrosion rate of the samples. Flow between the tanks was maintain via a pump & a drain.

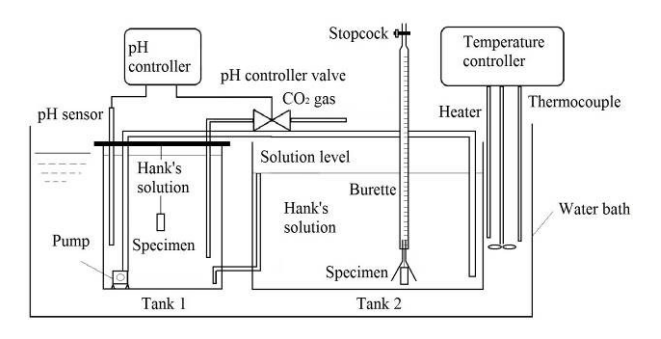


Fig. 1: Immersion testing apparatus

**RESULTS:** The average  $P_m$  for the samples was compared to the average pH of the immersion solution, as presented in figure 2. The average solution pH levels were: 6.6, 6.9, 7.4 & 8.2.

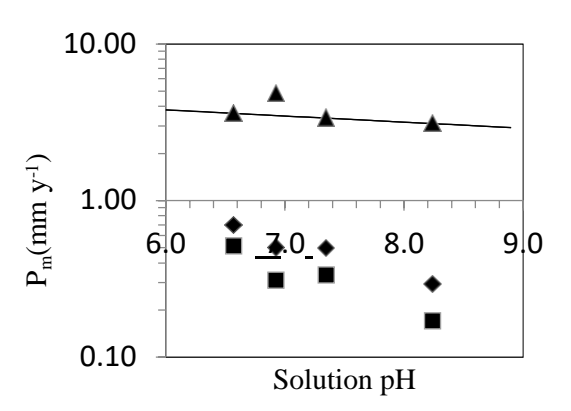


Fig. 2:  $P_m$  against average solution pH for HP Mg (diamonds), AZ91 (squares), & ZE41 (triangles).

As can be seen from figure 2, a negative correlation was found for all three alloys between  $P_m$  & average solution pH. This correlation was seen more strongly in the slower corroding alloys (HP Mg & AZ91). The average  $P_m$  of the samples in tank 1 versus tank 2 were also compared for all three alloys, across the average solution pH levels. It was found that the  $P_m$  of tank 1 samples were always either higher, or within experimental error of, samples in tank 2. The hydrogen evolution data collected for HP Mg & AZ91 samples was very inconsistent, & often measure negative evolution values. The evolution data gathered for ZE41 allowed a comparison between  $P_H$  &  $P_m$ . The ratio of  $P_H$ : $P_m$  was found to be 0.5.

**DISCUSSION & CONCLUSIONS:** The  $P_m$  of all three alloys was found to be negatively correlated with average solution pH. This was attributed to the higher stability of the oxide layer at higher pH values. Flow rate across the sample was also found to influence the  $P_m$  of the samples & this was again attributed to the higher stability of the oxide layer in stagnant conditions. The ratio of  $P_H:P_m$  was found to be 0.5 for ZE41. It is believed some hydrogen is absorbed into the Mg matrix.

**ACKNOWLEDGEMENTS:** This template was modified with kind permission from eCM Journal.

### Overview of long term clinical study performed in Korea

HS Han<sup>1</sup>, HK Seok <sup>1,2</sup>, YC Kim <sup>1,2</sup>

<sup>1</sup>Center for bio-materials, Korea Institute of Science and Technology, Korea, <sup>2</sup>Department of Biomedical Engineering, University of Science & Technology, Korea

**Abstract:** Research on Magnesium (Mg) and its alloys as alternative orthopedic materials have received increasing attention due to unique biodegradability, good biocompatibility and similar mechanical properties to natural bone.

Over the past eight years, our research teams have created a road map to the next generation of magnesium implant materials with the addition of completely biocompatible elements. More than 20 patents have been filed and various in vivo and clinical studies were performed in collaboration with major hospitals in Korea to evaluate developed alloy's performance as the simple degradable bone screw, bone plate, and bone graft.

We would like to go even further and use the vast experience in the biodegradable research field to develop more advanced biocompatible implant material with higher strength, elongation and corrosion resistance. New material can be applied to more complex load bearing orthopedic implants such as spinal cage, bone plate, k-wire and scaffold.

This presentation will cover the long term clinical study of biodegradable magnesium screw performed in South Korea during 2013-2015. Over 60 patients have successfully received the implantation and long term follow up data including x-ray images will be presented for the first time.

Manuscript of above mentioned clinical study is in preparation right now and this abstract will be updated accordingly.

**ACKNOWLEDGEMENTS:** This research was supported by KIST Project (2E25260)

## Vascularized bone grafting fixed by biodegradable magnesium screw for treating osteonecrosis of the femoral head – a pilot clinical trial

D Zhao<sup>1\*</sup>, B Wang<sup>1</sup>, S Huang<sup>1</sup>, Faqiang-Lu<sup>1</sup>, L Qin<sup>2\*</sup>, Y Li<sup>3</sup>

<sup>1</sup> Department of Orthopedics, Affiliated Zhongshan Hospital of Dalian University, Dalian, China.
<sup>2</sup> Musculoskeletal Research Laboratory, Department of Orthopaedics & Traumatology, The Chinese University of Hong Kong, Hong Kong SAR, China. <sup>3</sup> Dongguan Yi'an technology company

**INTRODUCTION:** To study prospectively the application of Biodegradable Magnesium Screw in the retention treatment of the femoral head and to discuss the follow-up evaluation of the pure magnesium biodegradable screws of stability, degradation and safety.

METHODS: 48 patients with ONFH met the inclusion criteria and were enrolled into the study from February 2013 to April 2014. The patients were randomly divided into two groups: the Mg screw group (vascularized bone grafting fixed by Mg screw) and the control group (vascularized bone grafting without fixation by Mg screw). The Mg corrosion rate, new bone formation, and the density around the Mg screw were determined. During the patients' 12 month follow-up period, the treatment effects including - imaging and functional recovery-Harris hip score (HHS) were assessed respectively. The serum levels of Mg, Calcium (Ca), Phosphorus (P) ions were determined at baseline (before operation) and postoperative.

**RESULTS**: It showed a slow degradation of the fixation Mg screw. The new bone formation and the density around the Mg screw increased with implantation over time. Compared to the control group, the HHS improved significantly in the Mg screw group. The angiography imaging showed more new bone formation and angiogenesis in Mg screw group. The postoperative serum levels of Ca, Mg, and P ions relevant for function of the liver and kidney were all within normal physiological range in all patients of both groups.



Fig. 1: Fig. 1: Pre and postoperative Imaging (posterior-anterior) of the control group.



Fig. 2: Pre and postoperative Imaging (posteri oranterior) of Mg screw group.

**DISCUSSION & CONCLUSIONS:** This is the first pilot randomized and perspective clinical trial on using pure Mg screw as a biodegradable and bioactive implant for the fixation of vascularized bone flaps indicated for surgical intervention in ONFH patients at ARCO Stage II and III. The pilot results suggested: 1) Treatment efficacy in terms of better stabilization of the bone flap as compared with conventional approach without any flap fixation using 'biodegradable polymer' permanent screws made of stainless steel or titanium. 2) Anabolic effects of degraded Mg ions as evidenced with more bone formed around the screw and flap fusion region. 3) The degradation rate was gradual without observable local gas production during Mg screw degradation and such degradation would not affect the initial fixation potential as it is compromised by healing or fusion taking place around the implanted bone flap. 4) The Mg screw is biocompatible as no tissue necrosis around screw and abnormal blood chemistry was found post-implantation. Mg screw of high purity provided a promising bone-screwfixation and had great potential for medical application.

#### Corrosion behaviour of 3 Mg-alloys in bone: a high-resolution investigation

S Galli<sup>1</sup>, JU Hammel<sup>2</sup>, J Herzen<sup>3</sup>, G Szakács<sup>2</sup>, F Lukáč<sup>4</sup>, M Vlček<sup>4</sup>, I Marco<sup>5</sup>, A Wennerberg<sup>1</sup>, R Willumeit-Römer<sup>2</sup>, R Jimbo<sup>1</sup>

<sup>1</sup>Malmö University, Sweden, <sup>2</sup>Helmholtz-Zentrum Geesthacht, Germany, <sup>3</sup>Technical University of Munich, Germany, <sup>4</sup>Charles University, Prague, Czech Republic, <sup>5</sup>KU Leuven, Belgium,

**INTRODUCTION:** Magnesium (Mg) and its biodegradable alloys are promising biomaterials for bone application. However, their corrosion behaviour is still poorly understood and the resorption mechanism is still unpredictable *in vivo*, due to the high complexity of the physiological environment [1]. Here we report on the *in vivo* degradation process of 3 Mg alloys as observed on synchrotron-based micro computed tomography (SR $\mu$ CT) and on corresponding histological sections. SR $\mu$ CT, thanks to the high contrast-tonoise ratio, enables to clearly detect the changes that the Mg alloys undergo during corrosion, in a non-destructive way and directly in the bone [2].

METHODS: Sixty mini-screws made of 3 Mgalloys (Mg2Ag, Mg10Gd and Mg4Y3RE) were implanted in the tibiae of 20 rats. After 1 and 3 months, screw-bone blocks were explanted and scanned for SRµCT (PETRA III - DESY, Hamburg). Reconstructed stacks of images were obtained (binned voxel edge: 4.8um) and the following parameters were quantitatively and qualitatively analysed: corrosion rates, corrosion layers morphology, bone formation and 3D boneto-implant contact (BIC%). After scanning, the specimens were embedded in resin and 30-µm thick non-decalcified sections were prepared. Histomorphometry and corrosion quantification were evaluated in the 2D slides and compared with the 3D results.

**RESULTS:** On the basis of the absorption coefficients, it was possible to segment the screws volume into the original alloy ( $\alpha$ -Mg phase), with dispersed high absorbing particles, and the corrosion layers, originating from the surfaces. The corrosion layers were less dense than the α-Mg phase at 1 month, but became gradually denser at 3 months. The Mg2Ag screws showed changes in shape and reduction in size at 3 months, while the other materials preserved the original shape. The total volume of Mg4Y3RE screws (alloy + corrosion layers) was 11% bigger after 3 months in bone then prior to implantation. The corrosion rates of the screws were calculated in mm/year as the decrease in volume of the  $\alpha$ -Mg phase, divided by the average initial screw area (Table 1). The different densities on the µCTs corresponded to

similar phases on the histological slides, where the screws appeared formed by a residual metal and a non-metallic material (Fig 1). Mg10Gd and Mg4Y3RE implants were surrounded by new bone and their BIC% increased from 1 to 3 months, while Mg2Ag showed almost no bone contact.

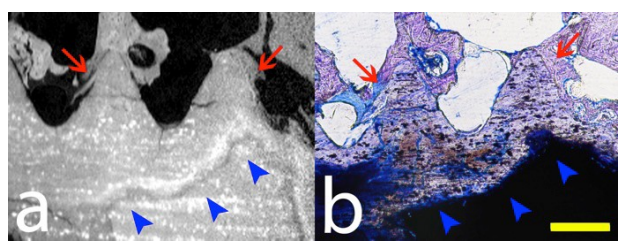


Fig. 1: The  $\mu$ CT slice (a) and the corresponding histology (b) of Mg4Y3RE. Blue arrows: contours of residual metallic alloy; red arrows: corrosion layer, still shaped as threads, in contact with bone (toluidine blue). Scale bar: 200  $\mu$ m.

Table 1. Volume change ( $\Delta V$ ) in % and corrosion rates (CR) in mm/year of the metallic alloys.

	0-1 m		0-3 m		1-3 m	
	$\Delta V$	CR	$\Delta V$	CR	$\Delta V$	CR
Mg4Y3RE	-17.3	.39	-31.8	.24	-17.6	.16
Mg10Gd	-34.4	.78	-35.8	.27	-2.2	.02
Mg2Ag	-21.6	.46	-44.6	.31	-29.3	.24

**DISCUSSION & CONCLUSIONS:** Surprisingly, Mg10Gd and Mg4Y3RE maintained the original screw shape while transforming in corrosion products. The corrosion rates decreased with time, although the inhomogeneous corrosion expanded the surface area of the residual metals. The 3months corrosion rates were similar for all materials, but the behaviour of the corrosion products differed. The relatively rapid solubilisation of Mg2Ag corrosion layers may explain the lower bone contact for these screws at month 3. In the other 2 alloys, the corroded layers looked stable during the observation time and were well osseointegrated.

**ACKNOWLEDGEMENTS:** Funding from the Marie Curie Actions (FP7/2007-2013) REA grant agreements: n° 289163 (MagnIM), n° 312284 (DESY).

### Influence of trace impurities on the *in vivo* degradation of biodegradable Mg–5Zn–0.3Ca

E Martinelli<sup>1</sup>, J Hofstetter<sup>2</sup>, S Pogatscher<sup>2</sup>, P Schmutz<sup>3</sup>, E Povoden-Karadeniz<sup>4</sup>, J Eichler<sup>1</sup>, A Myrissa<sup>1</sup>, T Kraus<sup>5</sup>, S Fischerauer<sup>1</sup>, P J Uggowitzer<sup>2</sup>, J F Löffler<sup>2</sup>, A Weinberg<sup>1</sup>

<sup>1</sup> Department of Orthopaedics, Medical University of Graz, Austria

<sup>2</sup> Laboratory of Metal Physics and Technology, Department of Materials, ETH Zurich, Switzerland

<sup>3</sup> Laboratory for Joining Technologies and Corrosion, EMPA, Swiss Federal Laboratories for Materials

Science and Technology, Switzerland

<sup>4</sup> Christian Doppler Laboratory for Early Stages of Precipitation, Vienna University of Technology, Austria

<sup>5</sup> Department of Paediatric Orthopaedics, Medical University of Graz, Austria

INTRODUCTION: Due to their excellent properties, magnesium (Mg) alloys are ideal candidates for the use in osteosynthesis [1]. Because a second operation for implant removal can be avoided, they might be of special interest in paediatric orthopaedics. However, degradation of conventional Mg alloys is too fast accompanied by the formation of high amounts of hydrogen gas [2]. It has been shown that the Mg degradation rate also strongly depends on the presence of specific impurity elements [3]. The aim of the present study was therefore to compare the in vivo performance of two Mg-Zn-Ca alloys (ZX50, Mg-5Zn-0.3Ca) of conventional purity (CP) and ultrahigh-purity (XHP) in a growing rat model.

**METHODS:** Both CP and XHP ZX50 were processed to extruded rods, and pins of 1.6 mm in diameter and 8 mm in length were produced for the *in vivo* tests [2]. The pins were implanted transcortically in the femoral bone of 12 male Sprague-Dawley rats (n = 6 per group). The degradation rate, gas amount, implant-bone interface, and new bone growth were observed within a period of 24 weeks by means of continuous online Micro-Computed Tomography ( $\mu$ CT) monitoring after 1, 4, 8, 12 [4] and 24 weeks. All animal experiments were conducted with ethical respect and ethical law and are authorized by the Austrian Ministry of Science and Research (BMWF-66.010/0087-II/3b/2011).

**RESULTS:** Animal experiments were performed to investigate the effect of trace impurity elements on the degradation behavior of CP and XHP ZX50. Especially, during the first period after implantation, XHP ZX50 degrades more homogeneously than CP ZX50, which has an increased impurity level. There is a significant difference up to 8 weeks after implantation, but this difference progressively vanishes towards the end of the in vivo

study. Both alloys are completely degraded after 24 weeks without any visible adverse effects on the bone morphology within the growing rat.

**DISCUSSION & CONCLUSIONS:** The lower trace impurity level in XHP ZX50 has a strong influence on the degradation behavior of the alloy. It increases the degradation rate within the first weeks after implantation and also increases the material's stability against local corrosion attacks. These effects lead to a more homogenous degradation performance compared to the alloy with conventional purity.

#### **ACKNOWLEDGEMENTS:**

The authors appreciate the support of the Laura Bassi Center of Expertise BRIC (Bioresorbable Implants for Children), FFG, Austria.

#### Dual in vivo behavior and biological effect of Mg in bone

A Chaya<sup>1,2</sup>, DT Chou<sup>2</sup>, D Hong<sup>2</sup>, S Yoshizawa<sup>1,3</sup>, K Verdelis<sup>1,3</sup>, P N. Kumta<sup>1,2,3</sup>, C Sfeir<sup>1,2,3</sup>

<sup>1</sup> Center for Craniofacial Regeneration, University of Pittsburgh, USA. <sup>2</sup> Department of Bioengineering, University of Pittsburgh, USA. <sup>3</sup> Department of Oral Biology, University of Pittsburgh, USA

INTRODUCTION: Magnesium (Mg) and its alloys have shown promise as degradable materials for bone fixation applications [1-3]. For this reason, we have studied 99.9% Mg fixation plates and screws using a rabbit ulna fracture model [4,5]. These studies demonstrated preliminary efficacy of the devices to facilitate fracture healing. In addition, we observed enhanced periosteal bone formation in the presence of their degradation. However, additional investigations are needed to fully understand the effects of alloy composition and degradation on the subsequent biological response. For these reasons, we are continuing to study Mg alloys as fixation devices to better understand their effect on bone biology.

**METHODS:** Plates and screws were machined from extruded WXQK (W: $0.5 \le Y \le 4 - X:0 < Ca \le 1 - Q:0.25 \le Ag \le 1 - K:0 < Zr \le 1$ ) and sterilized using gamma radiation. Rabbit ulnar osteotomies were created and secured with one plate and four screws each. After 8 and 16 weeks, forearms were assessed by microCT, histological staining, and mechanical testing.

**RESULTS:** MicroCT volume quantifications showed a significant reduction in WXQK volume after 8 weeks with corrosion product formation around all devices.

As previously described with 99.9% Mg, progressive bone formation was observed around WXQK devices throughout the study. Interestingly, this newly formed bone appeared highly porous when compared to that observed with 99.9% Mg. MicroCT quantification of pore volumes revealed significantly larger pores throughout periosteal bone around WXQK devices compared to 99.9% Mg after 16 weeks.

In contrast to bone formation above the degrading devices, proximal cortical bone loss was observed beneath most devices. When compared to cortical bone volumes beneath 99.9% Mg devices, the average bone volume beneath WXQK devices was significantly reduced after 8 and 16 weeks.

Despite observations of cortical bone loss, three point bend testing revealed no difference in the flexure load response for fractured ulnae after 16

weeks when compared to ulna fixed with 99.9% Mg and healthy controls.

**DISCUSSION & CONCLUSIONS:** These results reveal important distinctions between the in vivo behavior and subsequent biological effect of WXQK and 99.9% Mg fixation devices. Specifically, our observations of cortical bone loss beneath degrading WXQK devices warrants additional investigations on the effect of alloy degradation on local ion concentrations and pH.

ACKNOWLEDGEMENTS: This study was supported by the NSF ERC RMB (grant 0812348), Commonwealth of Pennsylvania (SAP 4100061184), and the University of Pittsburgh's Center for Craniofacial Regeneration. The authors thank Andrew Holmes for device fabrication, Dr. Michael Epperly for device sterilization, and Dr. Alejandro Almarza for assistance with mechanical testing (University of Pittsburgh).

## FACS based analysis of the early inflammatory reaction to biodegradable and not biodegradable implanted materials in rats

MC Heinze<sup>1,2</sup>, T Schmidt<sup>1,2</sup>, S Krummsdorf <sup>1,2</sup>, M Geiling <sup>1,2</sup>, Z Kronbach<sup>1,2</sup>, F Witte<sup>1,2</sup>

<sup>1</sup> Julius Wolff Institute, Charité- Universitaetsmedizin Berlin, <sup>2</sup> Berlin Brandenburg Center for Regenerative Therapies (BCRT), Charité- Universitaetsmedizin Berlin

INTRODUCTION: Biodegradable implants based on magnesium offer several advantages mainly the lack of the need for implant retrieval. However, the degradation products could cause negative side effects. Therefore, biocompatibility has to be proven before clinical use. In this study the local inflammatory reaction to biodegradable and not biodegradable implants was characterized using a newly established FACS immune cell panel which allows for quantitative single cell analysis.

**METHODS:** Round shaped implants (0.8cm) made from PEEK (negative control), polystyrene (PS, positive control) or pure magnesium (MG) were implanted one intramuscularly (i.m.; M. gluteus) and one subcutaneously in the back of 108 female 12 weeks old Lewis rats. After 1, 3, 7, 14, 21 or 28 days animals were sacrificed (each material n=6) and the capsules formed around the implants were harvested (*Fig. 1*). Tissue was minced and digested with collagenase buffer (1h, 37°C). Samples were stained for CD45, CD3, CD4, CD8, HIS48 and HIS36 as a marker for ED2 tissue macrophages following the instructions of the manufacturer (eBioscience).

FACS analysis was performed on MACS-Quant. Values are presented as % from CD45+ cells (all leukocytes). Statistics: two-way ANOVA, p≤0.05.

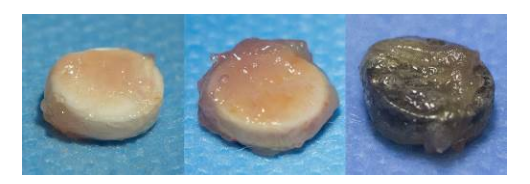


Fig. 1: Harvested i.m. capsules of PS, PEEK, MG around the implants at day 14

RESULTS: Granulocytes peaked at day 1 in MG, PS, PEEK s.c. and i.m., decreased significantly up to day 3 and stayed constant afterwards (*Fig.* 2). Macrophage number was low after one day but significantly increased up to day 28 in MG, PS and PEEK s.c. and i.m. with highest values after 7 (MG i.m), 14 days (PEEK, PS i.m., PS, MG s.c.) or 21 days (PEEK s.c.). T helper cells (CD3+CD4+) significantly increased up to day 28 in MG and PS s.c. and i.m. as well as in PEEK s.c. (p≤0.003). Number of T helper cells in MG was

increased compared to PS and PEEK from day 7. Cytotoxic T cells (CD3+CD8a+) i.m. peaked at day 7 and stayed constant afterwards in MG, PS and PEEK. Cell number in MG was decreased compared to PS and PEEK from day 7.

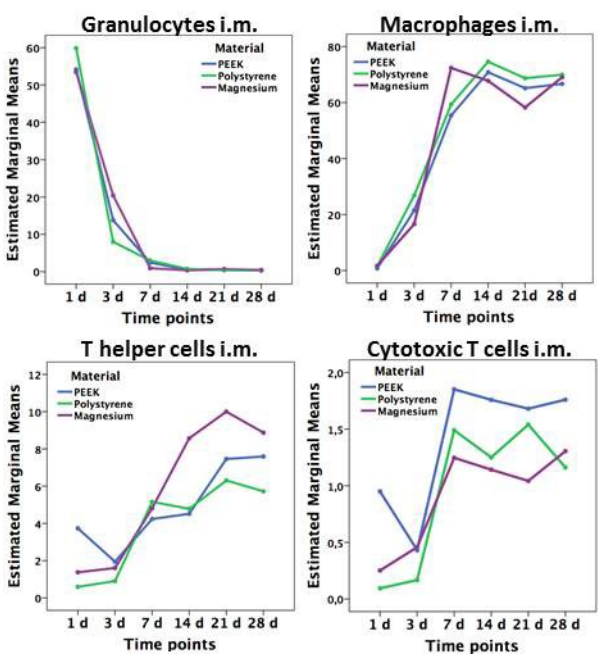


Fig. 2: Estimated marginal means of granulocytes, macrophages, T helper cells and cytotoxic T cells in % of the CD45+cells in i.m. capsule depending on time points (two-way ANOVA)

DISCUSSION & **CONCLUSIONS:** established FACS panel is a good tool to quantify the inflammatory response to implants in rats. Our results show a comparable moderate local foreign body reaction to the implants with an early immigration of granulocytes to the implant side followed by macrophages and T cells at both implant locations. The degradation of the magnesium did not increase the number of inflammatory cells in general indicating a good biocompatibility of the material. However the role of the changed T cell pattern in MG compared to PS and PEEK has to be investigated in further studies.

**ACKNOWLEDGEMENTS:** Dr. Désirée Kunkel, BCRT Flow Cytometry Lab

#### *In-vitro* and *in-vivo* characterization of biodegradable zinc coronary stent

J Zhou, H Gong, X Miao, Y Wang, X Yan, Y Zhang, G Guo, M Zhao, G Qu

Xi'an Advanced Medical Technology, China

**INTRODUCTION:** Zinc (Zn) as a novel biodegradable metal holds great potential in biodegradable implant applications since it is more corrosion resistant than Magnesium (Mg). However, the mechanical properties, In-vitro and In-vivo biodegradation behaviors of Zn remained as concerns. In this study, pure Zn tube, wire and pure Zn stent were tested In-vitro and In-vivo.

**METHODS:** Pure Zn wire ( $\Phi$  250µm, 99.9% purity) was purchased from Alfa Aesar, USA. Pure Zn tube ( $\Phi$  1.5mm, 150µm thickness, 99.99% purity) was purchased from EuroFlex, Germany. Zn stents (\$\Phi 1.5mm \times 10mm\$) were laser cut from Zn tube. To investigate In-vitro biodegradation behavior of Zn tube, immersion test was performed according to ASTM-G31-72. Simulated body fluid (SBF) was added by the surface area to solution volume to 1 cm<sup>2</sup>:20 ml and temperature was kept at 37 °C. Zn wires were inserted in New Zealand rabbit aorta abdominalis. Zn stents were implanted in New Zealand rabbit aorta abdominalis through left femoral artery using a balloon catheter (Φ 2.5mm×16mm). To examine morphology and atom biodegradation composition of specimens were fixed in resin and ground by silicon carbide abrasive papers with successive grades from 400 to 2000, and polished with 0.5 µm diamond suspension. Polished specimen were examined with Scanned Electron Microscope (SEM) equipped with Energy-dispersive X-ray spectroscopy (EDX) and backscattered electron (BSE) detectors. Phase composition of Zn tube biodegradation products were analyzed using Xray Diffraction (XRD).

RESULTS: Zn biodegradation product can be described as light grey under SEM. Similar biodegradation morphology were found in In-vitro tested Zn tube (Fig. 1A) and In-vivo tested Zn wire (Fig. 1B). Mostly it was found as a compact and continuous whole piece, without significant expansion or dislocated granular products. External layer of biodegradation products of In-vivo tested Zn wire were mainly composed of Zn, C, O, Cl, P and Ca (Tab. 1). It's reasonable to assume that products may contain ZnO, Zn(OH)<sub>2</sub>, Zn<sub>3</sub>(PO<sub>4</sub>)<sub>2</sub> and Ca<sub>3</sub>(PO<sub>4</sub>)<sub>2</sub>, but XRD examination found that ZnO and Zn<sub>5</sub>(OH)<sub>8</sub>Cl<sub>2</sub>·H<sub>2</sub>O were the

major composition of Zn biodegradation product. This is probably because that only a small amount of Ca and P existed in a thin external layer (Tab. 1). Implantation and expansion of pure Zn stent was successful without any broken struts (Fig 1C). Endothelialization was completed at the 28th day (Fig 1D).

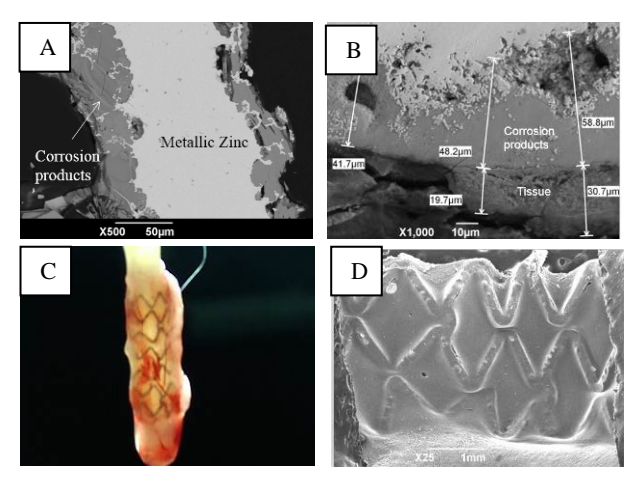


Fig. 1: A) In-vitro corrosion of Zn tube, B) In-vivo corrosion of Zn wire, C) Implantation of Zn stent in rabbit aorta abdominalis, D) 28 days after implantation of Zn stent

Tab 1. Atom percentages of Zn In-vivo corrosion products

	Zn	C	O	Cl	P	Ca
Internal	17.4	14.9	56.8	10.7	N	N
	6	4	6	4		
Externa	9.51	10.2	63.7	0.42	11.0	5.0
1	ı	8	1		5	3

DISCUSSION & CONCLUSIONS: The main advantage of Zn over Mg alloy is its high corrosion resistance in body fluid environment, considering current Mg alloy implants often suffer from fast-corrosion and consequent release of hydrogen bubble and early dislocation and disruption. From this study, it's believed that Zn with uniform and slow biodegradation and good biocompatibility is a suitable candidate material for load-bearing biodegradable implant application.

## Early experiences with the biocompatibility of zinc and its alloys in the murine aorta

PK Bowen<sup>1</sup>, RJ Guillory II<sup>2</sup>, ER Shearier<sup>2</sup>, <u>J Drelich</u><sup>1</sup>, <u>J Goldman</u><sup>2</sup>

<sup>1</sup> <u>Department of Materials Science and Engineering</u> <sup>2</sup> <u>Department of Biomedical Engineering</u>, Michigan Technological University, Houghton, Michigan, USA

INTRODUCTION: An ideal metal degradable endovascular stent material would perform its mechanical function for several months and be absorbed post-implantation. To circumvent the rapid degradation of magnesium, the authors recently introduced metallic zinc as a stent base material. Zinc exhibited a near-ideal in vivo corrosion rate [1], and alloying holds promise in producing a material with suitable mechanical properties. However, the biocompatibility of metallic zinc and its corrosion products are largely unknown. Characterization of cellular and tissue responses to zinc over time is crucial to gauge the compatibility of zinc and its alloys with arterial tissues, and to guide rational bulk and surface modifications to improve implant performance. Here, selected results are discussed from a 22month in vivo study of Zn and a series of alloys.

METHODS: High purity (99.99%) Zn was acquired in wire form (Ø=250µm) from Goodfellow, Inc. Electropolished strips of lower purity (standard high grade; nominally>99.7%) and experimental alloys were fabricated in-house with an approximately 250×250µm square crosssection. In vivo corrosion experimentation utilized an established abdominal aortic wall implant in Sprague-Dawley rats [2]. After 1–22 mo in the murine aorta, the wires were excised, snap-frozen in liquid N<sub>2</sub>, and cross-sectioned transversely. Important aspects of biocompatibility, including inflammation, dysplasia, cytotoxicity, and FBR were evaluated through histological examination. Sections were stained with H&E Masson's trichrome, and Verhoff-Van Gieson for light microscopy. Key fluorescent probes were also used, including DAPI,  $\alpha$ -actin, and CD-31.

**RESULTS**: Selected light and fluorescent microscopy results are shown in Fig. 1 and Fig.2, respectively. Low-magnification light microscopy results (Fig.1A) illustrate the presence of corrosion product and matrix within the original implant

footprint at 3 mo. A close-up view (Fig. 1B) shows matrix synthesis resident cells within the implant footprint. Immunofluorescence also indicated a

lack of  $\alpha$ -actin, and therefore smooth muscle cells, near the zinc surface (Fig. 2).

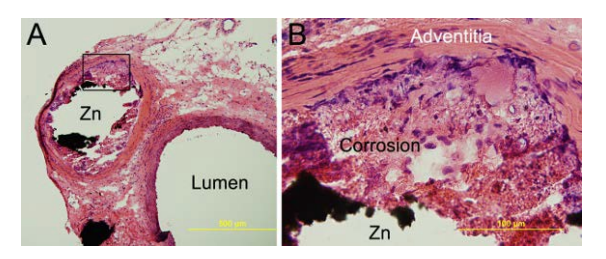


Fig. 1: H&E stain of an alloy after 3 mo in the arterial wall. 500 (A) and 100 (B) µm scale bars.

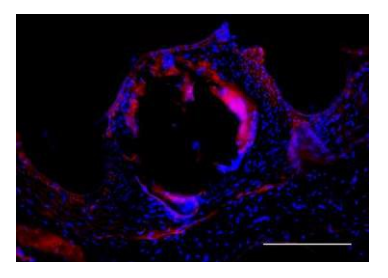


Fig. 2: Immunofluorescent image of luminal implant showing nuclei (DAPI, blue) and α-actin (smooth muscle cells) (red). 100 μm scale bar.

**DISCUSSION & CONCLUSIONS**: The arterial response to metallic zinc is positive. Matrix remodeling and repopulation in addition to a lack of smooth muscle cell proliferation and other contributors to restenosis indicate that this could be an effective degradable metallic stent material.

**ACKNOWLEDGEMENTS**: PKB was funded by an AHA predoctoral fellowship. Project funds from NIH NIBIB award 5R21EB019118-02.

### Preliminary in vivo study on iron-based alloy implantation in rat model

A Purnama<sup>1,2</sup>, MC Drolet<sup>1</sup>, J Couet<sup>1</sup>, D Mantovani<sup>2</sup>

<sup>1</sup> <u>Institut Universitaire de Cardiologie et de Pnemulogie de Ouébec</u>, Department of Medicine, Laval University, Canada <sup>2</sup> <u>Laboratory for Biomaterials and Bioengineering</u>, Department Min-Met-Materials, Laval University, Canada

**INTRODUCTION:** The need of temporary scaffolding function for cardiovascular stent has led the development of iron-based alloys. Iron-based alloy are preferable due to their superior mechanical properties compared to magnesium and zinc-based alloys. However, the degradation rate of iron for cardiovascular application is considered slow. Powder metallurgy<sup>1</sup> and electroforming<sup>2</sup> have been used as a new fabrication approach to accelerate the degradation rate of iron. Manganese (35% w/w) was added to form binary Fe-35Mn alloy<sup>1</sup>. Iron is an essential element for human body, therefore the toxicity of their degradation products is unlikely. More over, pure casted iron<sup>3</sup>, pure electroformed iron<sup>2</sup>, and Fe-35Mn<sup>1</sup> have been shown as potential candidates for cardiovascular biodegradable stent with mechanical properties similar to those of the stainless steel. Previously, electroformed iron and Fe-35Mn alloy have been shown to reduce the proliferation of the smooth muscle leading to their potential to avoid in-stent restenosis. This result suggested further study with in vivo model to understand better the interaction of iron-based alloy with the living tissue. The iron-based alloy discs were then implanted subcutaneously using rat model and the tissue reaction within the surrounding tissue was observed.

METHODS: Iron-based alloys consist of electroformed iron (E-Fe), annealed Fe (A-Fe), and Fe-35Mn were cut into disc-shape implants with 5 mm diameter. Stainless steel 316L was used as a reference material. Subsequently, the discs were implanted in the back of male a Wistar rat subcutaneously for 1 and 3 months. Each rat received one type of disc and there were six rats involved within each group. After incubation period attained, the rats were sacrificed and then followed by

the observation of the discs and the surrounding tissue.

**RESULTS:** The results showed that there were no signs of systemic toxicity observed in all implantation groups. However, there was a tendency of elevated weight gain observed within the groups that received iron-based alloy implants. Moreover, the presence of macrophage within the surrounding implantation site was observed. The presence of macrophage was more evident within the group that received E-Fe. This was suggestively due the faster degradation rate of E-Fe compared to other iron-based alloys.

**DISCUSSION & CONCLUSIONS:** The results demonstrated a moderate presence of macrophage around the degradable metals implying a promising potential of the tested materials although further study is suggestively needed to confirm their functional biocompatibility with bigger animal model.

ACKNOWLEDGEMENTS: The authors would like to acknowledge the hospital animal center and the kind financial support from the Natural Science and Engineering Research Council (NSERC) of Canada, the Collaborative Health Research Projects of NSERC and the Canadian Institutes of Health Research (CIHR).

## In-vivo suitability studies of magnesium based screws concerning handling and ingrowth outcome

L Berger<sup>1</sup>, J Eichler<sup>2</sup>, E Martinelli<sup>2</sup>, C Kleinhans<sup>2</sup>, P Uggowitzer<sup>3</sup>, J Löffler<sup>3</sup>, A Weinberg<sup>2</sup>,

<sup>1</sup> Insitute for Building Construction and Technology, TU Wien, Vienna, AT

<sup>2</sup> Department of Orthopaedic and Orthopaedic surgery, Medical University of Graz, Graz, AT

<sup>3</sup> Laboratory of Metal Physics and Technology, ETH Zurich, Zurich, CH

**INTRODUCTION:** Magnesium (Mg) possesses ideal characteristics in mechanical properties and biological acceptance and thus is promising to be used as implant material particularly in surgical stabilisation of bone fractures. In addition, the degradation ability avoids second surgeries for removal<sup>1</sup>. Besides a reliable degradation profile and good bone ingrowth, the handling and suitability of Mg based implants must be tested. The purpose of this study was to analyse the applicability of Mg based screws for the usage in cortical bone.

**METHODS:** The biodegradable Mg alloy XHP ZX00 (Mg-0.3Zn-0.4Ca) was selected for drymachining of screws (Ø=3.5 mm, L=16 mm), which were gamma sterilized and inserted into an ovine right tibia (experimental, N=1) with precedent drilling and tapping of insertion sites. The same screws were implanted in the cadaveric right tibia (control, N=1) after sacrificing the animal at 6 weeks after implantation. All animal studies were performed in accordance to the Austrian Ministry of Science and Research that authorized these experiments (accreditation number BMWFW-66.010/0190-WF/V/3b/2014). An axial pull-out was performed on 3 screws of the experimental group after 6 weeks (w) in vivo. The same method was conducted with the cadaveric control bone with 2 screws in cortical bone.

**RESULTS:** The pull-out test revealed a lower normalized strength of the screws that stayed in the tibia for 6w in comparison to the control group (Fig. 1).

The cross section of the bone at the implant site showed small gas pockets in the medullary cavity. The screws failed by partly shearing-off the thread flanks and partly failure of the bone tissue.

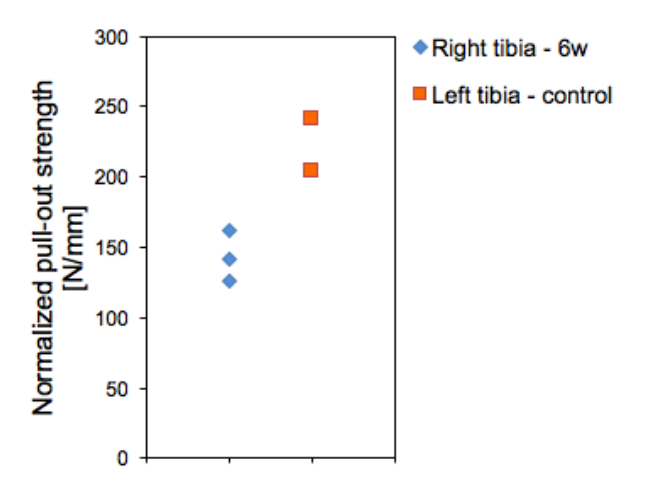


Fig. 1: Pull-out test of XHP ZX00 screws inserted in ovine tibia (diaphysis) for 6 weeks vs ex vivo control group.

**DISCUSSION & CONCLUSIONS:** This first experiments show that Mg XHP ZX00 screws are suitable for the application in cortical bone. The strength is sufficient for an application after predrilling and tapping. After 6 weeks of implantation the pull-out test revealed lower load bearing capacity in comparison to the control, however the interface strength still sufficient enough for clinical applications. Gas evolution during the degradation in bone tissue and medullary cavity may influence bone structures and additionally lead to a lower pull-out strength of the screw. Further studies need to be performed to evaluate degradation, ingrowth and tissue reactions in more detail.

**ACKNOWLEDGEMENTS:** This work was financially supported by Laura Bassi BRIC.

# Ceramized magnesium scaffolds with submillimetre channel structures for bone reconstruction: *in vitro* characterization and preliminary *in vivo* results

A Kopp<sup>1</sup>, O Jung<sup>2</sup>, P Hartjen<sup>2</sup>, H Hanken<sup>2</sup>, R Smeets<sup>2</sup>, C Ptock<sup>1</sup>, D Porchetta<sup>1</sup>, S Schneider<sup>3</sup>, A Klink<sup>3</sup>, F Klocke<sup>3</sup>

<sup>1</sup> Meotec GmbH & Co. KG, Aachen. <sup>2</sup> Department of Oral & Maxillofacial Surgery, University Medical Center Hamburg-Eppendorf, Hamburg. <sup>3</sup> Manufacturing Technology, Laboratory for Machine Tools and Production Engineering (WZL) of RWTH Aachen University, Aachen.

#### **INTRODUCTION:**

Bioresorbable metals show a high potential for load-bearing applications in medical device technology, especially in the field of osteosynthesis. Depending on the alloy, bioresorbable magnesium alloys can show bone-like properties regarding strength and promising biocompatibility. Still, there are disadvantages as excessive hydrogen gas evolution and rapid degradation to overcome. While smallest implants like screws and others seem within reach, there is a special need to minimize material and allow for appropriate bone in-growth in large-volume bone-replacement, e.g. replacement of the mandible or long bones. In order to show the feasibility of large-scale bone replacement, ceramized magnesium scaffolds have been tested *in-vitro* and *in-vivo*.

#### **METHODS:**

Magnesium scaffolds made of magnesium WE43 with an innerconnecting square channel geometry of 0.4, 0.6 and 0.8 mm in length were manufactured. To instantiate such small bores with high aspect ratio, EDM (electro discharge machining) has been employed. Plasma-electrolytic oxidation treatment (PEO) is used to ensure a proper cell attachment and to intermittently restrain degradation of the significantly enhanced inner and outer surface of scaffold. Prior to in-vivo testing designated material combinations have been tested regarding cytocompatibility and degradation behavior in-vitro. For comparison of degradation behavior, alloy and different surface coatings have been qualitatively compared by electrochemical corrosion measurements, i.e. PDP and EIS. In vitro cytocompatibility was assessed according to DIN ISO 10993-5 and -12 using indirect XTT-, BrdU- and LDH- and direct livedead staining assays. For in-vivo assessment the three different scaffold scructures combining the magnesium WE43 alloy and a favourable surface modification were implanted transcortically into the femur of 60 new zealand white rabbits. The degradation in-vivo was monitored utilizing computer tomography (CT). After 6 and 12 months respectively, the animals were sacrificed to

evaluate osseointegration and bone regeneration by  $\mu CT$  and histomorphometric studies.

#### **RESULTS:**

While the blank WE43 alloy and different surface modifications showed diminished cytocompatibility due to assay interferences or rapid initial corrosion, one of the examined specimen exhibited excellent cytocompatibility with no significant difference compared to the titanium reference. Stained L929-fibroblasts, seeded directly on the surface, showed dense colonization with living, spindle-shaped cells, indicating viability. Indirect testing by XTT-, BrdU- and LDH-assays gave no evidence for cytotoxicity caused by the materialextracts. Evaluation of degradation behavior showed, that the average H<sub>2</sub>-release was significantly lower with ceramized specimen in comparison to uncoated samples. Concordantly, implants showed good osseointegration, low gas evolution and moderate foreign body reaction in-vivo.



Fig. 1: Magnesium scaffold after fabrication and during insertion in femur for in-vivo testing

#### **DISCUSSION & CONCLUSIONS:**

Magnesium scaffolds with different structures have been manufactured successfully by combining innovative production technologies, materials and surface modifications derived from *in-vitro* testing. Preliminary results of the *in-vivo* testing show that the inserted scaffolds were well tolerated by the animals throughout the first testing-period of 6 months.

### MgO forms a bone-inducing matrix when implanted in bone marrow

H Nygren<sup>1</sup>, M Chaudhry<sup>1</sup> and S Gustafsson<sup>2</sup>

<sup>1</sup>Institute of Biomedicine, University of Gothenburg, POB 420 405 30 Goteborg, Sweden, <sup>2</sup>Department of Applied Physics, Chalmers University of Technology, 412 96 Goteborg, Sweden

INTRODUCTION: Magnesium oxide, which has been shown to stimulate bone growth, was used as bone cement around Ti-implants, and the outcome of pull-out tests were compared between experiment and control groups. The results show improved fixture retention in the group treated with MgO-paste[1]. The mechanism behind this effect was elucidated by analyzing bone samples with implanted MgO by light microscopy and environmental scanning electron microscopy and EDX analysis of histological bone preparations.

METHODS: Surgery. Pure MgO-powder (Sigma-Aldrich® Schnelldorf, Germany) and titanium cylinders (Elos Medtech, Sweden) were heat sterilized. Male Sprague Dawley rats (Charles River, Holland) were used throughout the study. The surgery has been described elsewhere [2]. Environmental scanning electron microscopy and EDX. The bone samples were dehydrated in ethanol, cut with a diamond saw and air-dried. An FEI Quanta 200 FEG ESEM operating at an accelerating voltage of 20 kV was used imaging. All images were acquired in the backscattered electron imaging mode. The atomic species of the samples were analysed by Energy dispersive X-ray (EDX). Data was recorded using an Oxford EDX detector and spectra were evaluated with the INCA software. Histology. Samples were fixed in 1% formaldehyde in phosphate-buffered saline (PBS) over night. The bone samples were decalcified for 2 weeks in 0.15 M EDTA, containing 0.5% paraformaldehyde. The samples were dehydrated and embedded in paraffin. Sections were cut and stained with hematoxylin and eosin and examined in a Zeiss Axioscope 2 microscope, equipped with an Axiocam ICc 1 digital camera.

**RESULTS:** A light micrograph from rat tibia implanted for 3 weeks with MgO paste is shown in Figure 1. Osteoblast differentiation, angiogenesis and bone formation is seen at the surface of an amorphous body. An ESEM backscatter image of the distribution of mineral in rat tibia 3 weeks after implantation is shown in Figure 2.

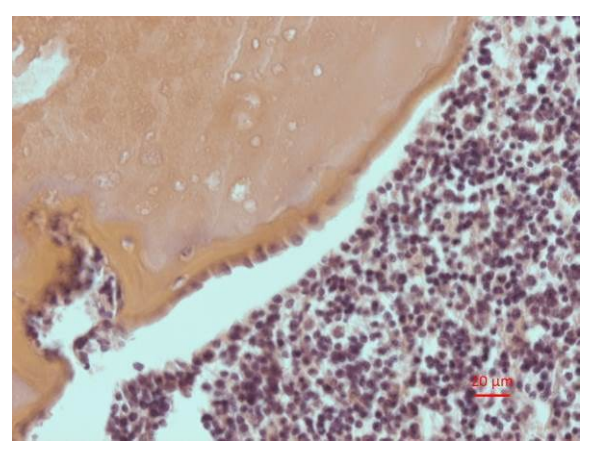


Fig. 1

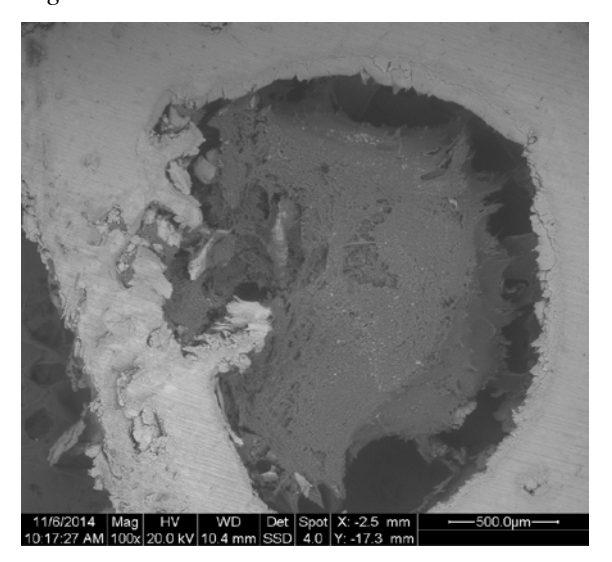


Fig. 2

**DISCUSSION:** Results obtained indicate that the distribution of Mg in the bone changes with time to become local bodies. These bodies induce bone formation.

## Pre-clinical characterization of full-size bioresorbable magnesium osteosynthesis implants in a growing sheep model

J Eichler<sup>1</sup>, SF Fischerauer<sup>1</sup>, E Martinelli<sup>1</sup>, A Myrissa<sup>1</sup>, T Kraus<sup>2</sup>, L Berger<sup>3</sup>, PJ Uggowitzer<sup>4</sup>, JF Löffler<sup>4</sup>, AM Weinberg<sup>1</sup>

<sup>1</sup>Department of Orthopaedics, Medical University Graz, Graz, AT. <sup>2</sup>Department of Paediatric Orthopaedics, Medical University Graz, Graz, AT. <sup>3</sup>Institute of Building Construction and Technology, Vienna University of Technology, Vienna, AT. <sup>4</sup>Metal Physics and Technology, Department of Materials, ETH Zurich, Zurich, CH.

**INTRODUCTION:** Elastic stable intramedullary nailing (ESIN) is a common method to treat paediatric long-bone fractures in an easy and effective way, allowing for early weight bearing without cast. However, metal removal is required when the fracture has healed, which leads to additional morbidity for the patient due to a second surgical intervention. Biodegradable Mg implants have great potential for deployment in paediatric fracture stabilization as they promise suitable mechanical properties and render a second surgical intervention. However, their major drawback is too rapid degradation. Thus rare-earth (RE) elements are frequently used for alloying, although they are considered to be noxious for the human body and obviously not suitable for a growing skeleton. The above desire for RE-free paediatric Mg implants led to the development of Mg-Zn-Ca alloys with 5 wt.% Zn (ZX50). However, these alloys showed a too high degradation rate with high amounts of gas in the bone [1]. Further research eventually led to Mg-Zn-Ca alloys with much lower Zn content (ZX10) [2], exhibiting a promising balance between degradation rate and hydrogen gas evolution in a living rat model. Aim of this pilot study was to evaluate the degradation of Zn-poor Mg-Zn-Ca ESIN implants in an in vivo sheep model to enable the use of fully sized ESIN implants due to clinical conditions, close to that of the paediatric trauma case.

**METHODS:** Two different RE-free magnesium alloys were investigated in 7 sheep tibiae (Austrian Ministry of Science, Research and Economy accreditation number BMWFW-66.010/0049-WF/II/3b/2014): alloy ZX10 (Mg-1Zn-0.3Ca, N =3) and alloy ZX00 (Mg-0.3Zn-0.4Ca, N=4). The materials were extruded to rods with a diameter of 3 mm and cut to a length of 25 cm, according to a preoperative length measurement of the sheep tibia. The operational procedure was performed similarly to a clinic paediatric trauma case. 2 ESINs (of diameter 3 mm) were used in the sheep tibia, filling 2/3 of the medullary cavity diameters according to standardized clinical conditions. A

group of 10 female lambs was used in this pilot study, including 3 control animals. The ESINs were implanted descending from the proximal tibia by a small lateral and medial approach. The medullary cavity was opened with a pricker and the nails were slightly bent and implanted to fit to the bone lengths. The protruding ends of the nails were cut and the wounds were closed in layers. All surgical interventions were performed under sterile clinical conditions. Degradation behaviour and gas amount were evaluated by continuous clinical CT imaging (Siemens Sensatom 64) at 2, 6, 12, 24 and 52 weeks after implantation. Volume, surface and gas evolution were quantified with Materialise MIMICS, ver. 17.

**RESULTS:** The implants were well tolerated by all animals and did not show adverse effects during the whole study period. Longitudinal radiological evaluations demonstrated a faster degradation and increased hydrogen gas production in the alloy ZX00, and visible degradation started after 2 weeks.

**DISCUSSION & CONCLUSIONS:** The aim of this study was to evaluate the degradation behaviour of fully sized RE-free implants in a living sheep model in which the ZX00 alloy showed faster degradation. Clinical CT evaluations were suitable for the distinction and characterisation of different rates of degradation and hydrogen gas release.

## Influence of impurities on the degradation performance of sintered and spark eroded Mg-0.9Ca alloy in an *in vivo* study

A Myrissa<sup>1</sup>, M Wolff<sup>2</sup>, E Martinelli<sup>1</sup>, J Eichler<sup>1</sup>, S Srinivasaiah<sup>1</sup>, R Willumeit-Römer<sup>2</sup>, U Schäfer<sup>3</sup>, AM Weinberg<sup>1</sup>

**INTRODUCTION:** Bioresorbable implants can be used in patients with bone fractures to avoid a secondary surgery for the implant removal. Common conventional pure Mg implants display higher corrosion rates than the High Pure and Ultra high pure Mg implants because of higher impurities [1]. For this reason, different alloying elements are used in implant processing to diminish the degradation rate. Recent *in vitro* biocorrosion tests of sintered Mg-0.9Ca material showed a corrosion rate of 0.6 mm/a. Due to this promising result, the implant material was used in this study to investigate its degradation performance under in vivo conditions.

**METHODS:** Mg-0.9Ca powder was pressed at 100 MPa and sintered at 635-645 °C for 8-64h under Argon atmosphere in a hot wall furnace (Xerion, Germany) [2]. Sintered Mg-0.9Ca parts were spark-eroded to cylindrical pins (d=1.6 mm, l=0.8 mm) and they were implanted transcortically to the femoral bones of male growing Sprague-Dawley rats. Micro CT scans were performed 1, 4, 12 and 24w after implantation (n=12). Pin volume, surface and gas evolution were evaluated with Materialise Mimics (V. 15.0). Degradation rate was calculated via the delta of pin volume and pin surface (n=6 bones). An untreated group was used as control and a Sham group with a drill hole at the same site of the femur was performed.



Fig. 1: Mg-0.9Ca (X1): left: sintered and sparkeroded part; right: pitting corrosion after 7d under cell culture conditions.

**RESULTS:** The Mg-0.9Ca alloy produced high amounts of gas due to an early corrosion in the first week after implantation, which led to the development of gas cavities within the intramedullary cavity and also the surrounding tissue. Gas volume showed further increase until

4<sup>th</sup>w post-operative. After 12 and 24w this behaviour was retarded. 24w after implantation, less than a third of the initial pin volume remained. As shown in fig.1 in vitro biocorrosion tests showed pitting corrosion of the pins, too. This corrosion type is unwanted. Additional SEM imaging and EDX-analysis displayed different particles consisting of e.g.: Fe, Cr, Ni, Cu, Zn as shown exemplary in fig. 2.



Fig. 2: SEM image of pin surface with particles

**DISCUSSION & CONCLUSIONS:** High loss of the pin volume at the end of the study as well as high amount of gas formation at the first time points of this study (1 and 4w) let us assume that existing impurities have a higher influence on the degradation behaviour as initially expected. The source of impurities might be due to the spark eroding process step. This indicates that key properties of material processing are: correct handling, surface quality and purity controls. Especially, in the manufacturing of magnesium alloys, all these production steps have to be optimised to gain a reproducible, homogenous degradation performance. However, a possible influence of tiny amounts of impurities on the surface and within the alloy on the degradation rate is still unknown and remains unclear and might be an explanation for the different in the corrosion behavior in vitro and in vivo.

**ACKNOWLEDGEMENTS:** This work is supported by the FP7 MSCA (Project Number: 289163) and by HVI VH-VI-523 (*In vivo* studies of biodegradable magnesium based implant materials).

<sup>&</sup>lt;sup>1</sup> <u>Department of Orthopaedic Surgery</u>, Medical University Graz, 8036 Graz, Austria, <sup>2</sup> <u>Institute of Materials Research</u>, Division Metallic Biomaterials, HZG, 21502 Geesthacht, Germany, <sup>3</sup> <u>Department of Experimental Neurotraumatology</u>, Medical University Graz, 8036 Graz, Austria

# Promotion of tendon-graft healing by magnesium-based interference screw in rabbit anterior cruciate ligament reconstruction model

P Cheng<sup>1</sup>, P Han<sup>1</sup>, C Zhao<sup>2</sup>, S Zhang<sup>2</sup>, X Zhang<sup>2</sup>, Y Chai<sup>1</sup>

<sup>1</sup> Shanghai Jiao Tong University Affiliated Sixth People's Hospital, Shanghai, China. <sup>2</sup> School of Materials Science and Engineering, Shanghai Jiao Tong University, Shanghai, China

**INTRODUCTION:** Within reconstruction of acterior cruciate ligment (ACL), interference screw is broadly used for tendon graft fixation to bone tunnel. Traditional interference screws is not effective in promoting fibrocartilaginous-type enthesis regeneration, which became the weak link in postoperative rehabilitation [1]. Magnesium based materials could provide a balance between mechanical strength and degradation [2], and shows potential in biological activities to promote firbrocartilage matrix [3].

METHODS: Interference screws were fabricated from 99.99% high purity magnesium (HP Mg) and shared same design with Titanium (Ti) screw as control. A total of 48 rabbits were used as ACL reconstruction model, and tendon graft was fixed by interference screw to femoral bone tunnel, 3.6.9 and 12 weeks after surgery, X ray scanning and range of motion (ROM) were performed for the analysis of functional recovery. Then femurtendon-tibia complexes were harvested for microcomputed tomography (microCT) scanning. The volume of bone tunnel was tested. Then samples were decalcified for hematoxylin and eosin (HE) staining and Safranin O/fast green staining. Furthermore, the biomechanical tests were conducted on samples for ultimate load to failure as well as related stiffness.

**RESULTS:** All rabbit resumed normal ambulation and ROM recovered 9 weeks after surgery. The insertion site and articular surface kept in good condition. No sign of dislocation or deformity was found in X ray images. In microCT analysis, HP interference screw performed degradation behavior without displacement in the bone tunnel. Furthremore, histologic images showed mature and calcified fabricartilagious layers in tendon-bone interfaces of HP Mg group, indicating formation of fibrocartilaginous-type enthesis. In contrary, fabricartilagious layer in Ti group exhibit smaller areas and lower histological scores. Furthermore, the ultimate load to failure in HP Mg group was comparable to Ti group, without significant differences.

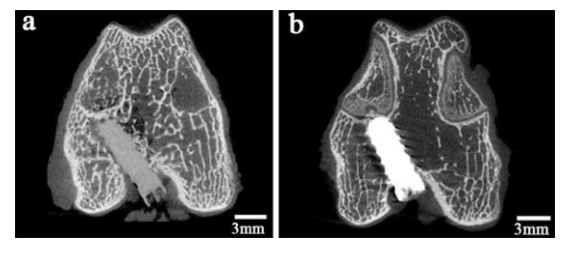


Fig. 1: 2D microCT images of rabbit femur with (a)HP Mg interference screw and (b)Ti interference screw 12 weeks after surgery.

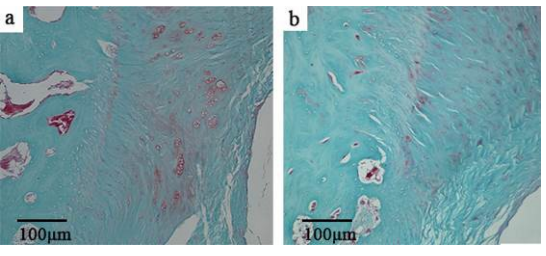


Fig. 2: Histological section of tendon-bone interface stained with Safranin O/fast green ( $\times 400$ ). (a) HP Mg group (b) Ti group.

**DISCUSSION & CONCLUSIONS:** HP Mg interference screw exhibited uniform degradation behaviour [4] and rigid fixation in bone tunnel. What is more important, HP Mg interference screw promoted regeneration of fibrocartilaginous-type enthesis, which might be due to its corrosion product. Thus Mg interference screw performed great potential in promoting tendon-bone healing in ACL reconstruction.

**ACKNOWLEDGEMENTS:** This work was supported by the Natural Science Foundation of China (No. 51271117, 81371935).

# Fixation of biodegradable high-purity magnesium screws in rabbit femoral intracondylar fractured model

P Han<sup>1</sup>, P Cheng<sup>1</sup>, P Hou<sup>1</sup>, C Zhao<sup>2</sup>, S Zhang<sup>2</sup>, X Zhang<sup>2</sup>, Y Chai<sup>1</sup>

<sup>1</sup> Shanghai Jiao Tong University Affiliated Sixth People's Hospital, Shanghai, China. <sup>2</sup> School of Materials Science and Engineering, Shanghai Jiao Tong University, Shanghai, China

**INTRODUCTION:** High-purity magnesium (HP Mg) (99.99%) shows great potential in controlling corrosion rate [1], reducing microgalvanic degradation of secondary phase particles in Mg alloys [2] and limiting the pathophysiology and toxicology of alloying elements [3]. In this study, we fabricated orthopeadics screw from HP Mg and investigated the in vivo behaviour in rabbit model of weight-bearing bone fracture.

**METHODS:** HP Mg went through rolling process and was fabricated into orthopaedics screws. Then screws were implanted into rabbit model in fixation of femoral intracondylar fracture, compared with commercial poly L lactic acid (PLLA) screw in same design. 4,8,16 and 24 weeks after surgery, femur samples were harvested micro-computed tomography (microCT) scanning. The bone volume and bone mineral density (BMD) were tested in the fracture gap as well as surrounding screws. 3D remodelling of HP Mg screw were performed for volume evaluation. Then, the samples went through hard tissue slicing process for analysis of bone implant contact (BIC) area and fracture healing process. Furthermore, HP Mg screws were retrieved for bending-force test, weight loss and SEM and EDS tests.

**RESULTS:** HP Mg screws performed uniform degradation morphology from both SEM scanning and 3D remodelling, and broken PLLA screws were observed from 16 weeks after surgery. The bending strength retention and corrosion rate of HP Mg screw were stable throughout the period of experimental observation. Good osseointegration was revealed surrounding HP Mg screws, and significantly higher bone volume, BMD and BIC were observed compared with PLLA screw 8 weeks after surgery. In aspects of fracture healing process, the fracture gap was filled with matured bone tissue 8 weeks after surgery and increased bone volume and BMD were obtained in HP Mg group as compared to PLLA group, with significantly higher value in HP Mg group at Week 8 and Week 16.

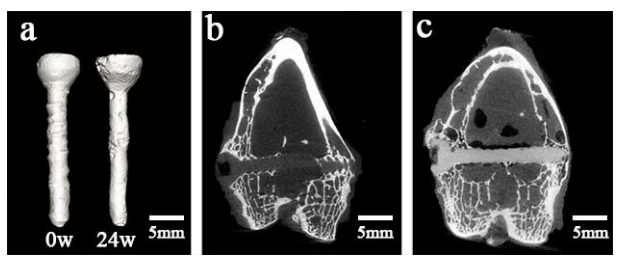


Fig. 1: In vivo 3D microCT remodelling of the implanted HP Mg screws (a) at Week 0 and Week 24. 2D microCT images of rabbit femur fixed by (b) HP Mg screw and (c) PLLA screw 24 weeks after surgery.

**DISCUSSION & CONCLUSIONS:** HP Mg screw performed a good balance between mechanical integrity and degradation in fracture fixation of weight-bearing bone. Bone formation surrounding Mg devices were observed, indicating good osseointegration in comparison with traditional PLLA screw. Fracture healing was achieved 16 weeks after surgery with higher mineral and bone accumulation in HP Mg group. These data suggested that Mg-based screws provided rigid fixation to facilitate fracture healing during degradation, and stimulated osseointegration surrounding screws as well as new bone formation in fracture gap.

**ACKNOWLEDGEMENTS:** This work was supported by the Natural Science Foundation of China (No. 51271117, 81371935), the Biomedical program of Science and Technology innovation project supported by Shanghai (No. 14441901800, No. 14441901802).

### Reduction of magnesium-induced biomineralization using matrix GLA protein

DD Hong<sup>1</sup>, F Witte<sup>3</sup>, C Sfeir<sup>1, 2</sup>

<sup>1</sup> Department of Bioengineering, University of Pittsburgh, Pittsburgh, PA. <sup>2</sup> School of Dental Medicine, University of Pittsburgh, Pittsburgh, PA. <sup>3</sup> Julius Wolff Institute and Center for Musculoskeletal Surgery, Charité - Universitätsmedizin Berlin, Germany.

**INTRODUCTION:** Bioabsorbable magnesium (Mg) and its alloys are gradually replacing the permanent implant biomaterials. traditional Orthopedic and cardiovascular implants are the two major research fields in developing the use of magnesium, especially the latter: various clinical trials have been conducted on magnesium stents with promising results. However, as shown both in vivo and in vitro, Mg degrades spontaneously in biological environment, triggering the deposition of biominerals on and around the material, which could be harmful for the purpose of soft tissue implantation<sup>1, 2</sup>. Hence, the **goal** of this study is to locally inhibit the biomineralization induced by the Mg degradation process, by using matrix GLA protein (MGP). MGP is a small secretory protein that has shown to inhibit soft tissue calcification. We propose to achieve our goal by incorporating MGP exterior of Mg implants for the binding of calcium ions that would otherwise be deposited onto the Mg surface.

**METHODS:** Pure Mg rods of 1.6mm in diameter and 0.5in in length were etched in acetone, acetic acid, and 70% nitric acid after polished using abrasive paper up to grit 1200. MGP was stably transfected into mammalian cells, which were then cultured for protein secretion. Sterilized Mg rods were placed on inserts and suspended in medium containing regular cells or cells secreting MGP for 4 days. Samples were imaged and analyzed by SEM and EDS for mineral deposition.

To obtain constant protein expression around Mg implant, MGP stably transfected cells were seeded into collagen scaffolds, and immunostained with MGP antibody. Mg implants were inserted in the middle of the scaffold and implanted intramuscularly in immunocompromised mice for four and eight weeks.

**RESULTS:** After 4 days of immersion in medium containing regular or transfected cells, the difference of Mg rods between two groups could not be distinguished morphologically via SEM. However, significantly higher weight percentage of calcium and phosphorous ions deposition were detected on the surface of Mg rods that were immersed in MGP secreting cells (figure 1).

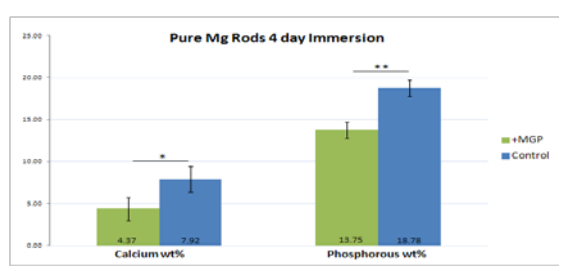


Fig. 1: Weight percent of calcium and phosphorous ions on pure Mg rods 4 days after immersion in medium.\*: p<0.005; \*\*p<0.001

H&E staining on various layers of the frozen section of the cells seeded collagen gel (figure 2a) showed uniform cells seeding in the scaffold. MGP antibody staining (figure 2b) confirmed that the cells were still expressing the protein after seeded into collagen gels.

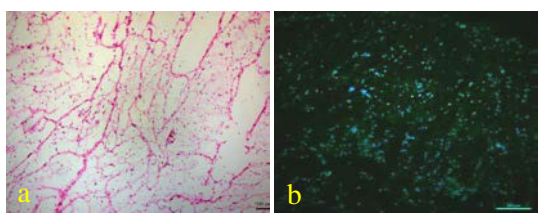


Fig. 2: (a) H&E (b) MGP antibody (MGP: green; DAPI: blue) staining on frozen section of the cells seeded collagen gel.

**DISCUSSION & CONCLUSIONS:** Still an ongoing study, the results from *in vivo* experiment are yet to be concluded. However, results from *in vitro* experiment demonstrated that MGP reduced the mineral deposition on the surface of Mg and its alloys. Further studies are needed to determine the total concentration of protein required for better biomineral inhibition on Mg implants.

**ACKNOWLEDGEMENTS:** We would like to acknowledge NSF-ERC for funding this project. Gratefully thank Dr. Mike Epperly for gamma sterilizing the samples.

#### Design concept and biocompatibility of iron-based biocorrodible scaffold

DY Zhang, WJ Lin, G Zhang, HP Qi and HT Sun.

R&D Center, Lifetech Scientific, Shenzhen China.

**INTRODUCTION:** The iron alloys are promising materials for temporary vascular scaffold with more controversies than magnesium. Main problems are slow in vivo corrosion and resorption as well as disqualified in vitro or in vivo biocompatibility, e.g. in vitro cytotoxicity. In this paper, we tried to solve above two problems using novel design of materials and novel test methodology.

**METHODS:** The iron based scaffold has similar pattern to mainstream permanent stents with total strut thickness 70 microns in which nitrided iron backbone thickness is 50-55 microns. A novel protection layer with thickness 300 nanometres is employed to delay the onset of iron corrosion to two or three months, ensuring the effective scaffold for dilated lesion. Outermost layer on struts is special designed polymer with sirolimus to not only control the drug release, but also control the iron corrosion profile and release of solid rust particulates. We extracted iron scaffold in different solutions with controlled pH value, oxygen, and measured the iron concentration in extracts, then incubated cell in those extracts to find the relationship of iron concentration with cell viability. We also implanted such scaffolds into rabbit abdominal aorta to check if any negative biological effects occurred. A novel way was developed to eliminate the further corrosion of iron during specimen preparation and to mitigate the influence of black iron rust on histological observation.

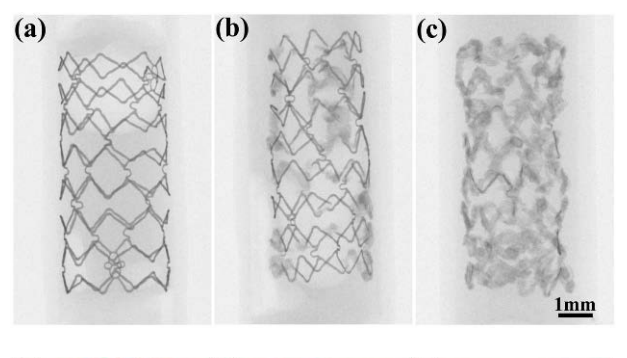
**RESULTS:** Such design of iron scaffold has similar or better mechanical performances, the same specifications, the same operation way without special or additional procedure in comparison with mainstream permanent stents. In terms of corrosion timeframe, the iron kept intact for about two months, then corroded more quickly when the protection layer on it was exhausted, totally corroded into rust about one year, while scaffold lost integrity and caging effect on vessels in about six to eight months.

Iron corroded into magnetite and soluble ions within polymer layer, meanwhile iron ions diffused into tissue and precipitated in tissue as

goethite and ferrous phosphate where pH value was higher and iron ions became oversaturated.

In vitro cytotoxicity test showed that cell viability has nothing to do with the iron concentration in extracts, instead, highly correlates to the particulates of specific dimensions in incubation media.

In vivo rabbit implantation showed iron scaffold may effectively scaffold without premature damage and corrode almost totally in 13 months. Iron corrosion particulates may be removed by phagocytosis, or moving between cells or stay in cells safely for long time.



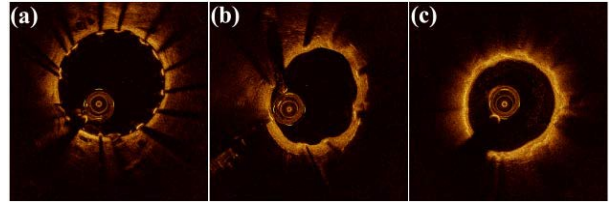


Fig. 1: MicroCT(above) and OCT(below) images of iron scaffold implanted in rabbit aorta for (a) three days, (b) six months and (c) 13 months

**DISCUSSION & CONCLUSIONS:** The ironbased scaffold has the same mechanical performance as the best permanent stents, and may effectively scaffold without premature structure damage and totally corroded in 13 months. The biocompatibility test methods based on ISO10993 should be modified for iron scaffold evaluation.

**ACKNOWLEDGEMENTS:** 863 program grant No 2011AA030103 from Chinese Ministry of Science and Technology.